

NASA Contractor Report 159628

{NASA-CR-159628) STUDIES OF THE ACOUSTIC  
TRANSMISSION CHARACTERISTICS OF COAXIAL  
NOZZLES WITH INVERTED VELOCITY PROFILES:  
COMPREHENSIVE DATA REPORT Final Report  
(Lockheed-Georgia Co., Marietta.) 182 p

N79-27933

Unclas  
63/71 30058

STUDIES OF THE ACOUSTIC TRANSMISSION  
CHARACTERISTICS OF COAXIAL NOZZLES  
WITH INVERTED VELOCITY PROFILES:  
COMPREHENSIVE DATA REPORT

P. D. Dean, M. Salikuddin, K. K. Ahuja  
H. E. Plumblee, and P. Mungur

LOCKHEED-GEORGIA COMPANY  
Marietta, GA 30063

CONTRACT NAS3-20797  
MAY 1979

**NASA**  
National  
Aeronautics and  
Space  
Administration

Lewis Research Center  
Cleveland, Ohio 44135



1. Report No. NASA CR-159628		2. Government Accession No.		3. Recipient's Catalog No.	
4. Title and Subtitle STUDIES OF THE ACOUSTIC TRANSMISSION CHARACTERISTICS OF COAXIAL NOZZLES WITH INVERTED VELOCITY PROFILES - Volume I				5. Report Date May 1979	
				6. Performing Organization Code	
7. Author(s) P. D. Dean, M. Salikuddin, K. K. Ahuja, H. E. Plumblee, and P. Mungur				8. Performing Organization Report No.	
9. Performing Organization Name and Address Lockheed-Georgia Company Marietta, Georgia 30063				10. Work Unit No.	
				11. Contract or Grant No. NAS3-20797	
12. Sponsoring Agency Name and Address National Aeronautics and Space Administration Washington, D. C.				13. Type of Report and Period Covered Contract Report	
				14. Sponsoring Agency Code	
15. Supplementary Notes Final Report. Project Manager, A. M. Karchmer, V/STOL and Noise Division, NASA-Lewis Research Center, Cleveland, Ohio. Lockheed Program Manager, H. E. Plumblee, Jr.					
16. Abstract An experimental study to determine the efficiency of internal noise radiation through a coannular exhaust nozzle with an inverted velocity profile was conducted. A preliminary investigation was first undertaken (1) to define the test parameters which influence the internal noise radiation, (2) to develop a test methodology which could realistically be used to examine the effects of the test parameters, and (3) to validate this methodology. The result was the choice of an acoustic impulse as the internal noise source in the jet nozzles. Noise transmission characteristics of a coannular nozzle system were then investigated. In particular, the effects of fan convergence angle, core extension length to annulus height ratio and flow Mach numbers and temperatures were studied. Main results of the study were described in reference 1. Relevant spectral data only is presented here in the form of normalized nozzle transfer function versus nondimensional frequency.					
17. Key Words (Suggested by Author(s)) Acoustic Measurements, Acoustic Sources, Duct Acoustics, Electric Spark, Engine Noise, Gun Shot, Internal Noise, Inverted Velocity and Temperature Coaxial Jets, Impulse Noise, Multilayer Flow, Nozzle Transfer Function, Refraction				18. Distribution Statement  Unclassified - Unlimited  STAR Category 71	
19. Security Classif. (of this report) UNCLASSIFIED		20. Security Classif. (of this page) UNCLASSIFIED		21. No. of Pages 179	
22. Price*					

## CONTENTS

	Page
1. Introduction . . . . .	1
2. Nozzle Transfer Function Amplitudes . . . . .	1
3. Nozzle Configurations . . . . .	3
4. List of Test Points and Data Plots . . . . .	3
5. Data Plots . . . . .	8
6. List of Symbols . . . . .	178
7. References . . . . .	179

## 1. INTRODUCTION

The present report complements Volume I (ref. 1) by presenting the acoustic data for all the coaxial nozzle configurations tested and described in reference 1. The data is presented in the form of plots of normalized nozzle transfer function as a function of  $kR$  for 'source in core' case and as a function of  $kh$  for 'source in fan' case. Nozzle configurations, test plan, methods of data acquisition and other details relevant to this report have already been given at length in Section 3 of Volume I. However, in order to minimize cross reference between the two reports, a few details presented in Volume I may be repeated here.

## 2. NOZZLE TRANSFER FUNCTION AMPLITUDES

The power spectra of edited in-duct and far-field signals are obtained by the Fourier transform of each pulse using the digital FFT signal analyzer. These data (512 spectral points of constant bandwidth) are recorded on cassettes and then transferred to a mini-computer for frequency response and atmospheric corrections. Each corrected record is then individually smoothed to remove fine detail of little practical interest. The transfer function spectra between the far-field and in-duct signals are then computed from these smoothed in-duct and far-field spectra.

The transfer function spectra between in-duct and far-field signals are also noisy in nature particularly in the higher frequency range. With this situation it is difficult to distinguish between the effect of any nozzle operating parameter, such as flow velocity, flow temperature, nozzle shape, etc. on the transfer functions. Therefore, to obtain a more meaningful comparison, an averaging procedure has also been used to smooth the transfer function spectra which is computed from the smoothed power spectra of individual signals. The smoothing technique used in this study can be illustrated as follows. The smoothed value of the function (or power spectra), at the  $l$ th frequency point is given by

$$\bar{F}(l) = \frac{F_1(l)}{X_{l+m} - X_{l-m}} \quad (1)$$

where

$$F_1(l) = \frac{H}{3} \left\{ F(l-m) + 4F(l-m+1) + 2F(l-m+2) + 4F(l-m+3) + \dots + 2F(l+m-2) + 4F(l+m-1) + F(l+m) \right\} \quad (2)$$

(Simpson rule for integrating  $2m+1$  points)

$X_l$  = coordinate of  $l$ th point

$H$  = difference between the coordinates of two successive points

$2m+1$  = number of points used for averaging

Let  $n = 2m+1$ .

In the smoothing procedure, the number of points  $n$  has been varied with respect to frequency. The number  $n$  is chosen such that it becomes equal to the 1/3 octave band for a given frequency, up to a maximum of 31 points. (The difference between two successive points is the bandwidth which is 200 Hz in this case.) The smoothing process is repeated three times to obtain a more uniform variation. The number of points,  $n$  used in smoothing is given by

$$n = 1/\sqrt{2} \quad (\text{rounded up}) \leq 31.$$

(If  $n$  comes out to be even, then it is increased by one.)

Nozzle transfer function  $\bar{F}(1)$  at a given frequency is further normalized by a procedure which relates the measured sound pressures at any fixed polar angle to that which would be given from a point source of equivalent power in free space. The standard normalization distance is one meter.

The basic assumption is that the measured incident pressure spectrum in the duct is uniform over the cross-section.

The in-duct power is then given by  $(1+M_D)^2 p_D^2 \cdot A_D / \rho_D c_D$  where  $M_D$  is duct mean flow Mach number,  $A_D$  is duct cross-section,  $\rho_D c_D$  is the characteristic in-duct acoustic impedance and  $p_D^2$  is the mean square pressure of the outgoing acoustic wave measured in-duct.

The intensity at one meter from the equivalent in-duct source is

$$I_D = \frac{p_D^2 A_D (1+M_D)^2}{\rho_D c_D 4\pi} \quad (4)$$

and the intensity at one meter transformed from far-field measurements at radius  $R_m$  meters is given by

$$I_{rad} = \frac{p_{rad}^2(\theta) R_m^2}{\rho_o c_o} \quad (5)$$

where  $p_{rad}^2(\theta)$  is the mean square pressure of the acoustic wave measured in the far field and  $\rho_o c_o$  is the characteristic free-field acoustic impedance.

The normalized nozzle transfer function is the ratio of  $I_{rad}/I_D$ , i.e.

$$NTF = \left( \frac{p_{rad}^2(\theta)}{p_D^2} \right) \left( \frac{4\pi R_m^2}{A_D} \right) \frac{\rho_D c_D}{\rho_o c_o} \frac{1}{(1+M_D)^2} \quad (6)$$

Note that the first term in brackets on the right-hand side of equation (6) is the measured transfer function obtained from the spectra of edited far-field and in-duct outgoing signals and is taken to be equal to  $\bar{F}(1)$  of equation (1) above for plotting purposes.

It is important to point out that the values of NTF at a given value of nondimensional frequency in the NTF spectra shown here are different from those plotted in directivity plots of Volume I. The reason for this is that the values used in directivity plots at the  $l^{\text{th}}$  frequency were obtained by averaging the smoothed transfer function data  $\bar{F}$  between the frequency points  $l/\sqrt{2}$  to  $l \times \sqrt{2}$  [see equation 3-3 of Volume I (ref. 1)] and normalized. Such averaging was not performed to the data presented here.

### 3. NOZZLE CONFIGURATIONS

The relevant geometric parameters for the coaxial nozzle system are given in Table 1. The convergence angle  $\alpha$ , of nozzles 1, 2, and 3 was  $20^\circ$  and that of nozzles 4, 5 and 6 was  $40^\circ$ .

#### Test Plan

The nozzle system consists of a primary and secondary (fan) nozzle, each with its own nozzle transmission coefficient. Two sets of measurements were thus required for primary and fan nozzle, respectively. As shown in Table 2, each of the outer nozzles was tested for the unheated conditions with the source located in the fan. With the source located in the primary (or core), only the outer nozzles designated 1, 2 and 3 were used.

The heated-jet tests were, however, limited to the measurement of the fan nozzle transmission coefficient only. Only two nozzles (#1 and #2) were tested.

The figures where the corresponding data appears are also listed in this table.

### 4. LIST OF TEST POINTS AND DATA PLOTS

The test points and the figure numbers where the corresponding data appear are given in Tables 3, 4 and 5.

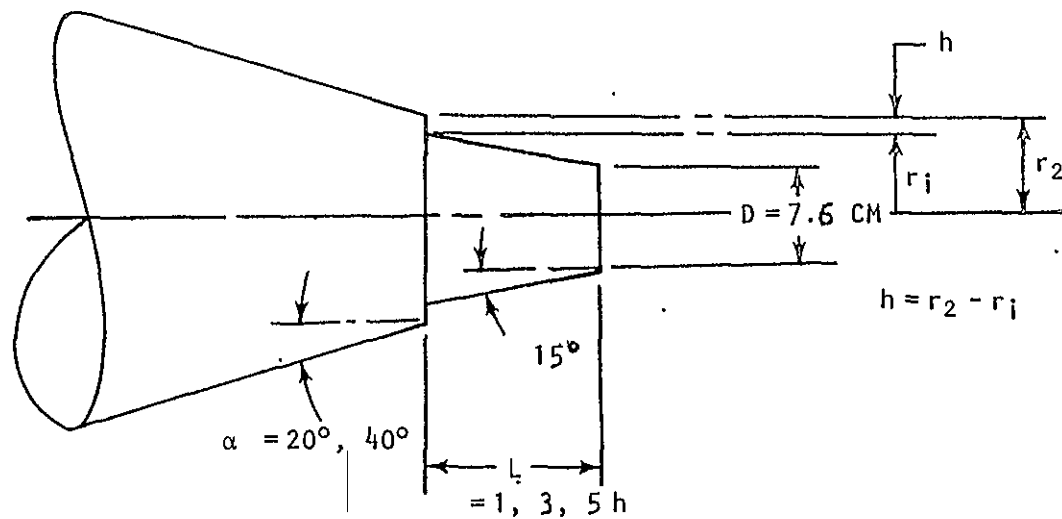


TABLE 1 RELEVANT GEOMETRIC PARAMETERS FOR COAXIAL NOZZLE SYSTEM

Nozzle Number		L/h	h (cm)	L (cm)	$r_1$ (cm)	$r_2$	Annulus Area $A_2$ (cm <sup>2</sup> )	Area Ratio* $A_2/A_1$
$\alpha = 20^\circ$	$\alpha = 40^\circ$							
1	4	1	1.37	1.37	4.12	5.49	41.45	0.91
2	5	3	1.71	5.12	5.12	6.83	64.14	1.41
3	6	5	2.26	11.30	6.78	9.04	112.21	2.46

\* $A_1$  = Primary Exit Area = 45.60 cm<sup>2</sup>.

TABLE 2 NOZZLE TEST SUMMARY

Outer Nozzle No.	Location of Source	Jet Condition	Figures Where the Data Appears
1,2 and 3	Primary	Unheated	1 - 19
1,2,3,4,5 and 6	Fan	Unheated	20 - 49
1 and 2	Fan	Heated	50 - 65

TABLE 3 DATA FOR UNHEATED JET WITH SOURCE IN CORE

Figure No.	$M_{J1}$	$M_{J2}$	$T_{R1}$ (K)	$T_{R2}$ (K)	$T_{amb}$ (K)
NOZZLE 1, $\alpha = 20^\circ$ , $L/h = 1$ ( $P_{amb} = 9.79 \times 10^4 \text{ N/m}^2$ )					
1	0.0	0.0	299.4	299.4	296.0
2	0.4	0.6	293.9	290.0	296.0
3	0.8	0.9	291.1	290.6	291.7
4	0.8	1.2	292.8	292.2	291.7
5	0.8	1.4	293.3	293.9	291.7
6	1.2	1.4	294.4	295.6	291.7
7	0.0	1.2	295.6	293.3	291.1
NOZZLE 2, $\alpha = 20^\circ$ , $L/h = 3$ ( $P_{amb} = 9.85 \times 10^4 \text{ N/m}^2$ )					
8	0.0	0.0	296.7	292.2	295.4
9	0.4	0.6	293.3	293.3	290.4
10	0.8	0.9	294.4	290.6	290.1
11	0.8	1.2	293.3	293.3	290.8
12	0.8	1.4	294.4	291.1	289.9
13	1.2	1.4	293.9	290.0	290.0
14	0	1.2	295.6	292.8	290.6
NOZZLE 3, $\alpha = 20^\circ$ , $L/h = 5$ ( $P_{amb} = 9.79 \times 10^4 \text{ N/m}^2$ )					
15	0.0	0.0	300.0	292.8	294.6
16	0.4	0.6	287.8	285.0	287.0
17	0.8	0.9	287.2	285.6	284.5
18	1.2	1.2	287.8	285.6	281.2
19	0.0	1.2	288.3	285.0	281.6



TABLE 4 DATA FOR UNHEATED JET WITH SOURCE IN FAN

Figure No.	MJ <sub>1</sub>	MJ <sub>2</sub>	TR <sub>1</sub> (K)	TR <sub>2</sub> (K)	T <sub>amb</sub> (K)
NOZZLE 1, $\alpha = 20^\circ$ , L/h = 1 (P <sub>amb</sub> = $9.83 \times 10^4$ N/m <sup>2</sup> )					
20	0.0	0.0	296.7	295.6	294.8
21	0.4	0.6	295.6	297.6	296.2
22	0.8	0.9	294.4	295.6	294.8
23	0.8	1.2	295.0	295.6	294.8
24	0.0	1.2	296.7	296.7	294.8
NOZZLE 2, $\alpha = 20^\circ$ , L/h = 3 (P <sub>amb</sub> = $9.90 \times 10^4$ N/m <sup>2</sup> )					
25	0.0	0.0	298.3	291.7	294.1
26	0.4	0.6	291.7	290.0	287.9
27	0.8	0.9	291.1	289.4	286.5
NOZZLE 3, $\alpha = 20^\circ$ , L/h = 5 (P <sub>amb</sub> = $9.83 \times 10^4$ N/m <sup>2</sup> )					
28	0.0	0.0	287.2	285.0	288.2
29	0.4	0.6	285.6	284.4	288.5
30	0.8	0.9	287.2	286.7	286.5
31	0.8	1.2	287.2	285.6	284.8
32	1.2	1.2	287.2	285.6	283.1
33	0.0	1.2	286.7	285.0	282.2
NOZZLE 4, $\alpha = 40^\circ$ , L/h = 1 (P <sub>amb</sub> = $9.91 \times 10^4$ N/m <sup>2</sup> )					
34	0.0	0.0	297.8	292.2	286.3
35	0.4	0.6	289.4	288.9	284.4
36	0.8	0.9	290.0	289.4	285.0
37	1.2	1.4	287.2	285.0	288.6
38	0.0	1.2	295.6	290.6	288.6
NOZZLE 5, $\alpha = 40^\circ$ , L/h = 3 (P <sub>amb</sub> = $9.70 \times 10^4$ N/m <sup>2</sup> )					
39	0.0	0.0	300.0	295.0	294.2
40	0.4	0.6	290.6	289.4	293.3
41	0.8	0.9	291.1	291.1	295.0
42	0.8	1.2	288.9	286.1	293.7
43	0.0	1.2	299.4	290.1	289.5
NOZZLE 6, $\alpha = 40^\circ$ , L/h = 5 (P <sub>amb</sub> = $9.70 \times 10^4$ N/m <sup>2</sup> )					
44	0.0	0.0	293.3	292.2	294.5
45	0.4	0.6	288.3	288.3	289.5
46	0.8	0.9	288.3	288.3	287.1
47	0.8	1.2	287.8	287.2	286.1
48	1.2	1.2	287.8	287.2	286.1
49	0.0	1.2	287.8	287.2	286.1

TABLE 5 DATA FOR HEATED JET WITH SOURCE IN FAN

Figure No.	$M_{J1}$	$M_{J2}$	$T_{R1}$ (K)	$T_{R2}$ (K)	$T_{amb}$ (K)
NOZZLE 1, $\alpha = 20^\circ$ , $L/h = 1$ ( $P_{amb} = 9.76 \times 10^4 \text{ N/m}^2$ )					
50	0.8	0.9	316.7	750.0	292.0
51	0.8	0.9	291.1	900.0	294.1
52	0.8	0.9	450.0	750.0	298.9
53	0.8	0.9	450.0	900.0	301.7
54	0.8	0.9	563.0	750.0	299.6
55	0.8	0.9	675.0	900.0	303.0
56	0.8	1.2	300.6	900.0	300.0
57	0.8	1.2	450.0	750.0	296.6
58	0.8	1.2	450.0	900.0	301.2
59	0.8	1.2	563.0	750.0	300.5
60	0.8	1.2	675.0	900.0	303.6
NOZZLE 2, $\alpha = 20^\circ$ , $L/h = 3$ ( $P_{amb} = 9.88 \times 10^4 \text{ N/m}^2$ )					
61	0.8	0.9	290.0	750.0	300.9
62	0.8	0.9	450.0	600.0	299.1
63	0.8	0.9	450.0	750.0	298.1
64	0.8	1.2	296.1	750.0	296.6
65	0.8	1.2	450.0	750.0	298.5

## 5. DATA PLOTS

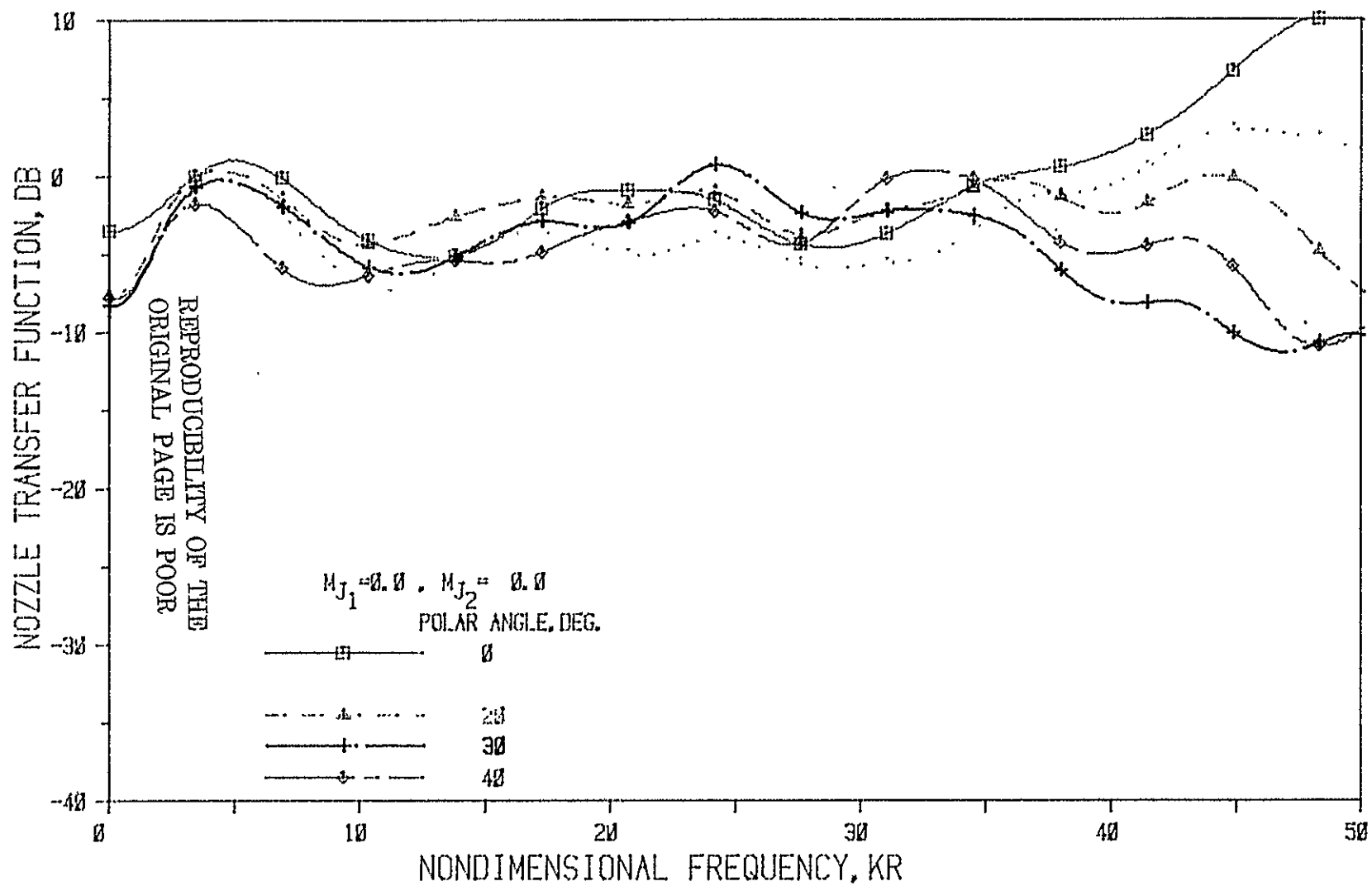


Figure 1(a) Nozzle N1 (  $L/h = 1$  , Convergence Angle = 20 Deg. ); Source At Core

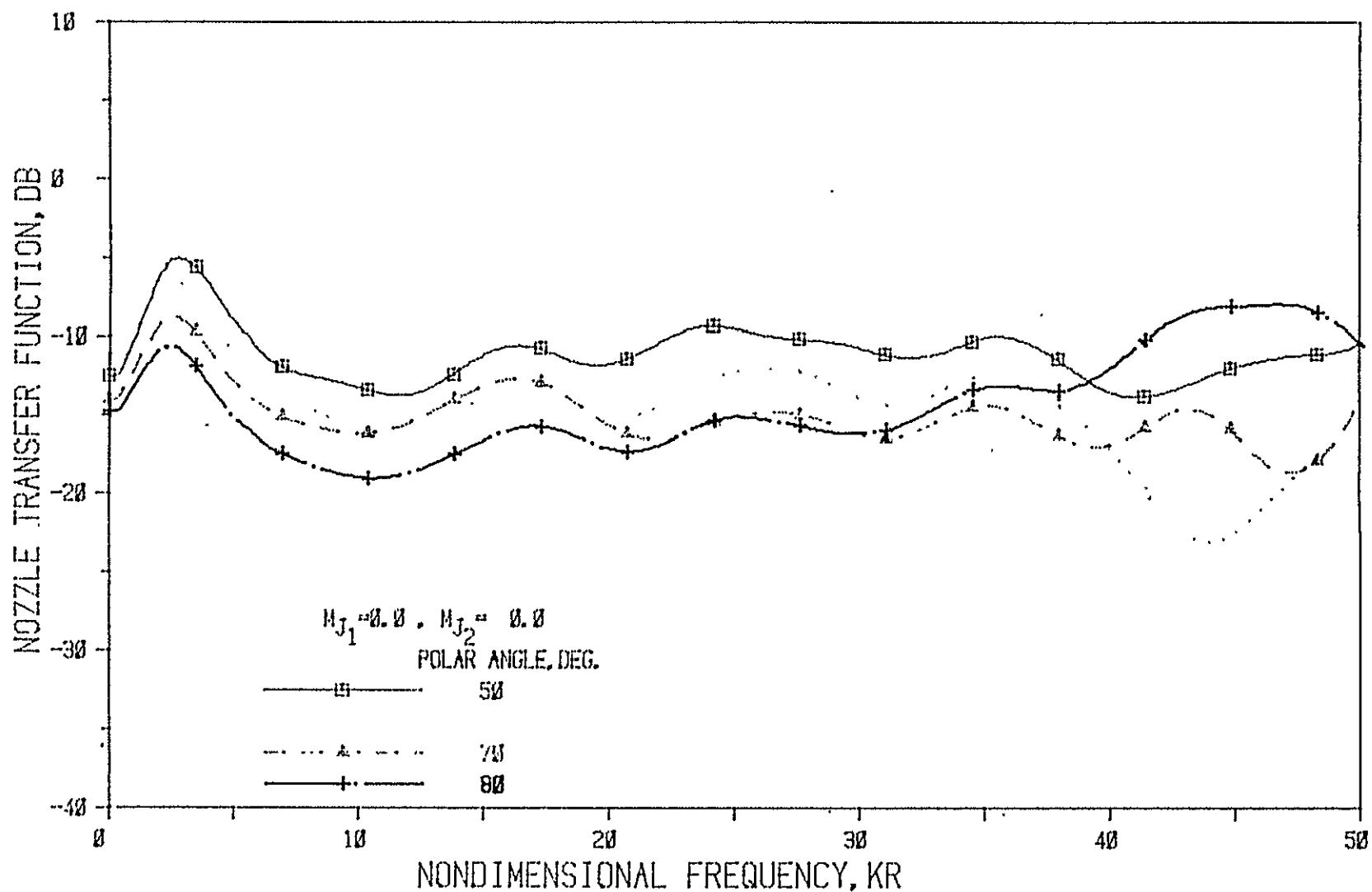


Figure 1(b) Nozzle N1 ( $L/h = 1$ , Convergence Angle  $= 20$  Deg.); Source At Core

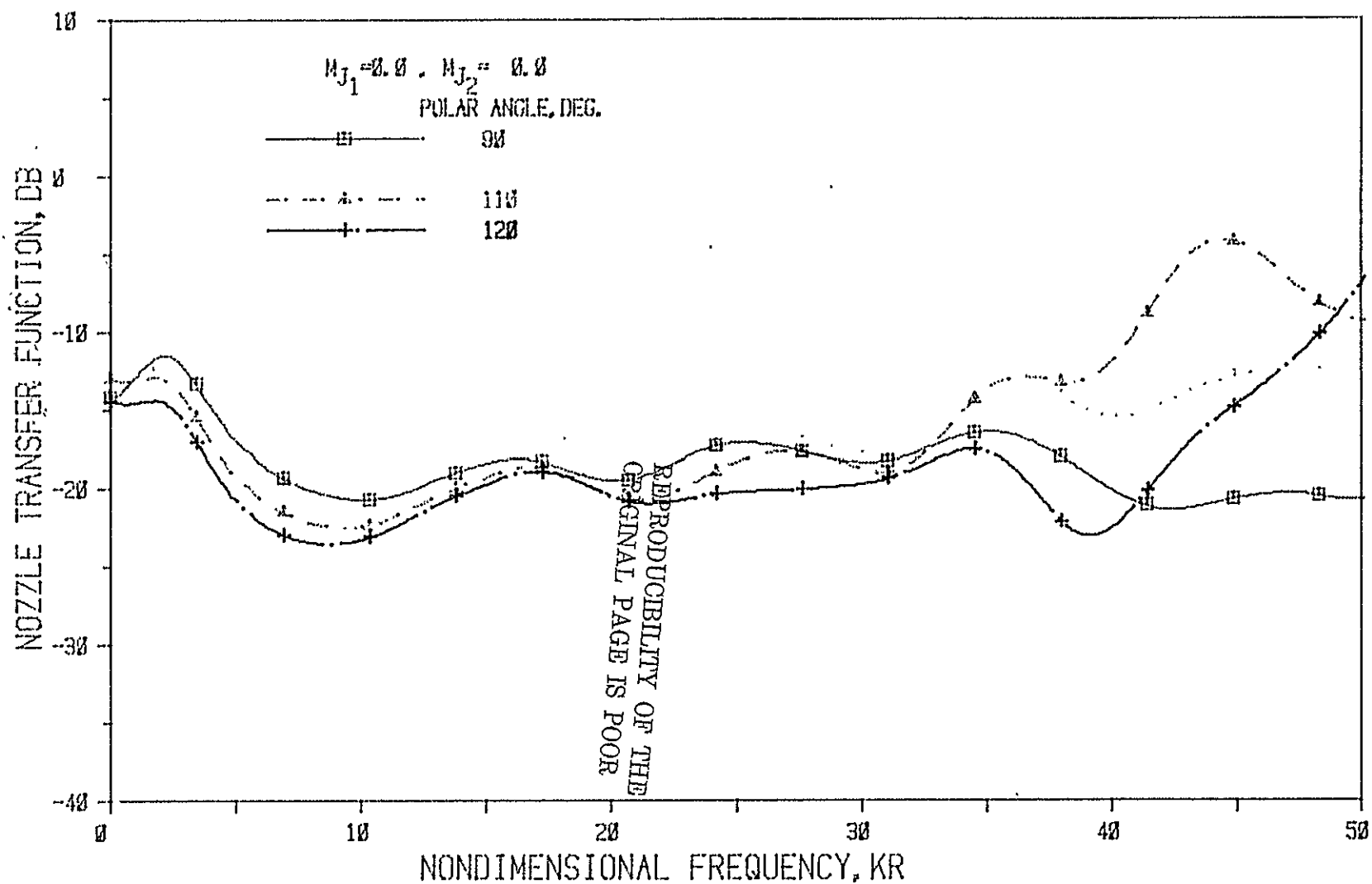


Figure 1(c) Nozzle N1 (  $L/h = 1$  , Convergence Angle = 20 Deg. ); Source At Core

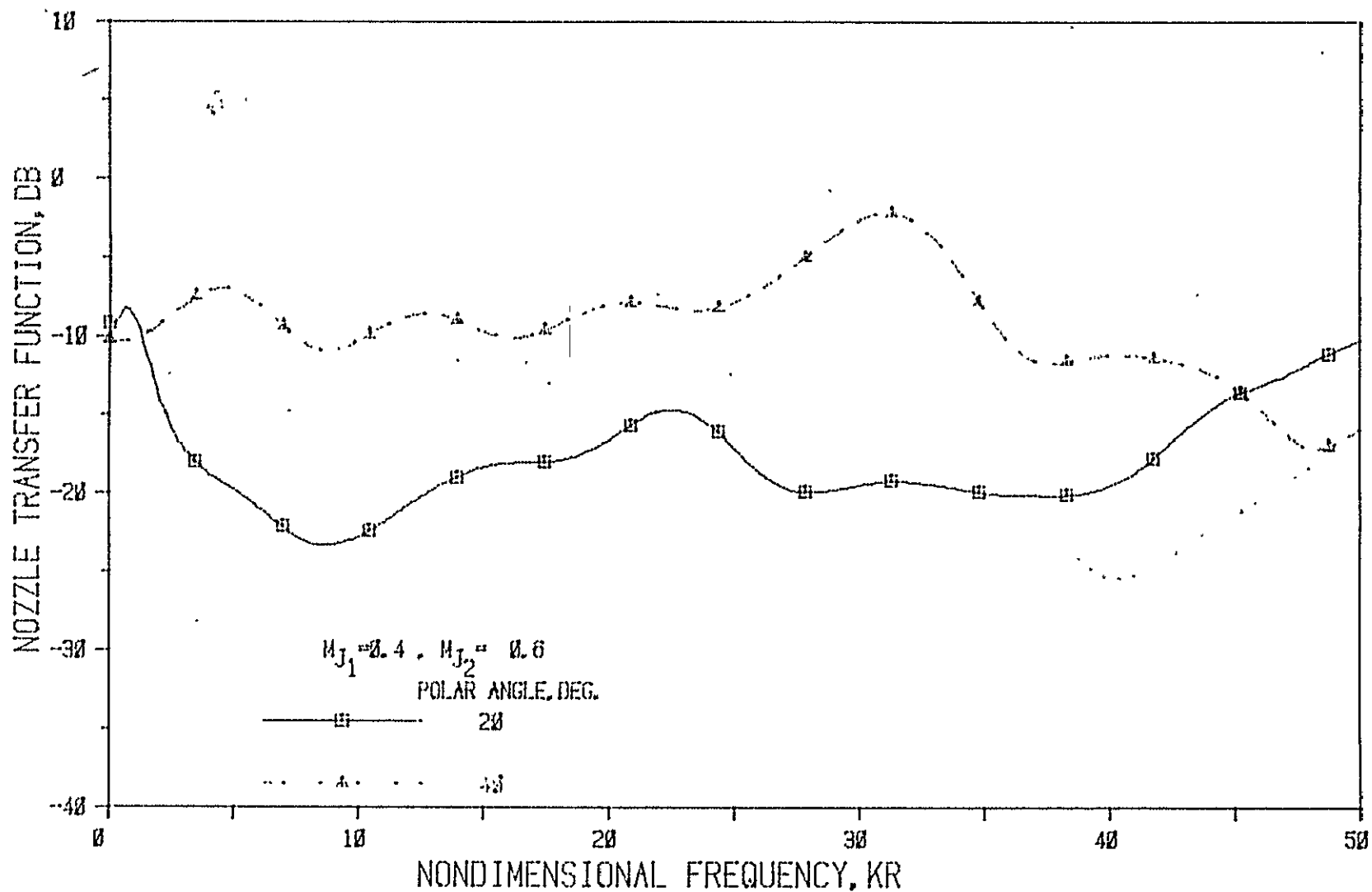


Figure 2(a) Nozzle N 1 (  $L/h = 1$ , Convergence Angle = 20 Deg. ); Source At Core

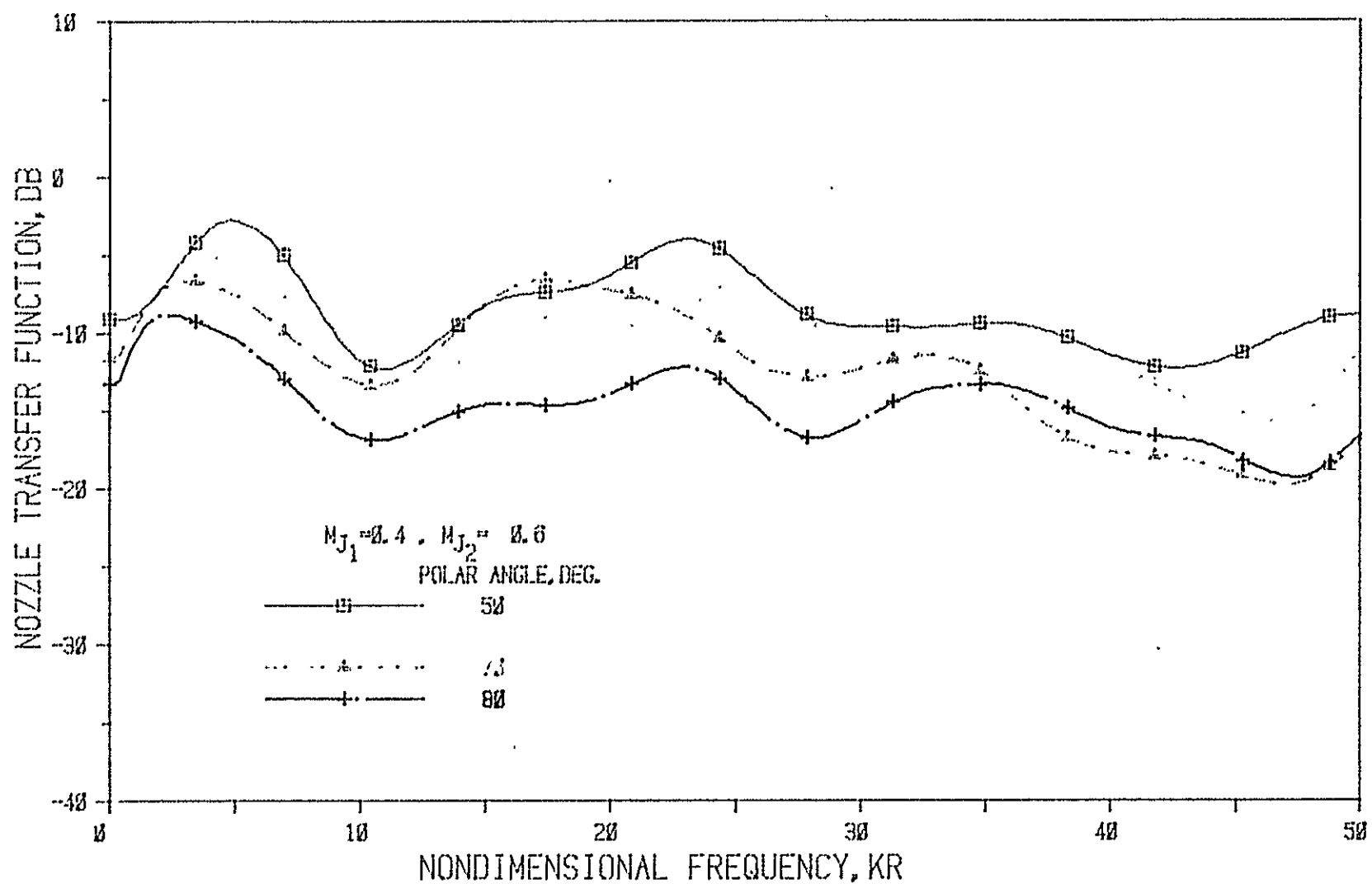


Figure 2(b) Nozzle N1 ( $L/h = 1$ , Convergence Angle = 20 Deg.); Source At Core



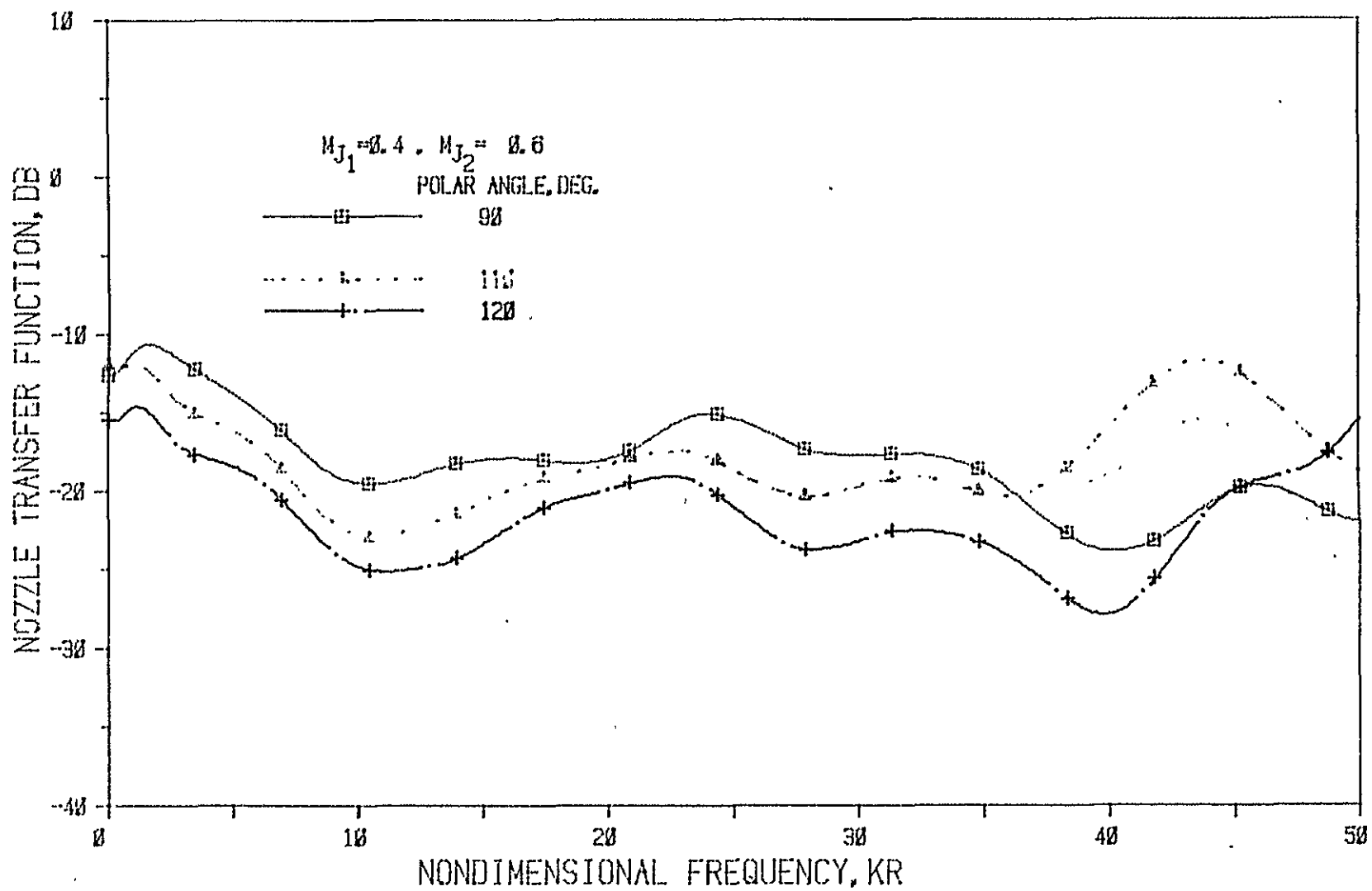


Figure 2(a) Nozzle N 1 (  $L/h = 1$ , Convergence Angle = 20 Deg. ); Source At Core

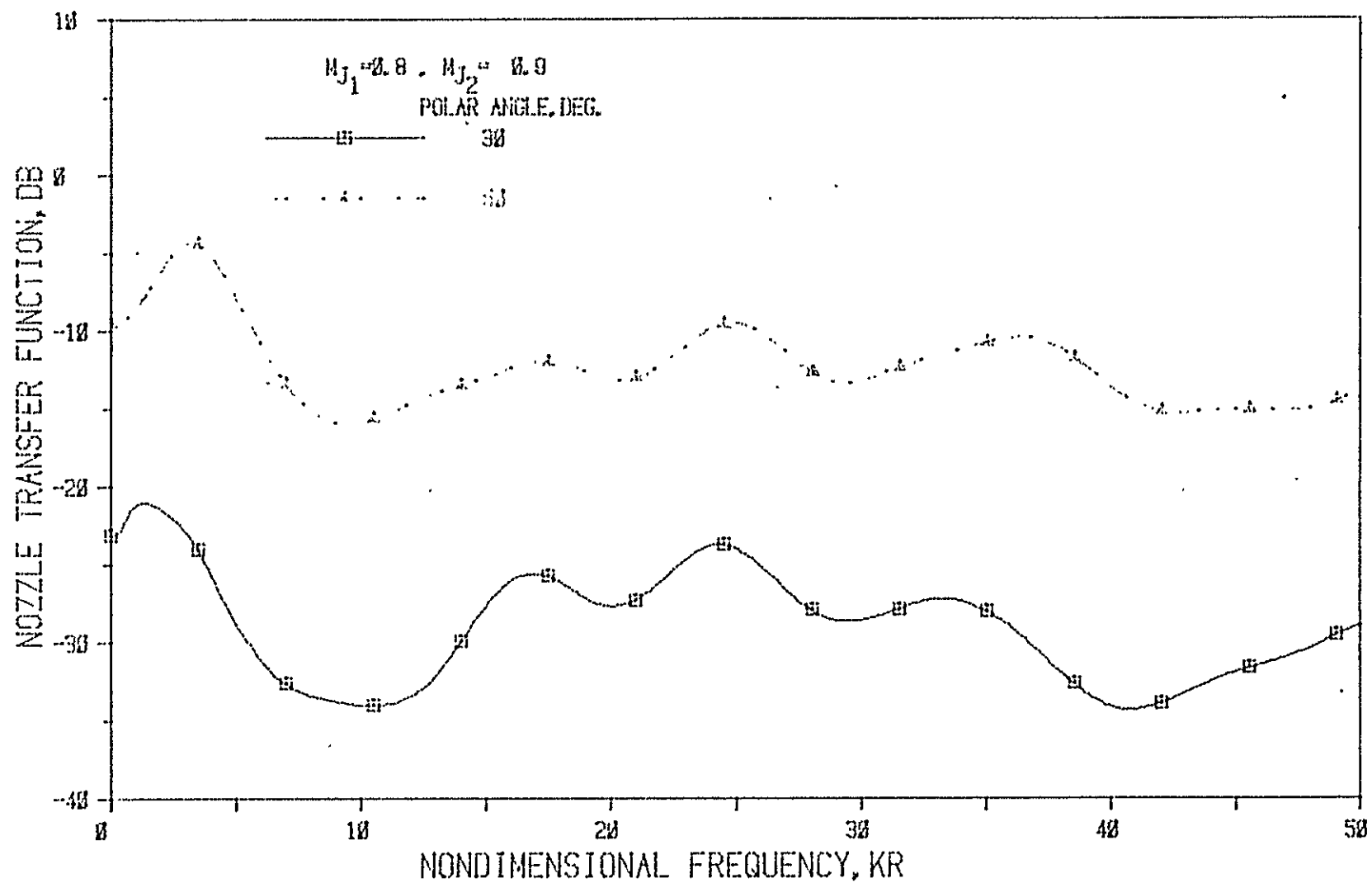


Figure 3(a) Nozzle N 1 (  $L/h = 1$ , Convergence Angle = 20 Deg.); Source At Core

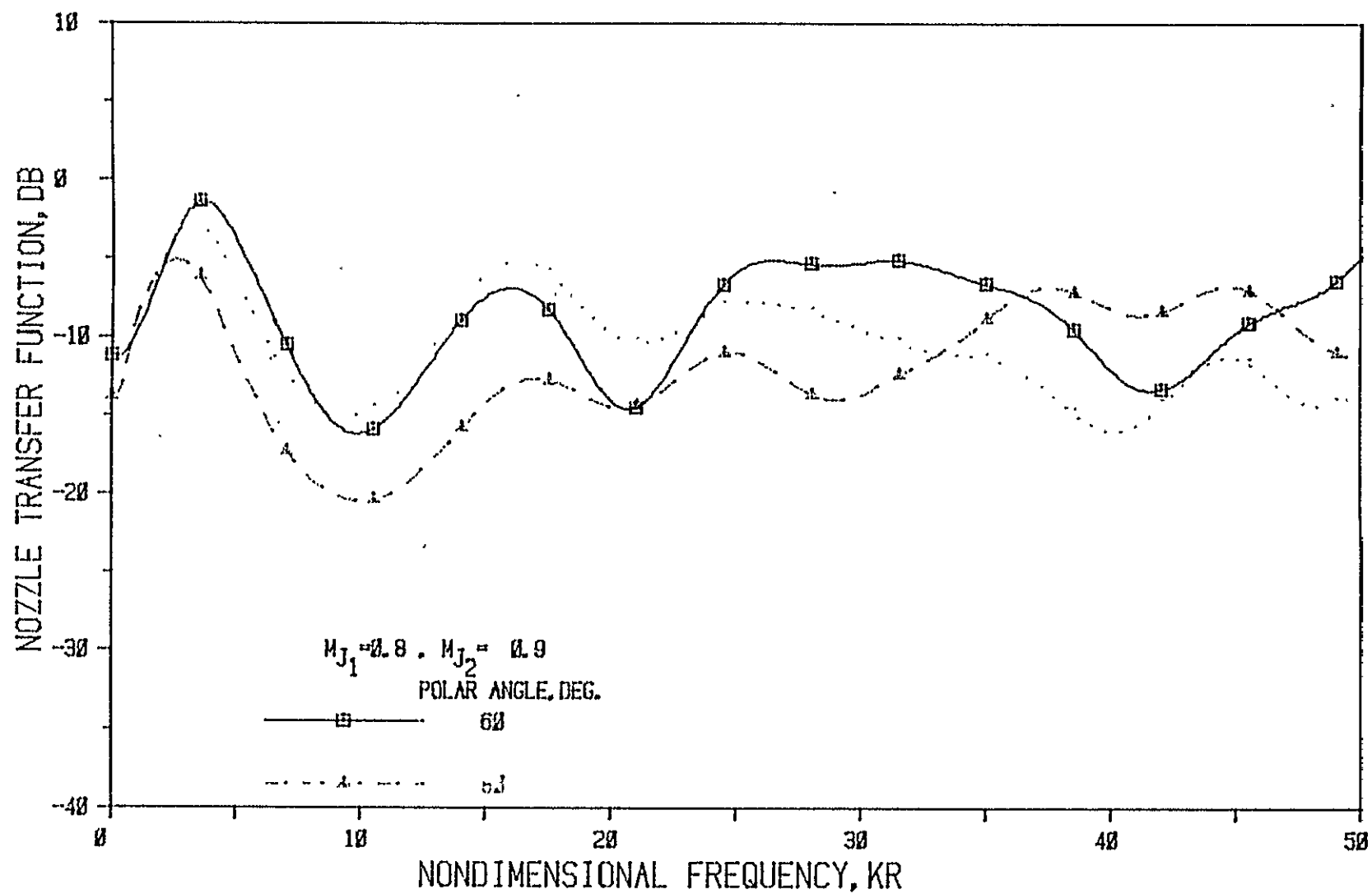


Figure 3(b) Nozzle N 1 (  $L/h = 1$  , Convergence Angle = 20 Deg. ); Source At Core

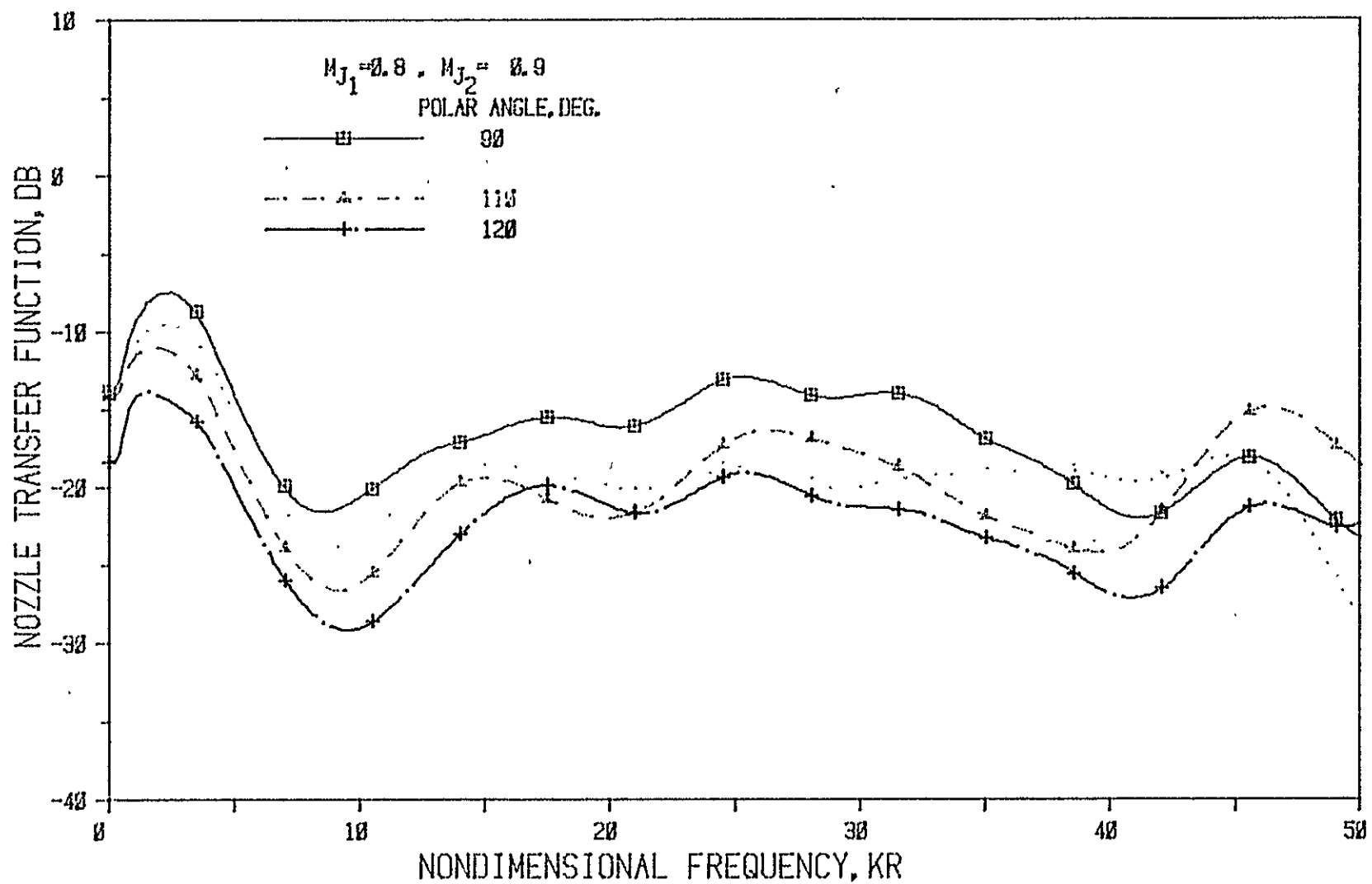


Figure 3(c) Nozzle N 1 (  $L/h = 1$  , Convergence Angle = 20 Deg. ); Source At Core

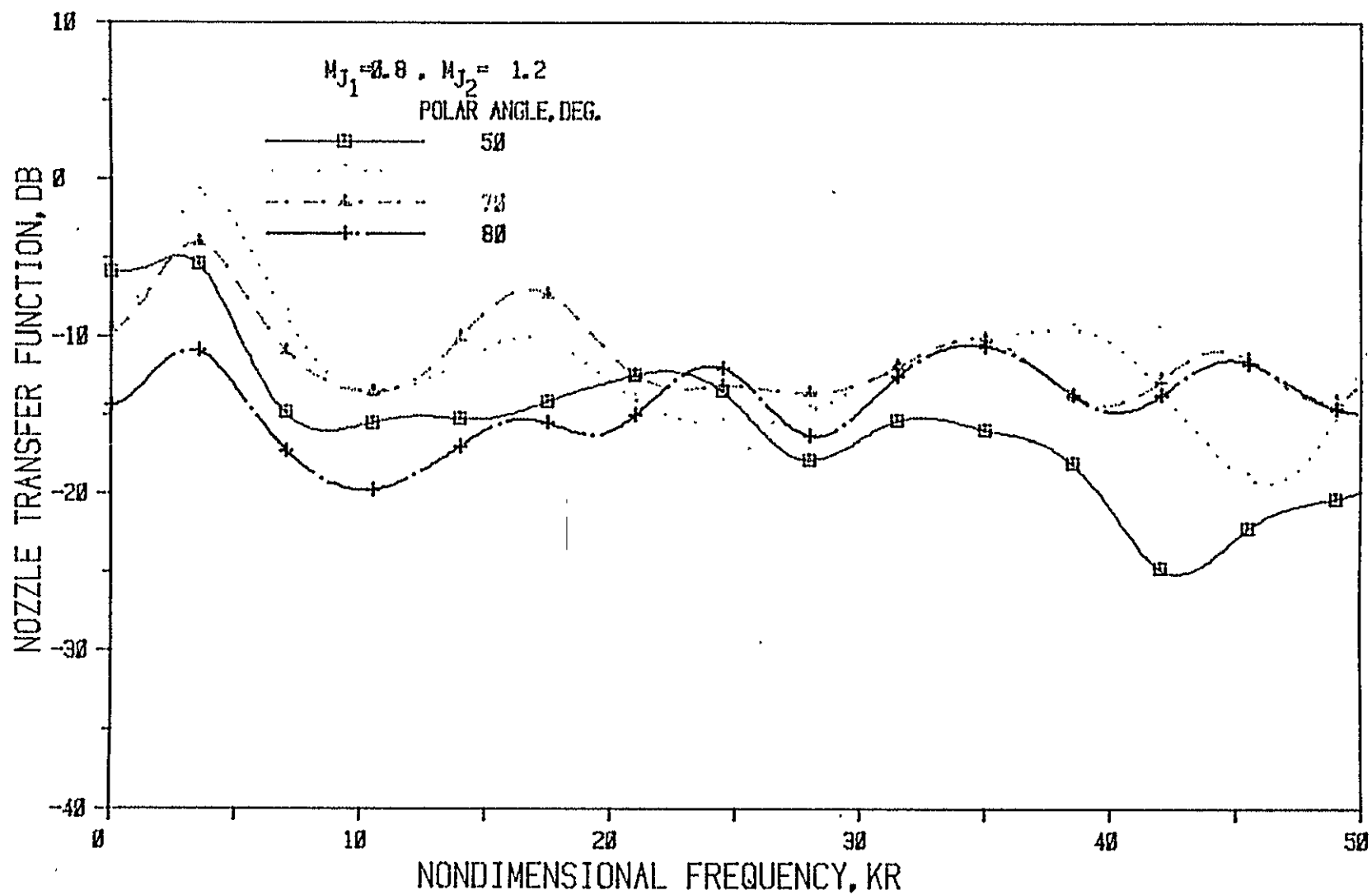


Figure 4(a) Nozzle N1 ( $L/h = 1$ , Convergence Angle = 20 Deg.); Source At Core

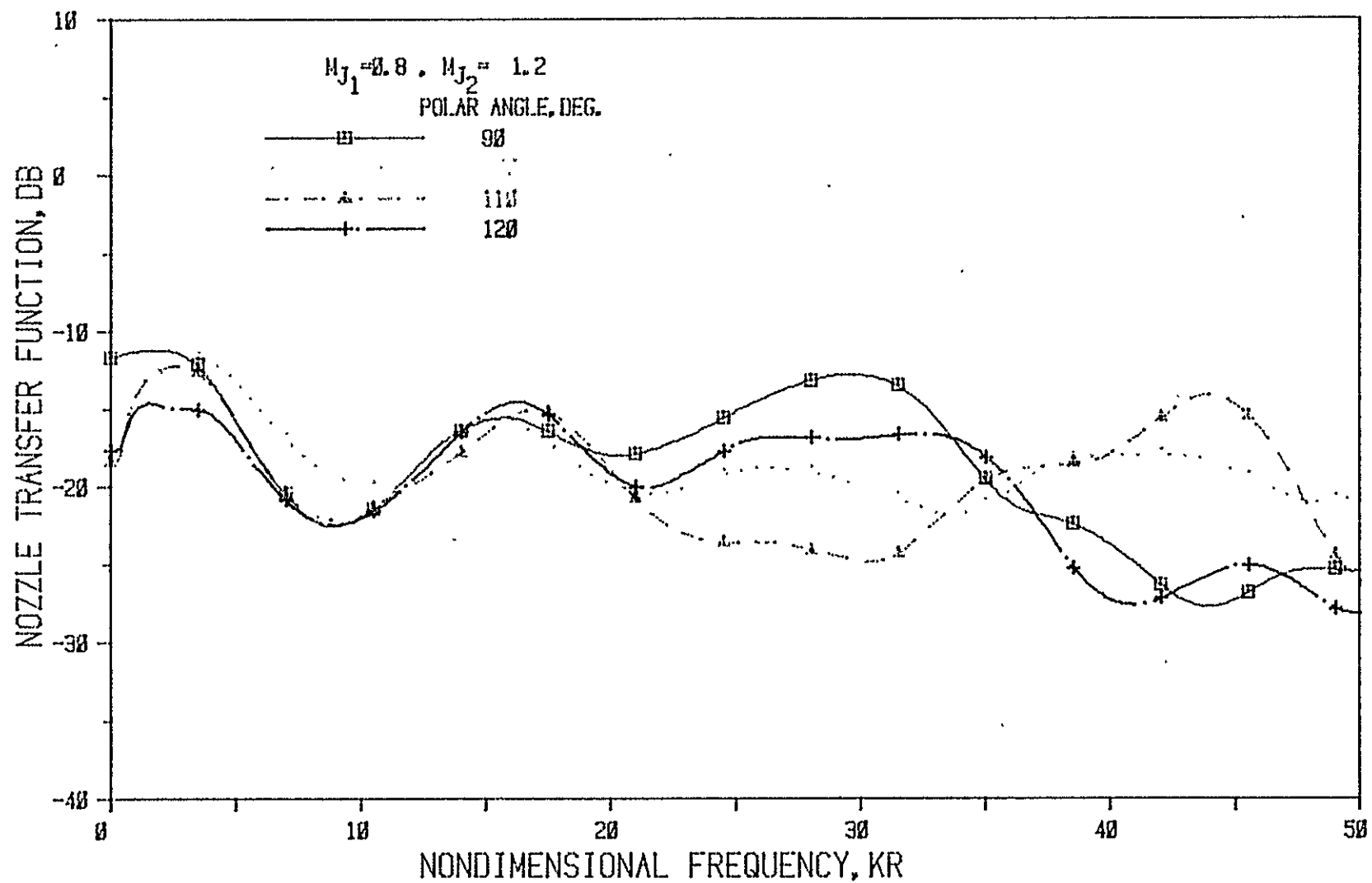


Figure 4 (b) Nozzle N1 ( $L/h = 1$ , Convergence Angle = 20 Deg.); Source At Core

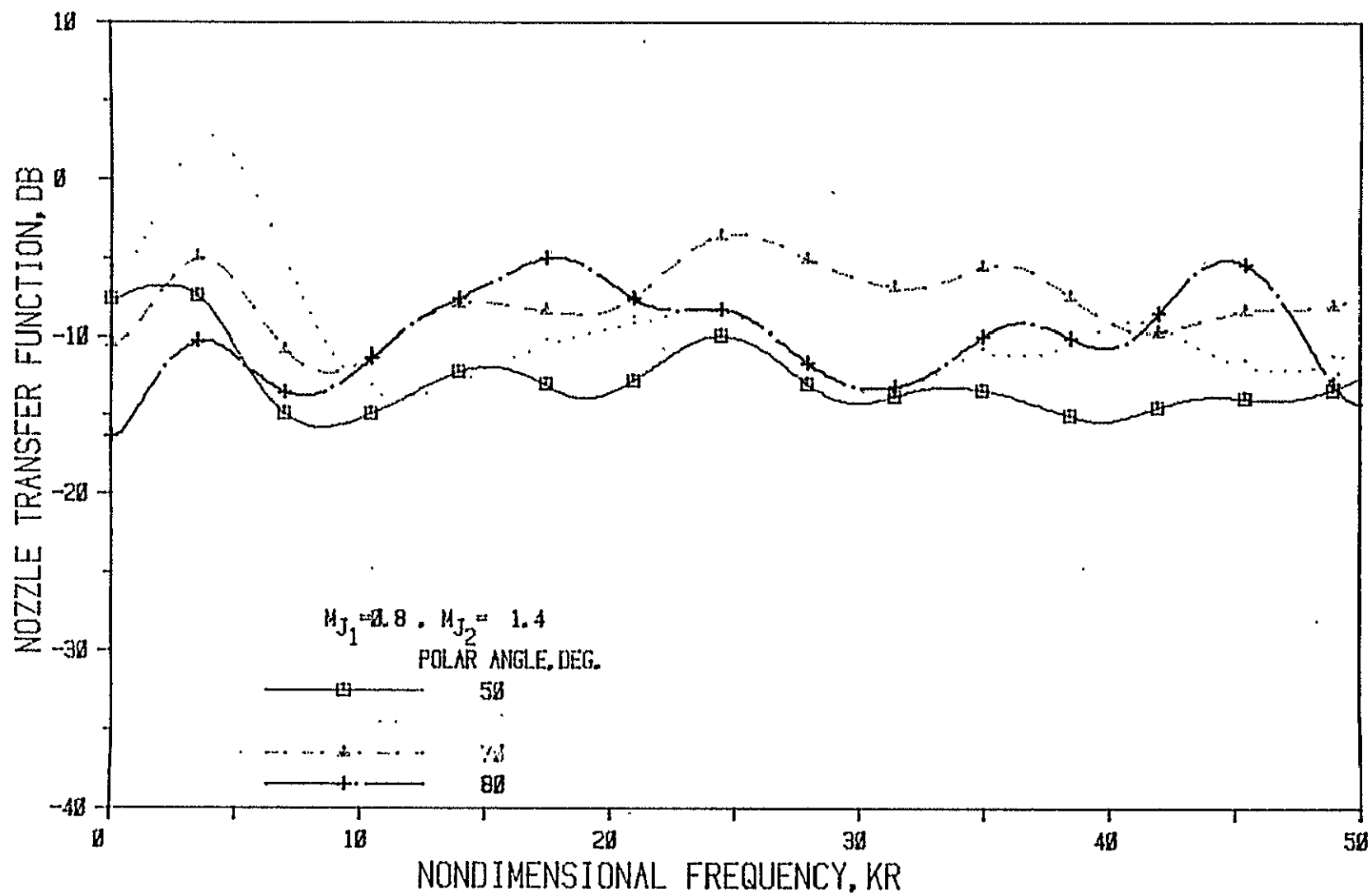


Figure 5(a) Nozzle N 1 (  $L/h = 1$  , Convergence Angle = 20 Deg. ); Source At Core

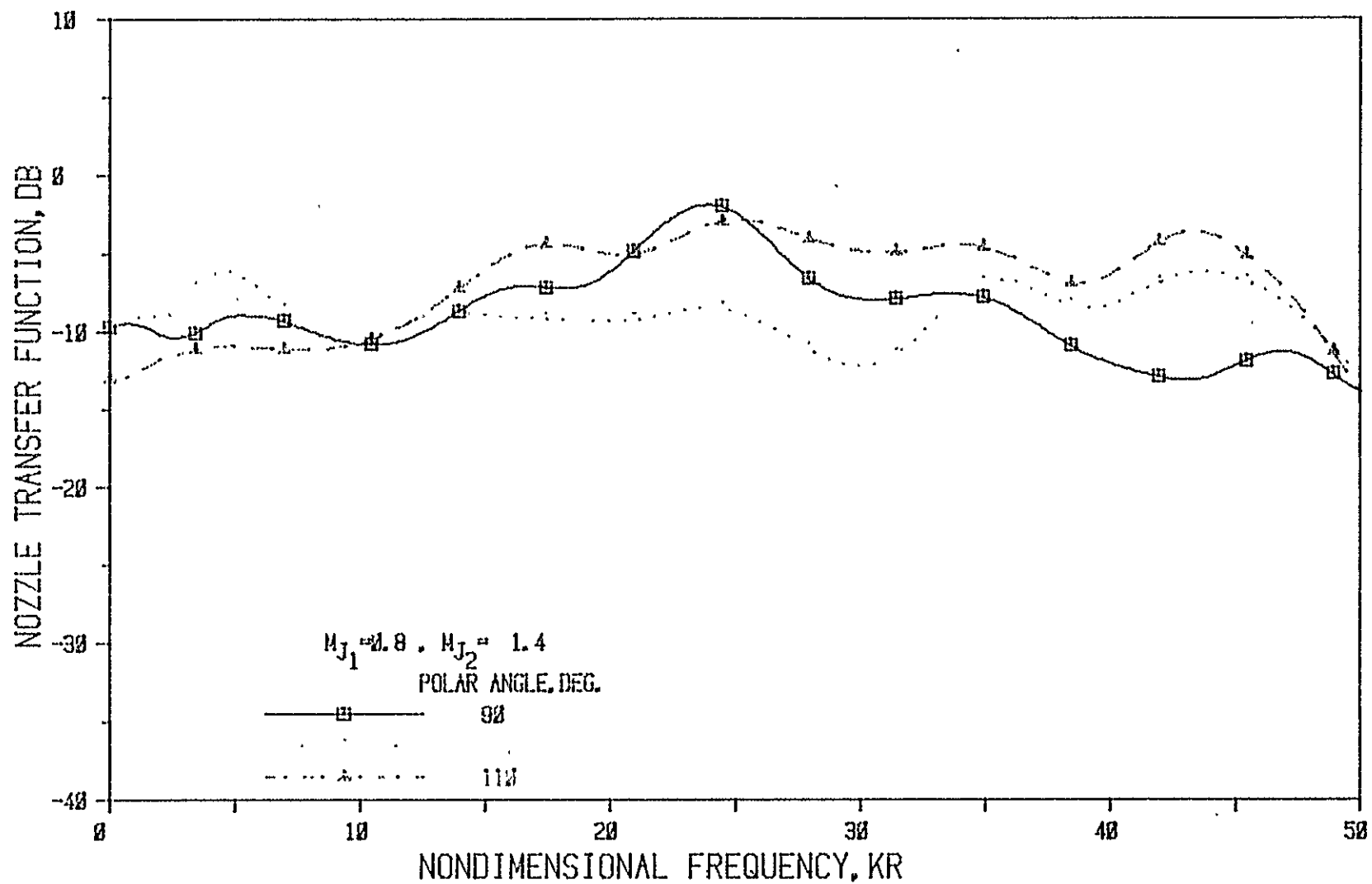


Figure 5(b) Nozzle N 1 (  $L/h = 1$ , Convergence Angle = 20 Deg.); Source At Core



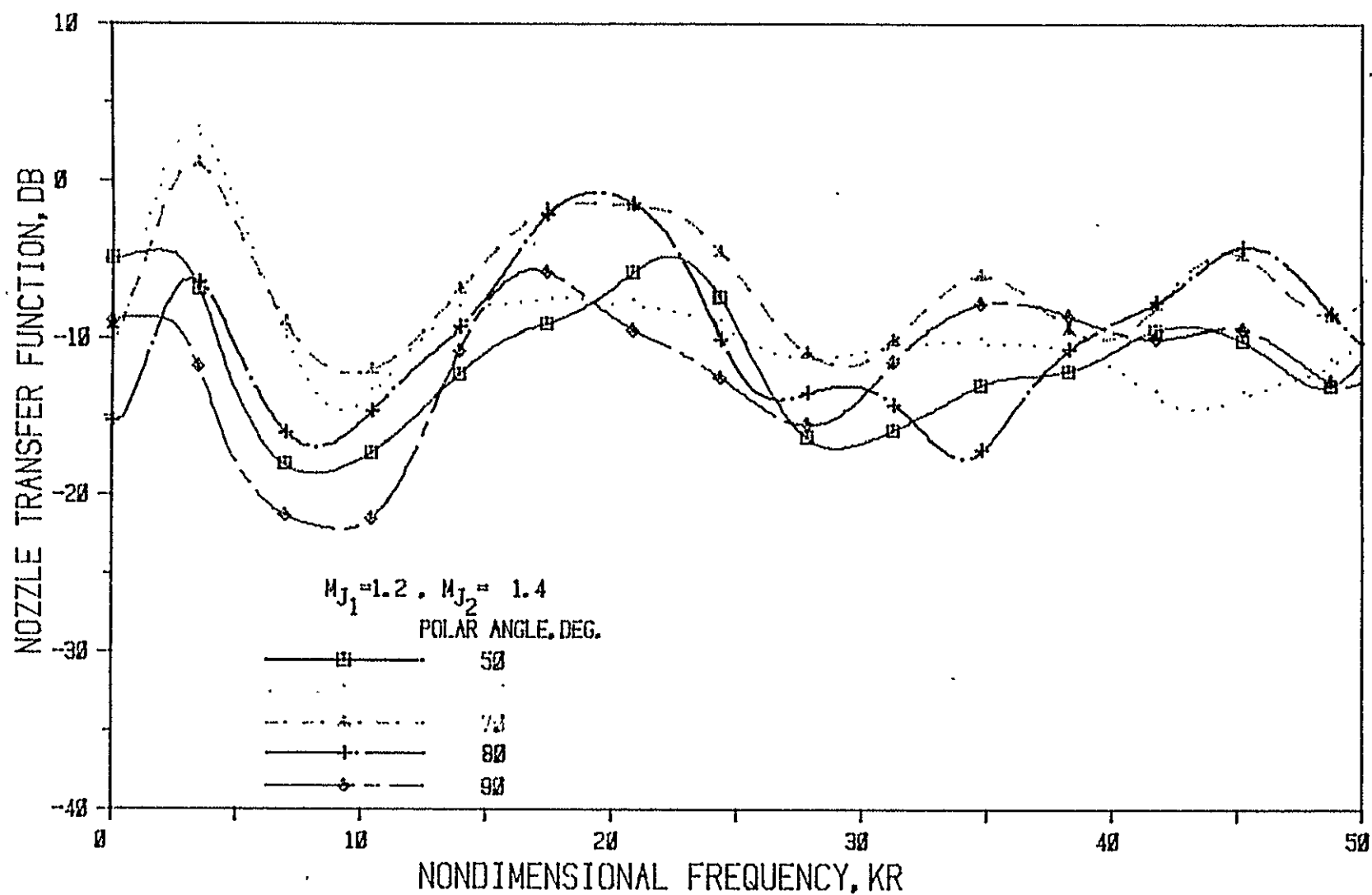


Figure 6 Nozzle N1 ( $L/h = 1$ , Convergence Angle = 20 Deg.); Source At Core

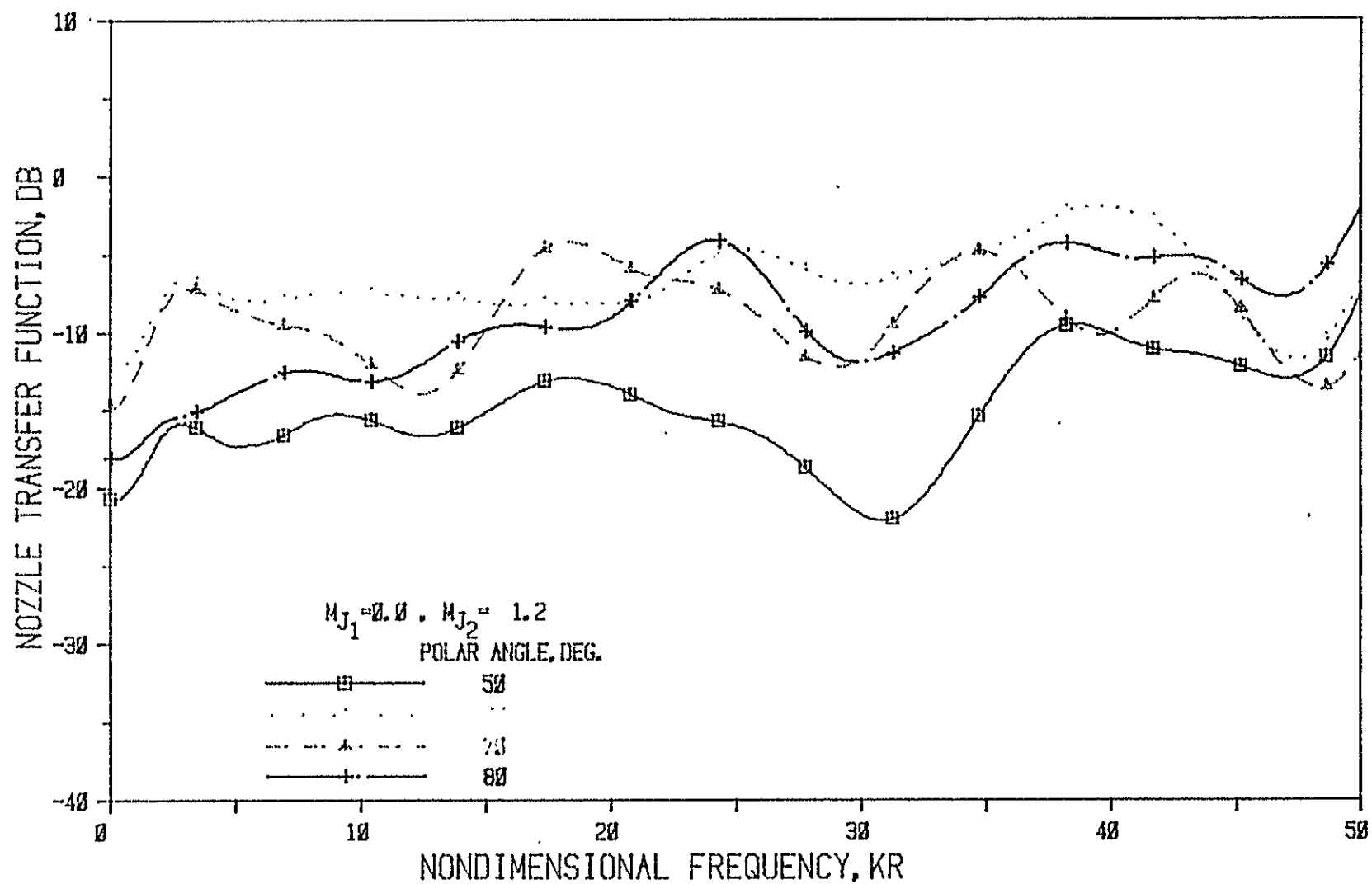


Figure 7(a) Nozzle N1 ( $L/h = 1$ , Convergence Angle = 20 Deg.); Source At Core

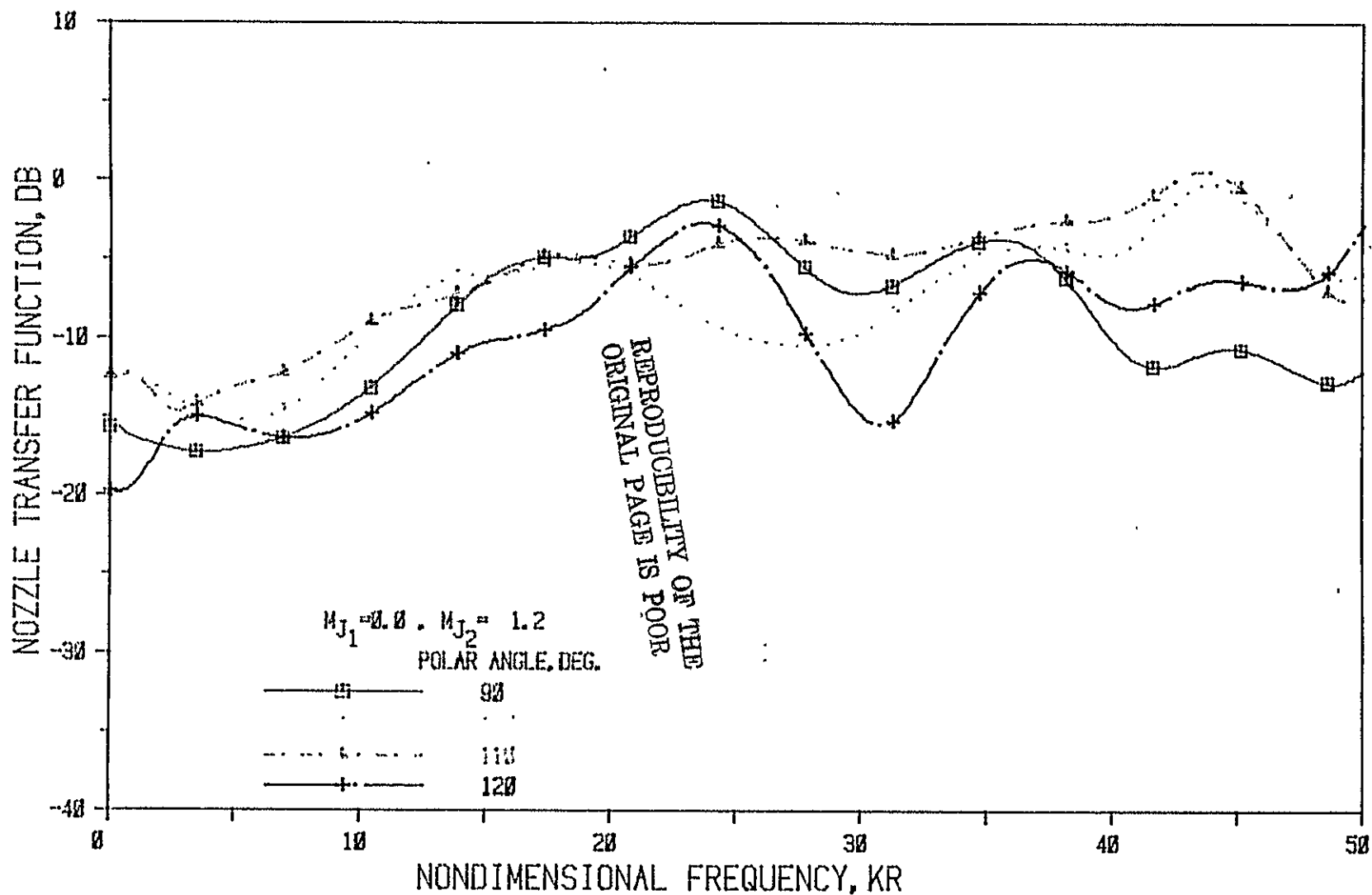


Figure 7 (b) Nozzle N1 ( $L/h = 1$ , Convergence Angle = 20 Deg.); Source At Core

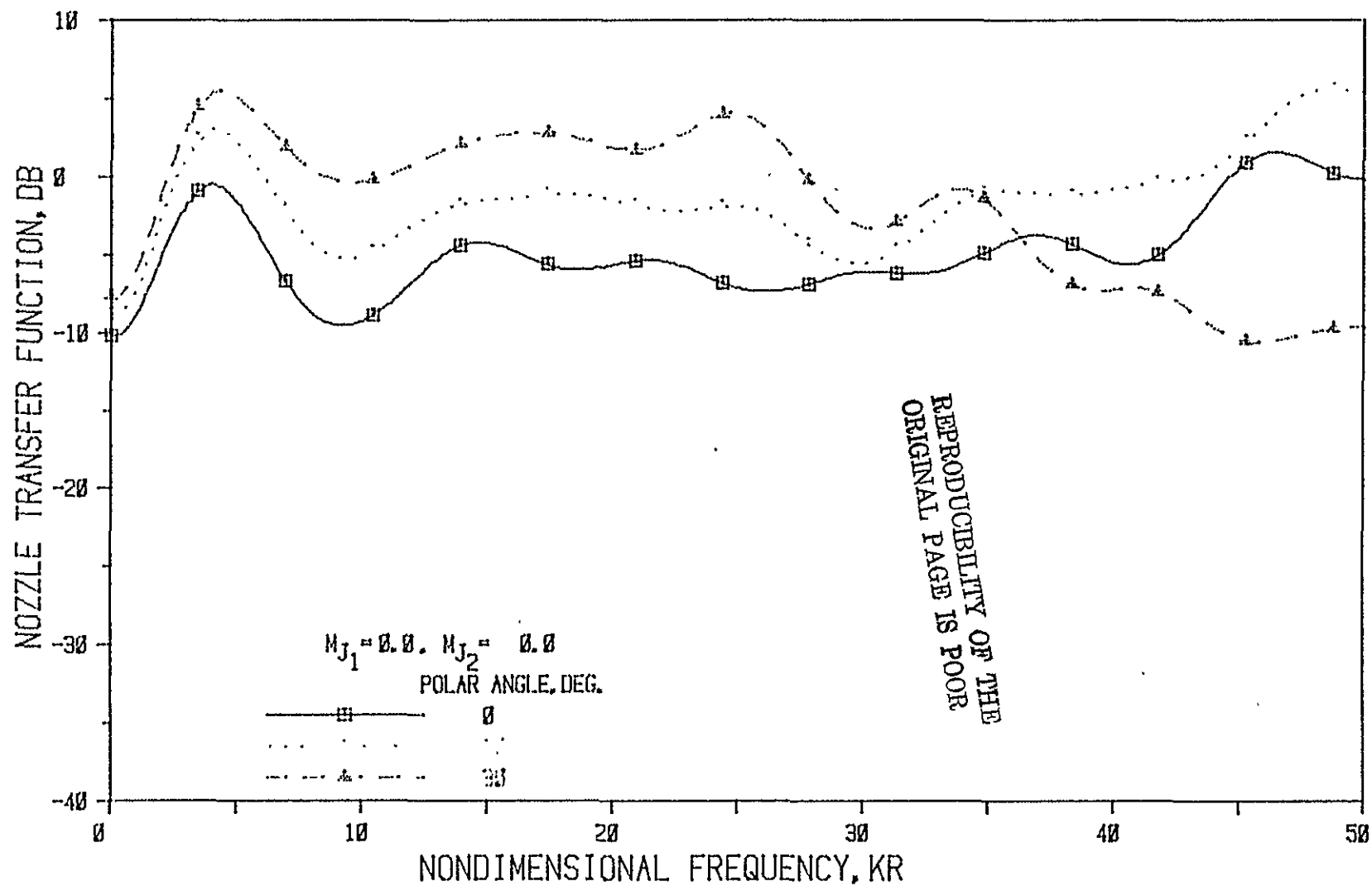


Figure 8(a) Nozzle N 2 (  $L/h = 3$ , Convergence Angle = 20 Deg.); Source At Core

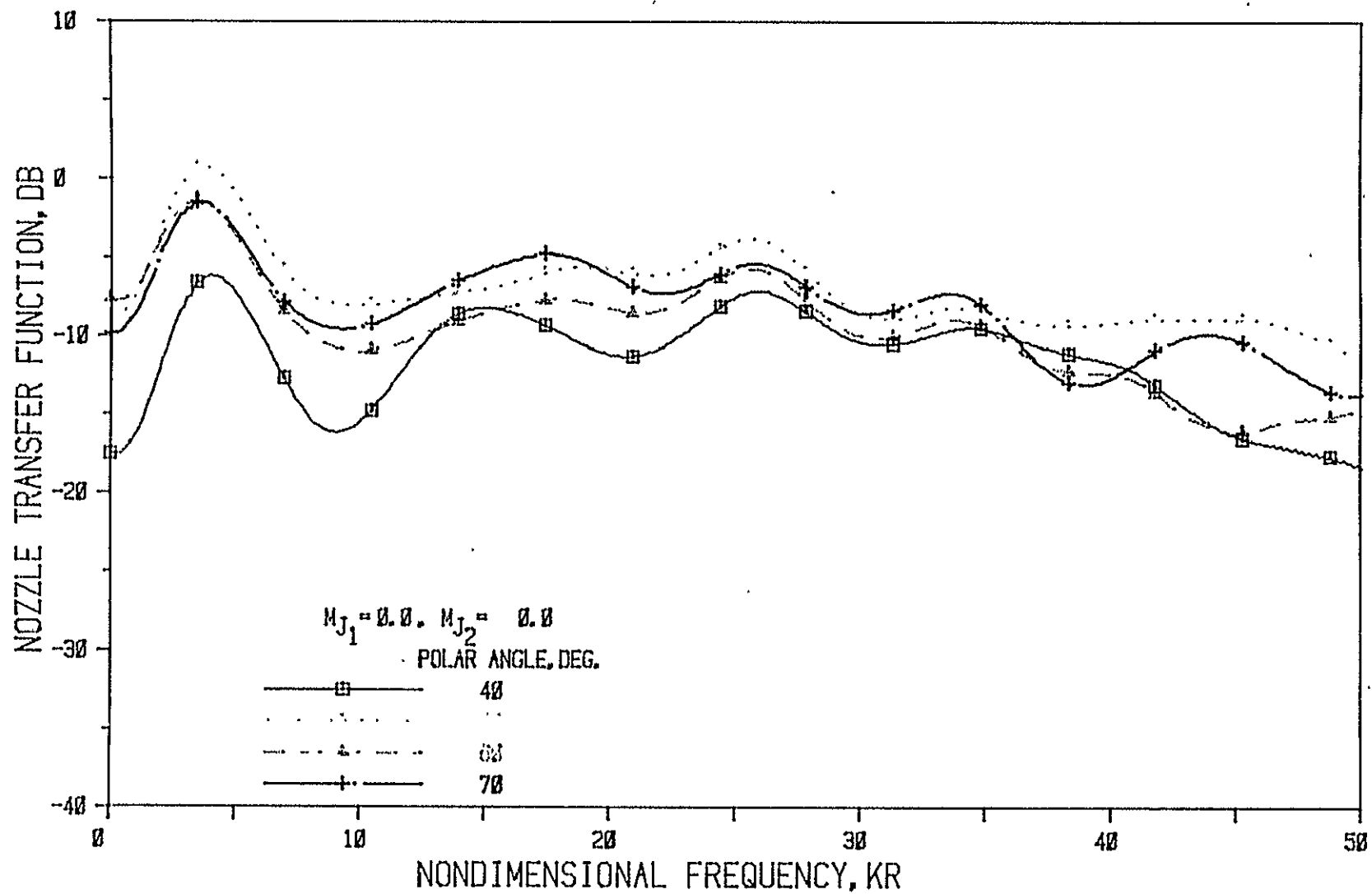


Figure 8 (b) Nozzle N 2 (  $L/h = 3$ , Convergence Angle = 20 Deg.); Source At Core

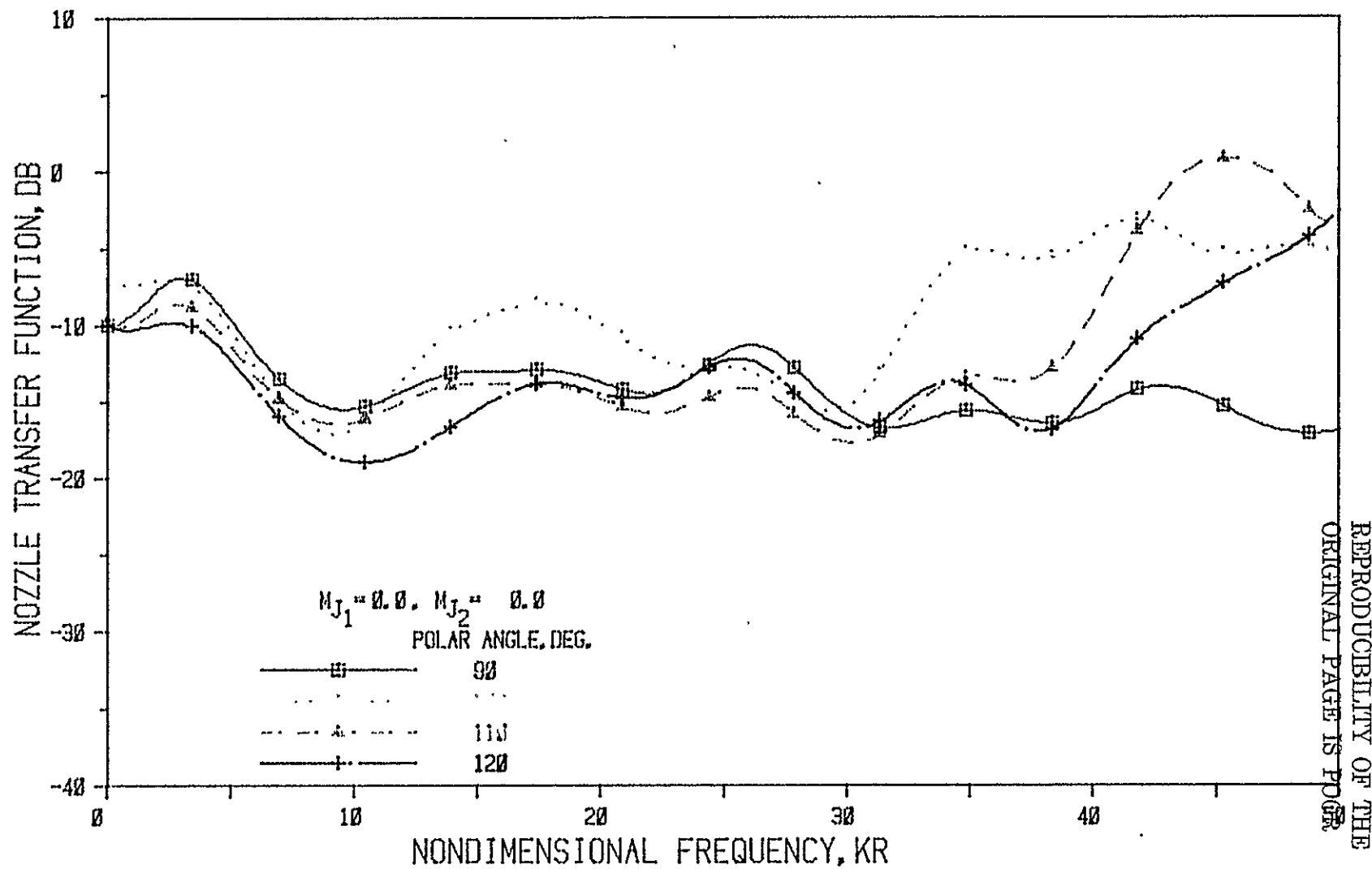


Figure 8(c) Nozzle N 2 (  $L/h = 3$ , Convergence Angle = 20 Deg.); Source At Core

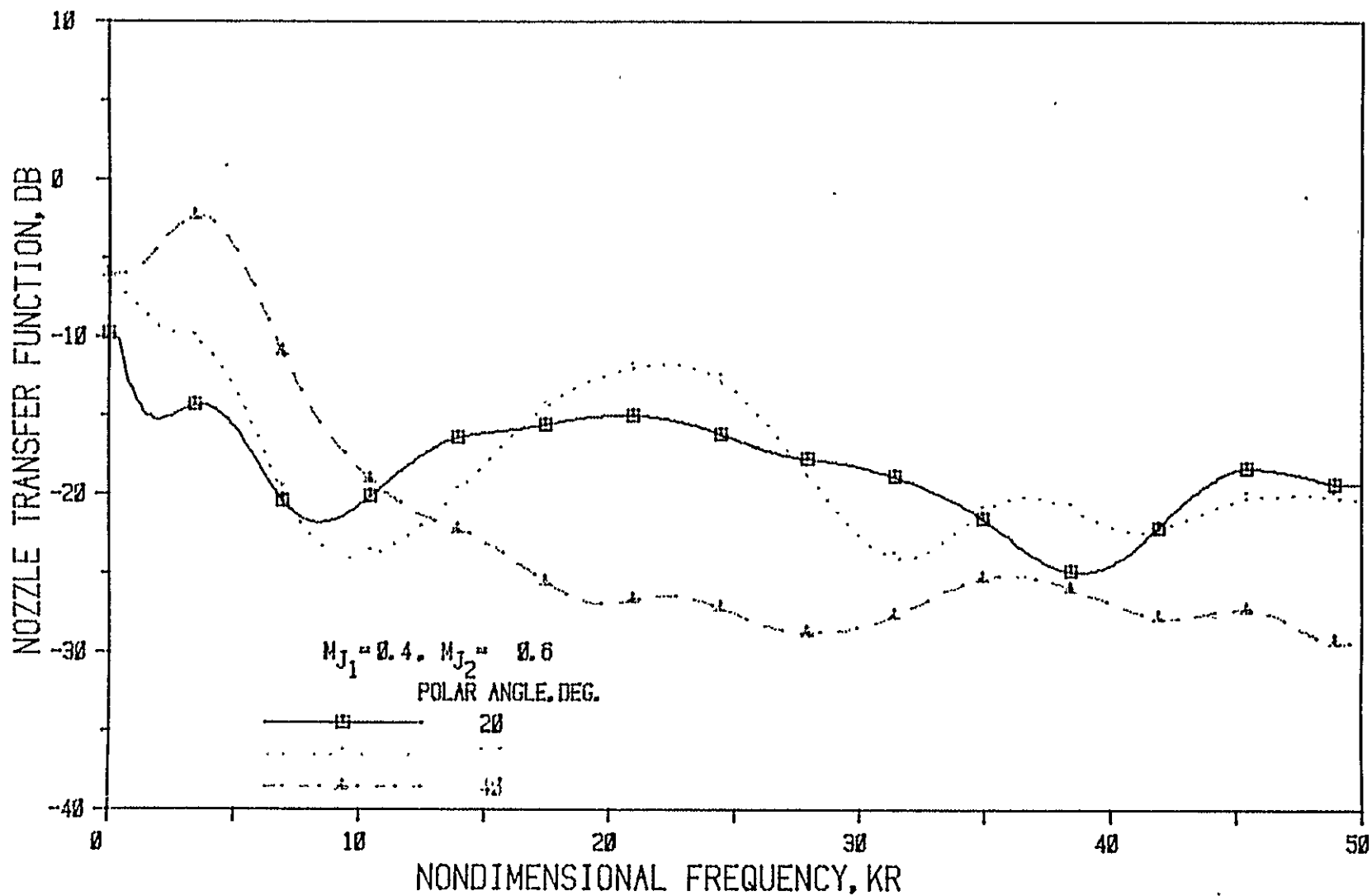


Figure 9(a) Nozzle N 2 ( $L/h = 3$ , Convergence Angle = 20 Deg.); Source At Core

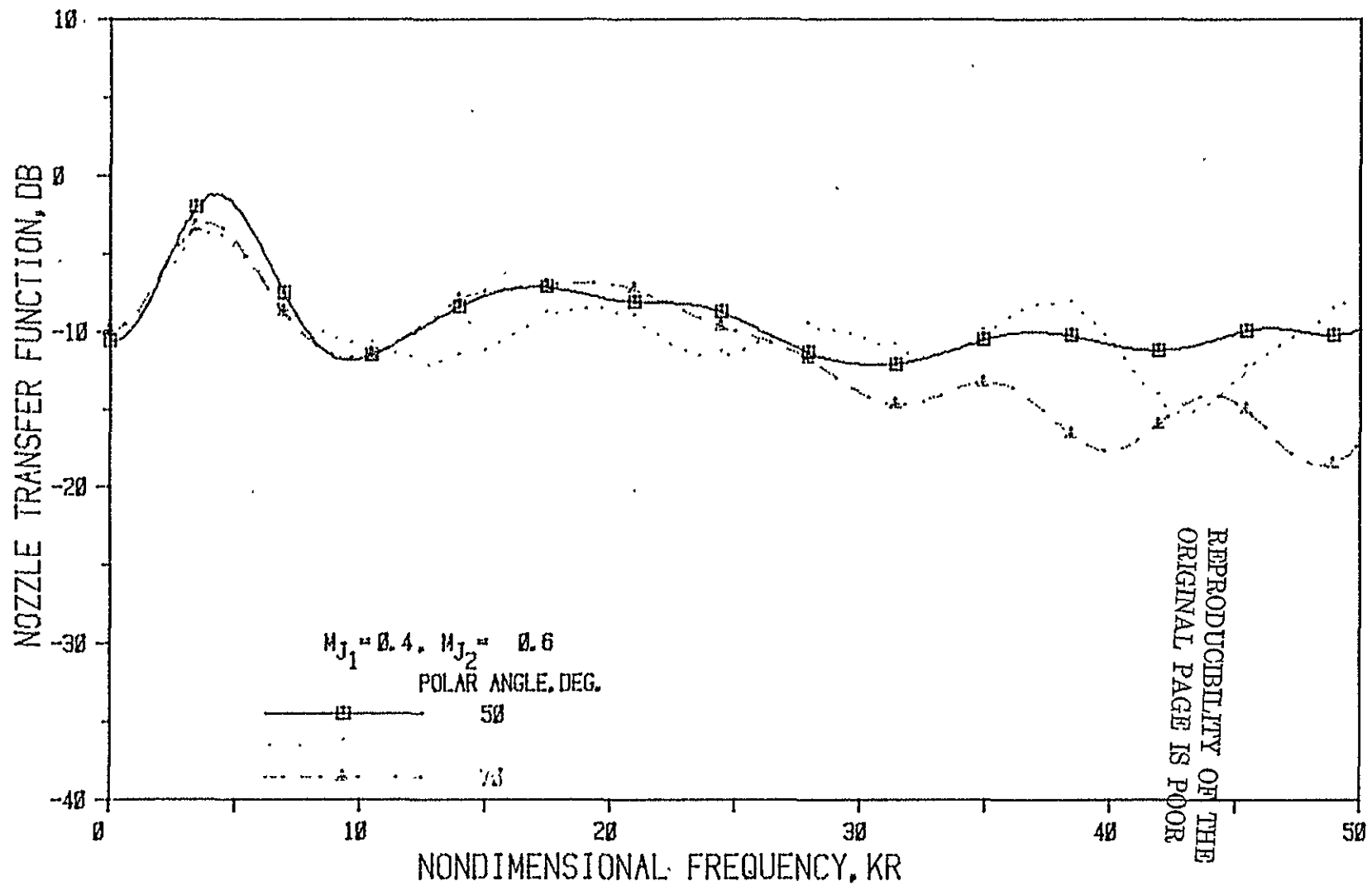


Figure 9 (b) Nozzle N 2 (  $L/h = 3$ , Convergence Angle = 20 Deg.); Source At Core



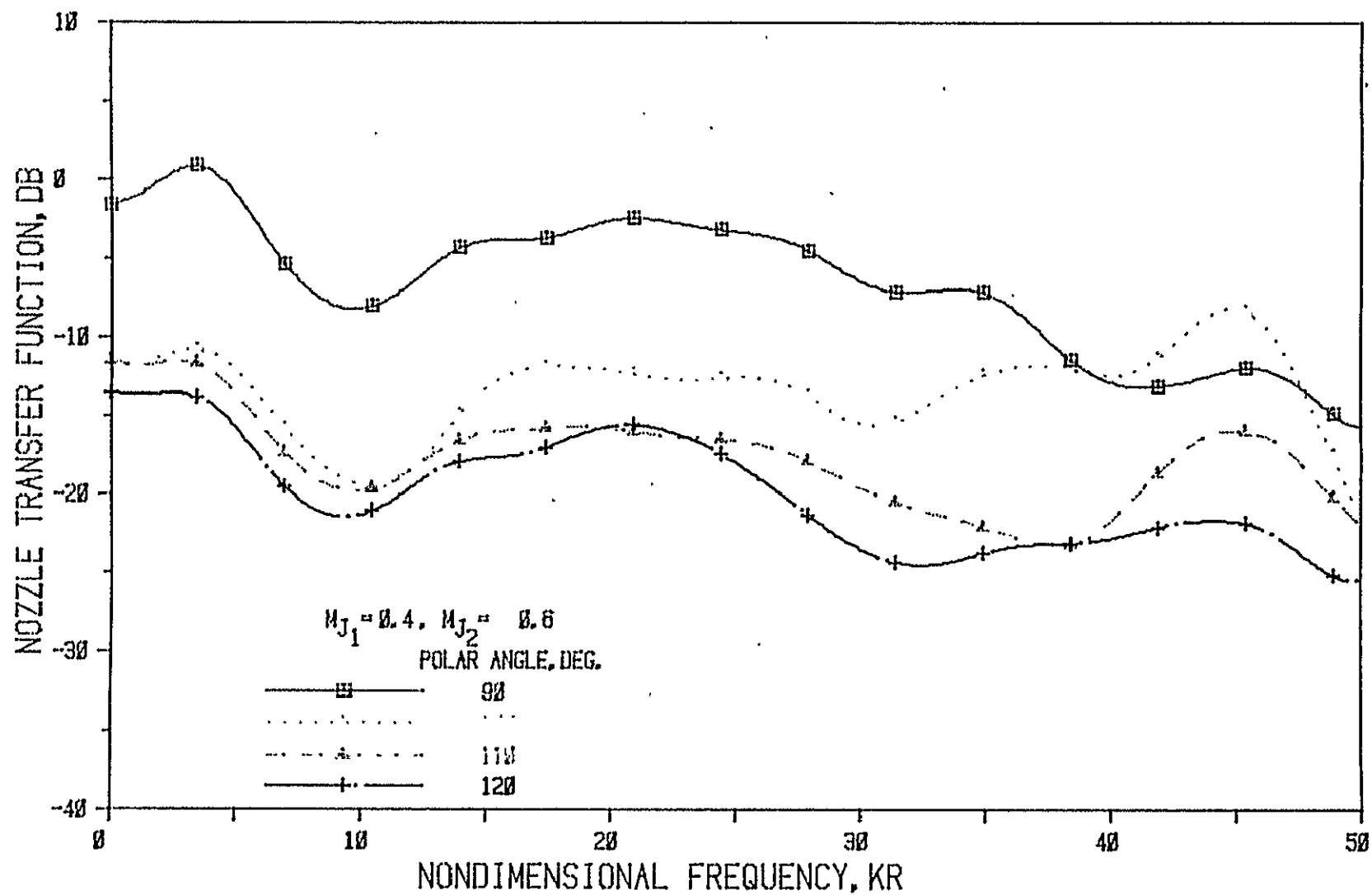


Figure 9(c) Nozzle N 2 ( $L/h = 3$ , Convergence Angle = 20 Deg.); Source At Core

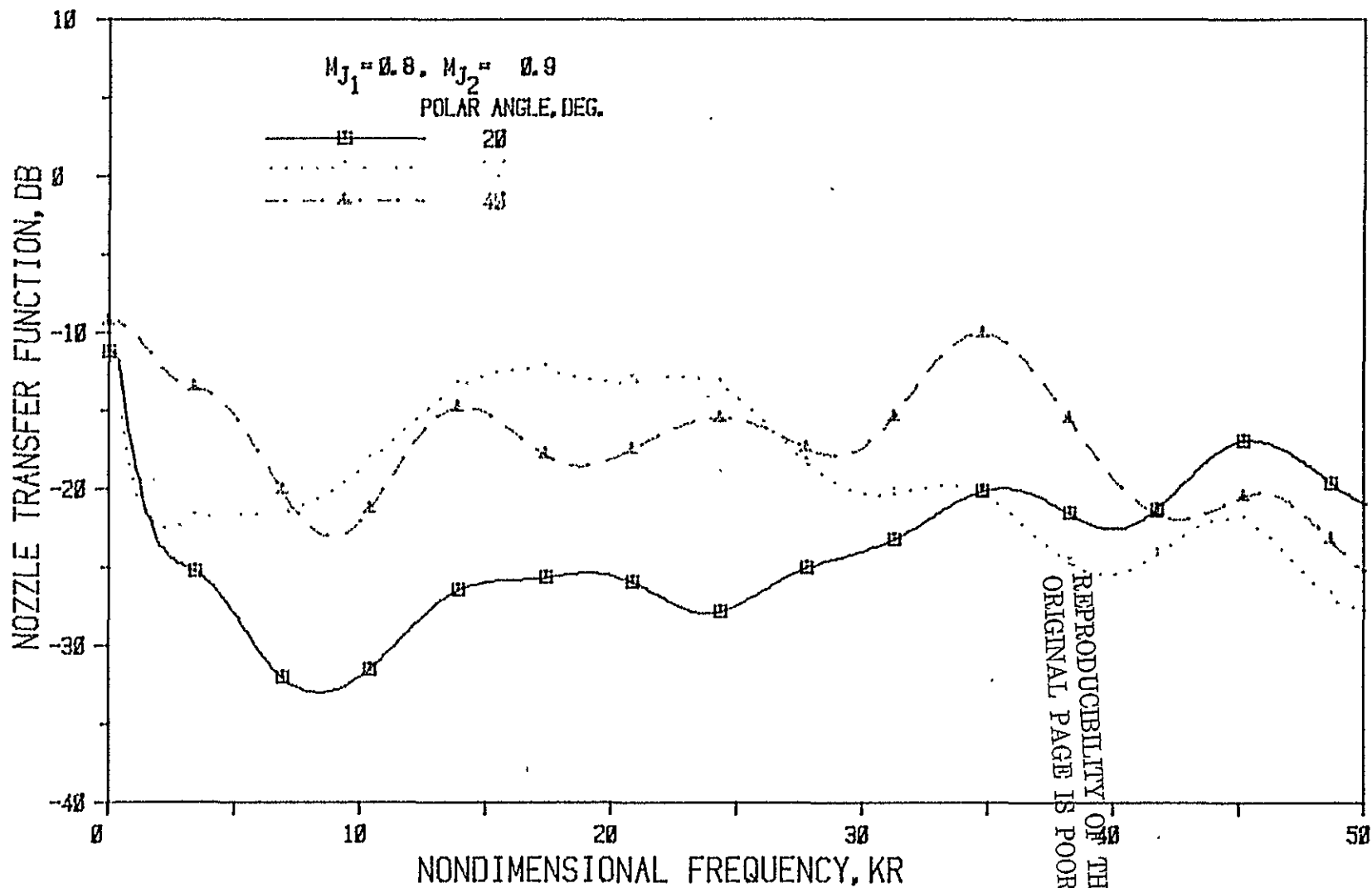


Figure 10(a) Nozzle N 2 (  $L/h = 3$ , Convergence Angle = 20 Deg.); Source At Core

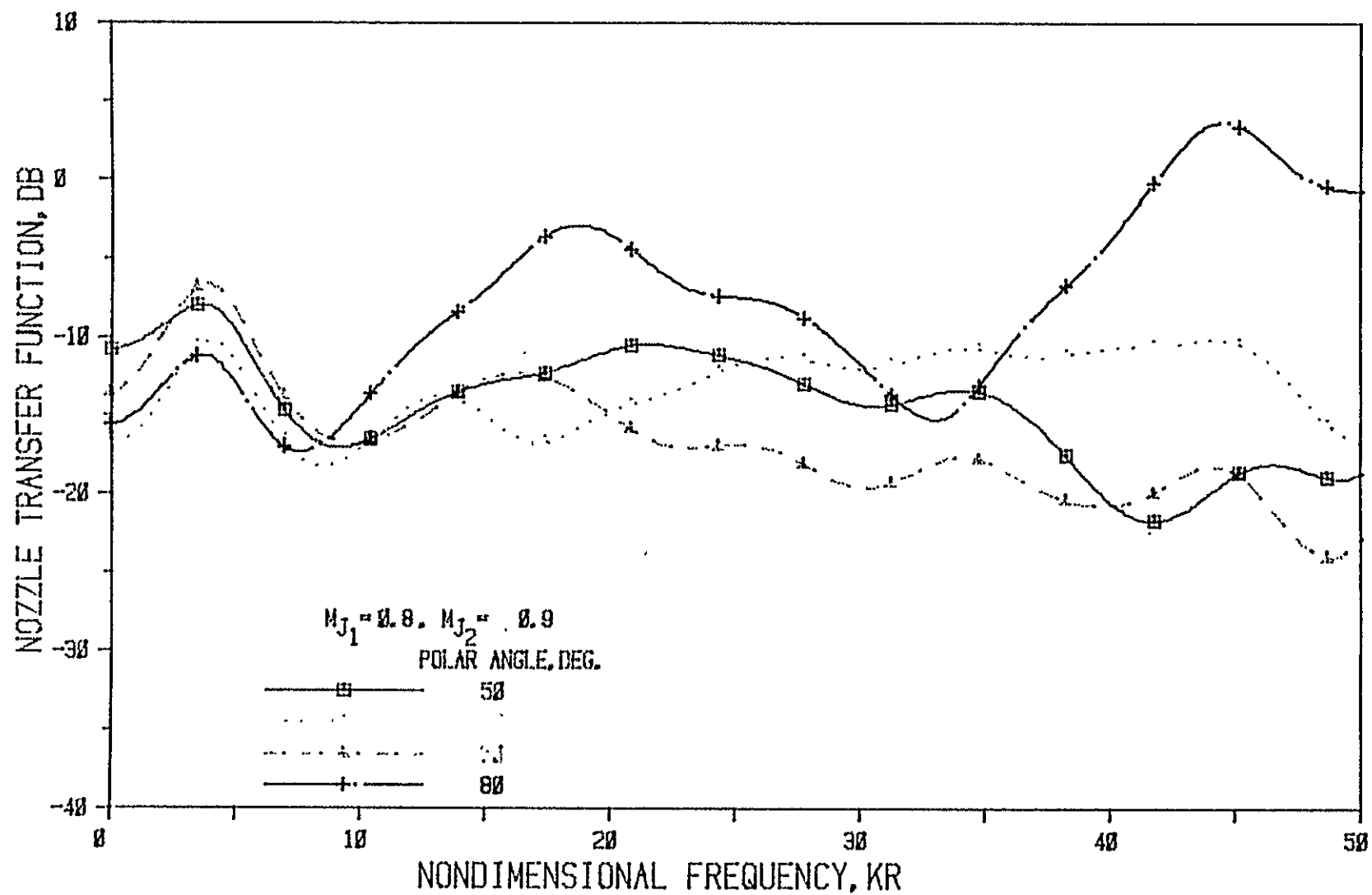


Figure 10(b) Nozzle N 2 ( $L/h = 3$ , Convergence Angle = 20 Deg.); Source At Core

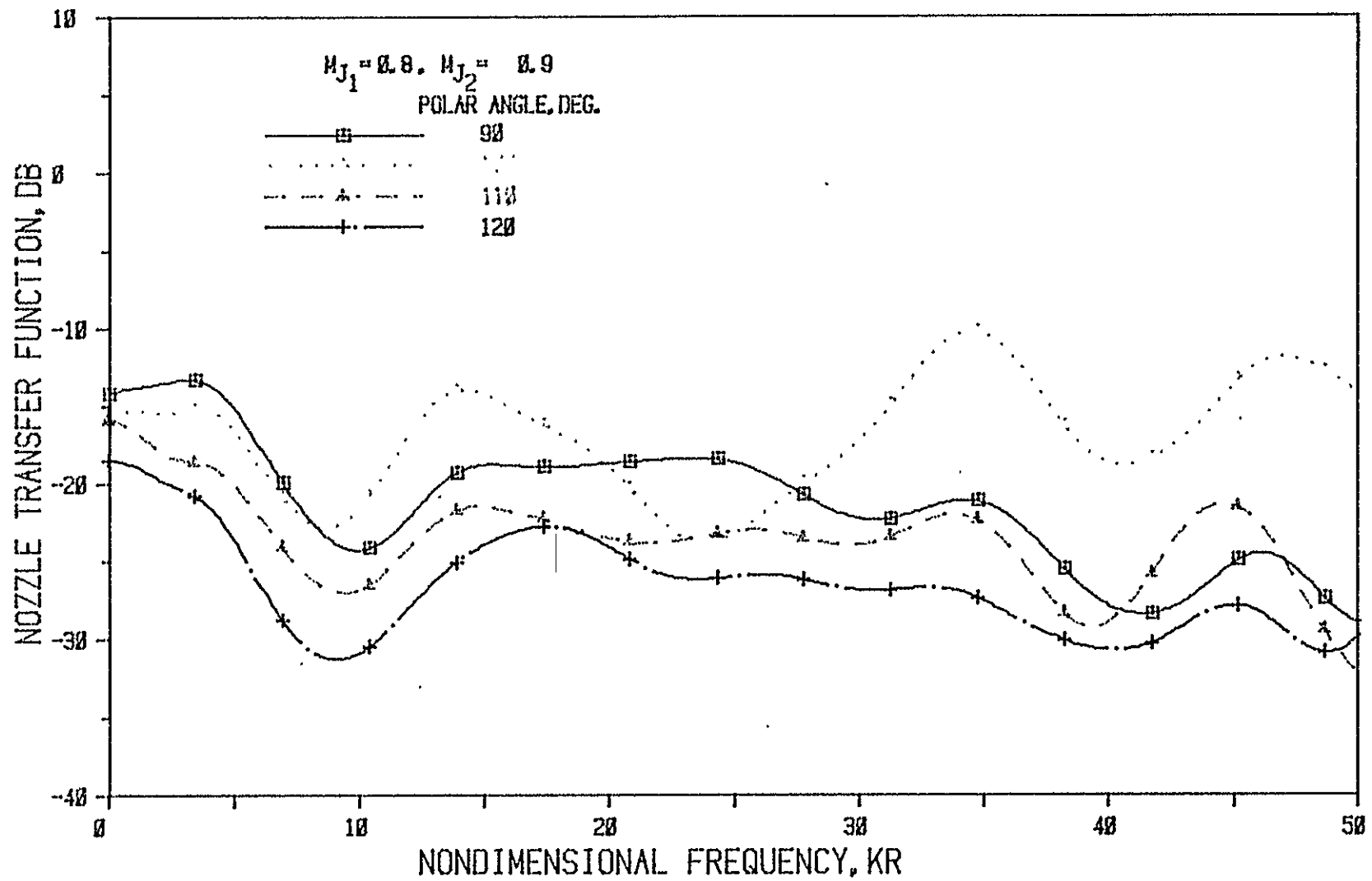


Figure 10(c) Nozzle N 2 (  $L/h = 3$ , Convergence Angle = 20 Deg. ); Source At Core

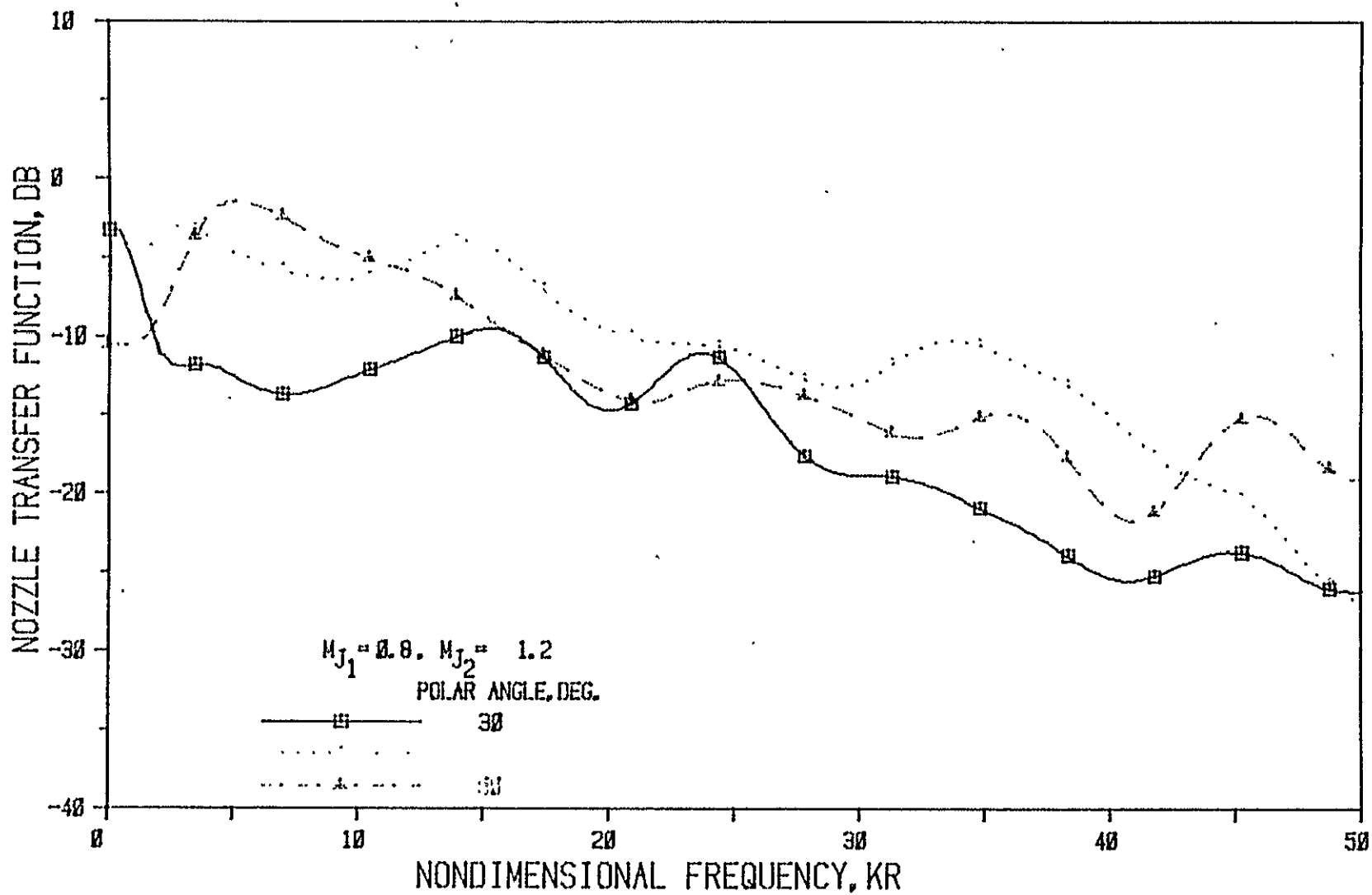


Figure 11(a) Nozzle N 2 ( $L/h = 3$ , Convergence Angle = 20 Deg.); Source At Core

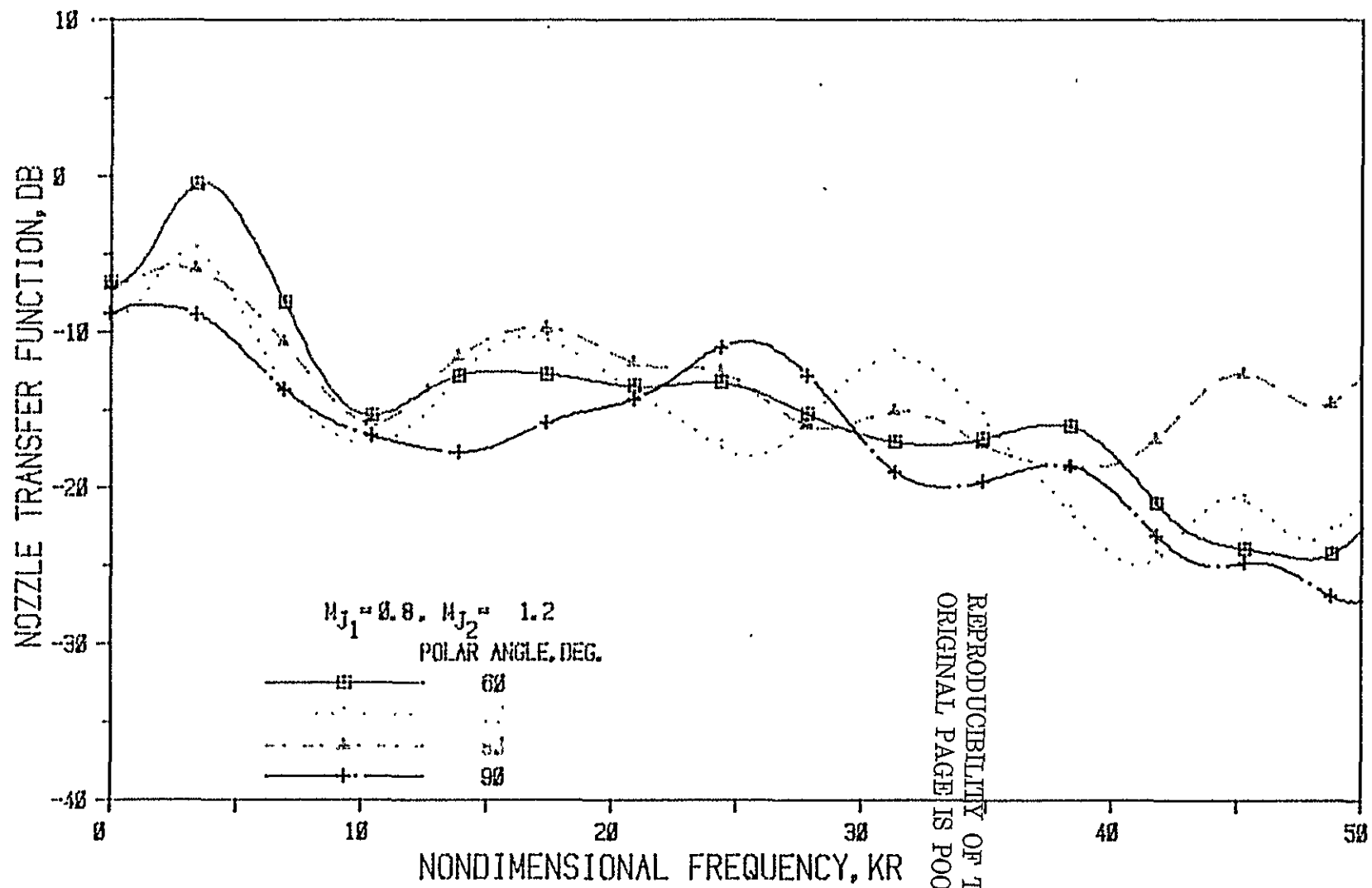


Figure 11(b) Nozzle N 2 (  $L/h = 3$ , Convergence Angle = 60 Deg. ); Source At Core

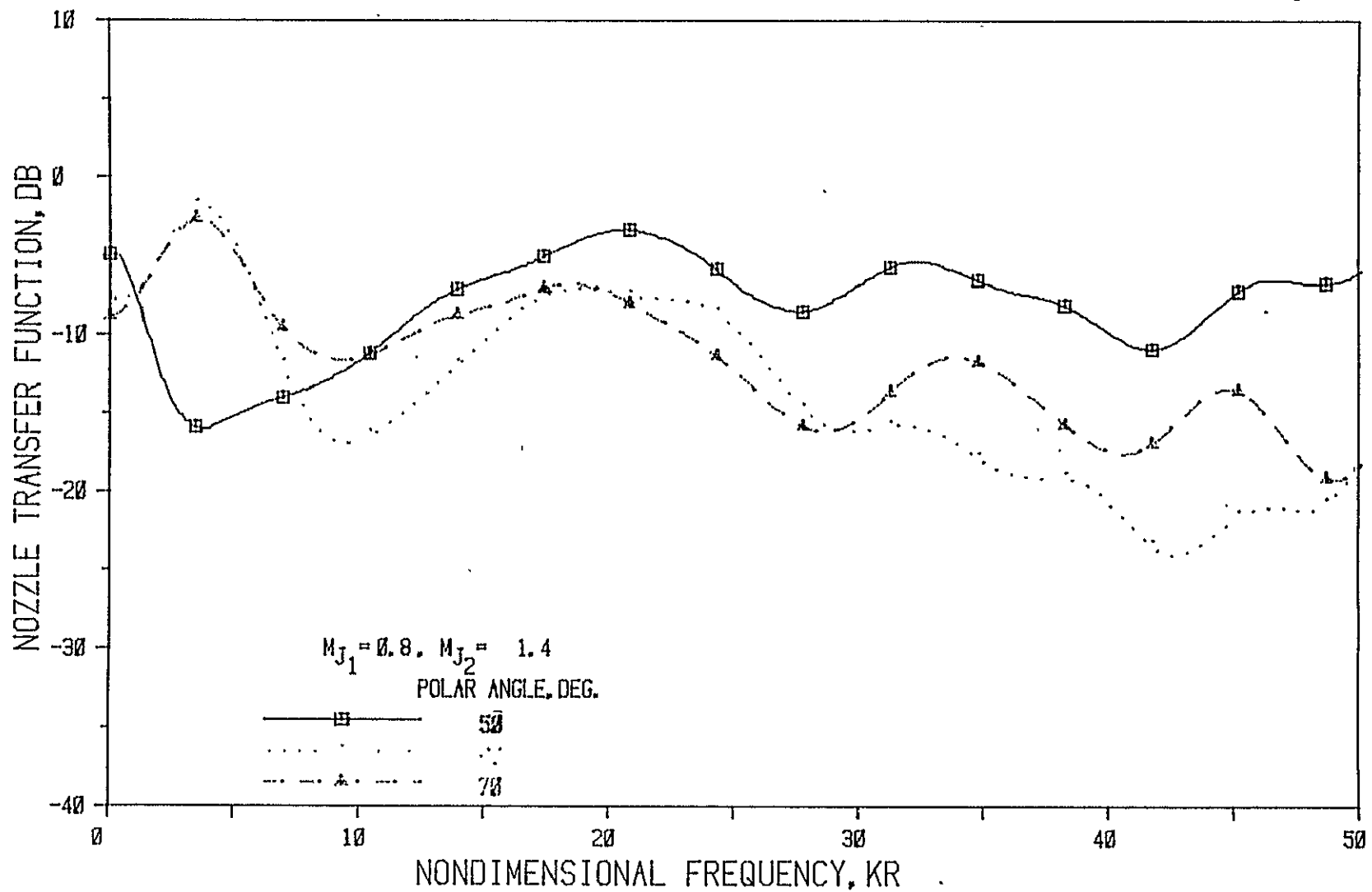


Figure 12(a) Nozzle N 2 ( $L/h = 3$ , Convergence Angle = 20 Deg.); Source At Core

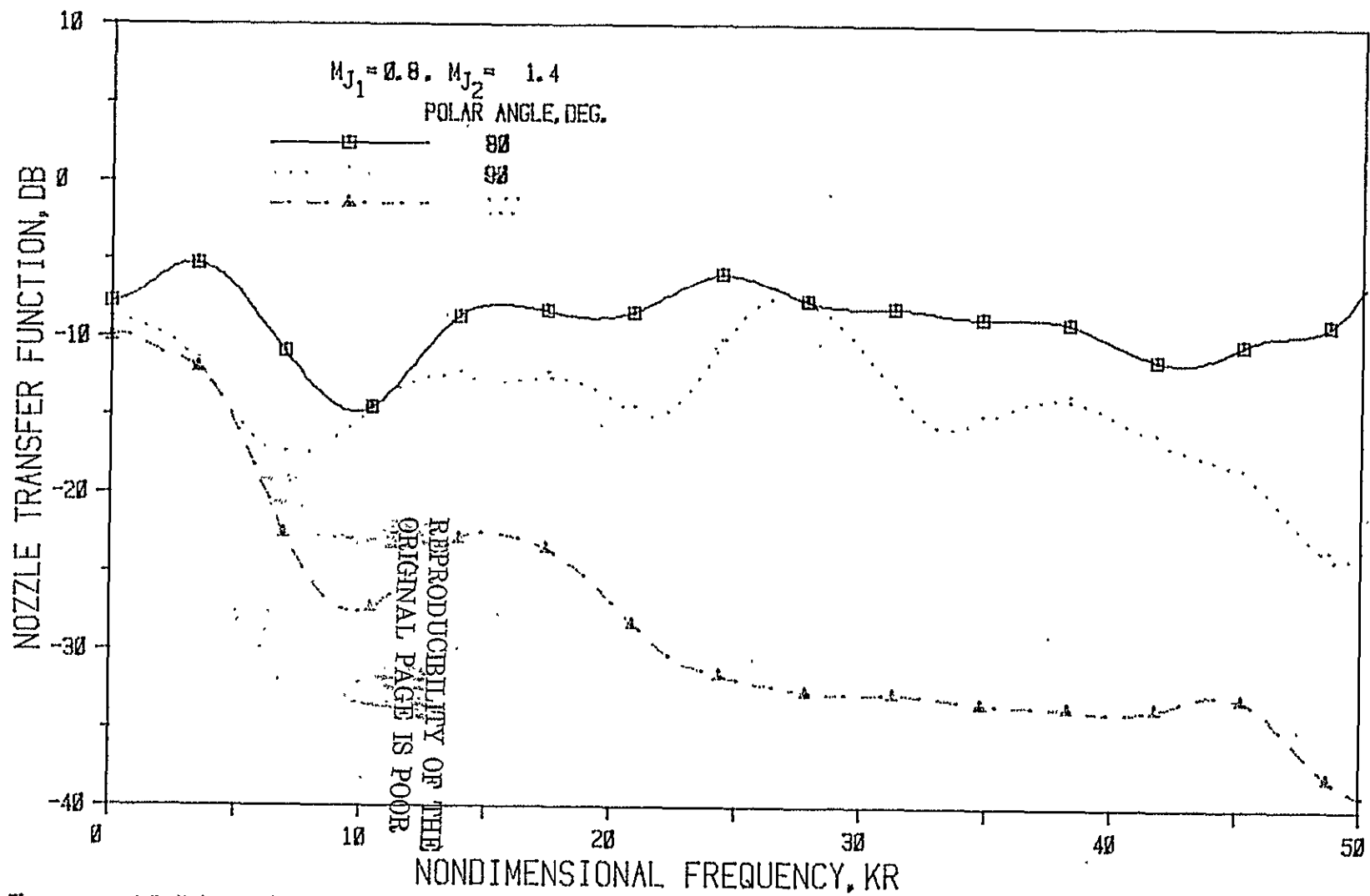


Figure 12(b) Nozzle N 2 (  $L/h = 3$ , Convergence Angle = 20 Deg.); Source At Core



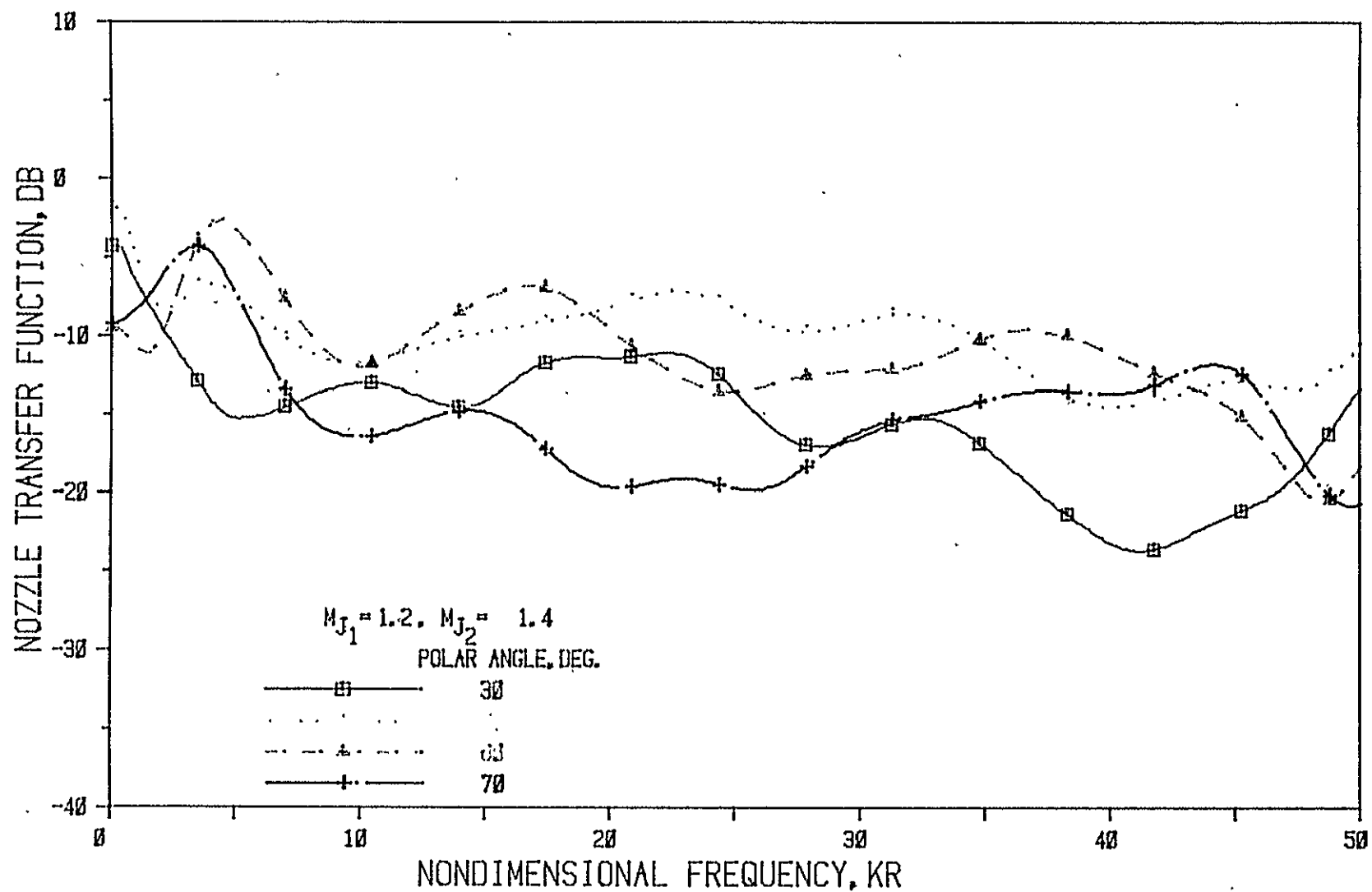


Figure 13(a) Nozzle N 2 ( $L/h = 3$ , Convergence Angle =  $20^\circ$ ); Source At Core

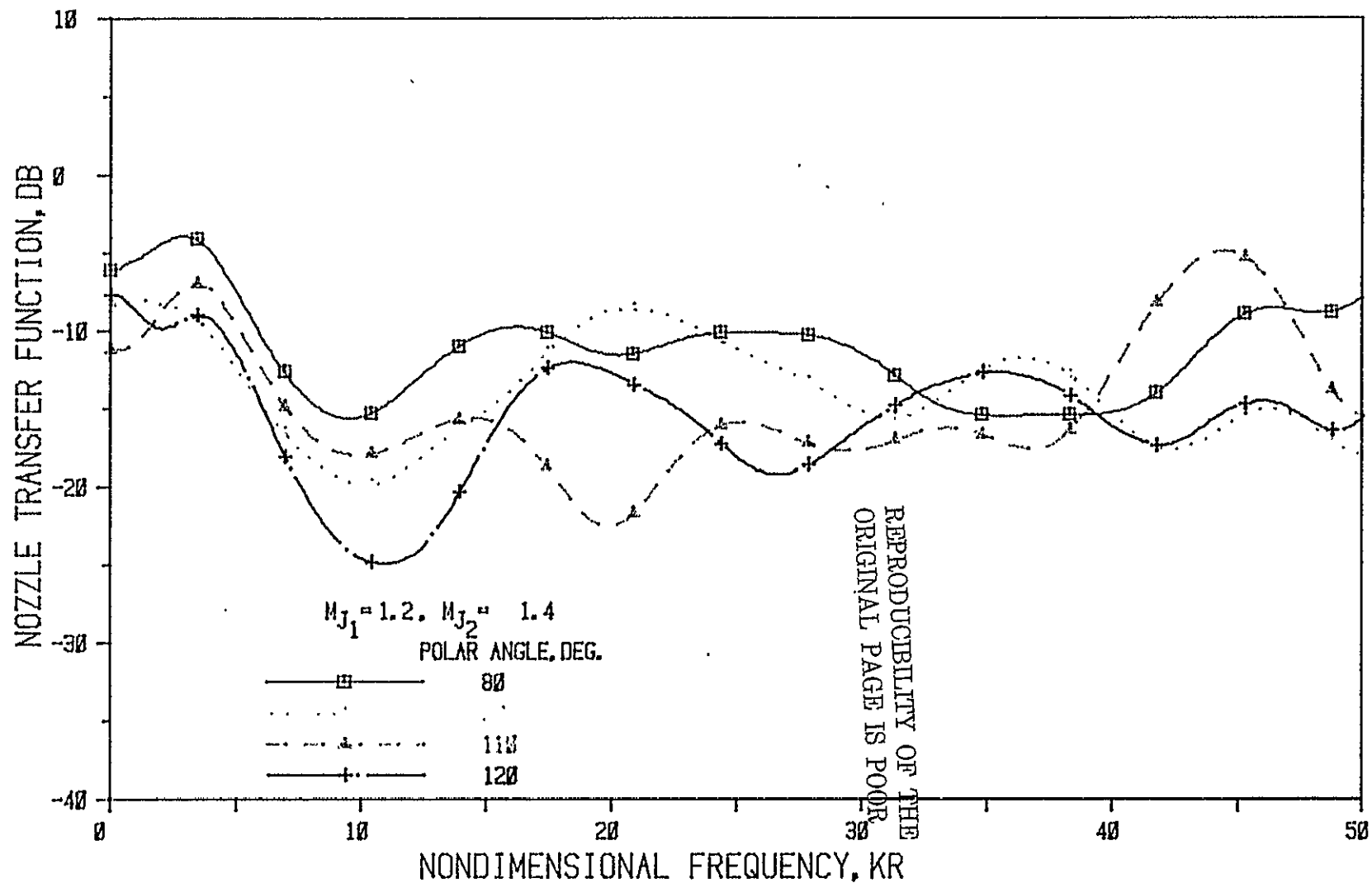


Figure 13(b) Nozzle N 2 (  $L/h = 3$ , Convergence Angle = 20 Deg.); Source At Core

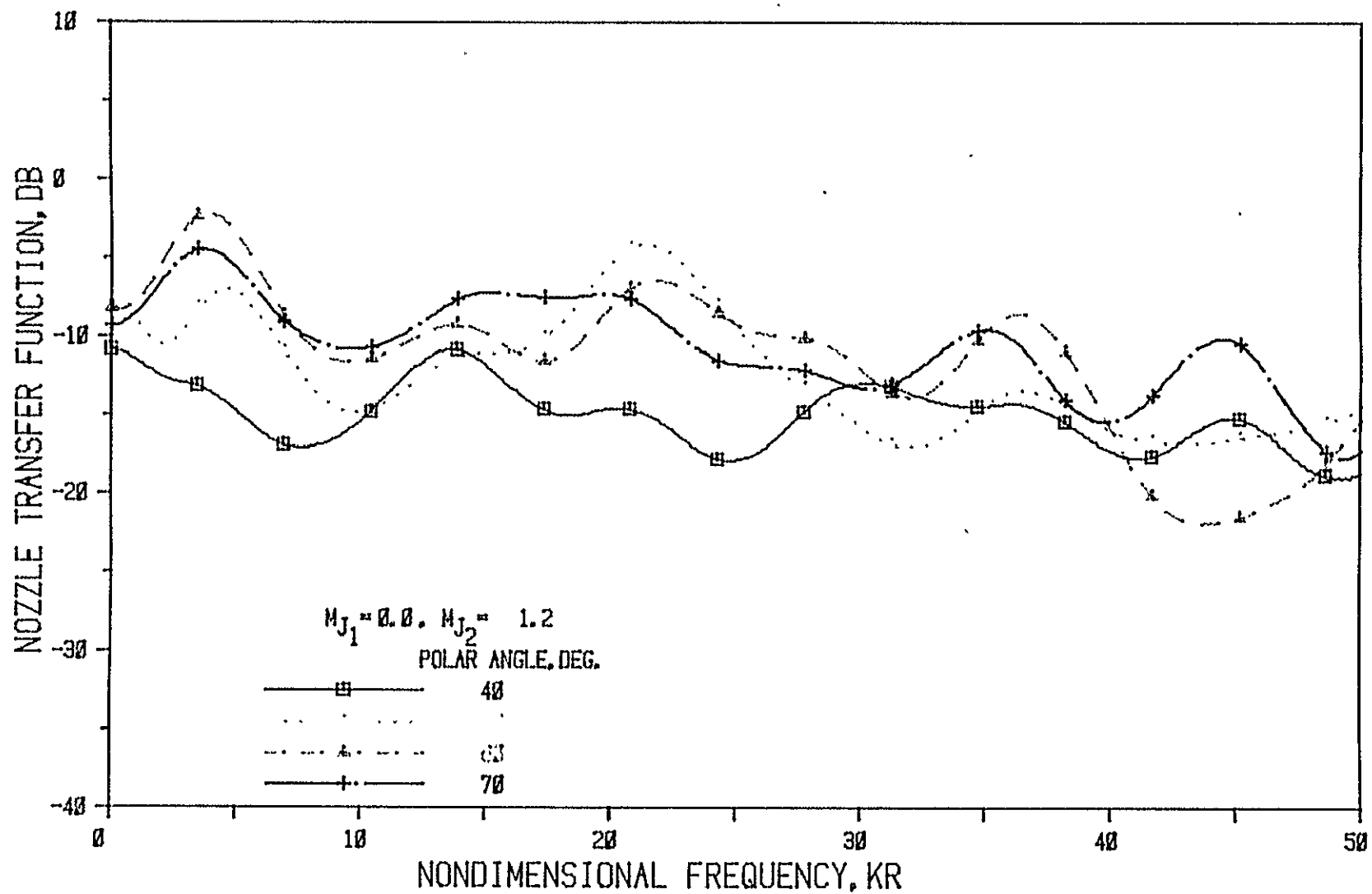


Figure 14(a) Nozzle N 2 (  $L/h = 3$ , Convergence Angle = 20 Deg. ); Source At Core

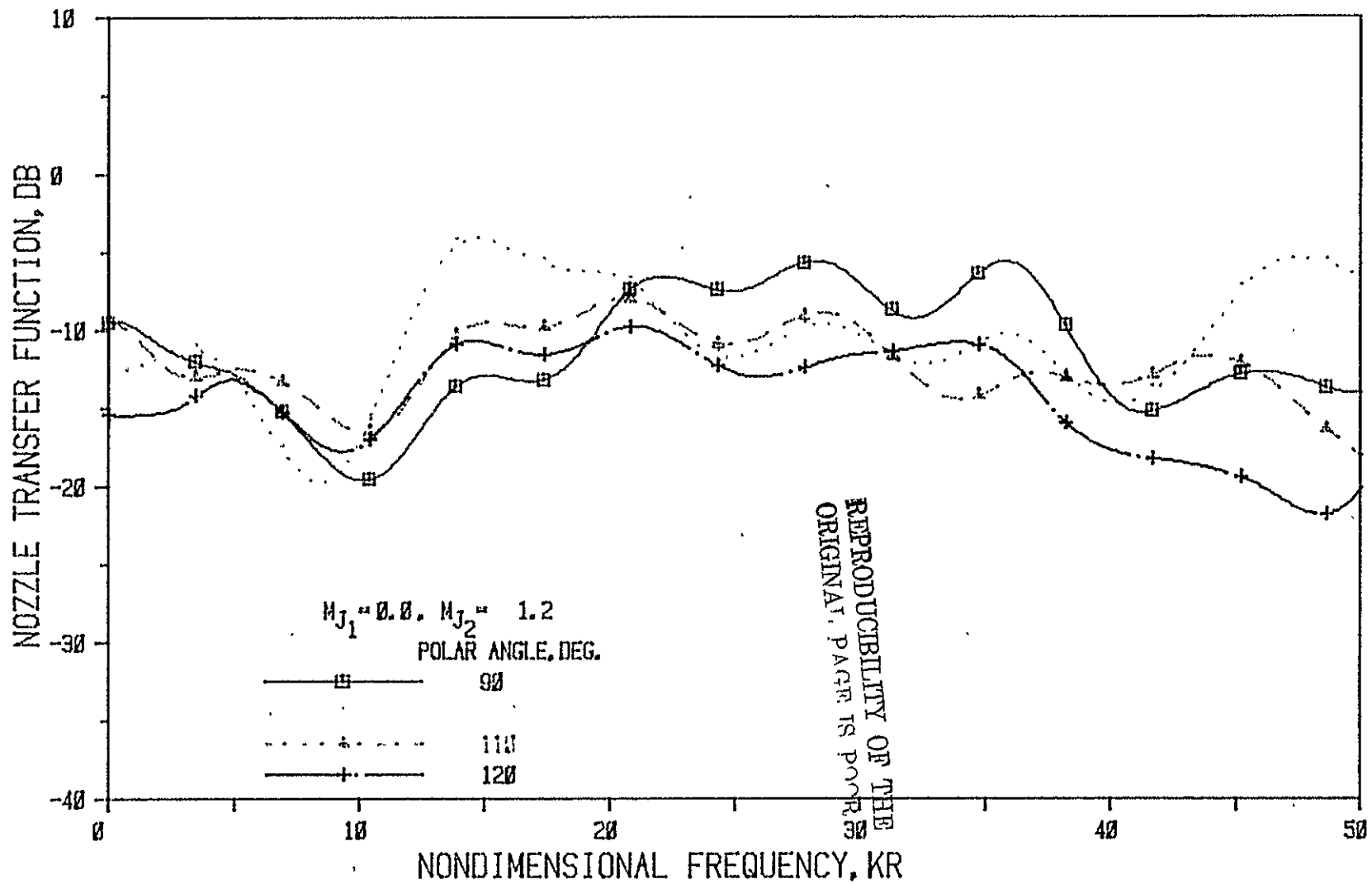


Figure 14(b) Nozzle N 2 (  $L/h = 3$ , Convergence Angle = 20 Deg. ); Source At Core

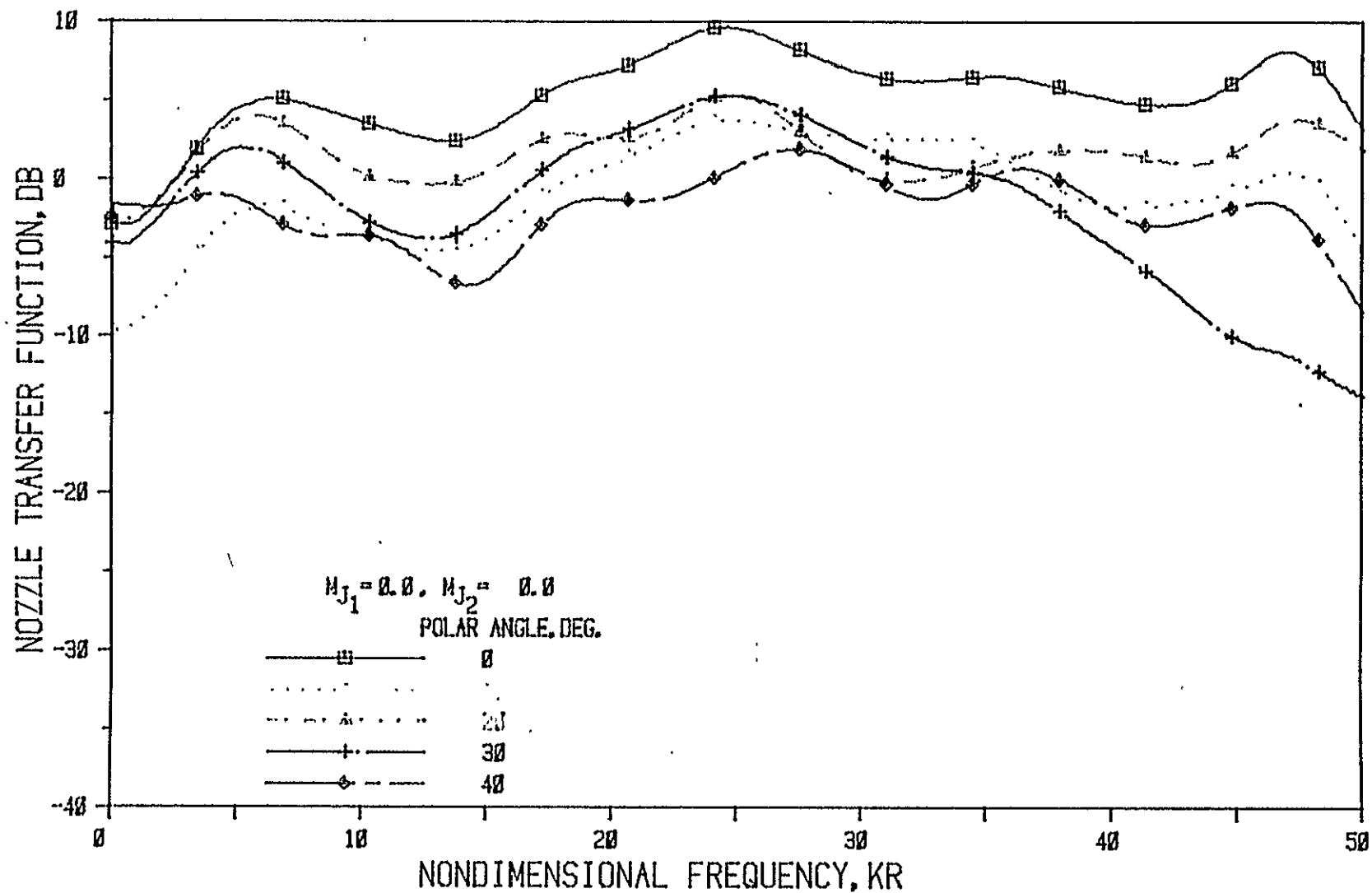


Figure 15(a) Nozzle N 3 ( $L/h = 5$ , Convergence Angle =  $20^\circ$ ); Source At Core

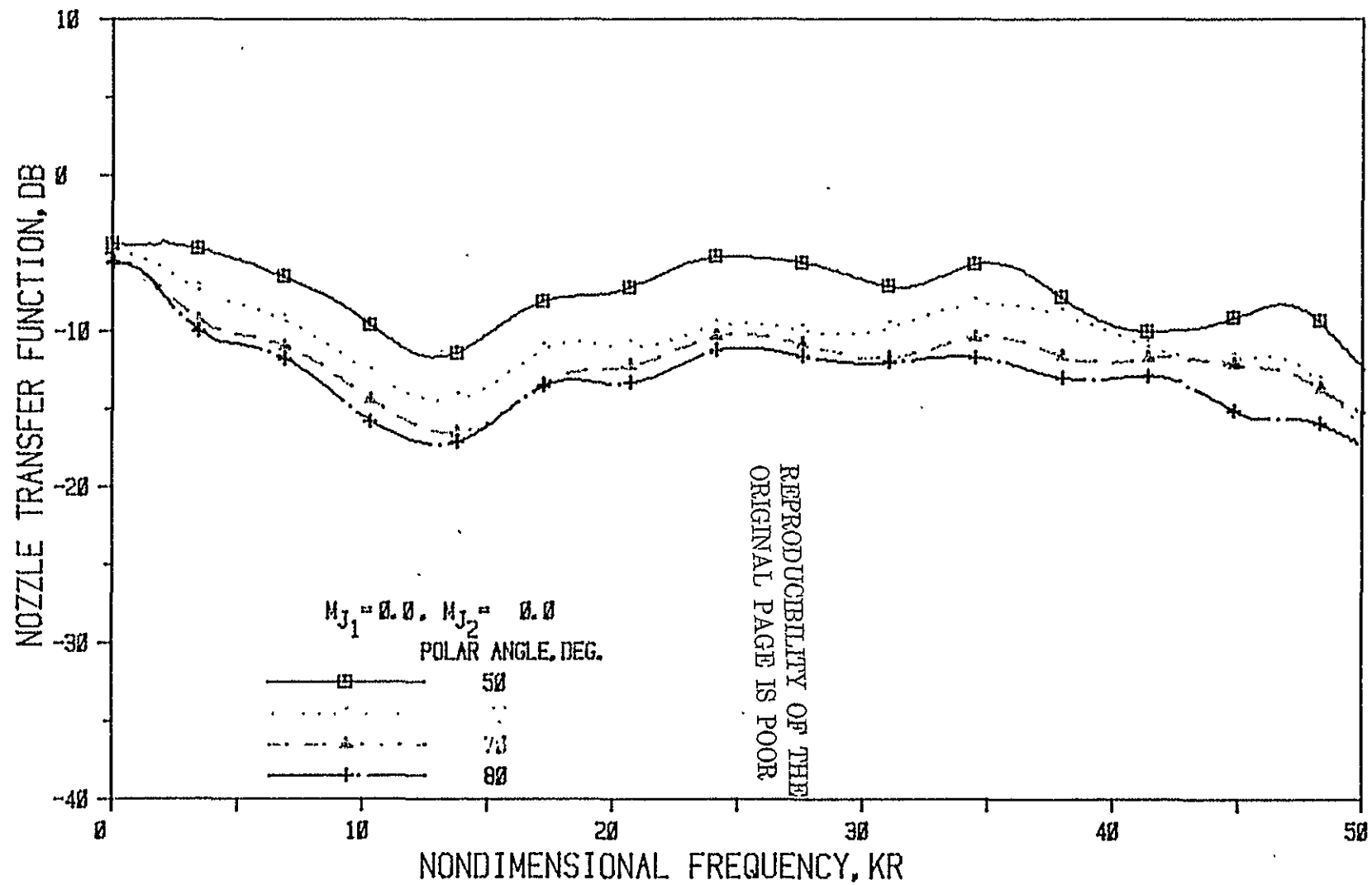


Figure 15(b) Nozzle N 3 (  $L/h = 5$ , Convergence Angle = 20 Deg.); Source At Core

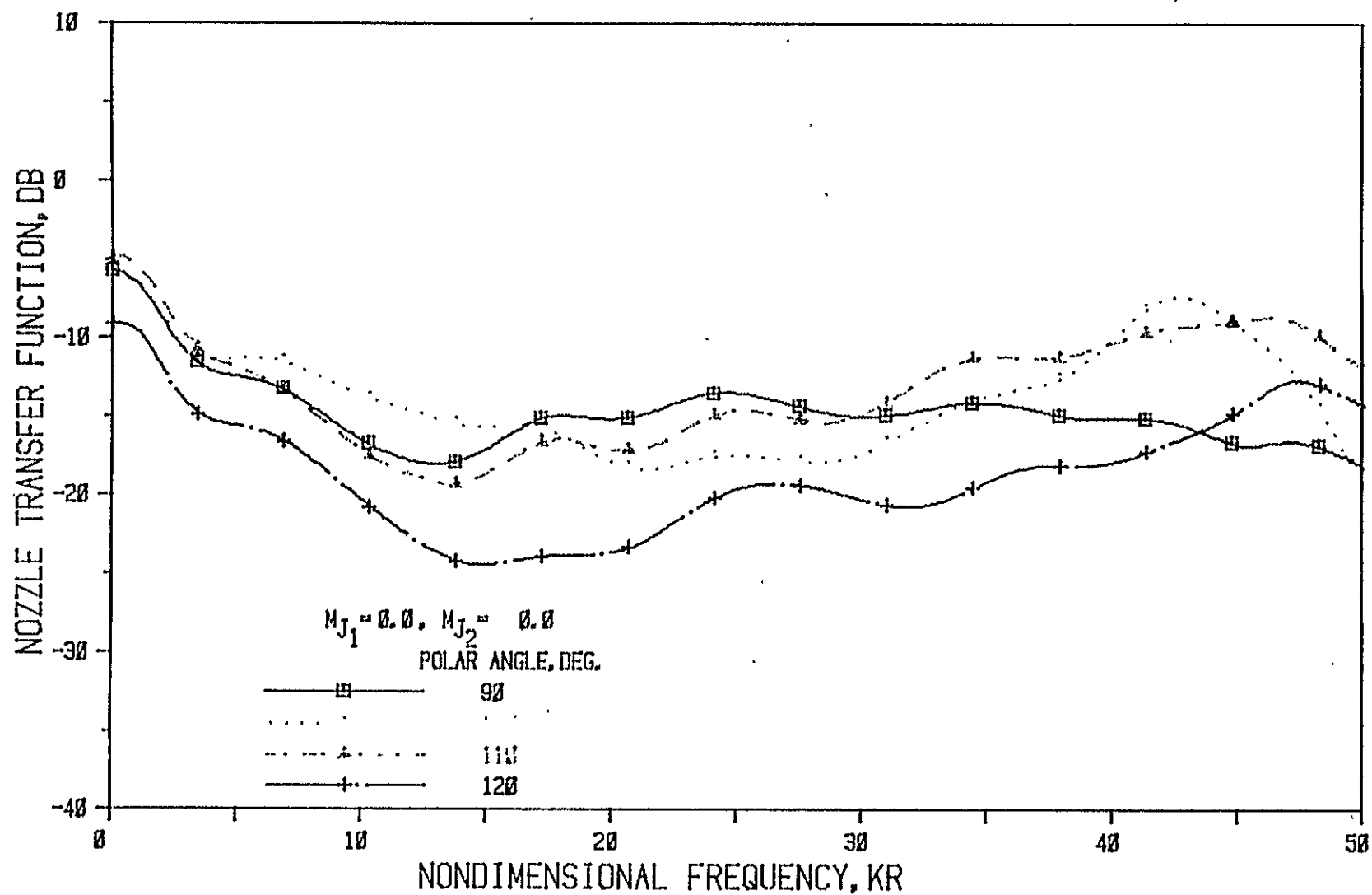


Figure 15(c) Nozzle N 3 (  $L/h = 5$ , Convergence Angle = 20 Deg.); Source At Core

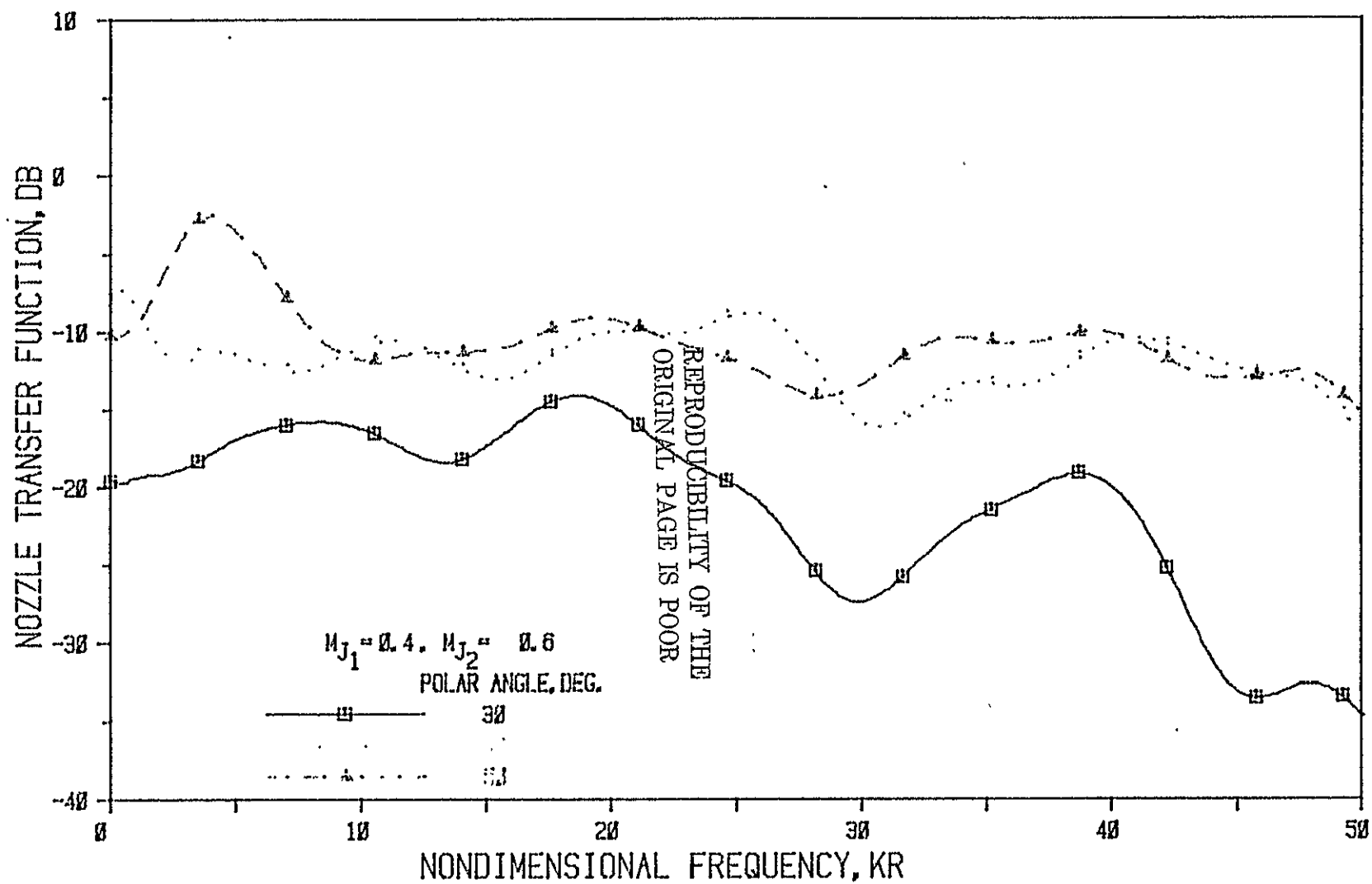


Figure 16(a) Nozzle N 3 ( $L/h = 5$ , Convergence Angle = 20 Deg.); Source At Core



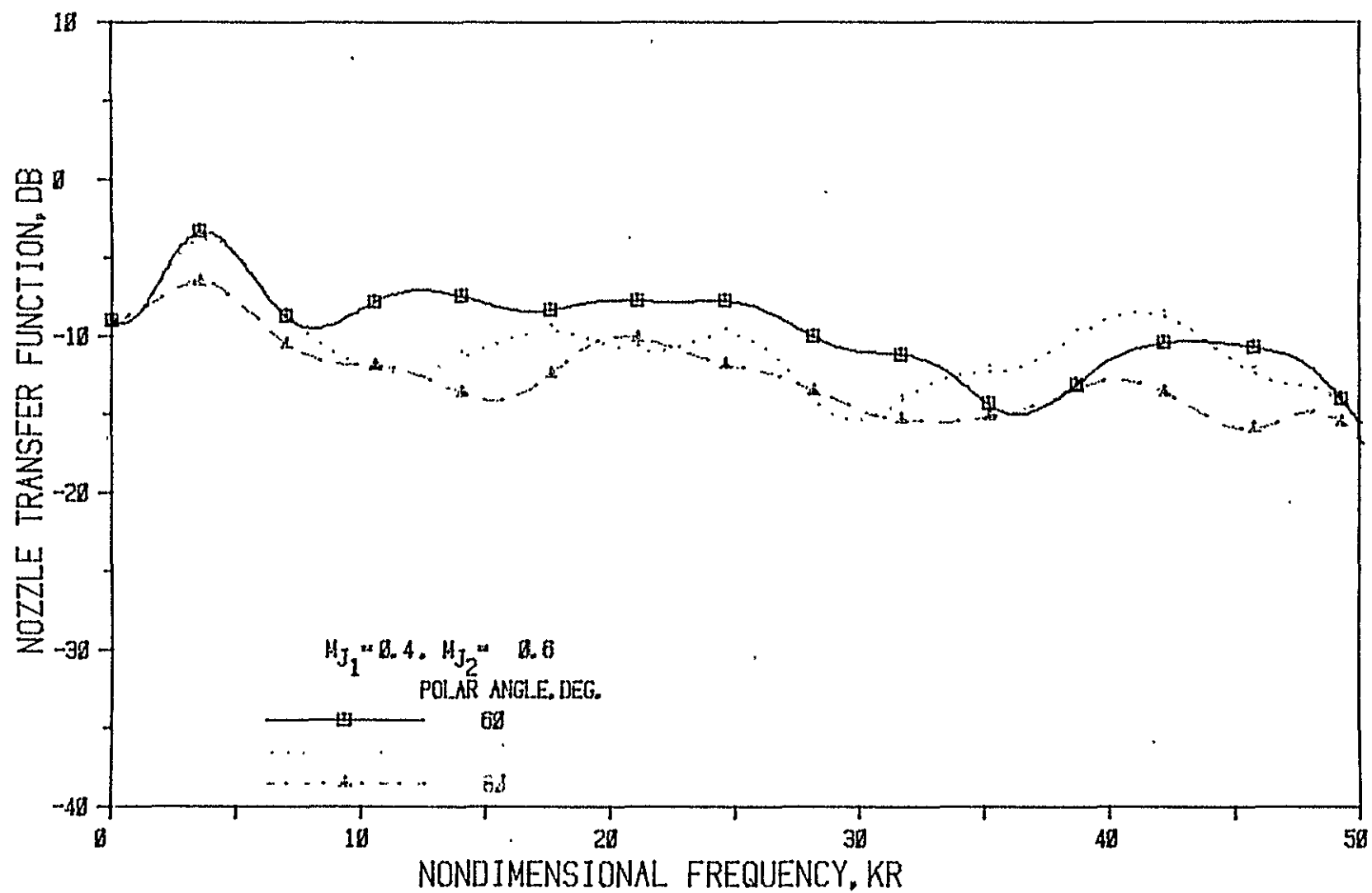


Figure 16(b) Nozzle N 3 (  $L/h = 5$ , Convergence Angle = 20 Deg. ); Source At Core

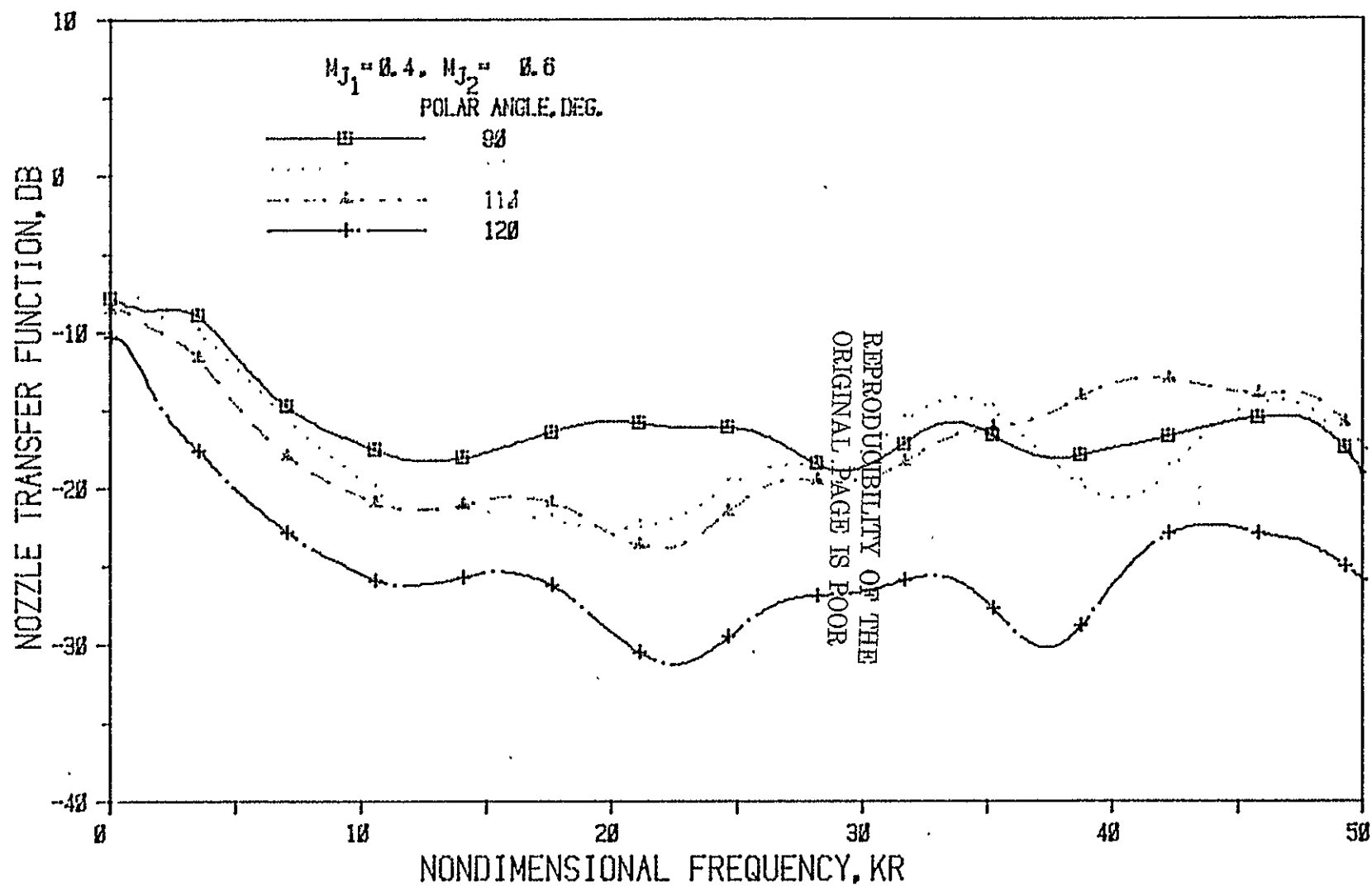


Figure 16(c) Nozzle N 3 (  $L/h = 5$ , Convergence Angle = 20 Deg. ); Source At Core

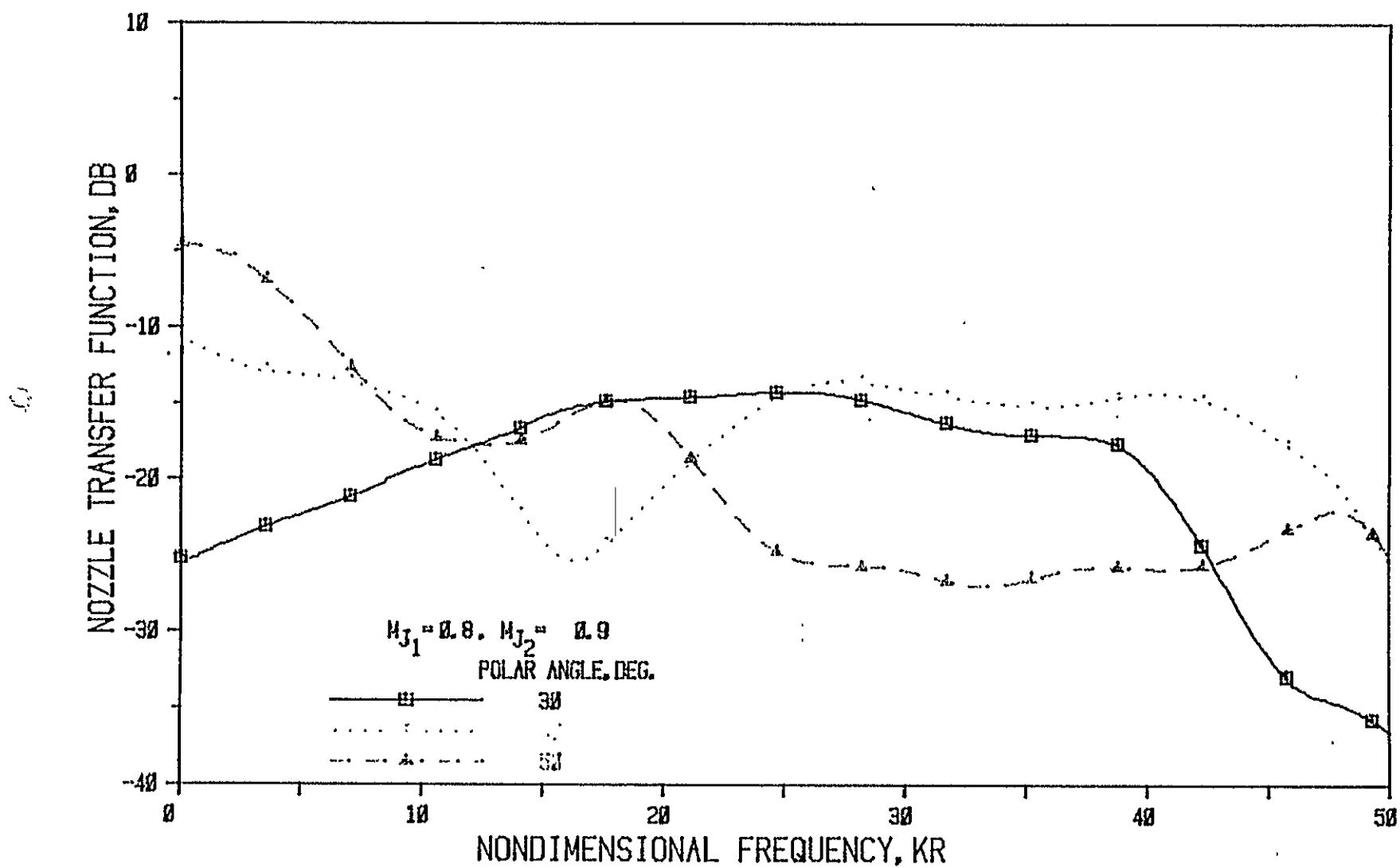


Figure 17(a) Nozzle N 3 ( $L/h = 5$ , Convergence Angle = 20 Deg.); Source At Core

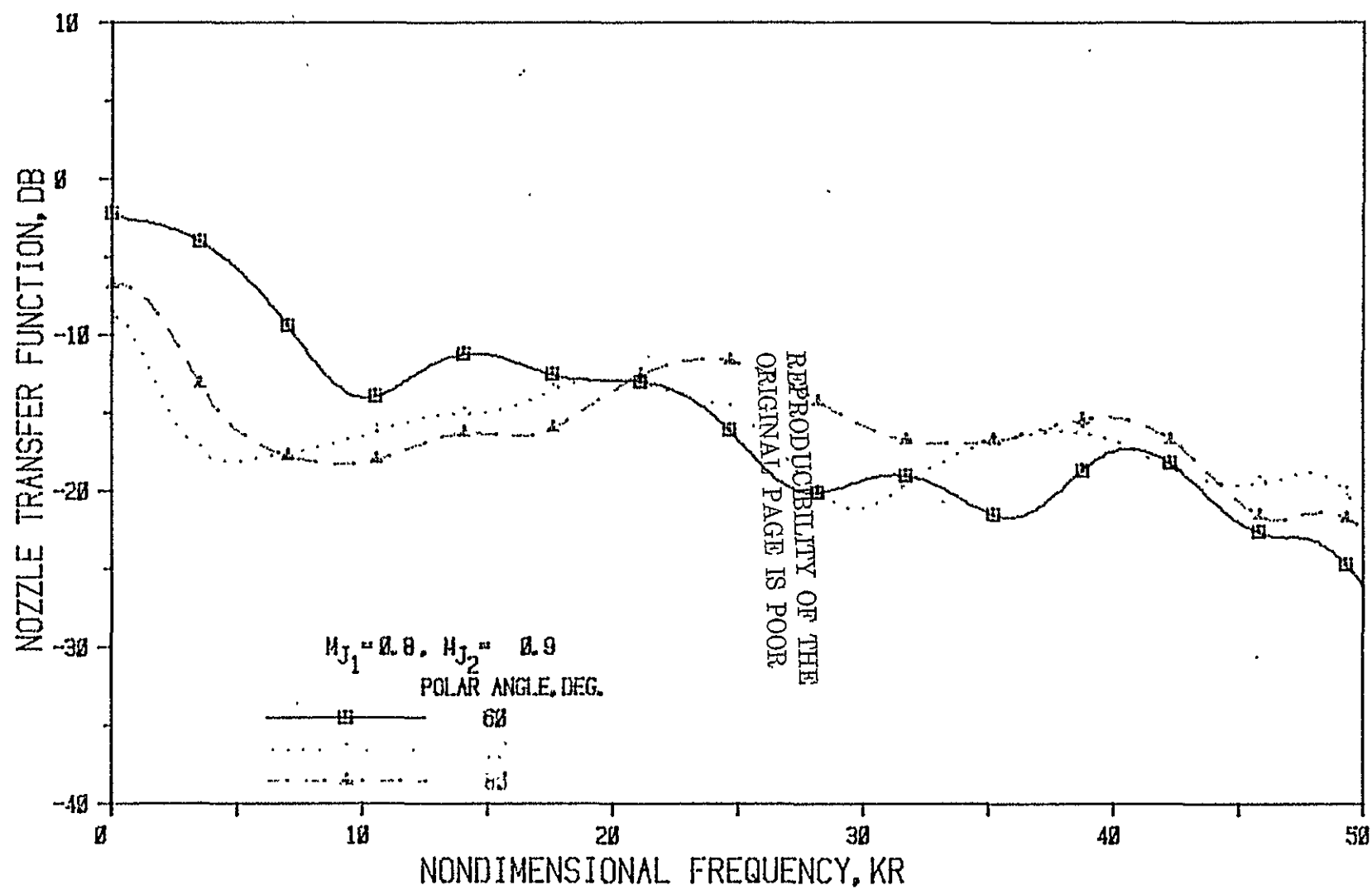


Figure 17(b) Nozzle N 3 ( $L/h = 5$ , Convergence Angle = 20 Deg.); Source At Core

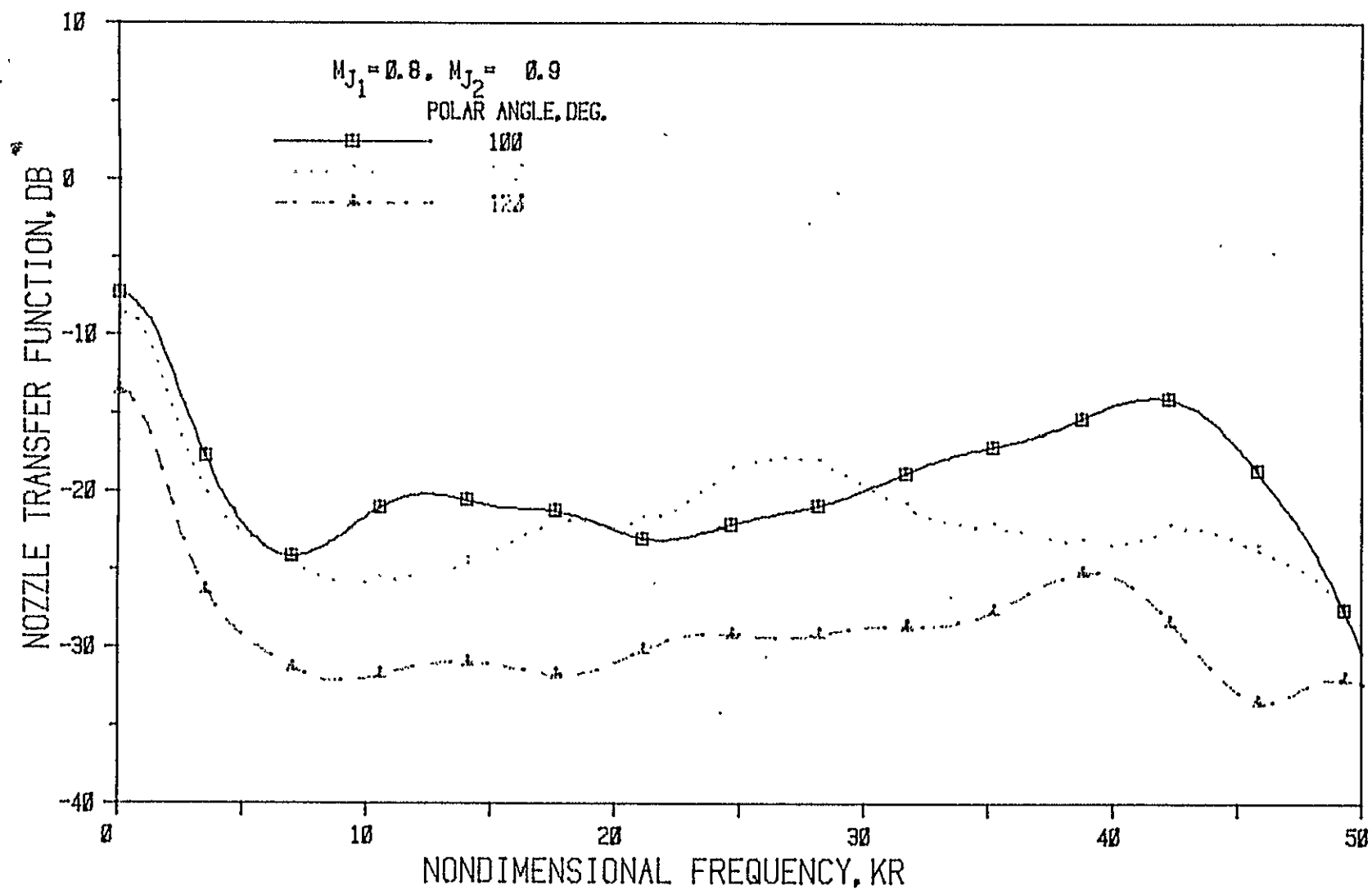


Figure 17(c) Nozzle N 3 (  $L/h = 5$ , Convergence Angle = 20 Deg.); Source At Core

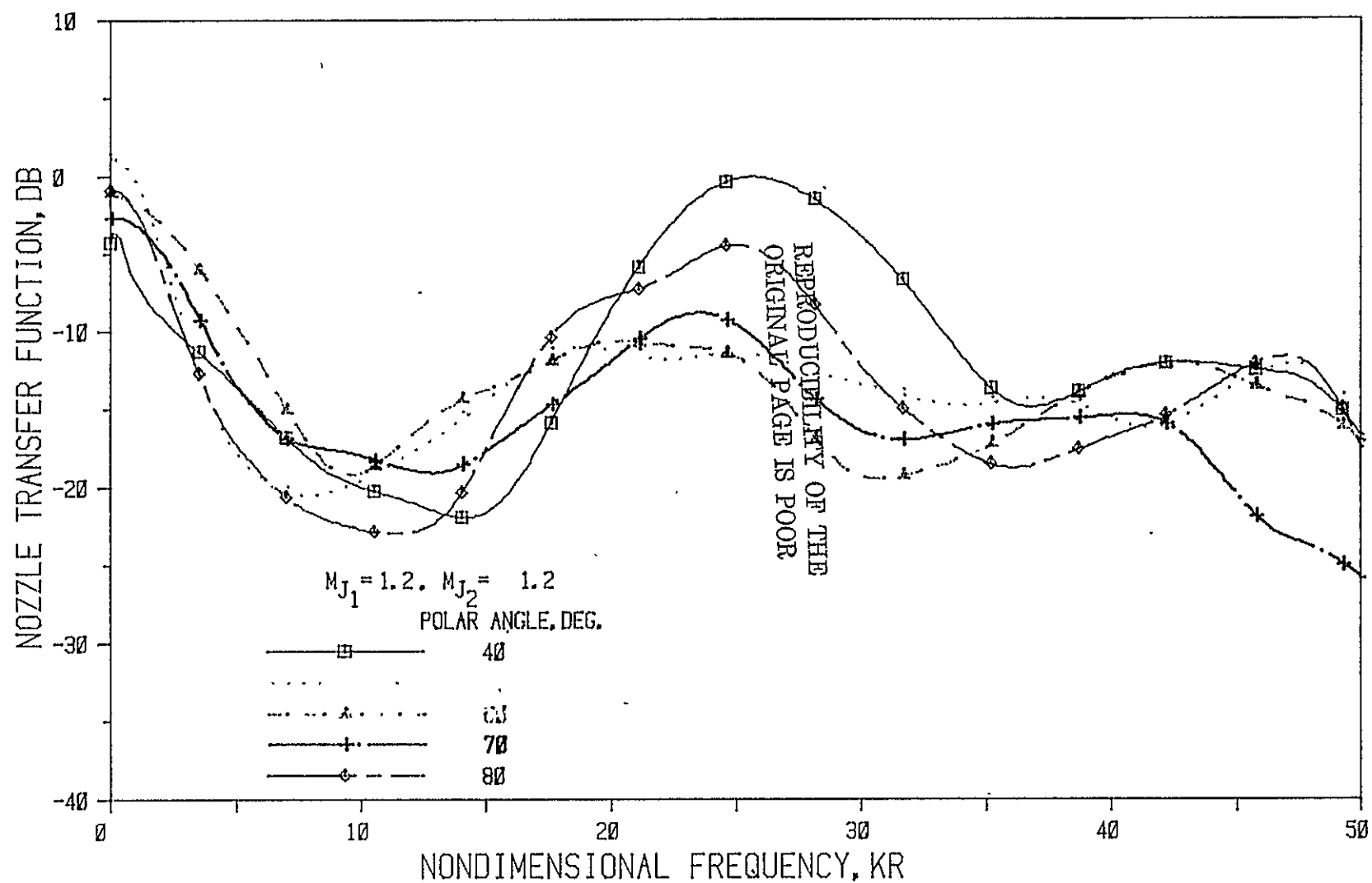


Figure 18 Nozzle N 3 (  $L/h = 5$ , Convergence Angle = 20 Deg.); Source At Core

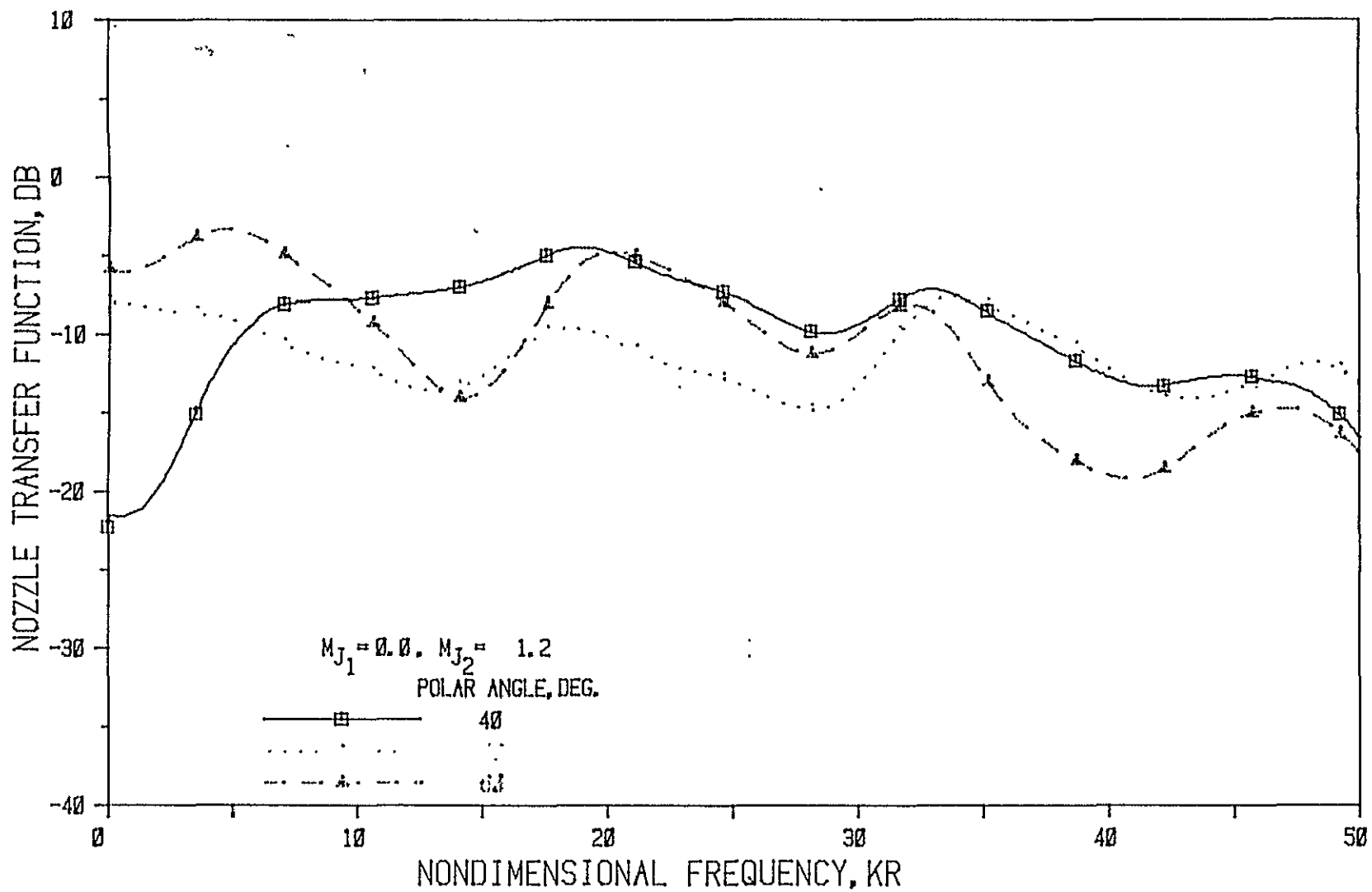


Figure 19(a) Nozzle N 3 (  $L/h = 5$ , Convergence Angle = 20 Deg.); Source At Core

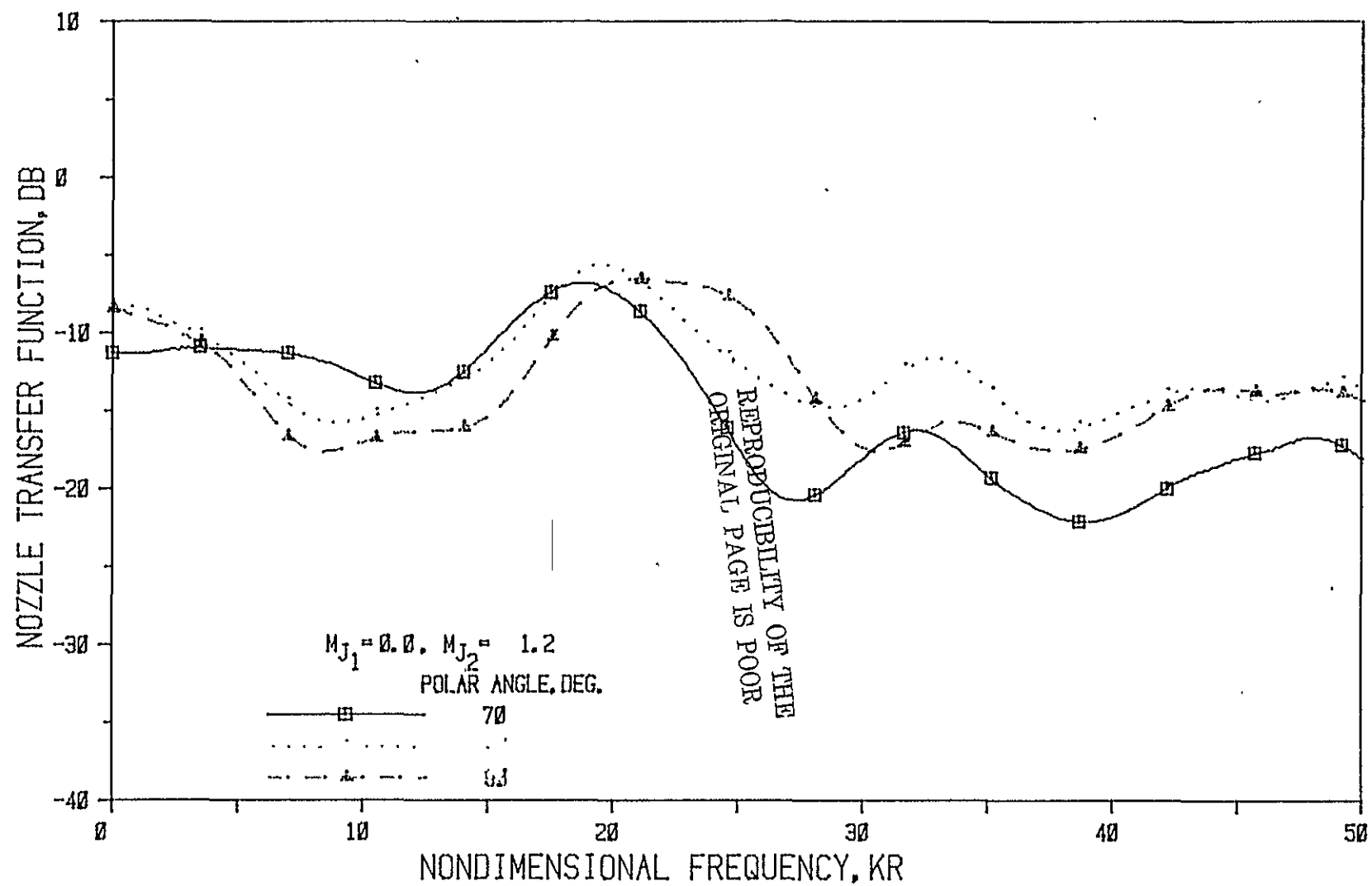


Figure 19(b) Nozzle N 3 (  $L/h = 5$ , Convergence Angle = 20 Deg.); Source At Core



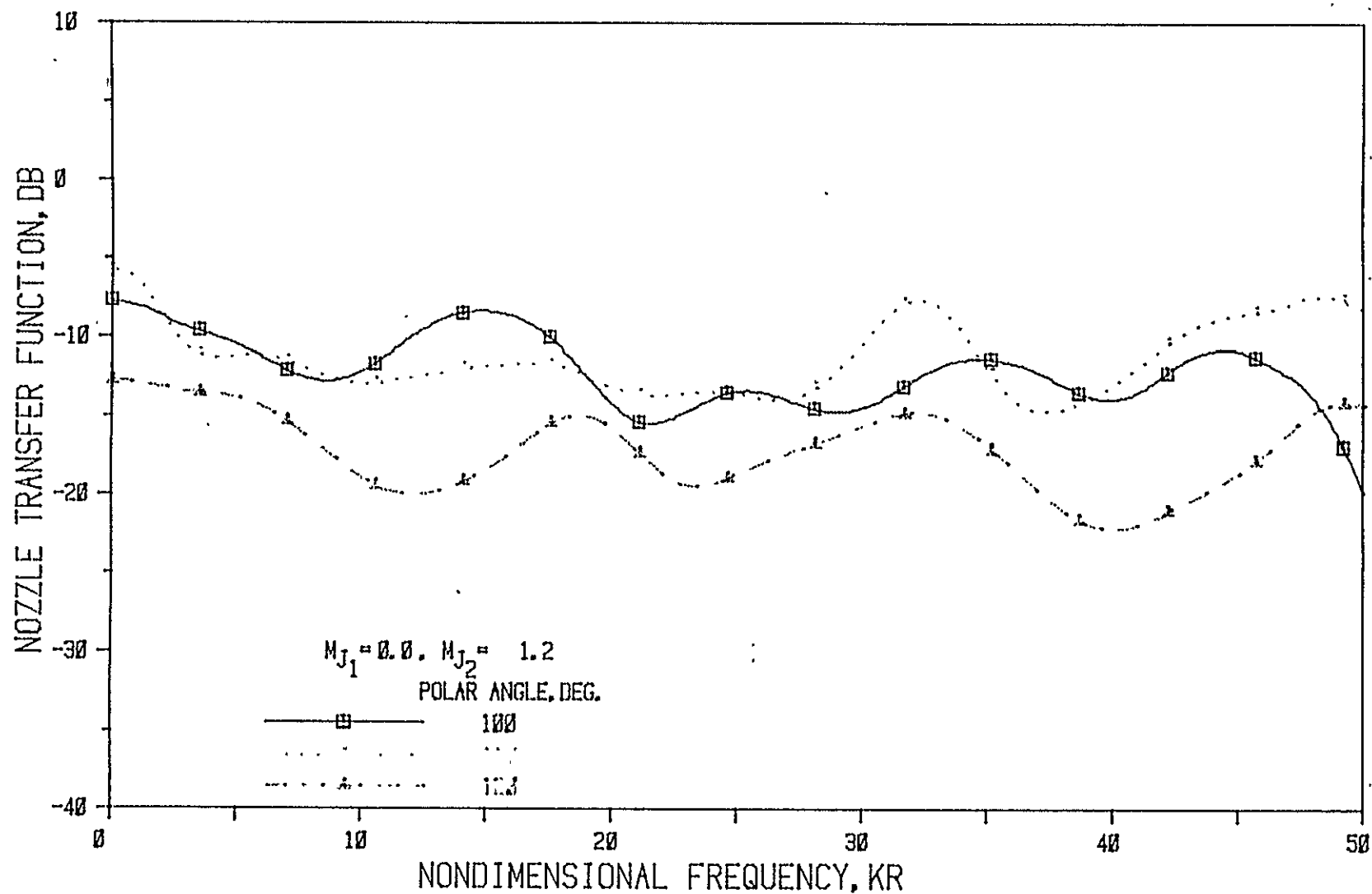


Figure 19(c) Nozzle N 3 (  $L/h = 5$ , Convergence Angle = 20 Deg.); Source At Core

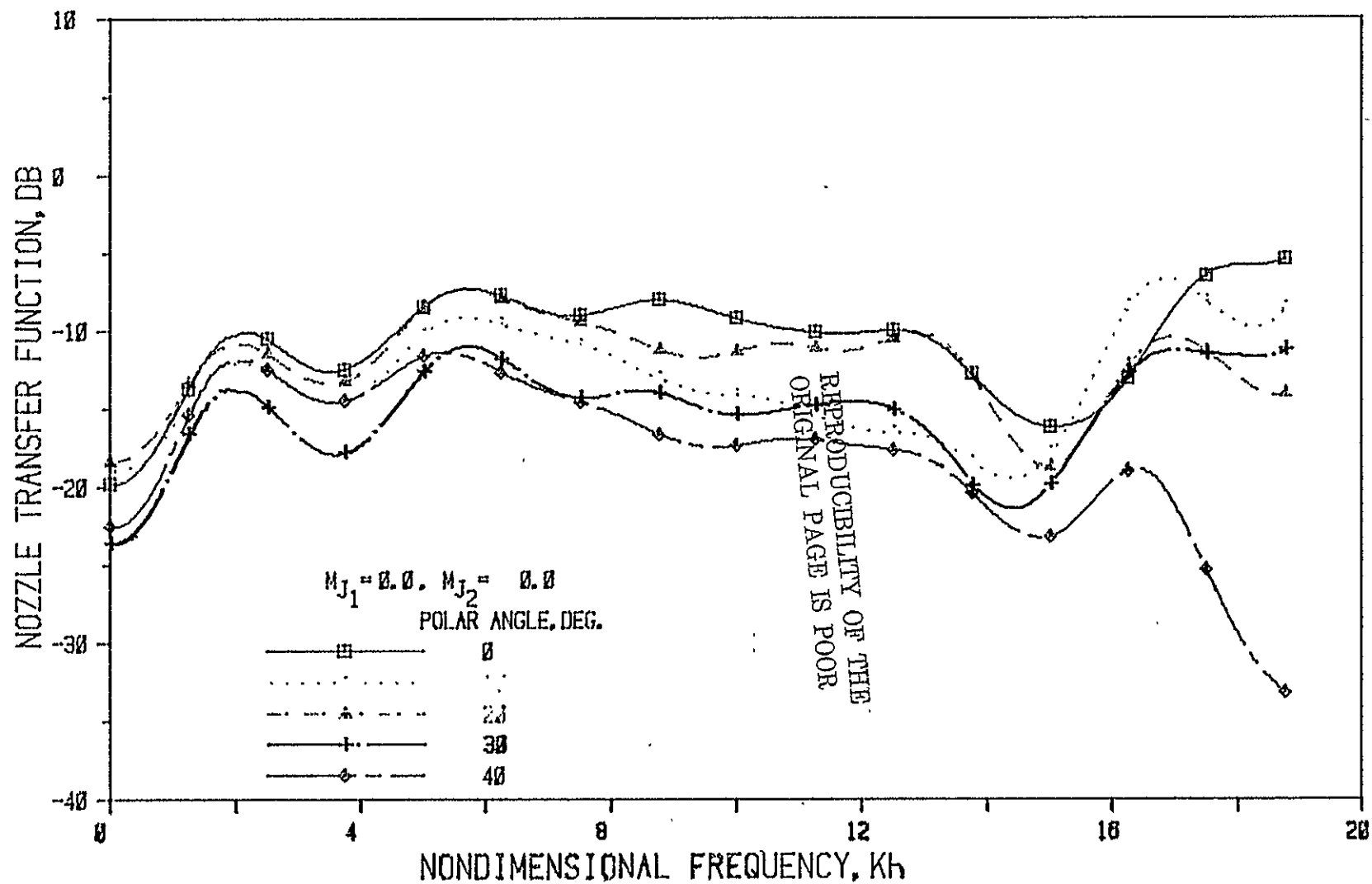


Figure 20(a) Nozzle N1 ( $L/h = 1$ , Convergence Angle = 20 Deg.); Source At Fan

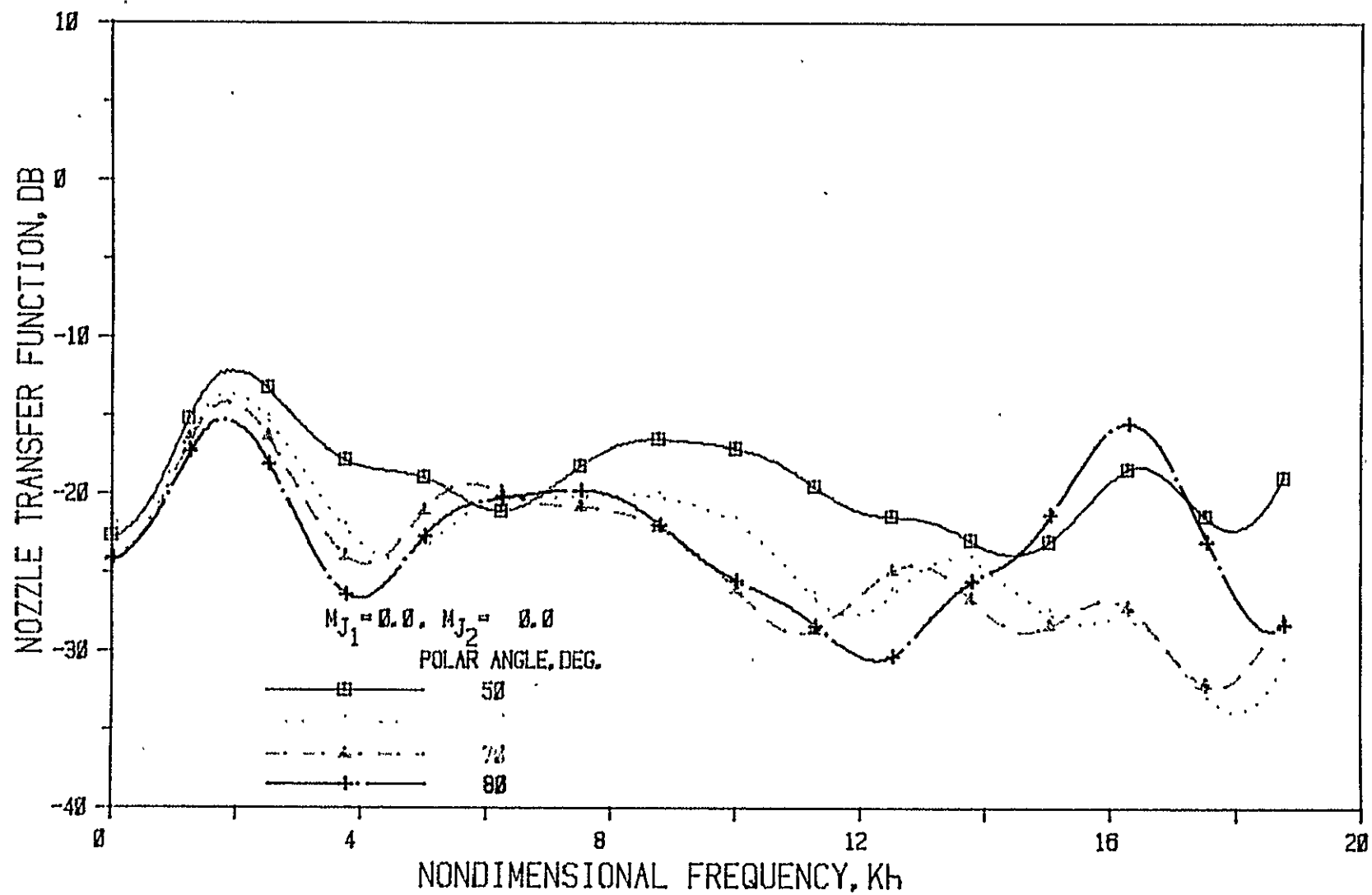


Figure 20(b) Nozzle N1 ( $L/h = 1$ , Convergence Angle = 20 Deg.); Source At Fan

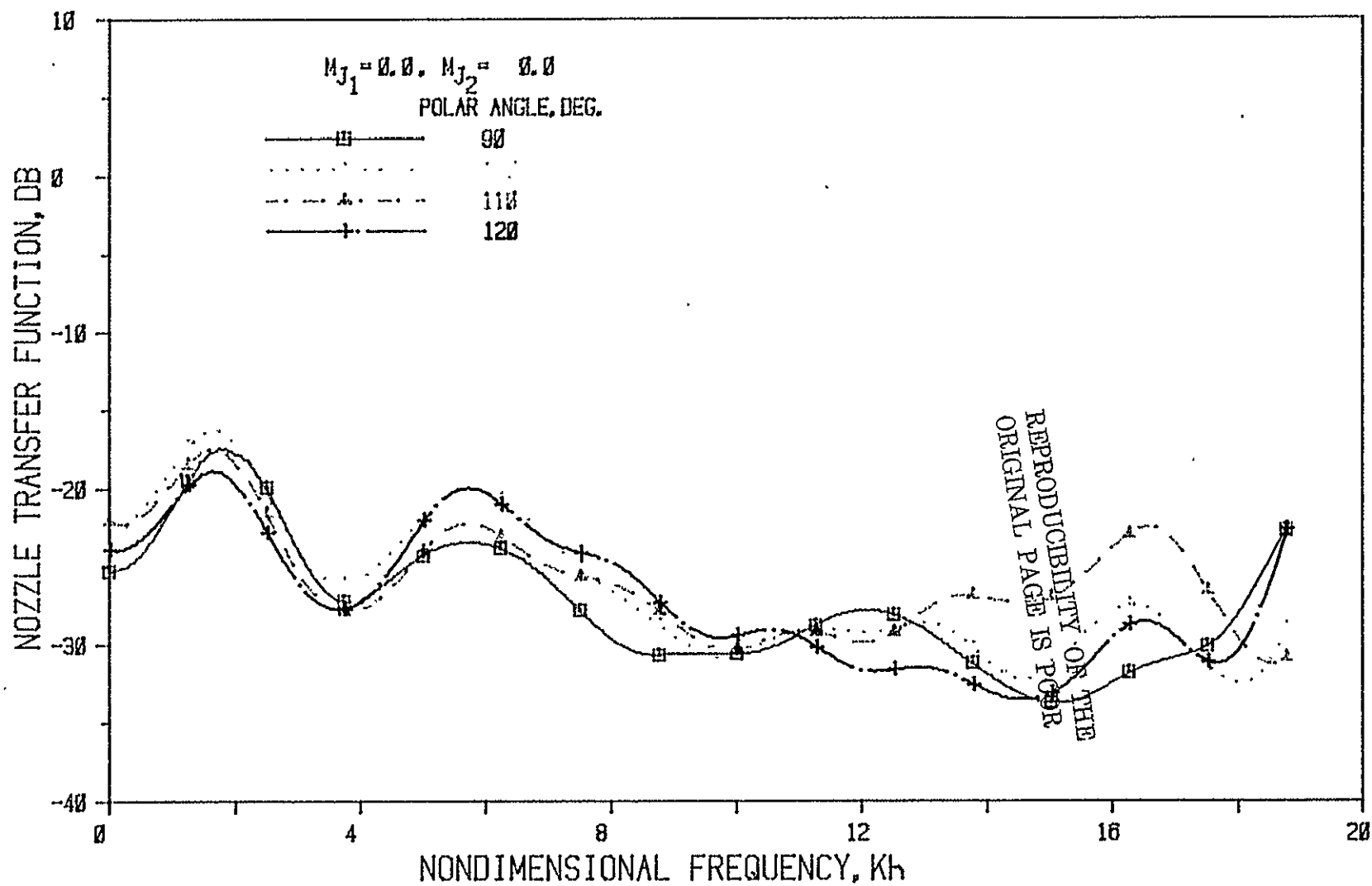


Figure 20(c) Nozzle N1 ( $L/h = 1$ , Convergence Angle = 20 Deg.); Source At Fan

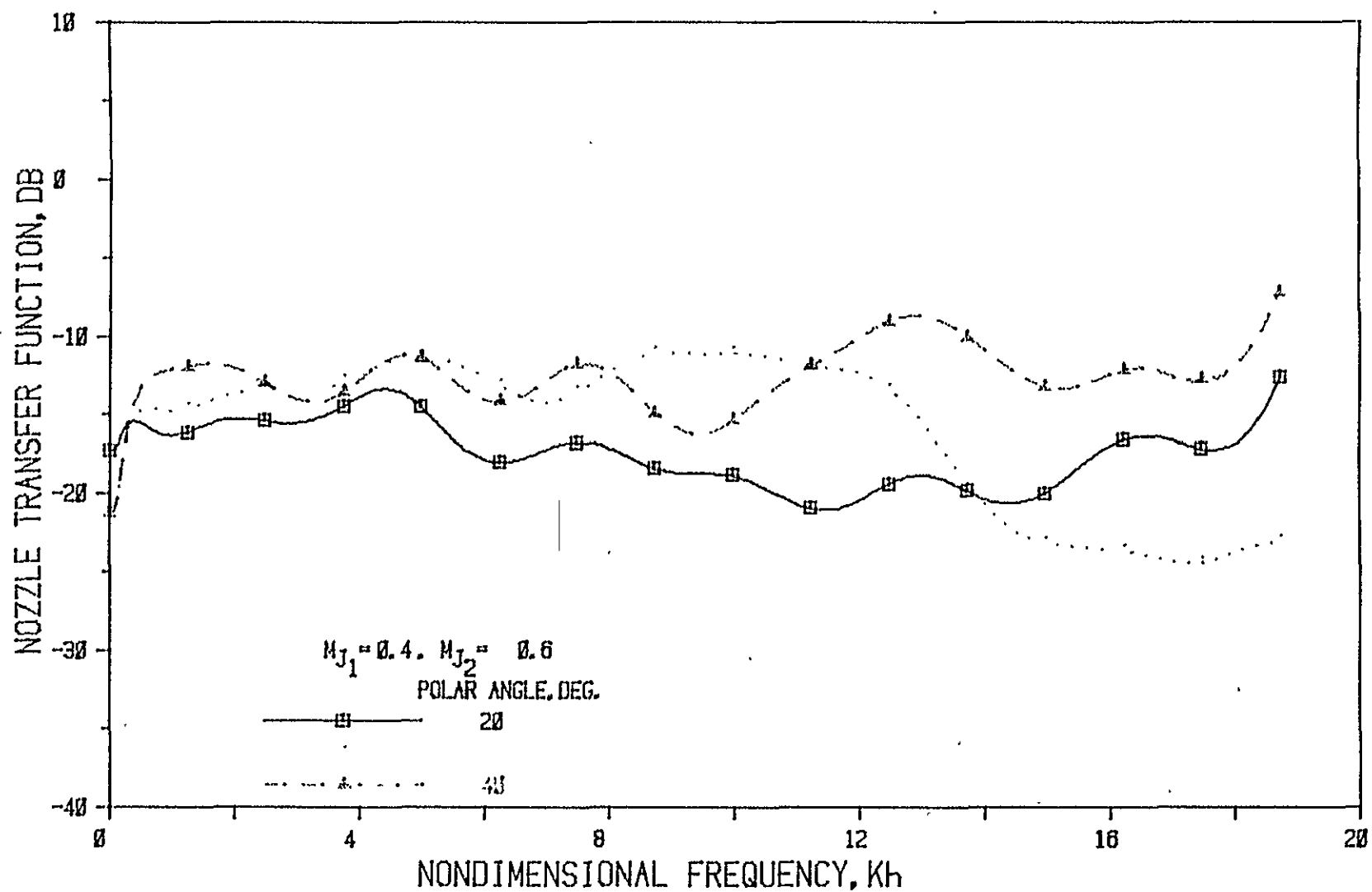


Figure 21(a) Nozzle N1 (  $L/h = 1$ , Convergence Angle = 20 Deg. ); Source At Fan

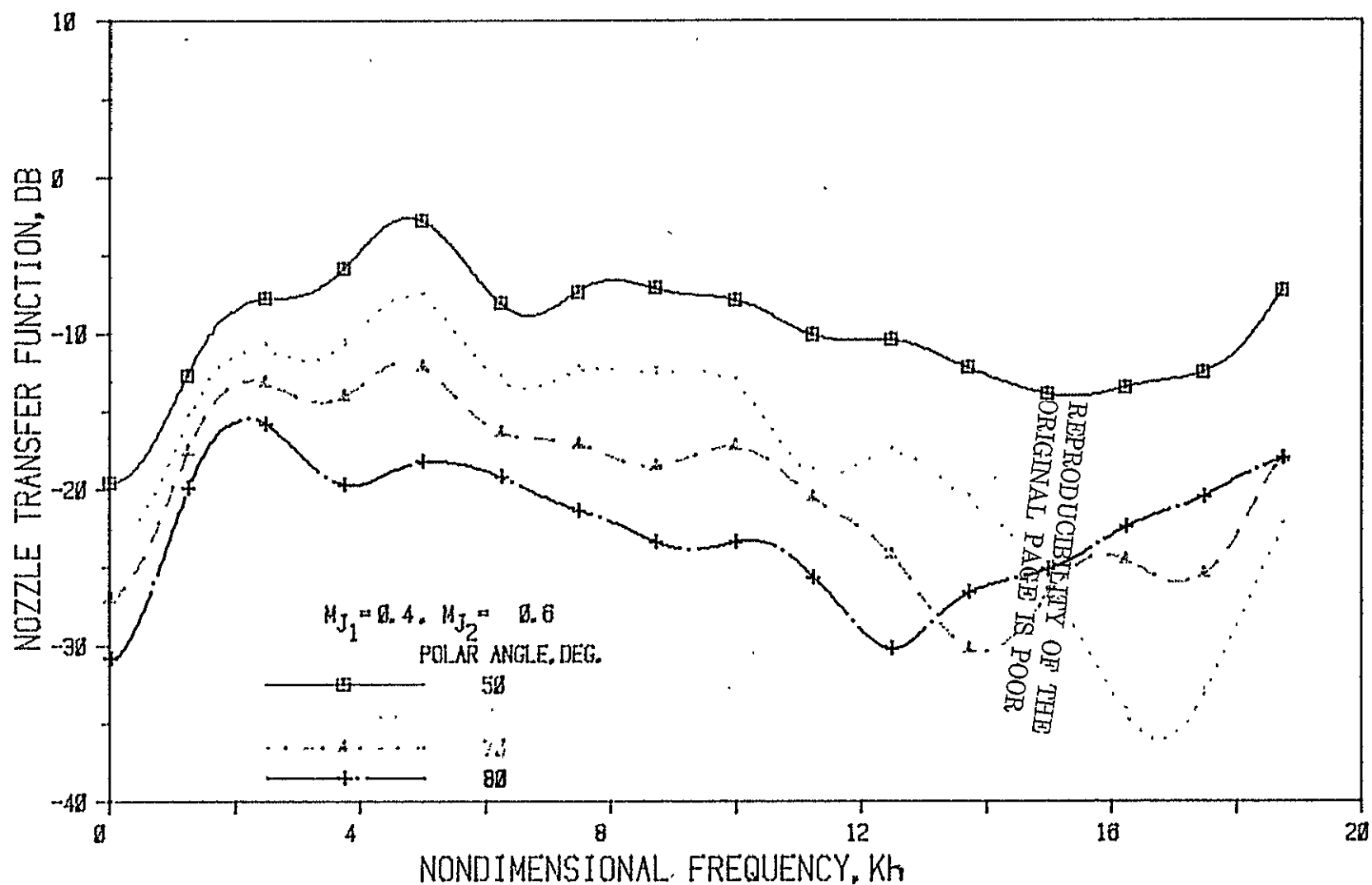


Figure 21(b) Nozzle N 1 ( $L/h = 1$ , Convergence Angle = 20 Deg.); Source At Fan

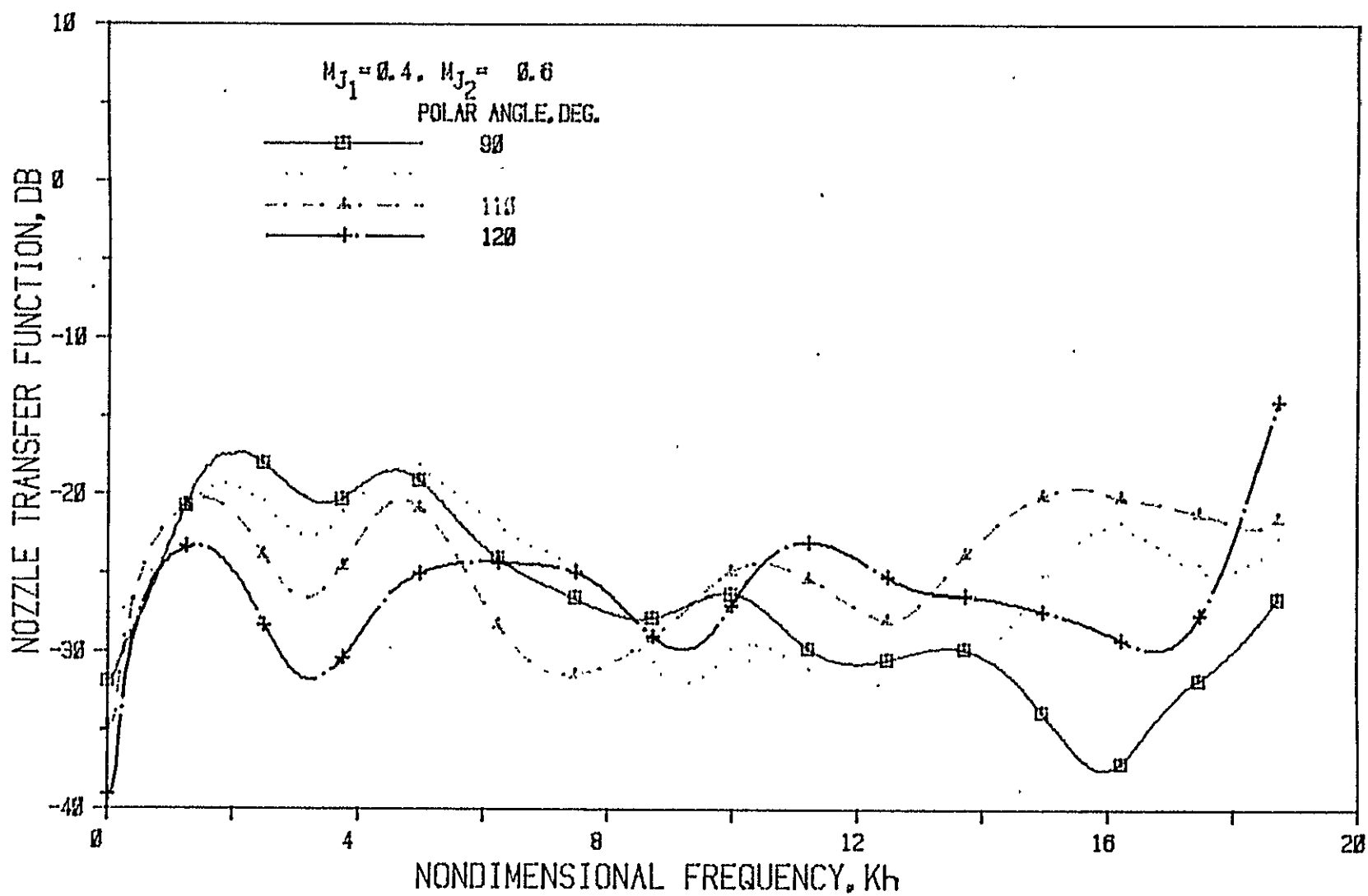


Figure 21(c) Nozzle N 1 (  $L/h = 1$ , Convergence Angle = 20 Deg. ); Source At Fan

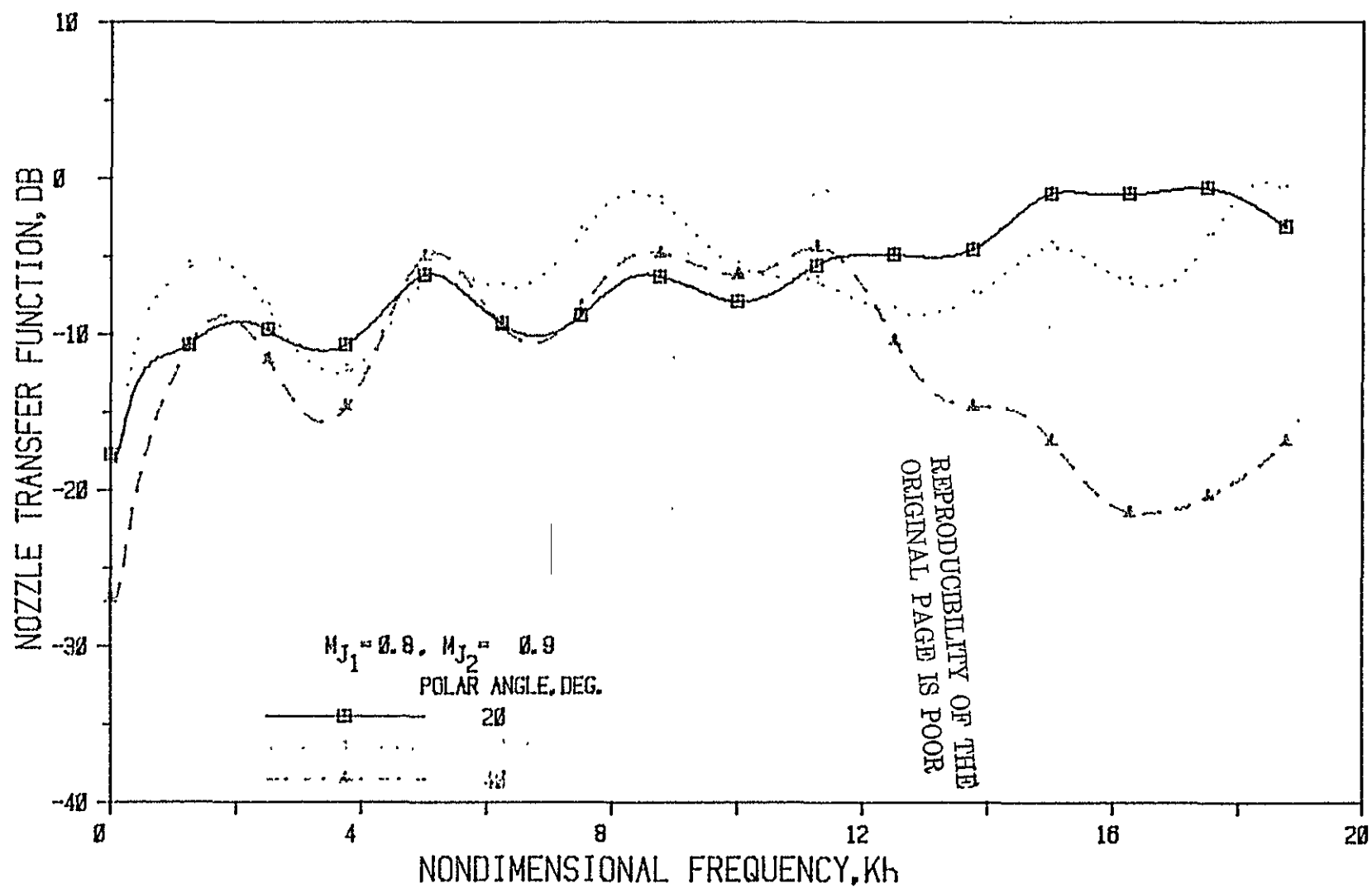


Figure 22(a) Nozzle N1 (L/h = 1, Convergence Angle = 20 Deg.); Source At Fan



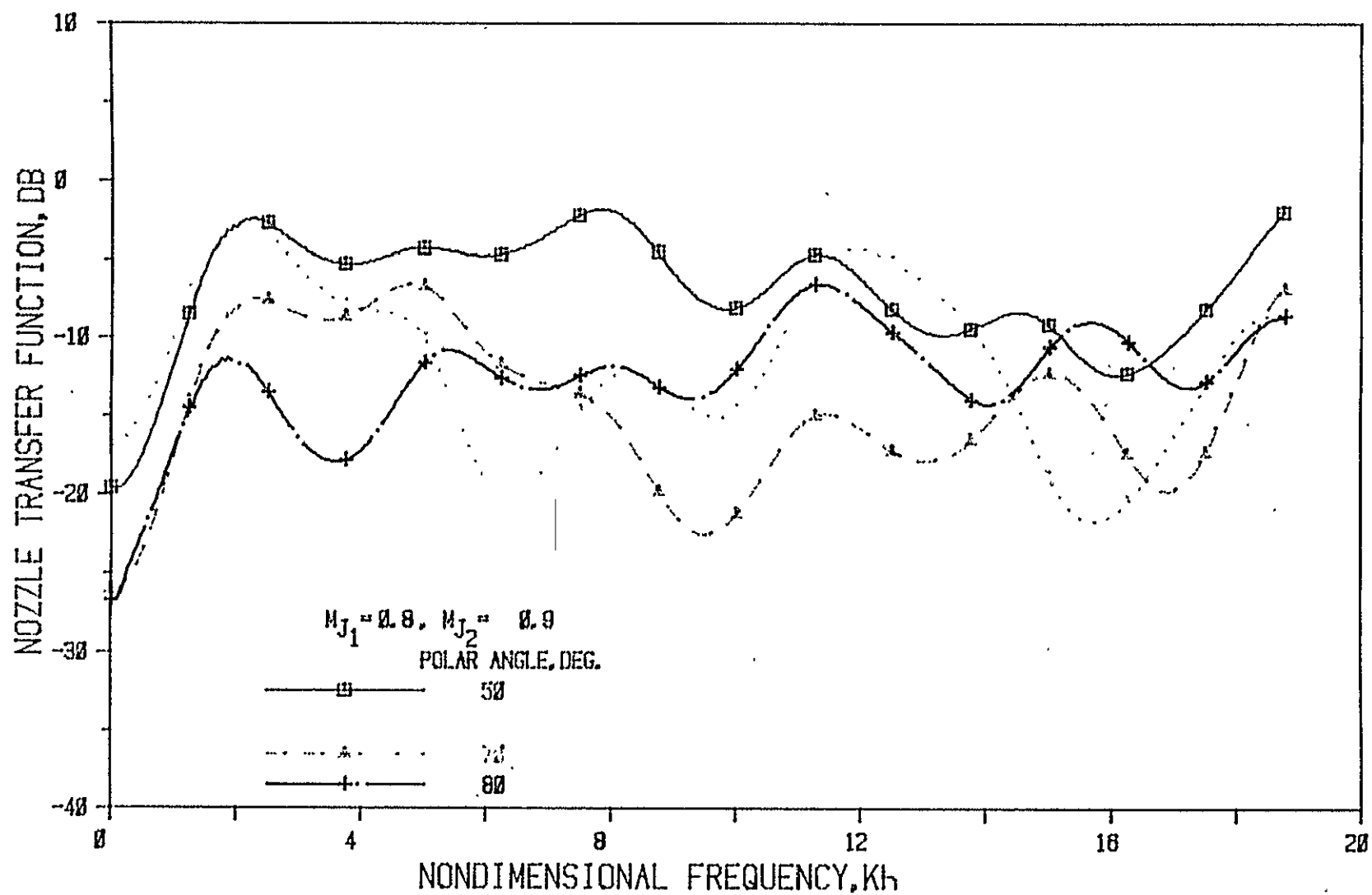


Figure 22(b) Nozzle N 1 ( $L/h = 1$ , Convergence Angle = 20 Deg.); Source At Fan

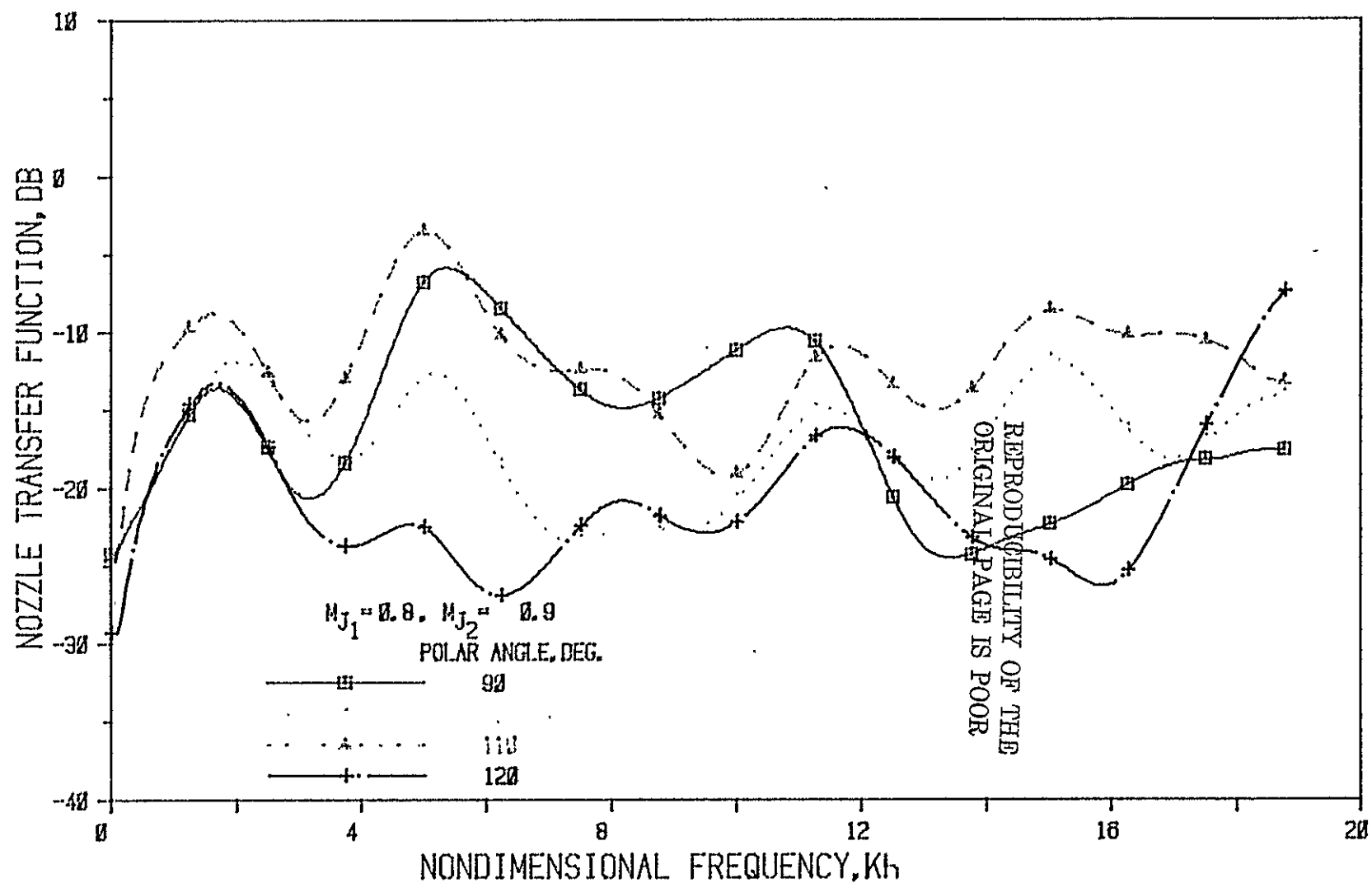


Figure 22(c) Nozzle N1 ( $L/h = 1$ , Convergence Angle = 20 Deg.); Source At Fan

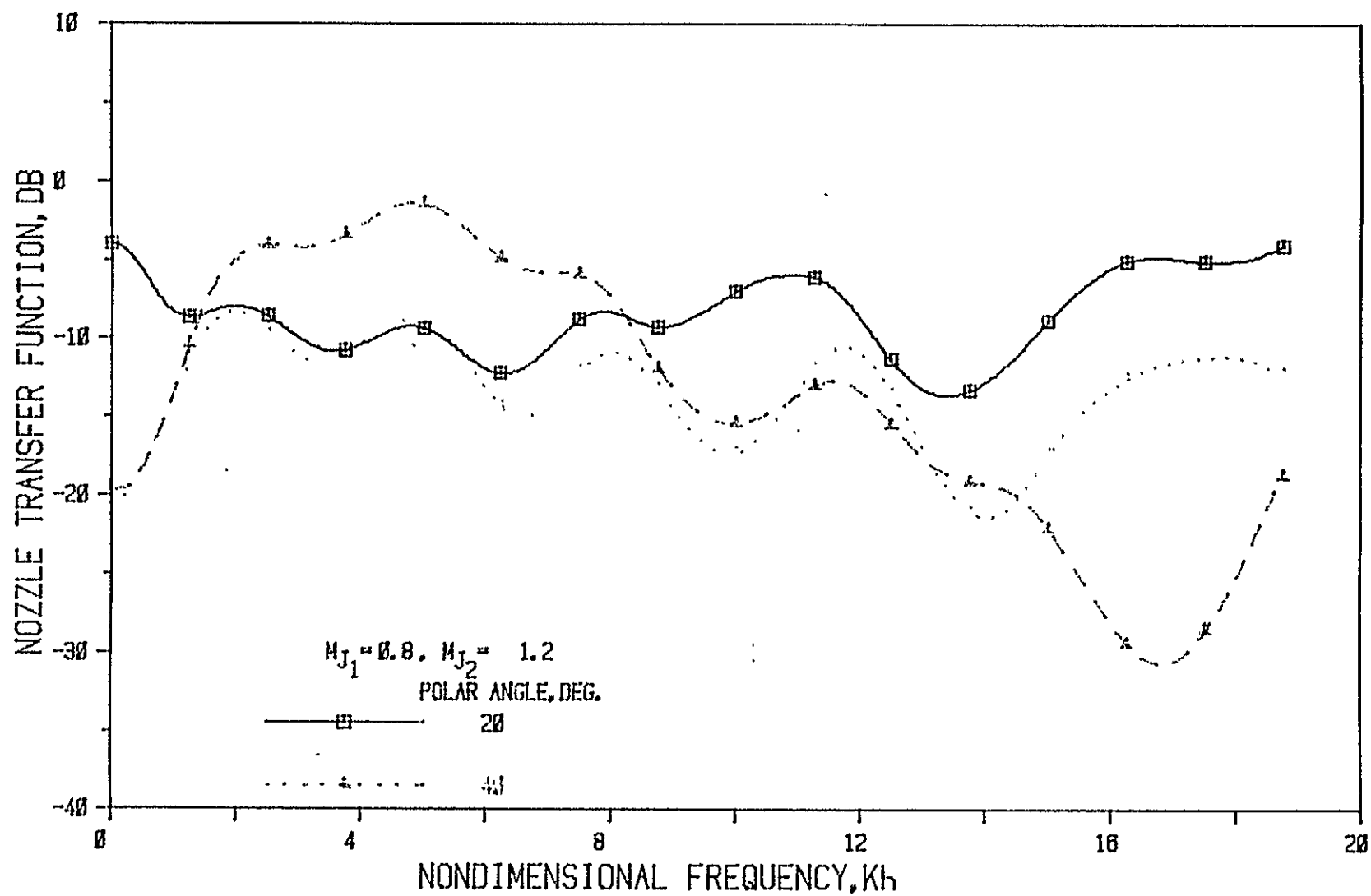


Figure 23(a) Nozzle N 1 ( $L/h = 1$ , Convergence Angle = 20 Deg.); Source At Fan

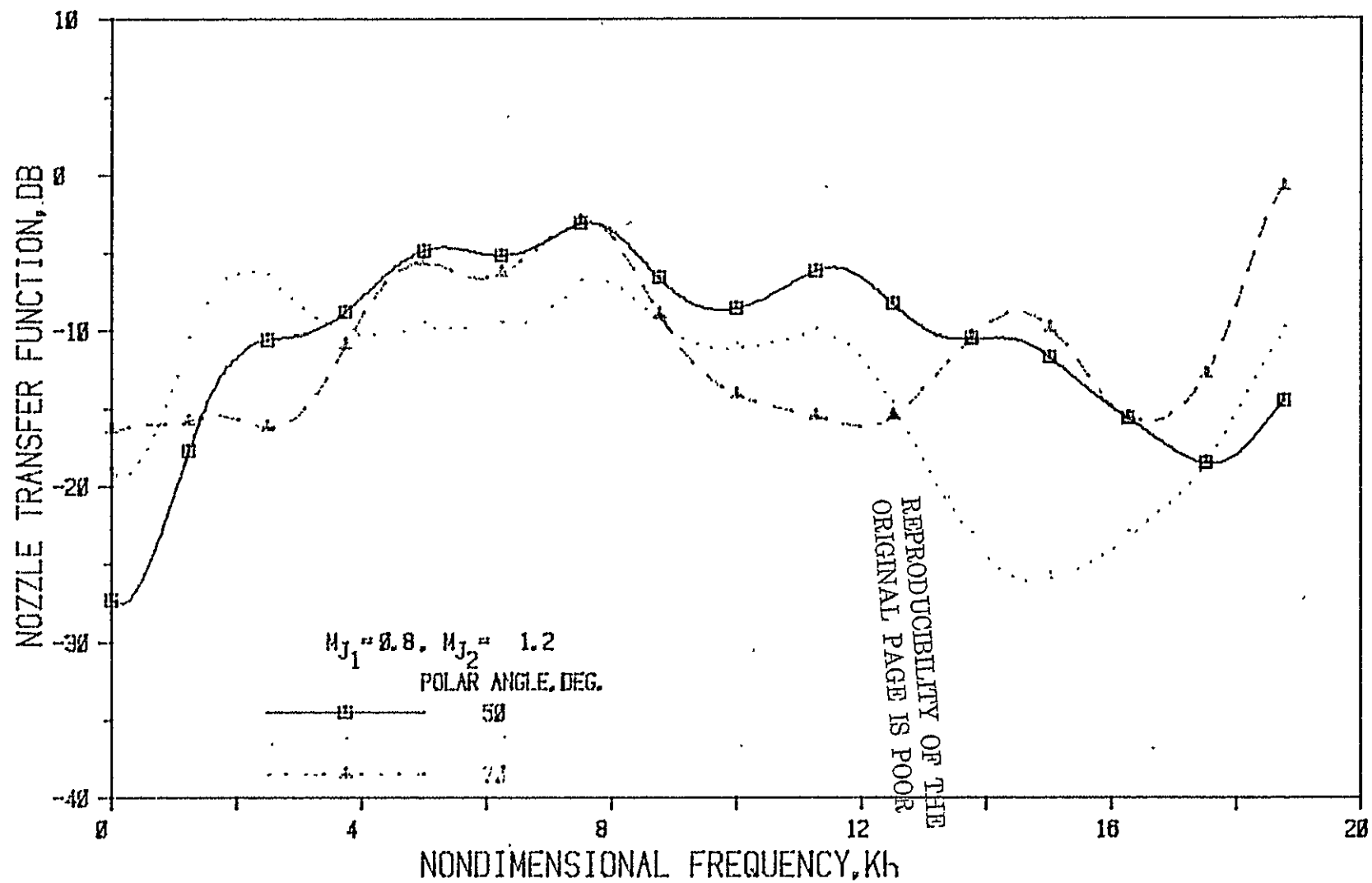


Figure 23(b) Nozzle N 1 (  $L/h = 1$ , Convergence Angle = 20 Deg.); Source At Fan

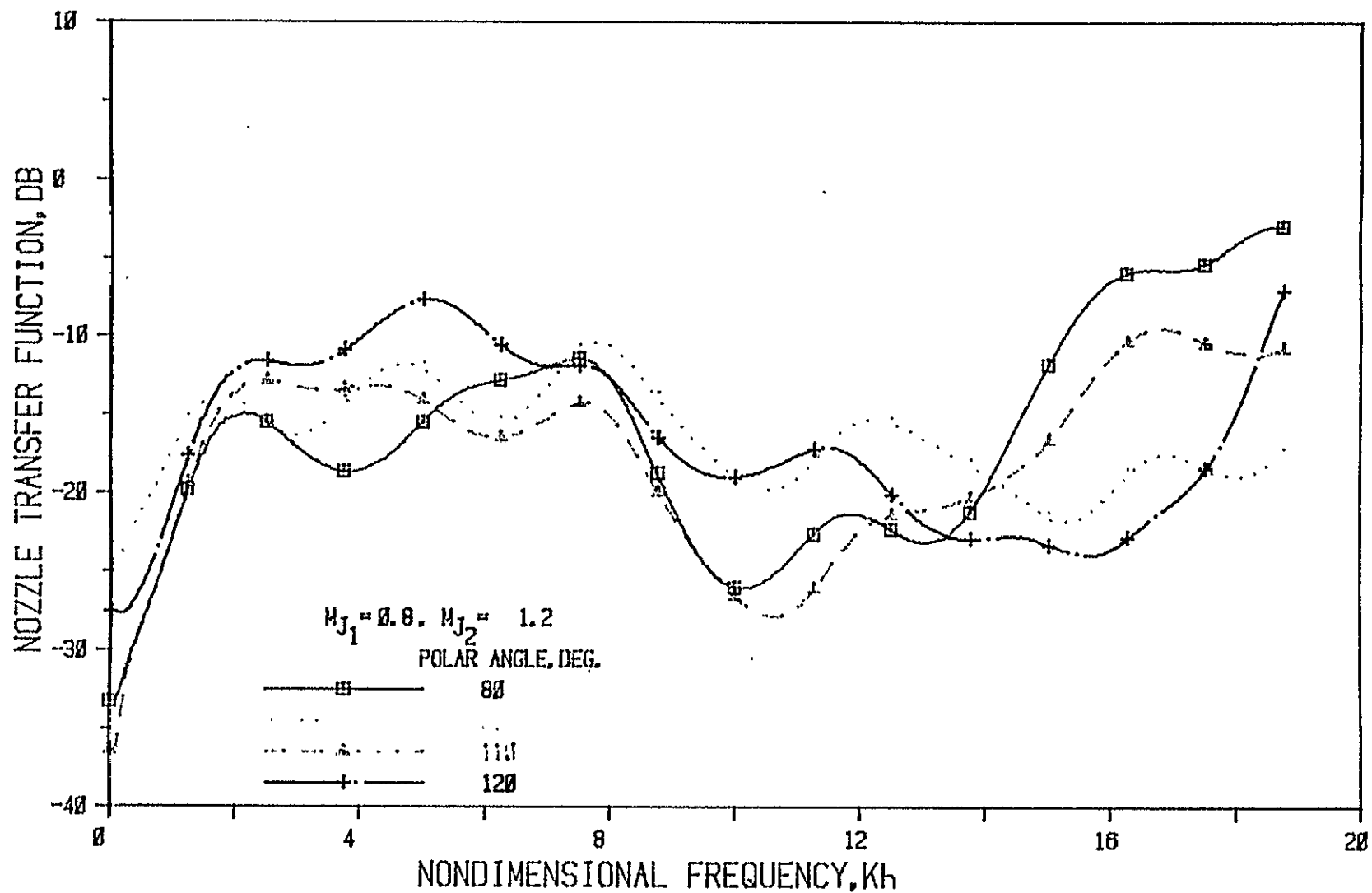


Figure 23(c) Nozzle N 1 ( $L/h = 1$ , Convergence Angle = 20 Deg.); Source At Fan

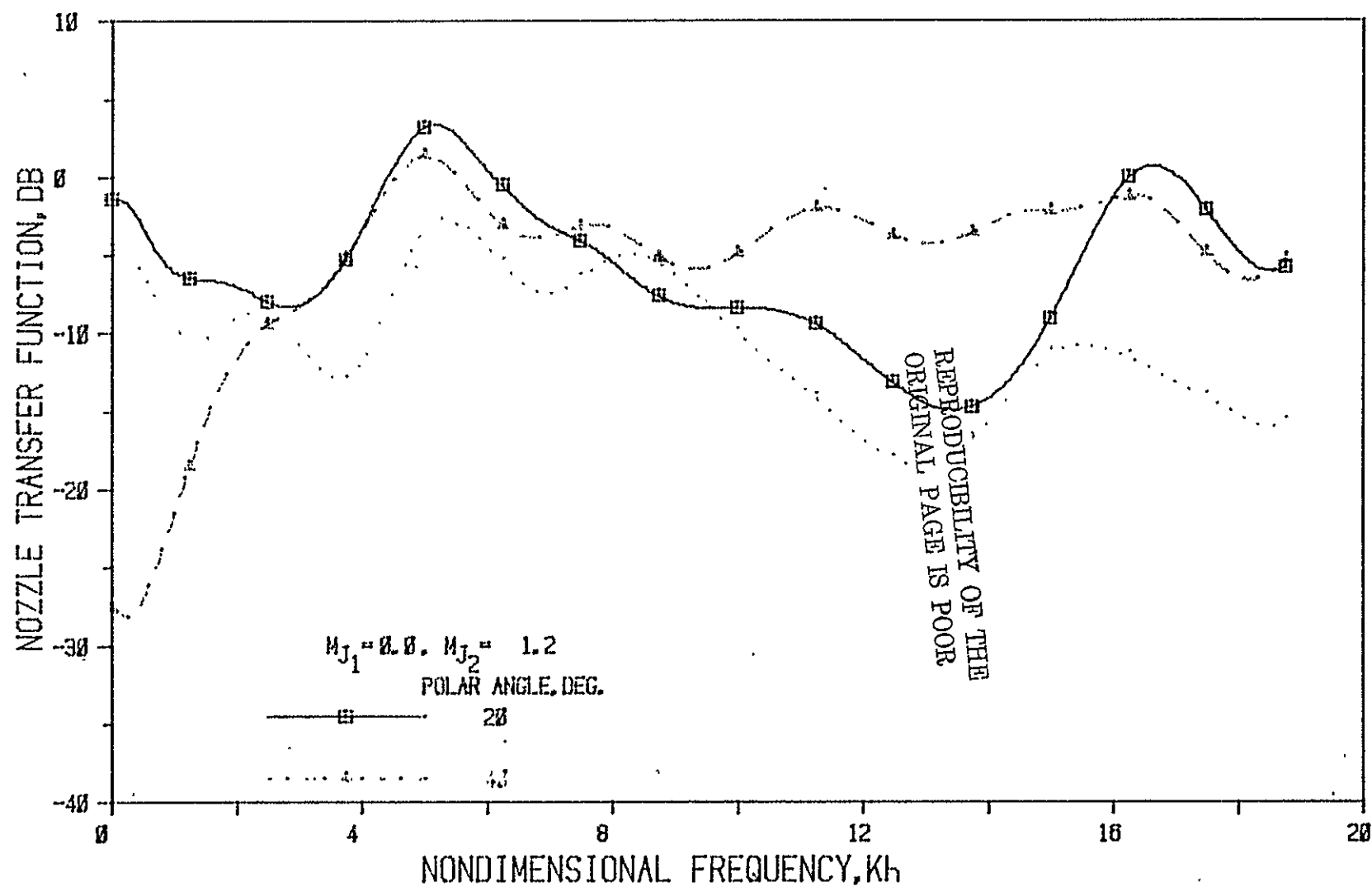


Figure 24(a) Nozzle N 1 (  $L/h = 1$ , Convergence Angle = 20 Deg.); Source At Fan

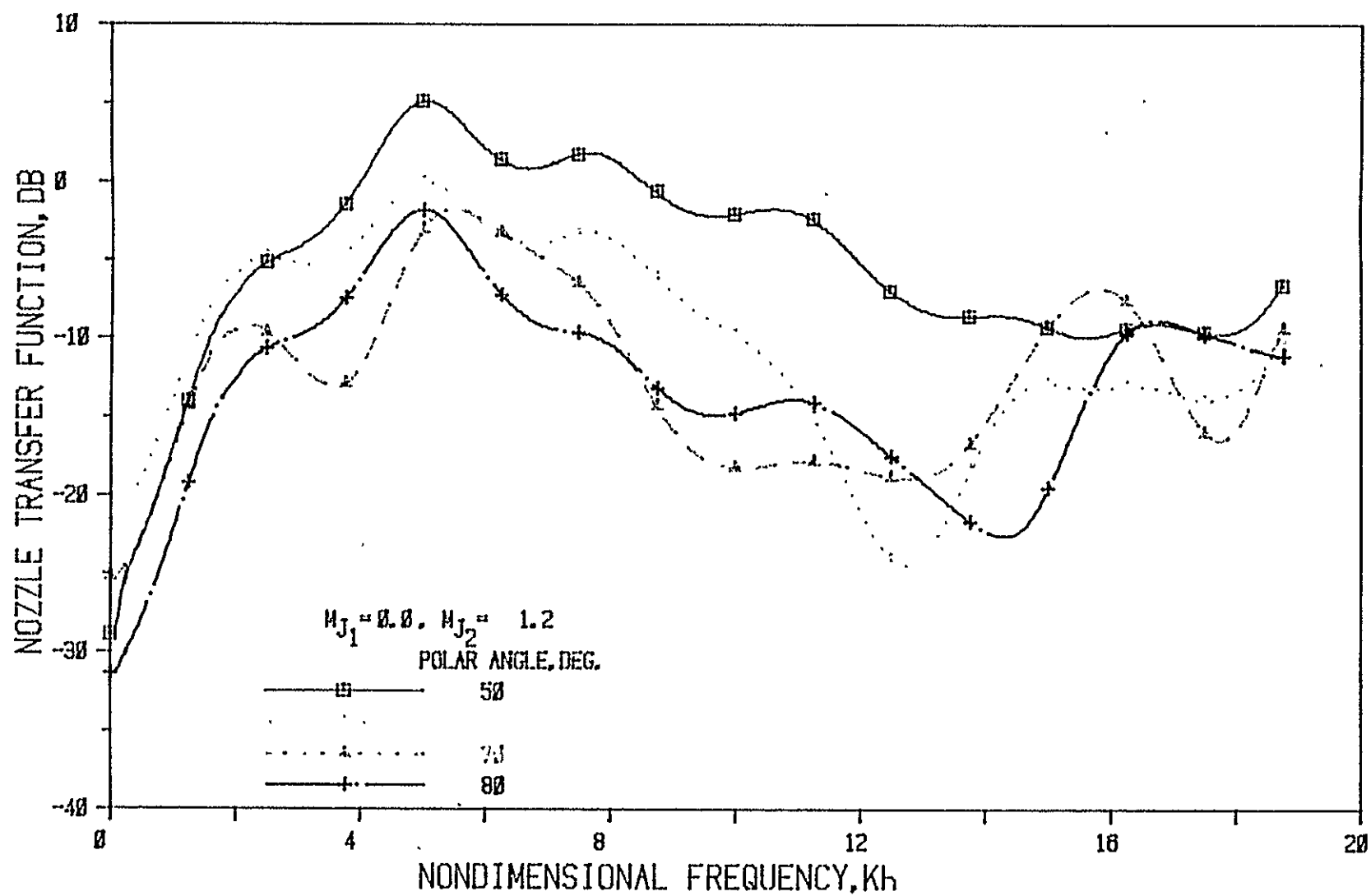


Figure 24(b) Nozzle N 1 ( $L/h = 1$ , Convergence Angle = 20 Deg.); Source At Fan

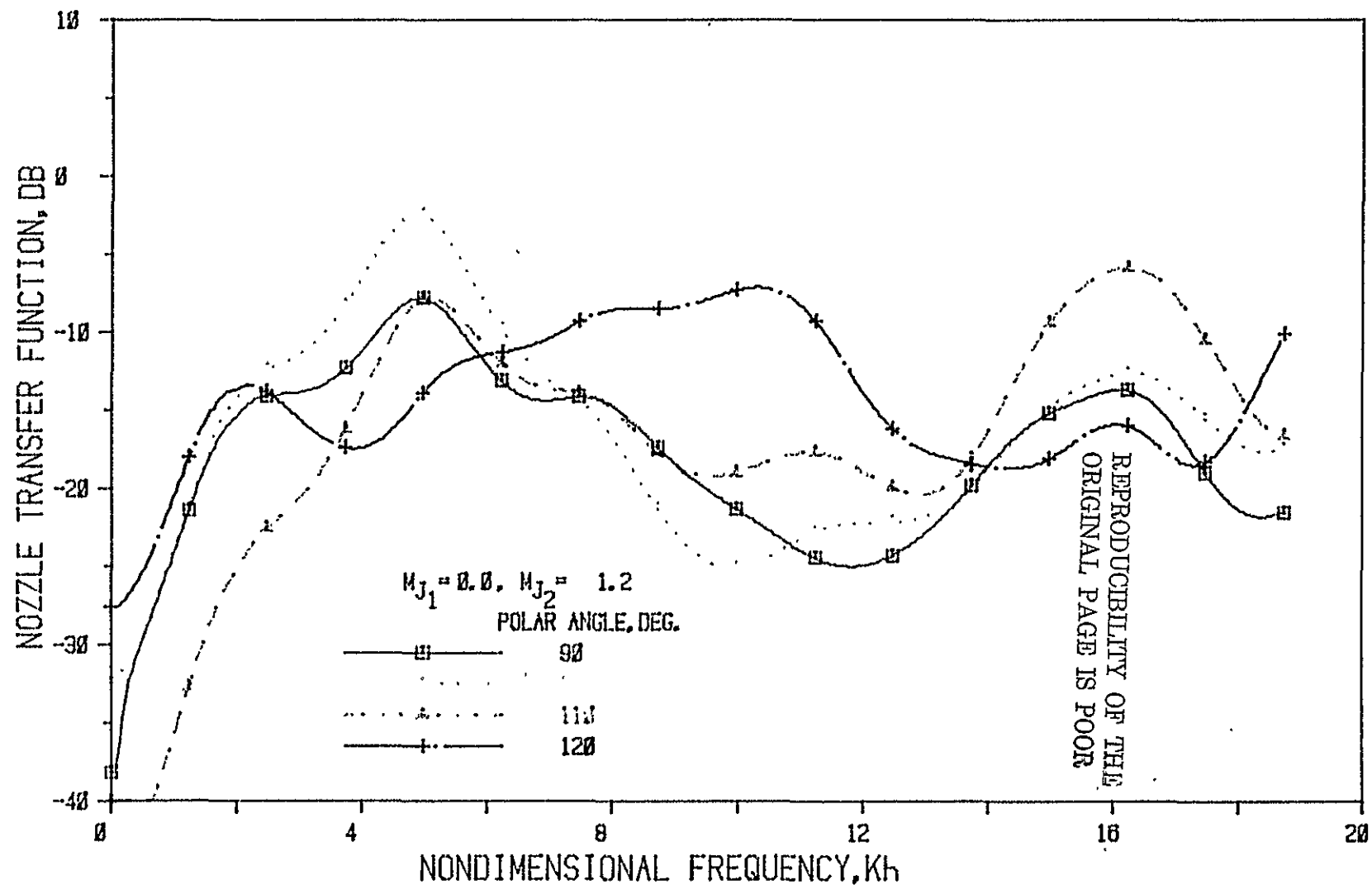


Figure 24(c) Nozzle N 1 (  $L/h = 1$ , Convergence Angle = 20 Deg.); Source At Fan



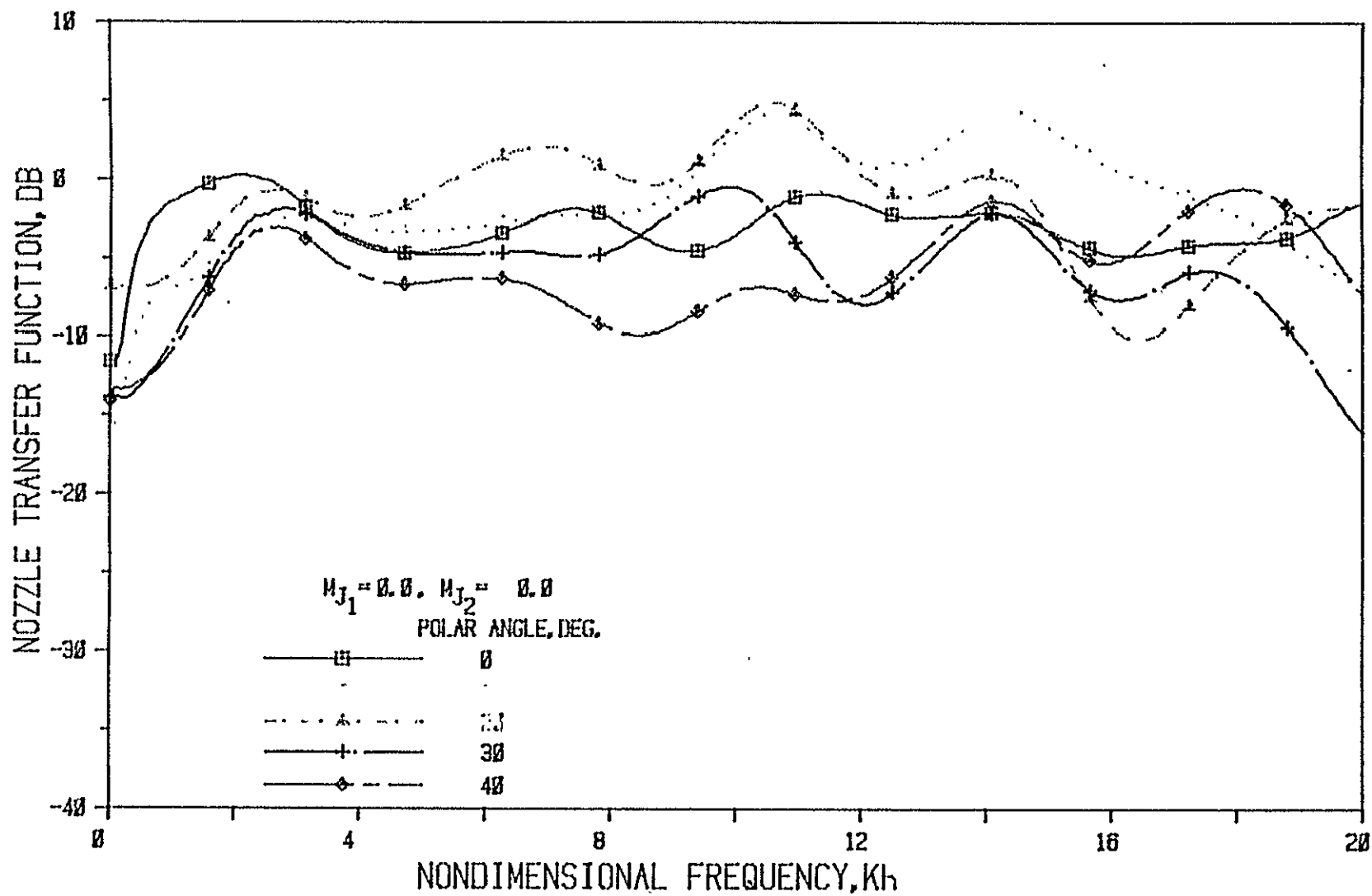


Figure 25(a) Nozzle N 2 ( $L/h = 3$ , Convergence Angle = 20 Deg.); Source At Fan

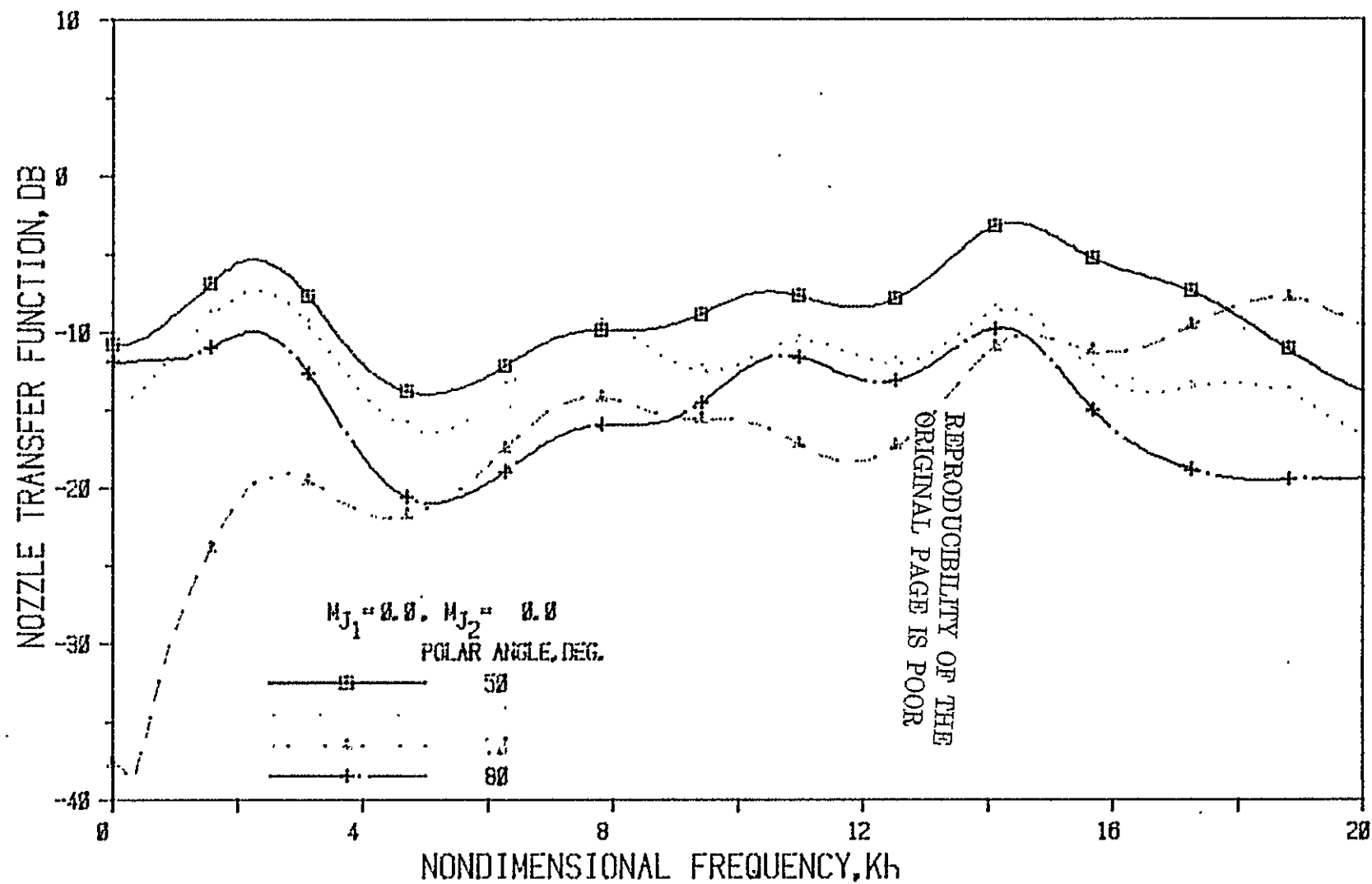


Figure 25(b) Nozzle N 2 ( $L/h = 3$ , Convergence Angle = 20 Deg.); Source At Fan

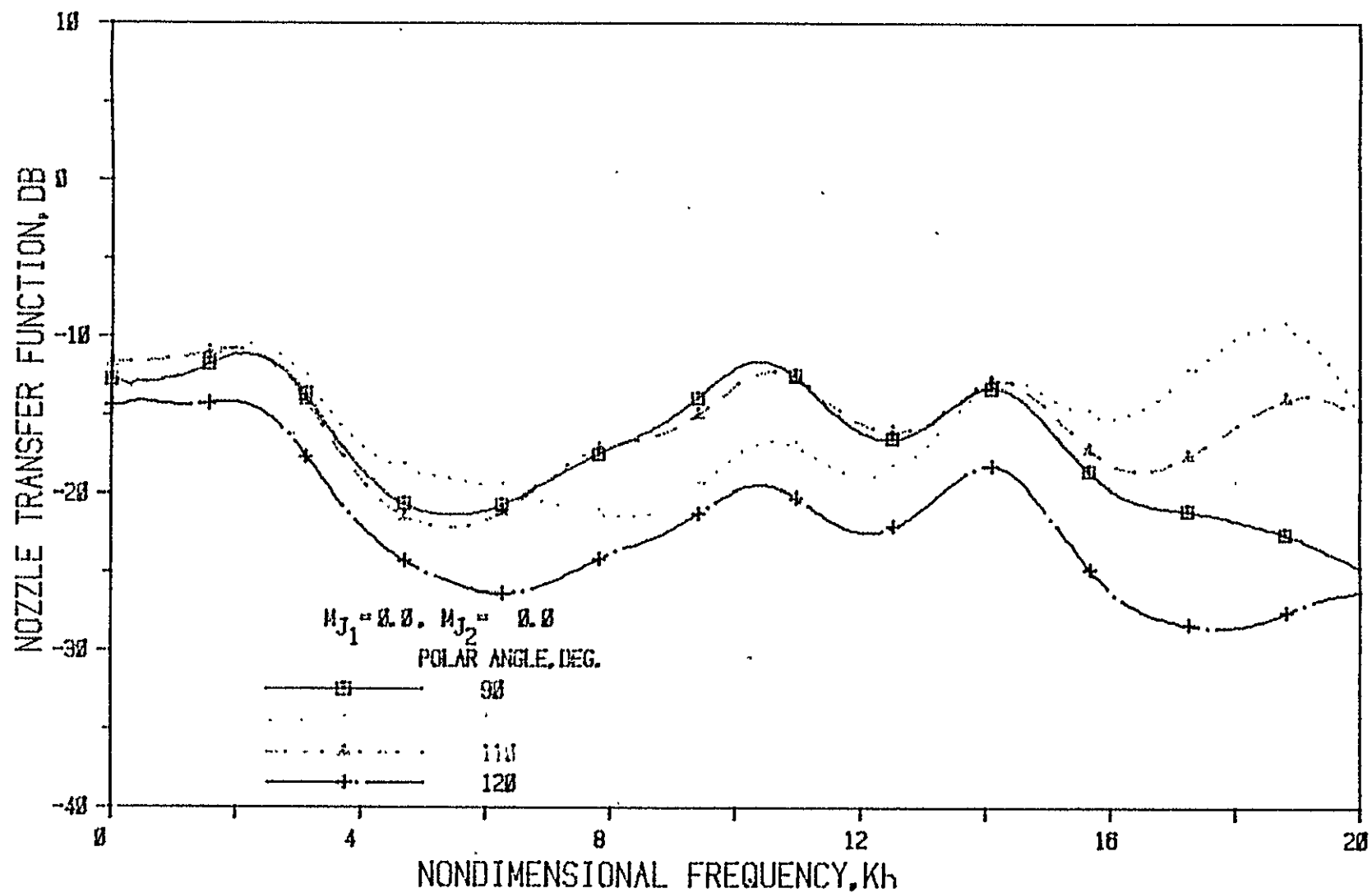


Figure 25(c) Nozzle N 2 ( $L/h = 3$ , Convergence Angle = 20 Deg.); Source At Fan

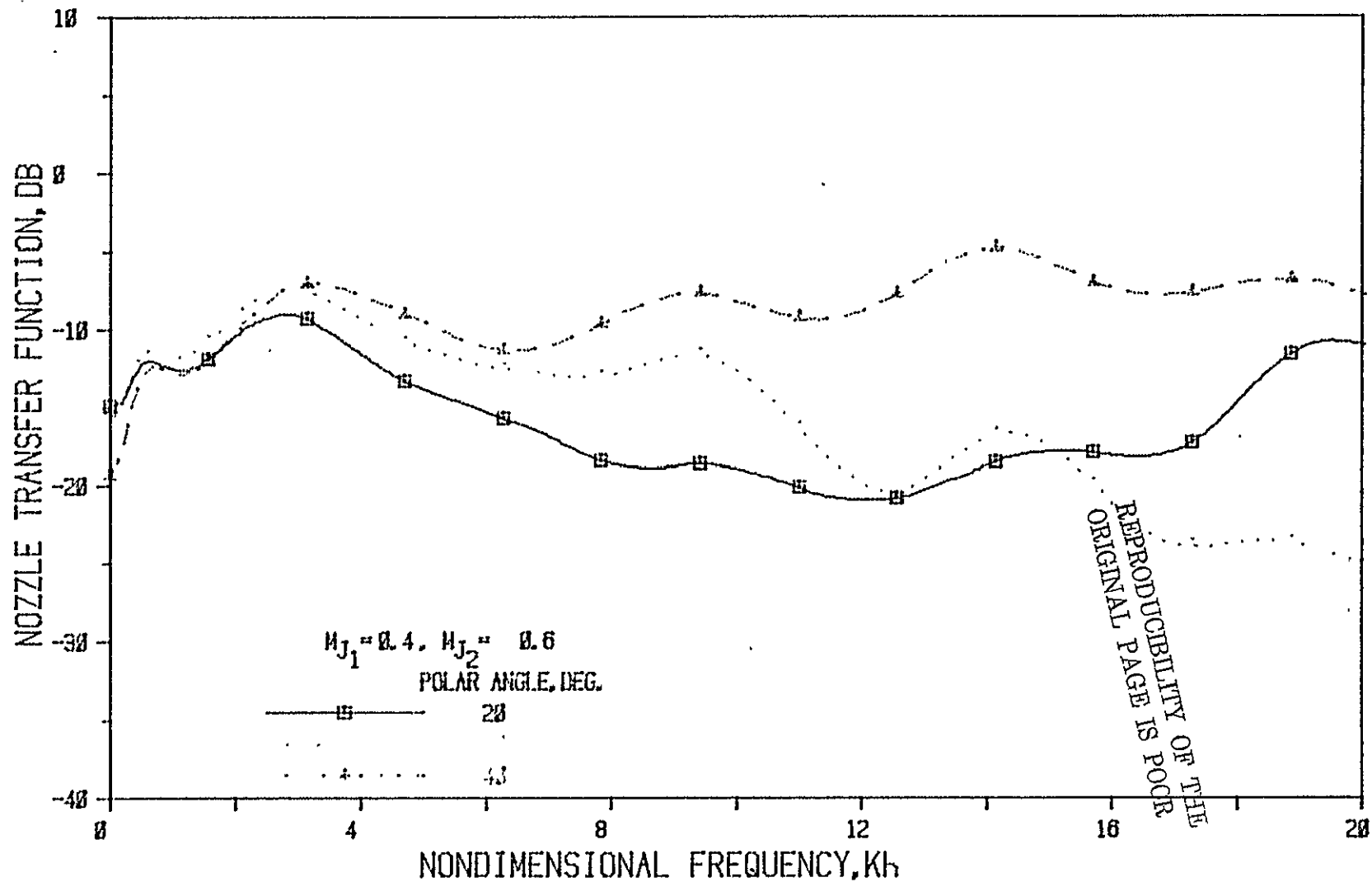


Figure 26(a) Nozzle N 2 (  $L/h = 3$ , Convergence Angle = 20 Deg.); Source At Fan

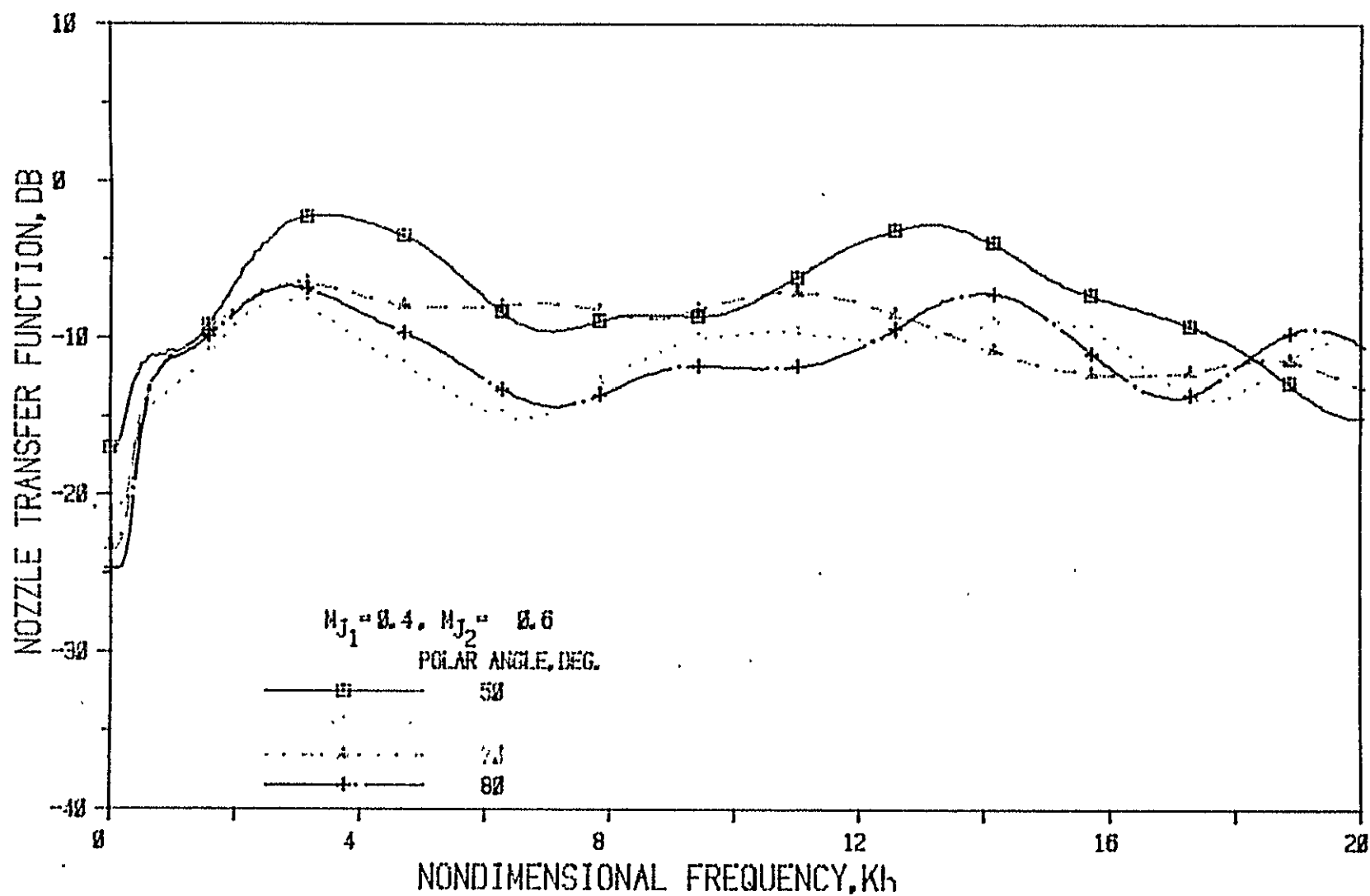


Figure 26(b) Nozzle N 2 (  $L/h = 3$ , Convergence Angle = 20 Deg. ); Source At Fan

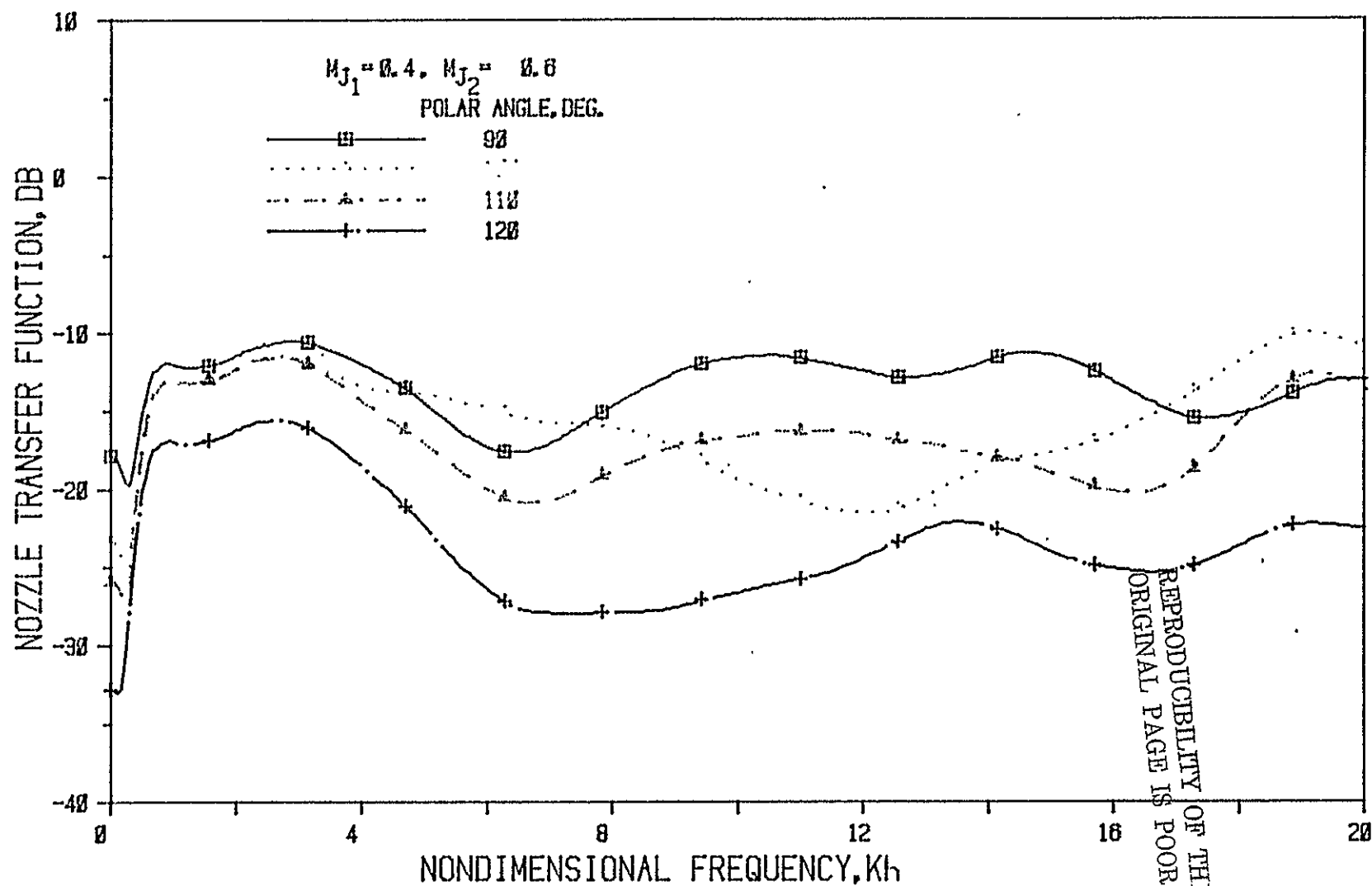


Figure 26(c) Nozzle N 2 (  $L/h = 3$ , Convergence Angle = 20 Deg.); Source At Fan

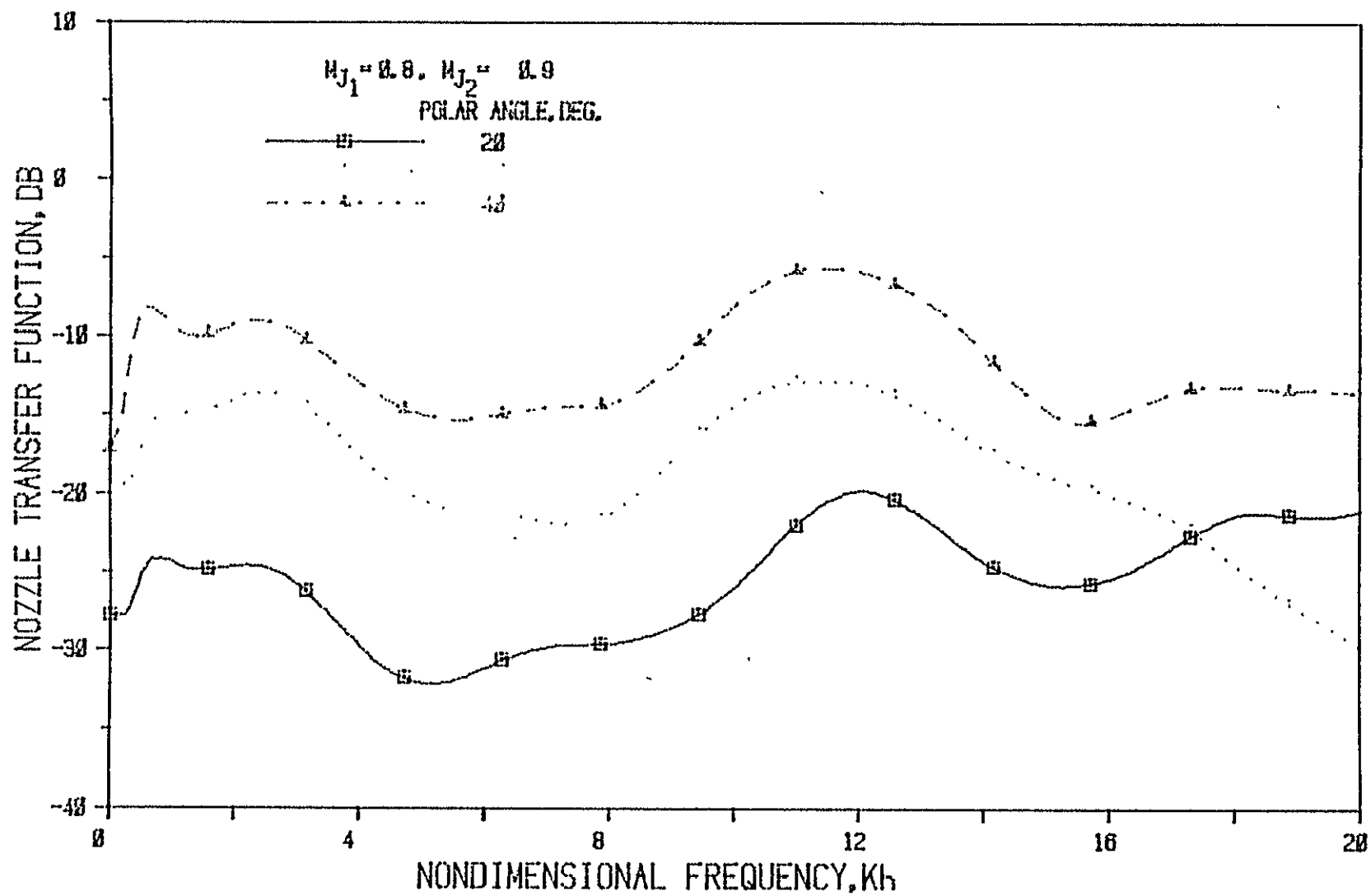


Figure 27(a) Nozzle N 2 ( $L/h = 3$ , Convergence Angle = 20 Deg.); Source At Fan

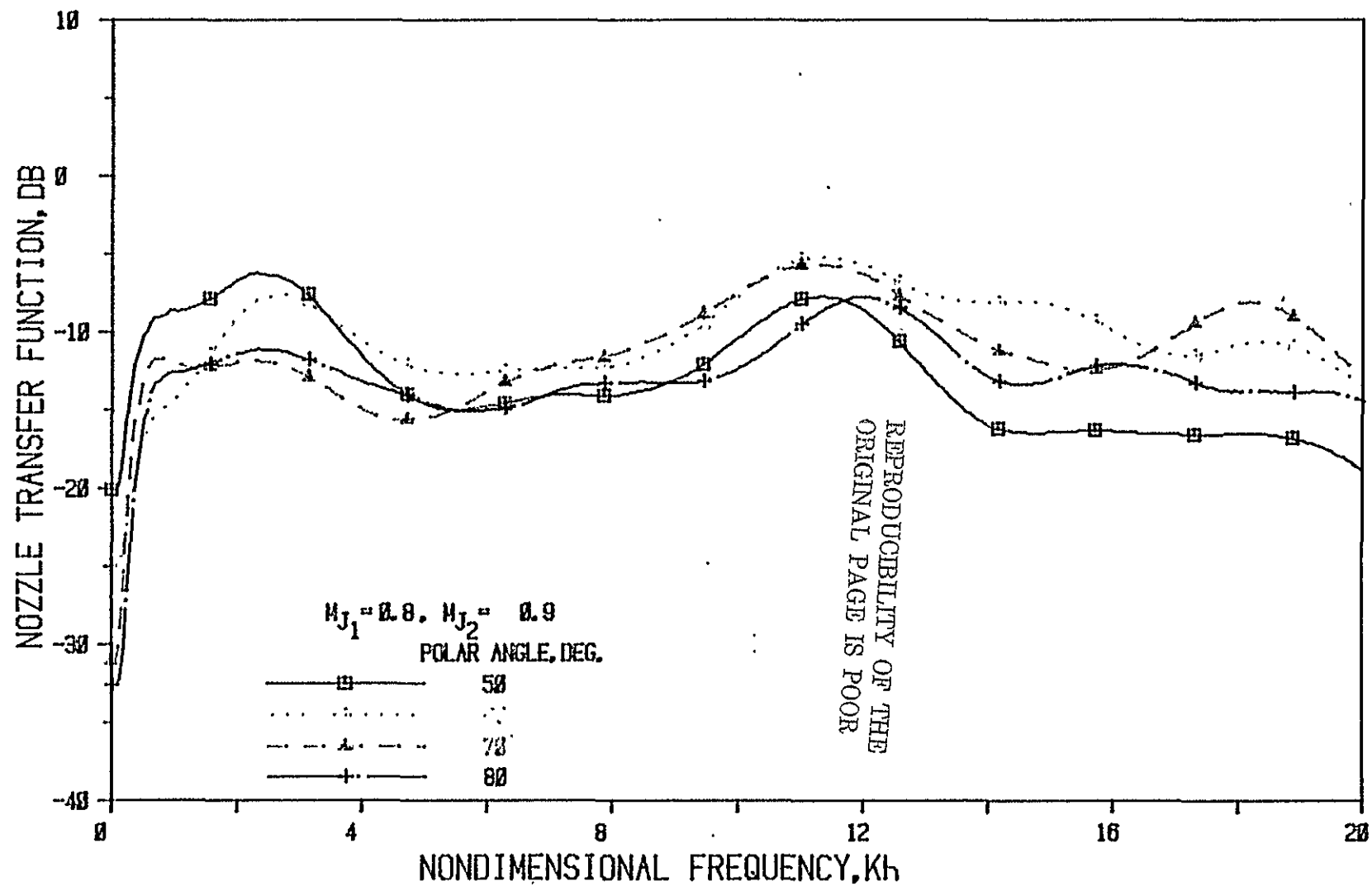


Figure 27(b) Nozzle N 2 ( $L/h = 3$ , Convergence Angle = 20 Deg.); Source At Fan



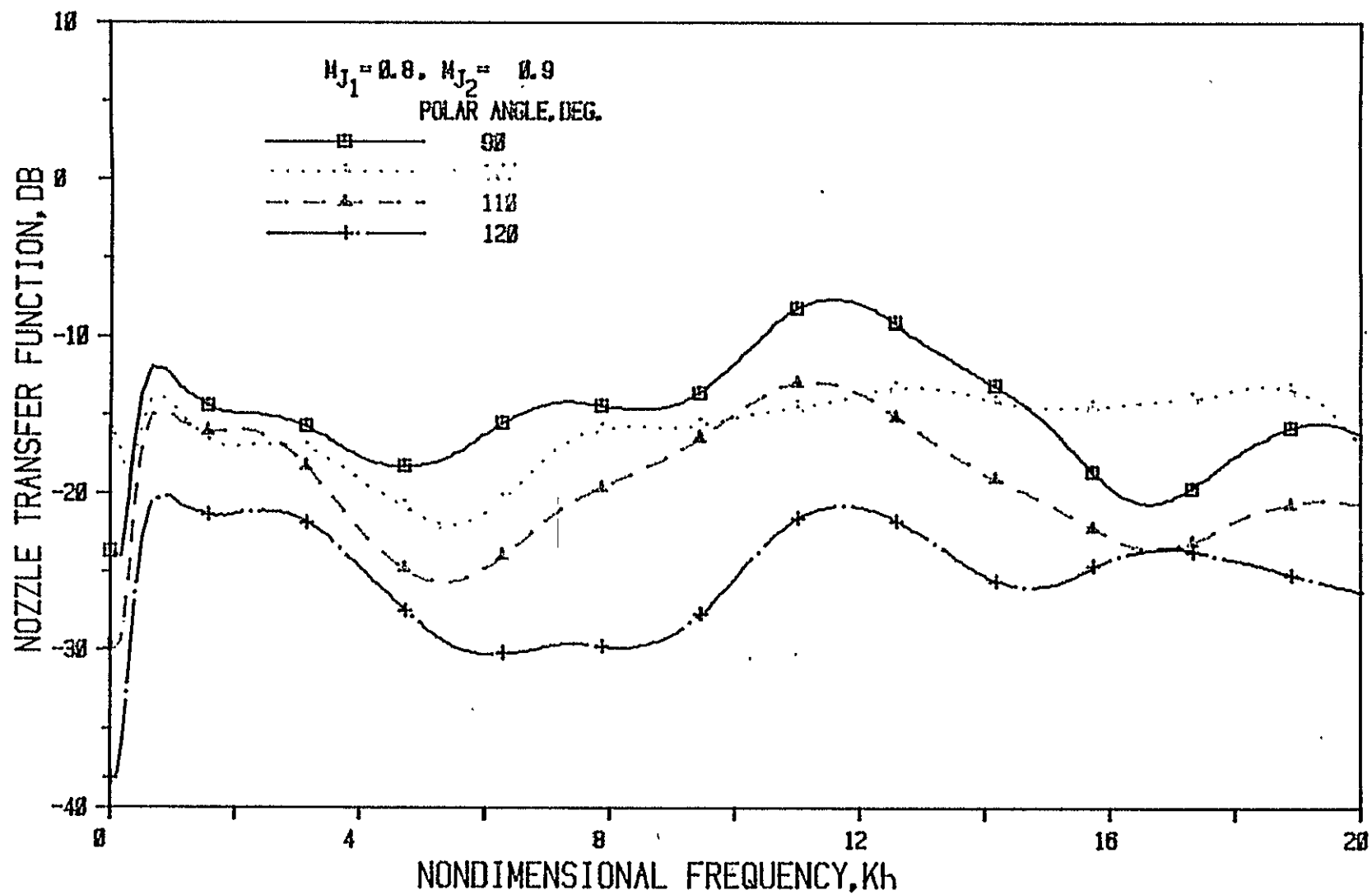


Figure 27(c) Nozzle N 2 ( $L/h = 3$ , Convergence Angle =  $20^\circ$ ); Source At Fan

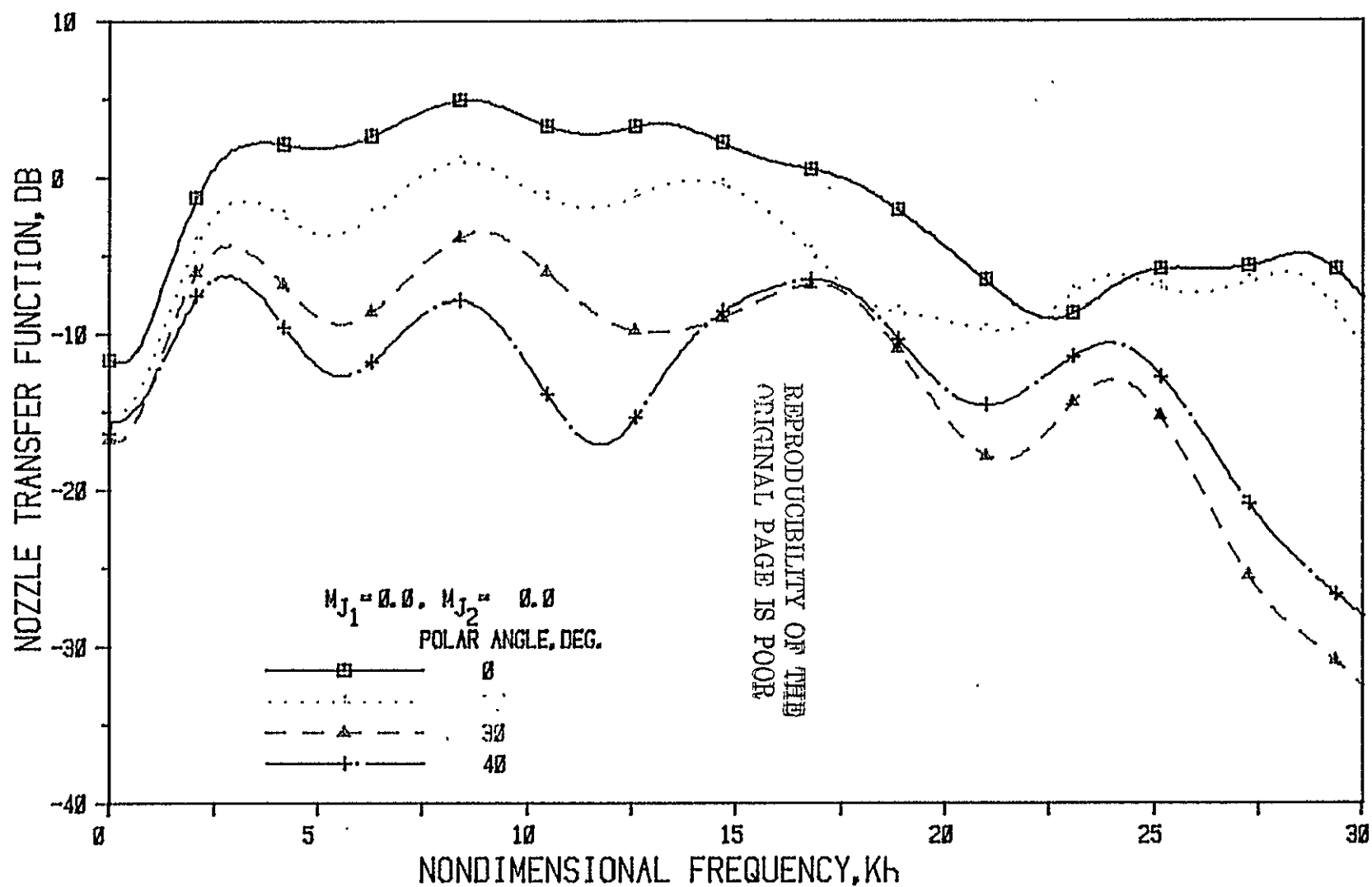


Figure 28(a) Nozzle N 3 (  $L/h = 5$ , Convergence Angle = 20 Deg.); Source At Fan

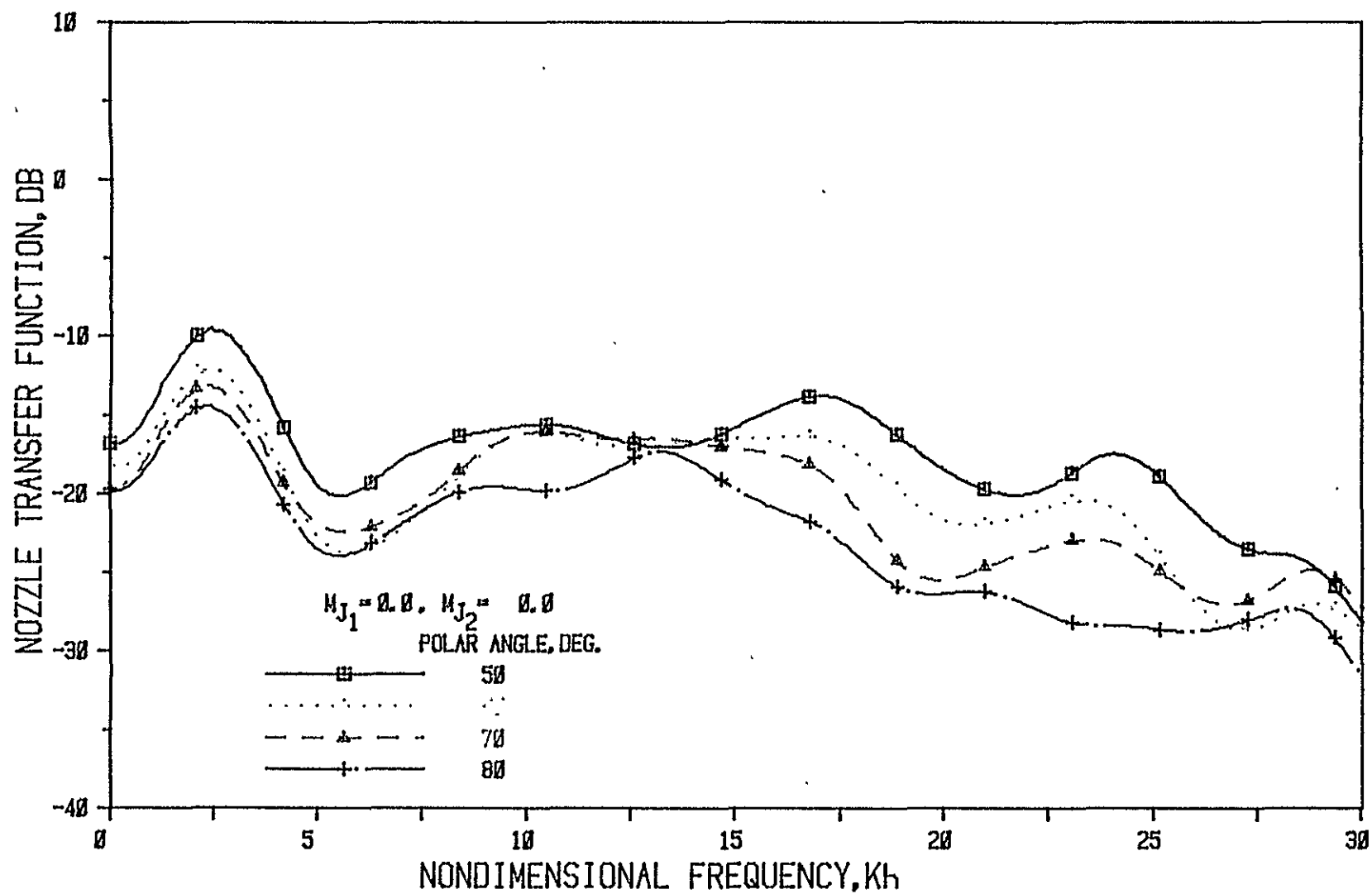


Figure 28(b) Nozzle N 3 ( $L/h = 5$ , Convergence Angle =  $20^\circ$ ); Source At Fan

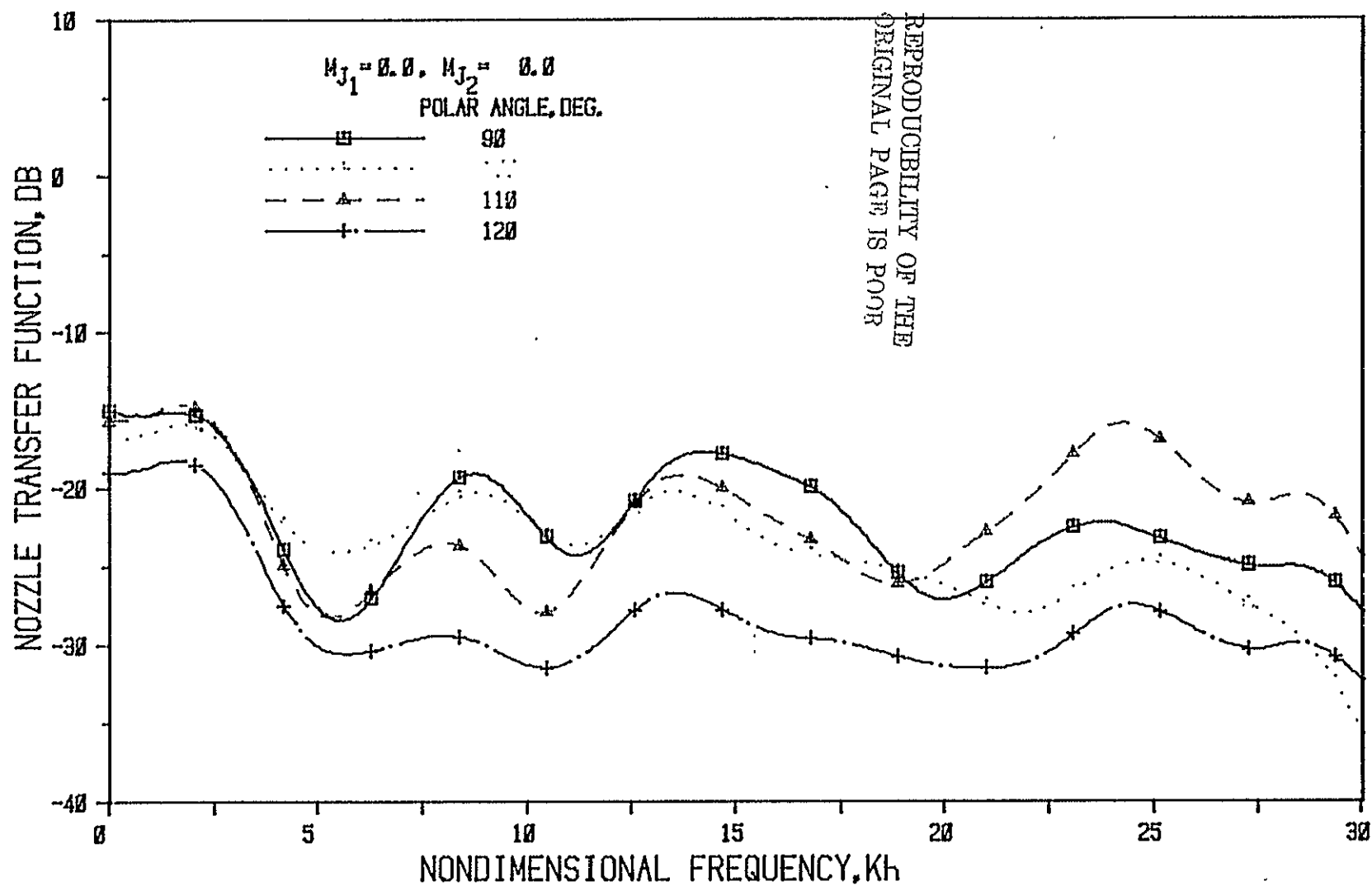


Figure 28(c) Nozzle N 3 (  $L/h = 5$ , Convergence Angle = 20 Deg.); Source At Fan

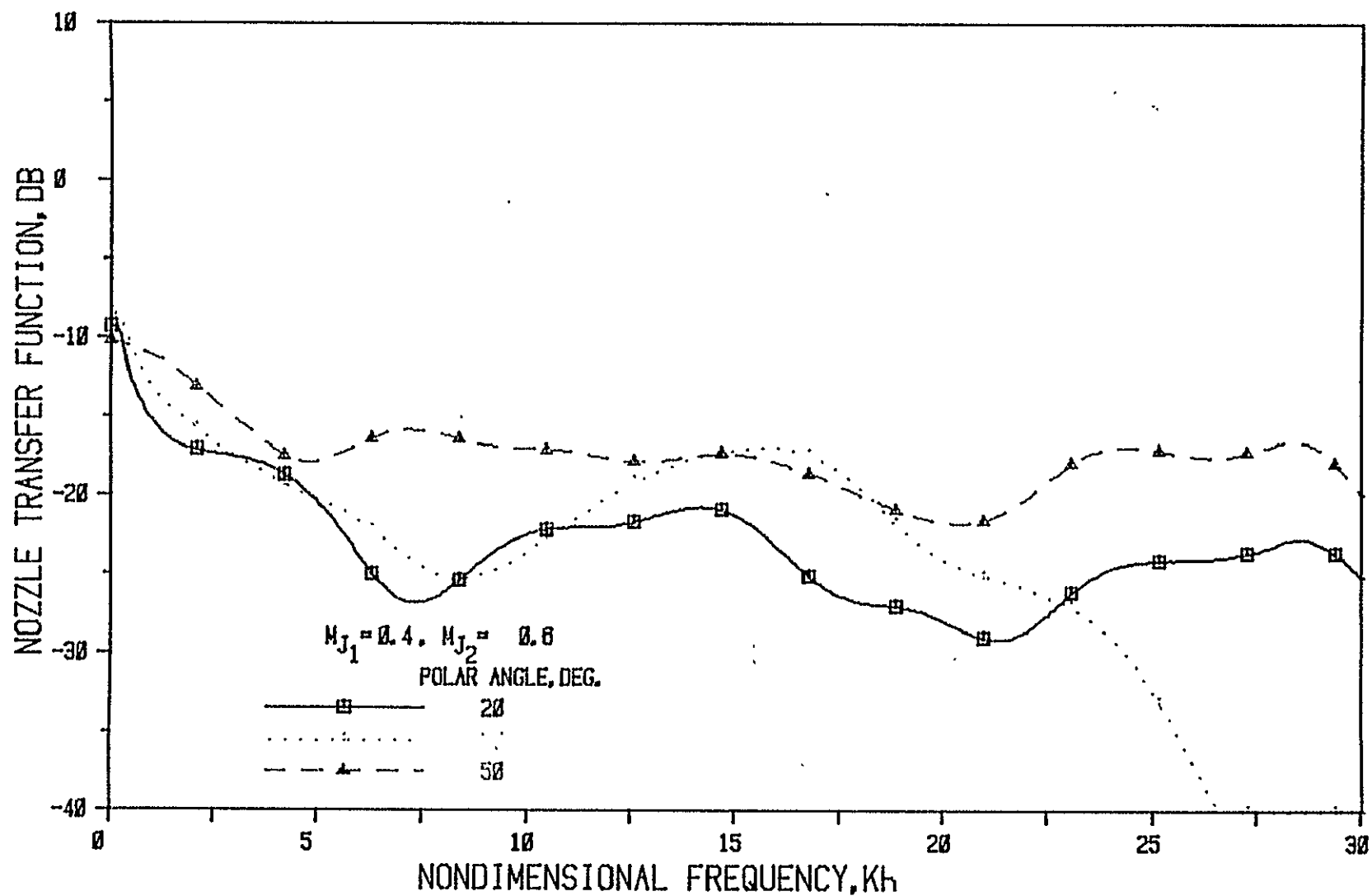


Figure 29(a) Nozzle N 3 ( $L/h = 5$ , Convergence Angle = 20 Deg.); Source At Fan

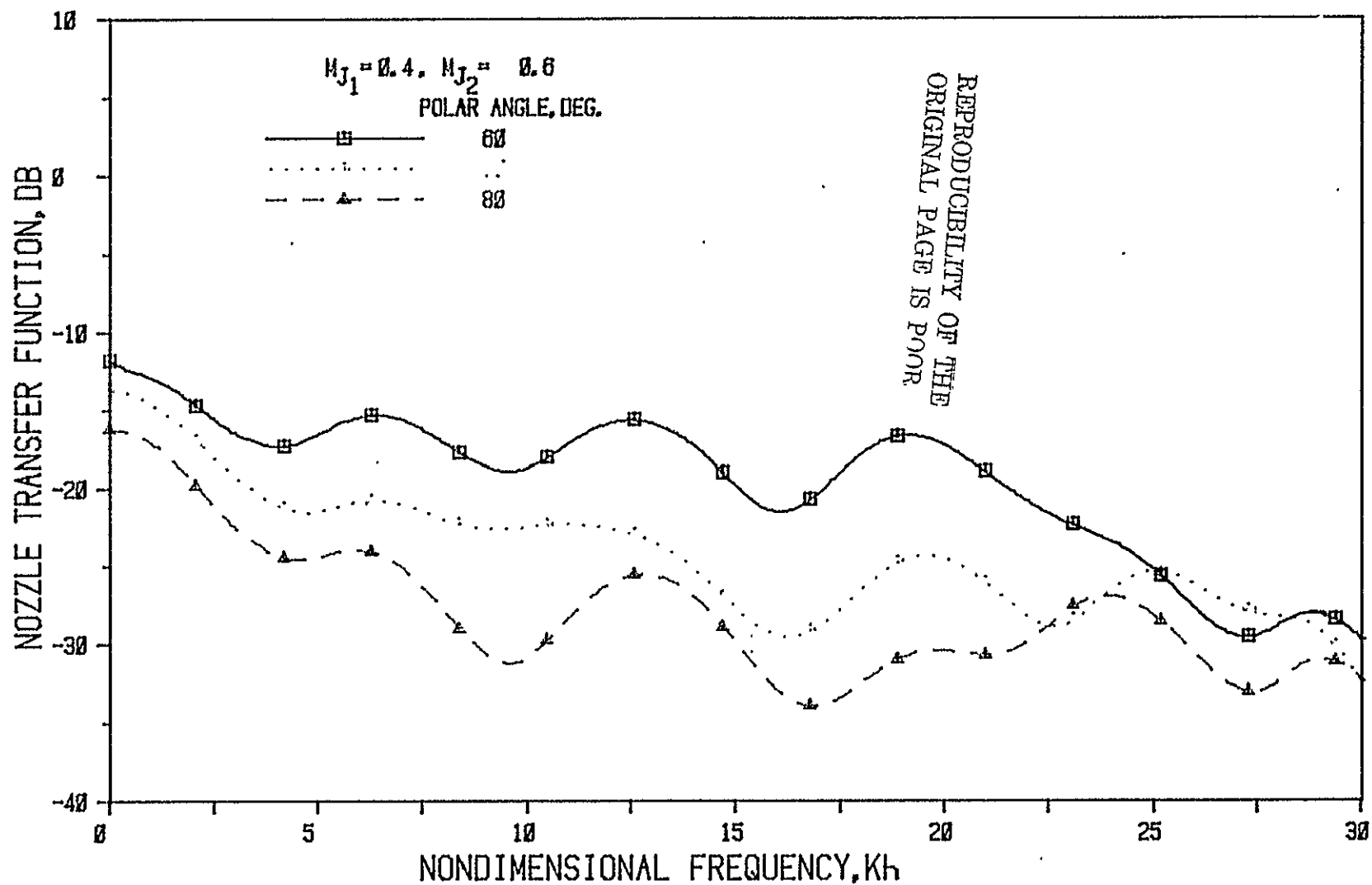


Figure 29(b) Nozzle N 3 (  $L/h = 5$ , Convergence Angle = 20 Deg.); Source At Fan

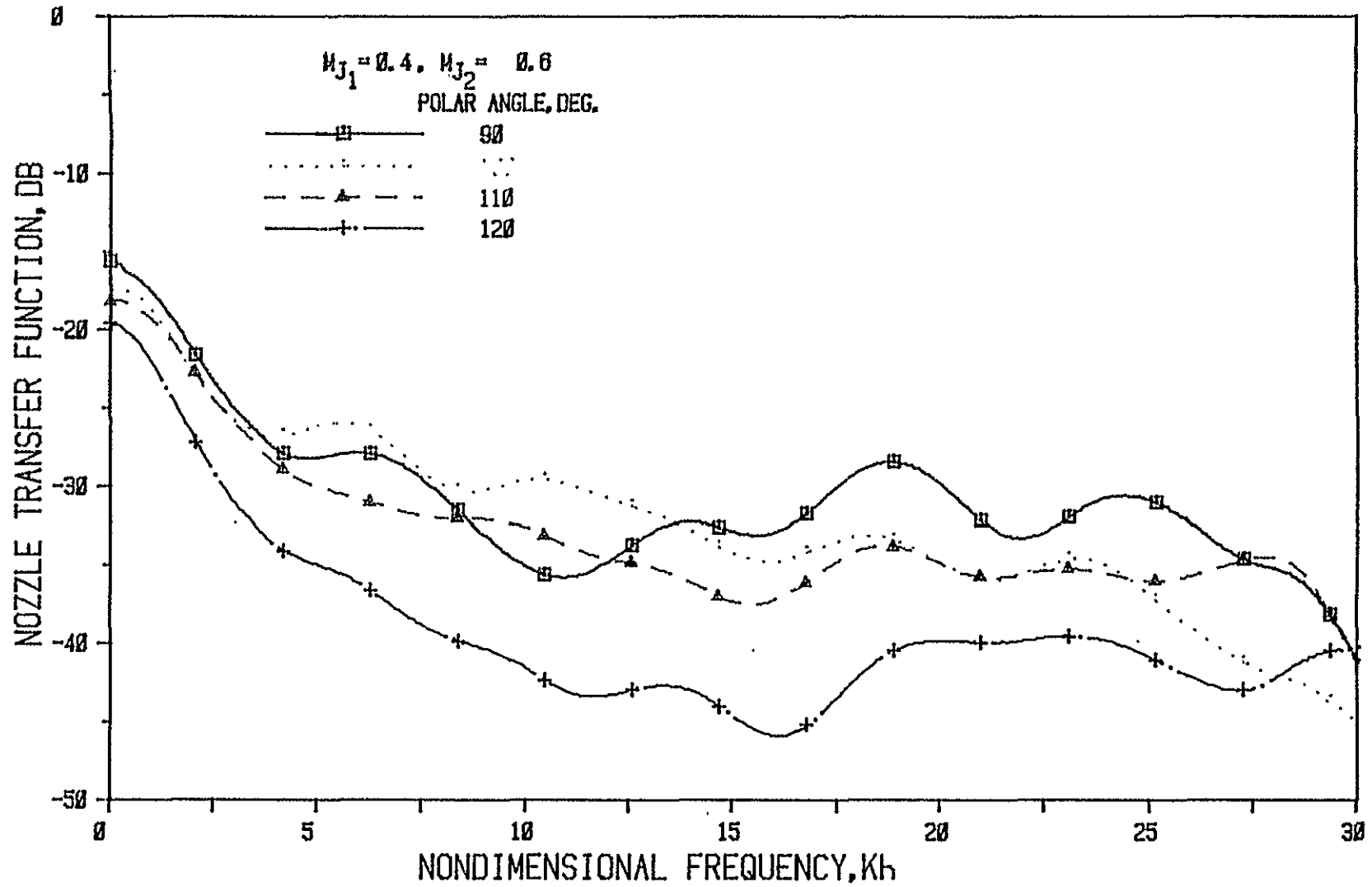


Figure 29(c) Nozzle N 3 ( $L/h = 5$ , Convergence Angle = 20 Deg.); Source At Fan

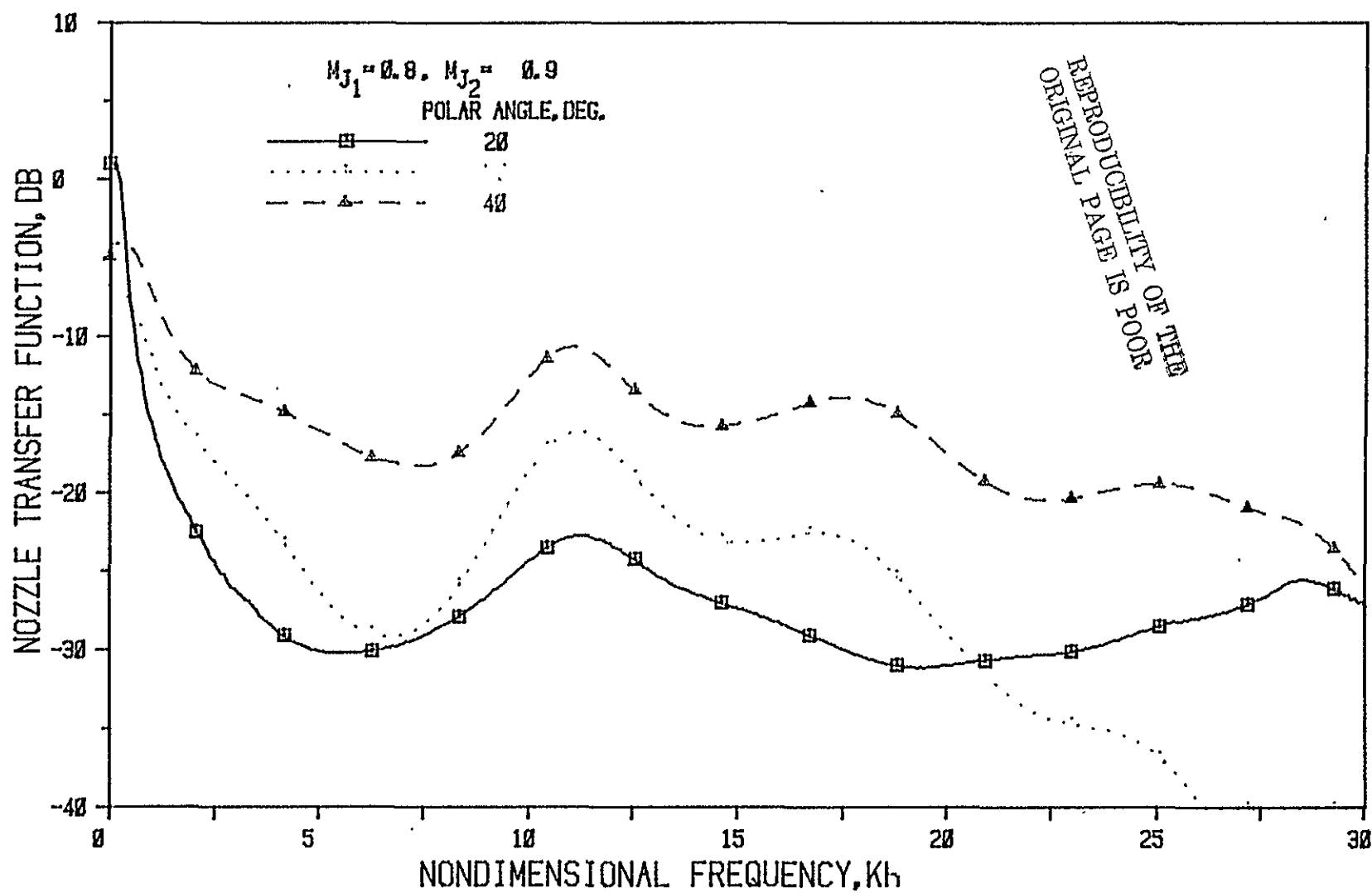


Figure 30(a) Nozzle N 3 ( $L/h = 5$ , Convergence Angle = 20 Deg.); Source At Fan



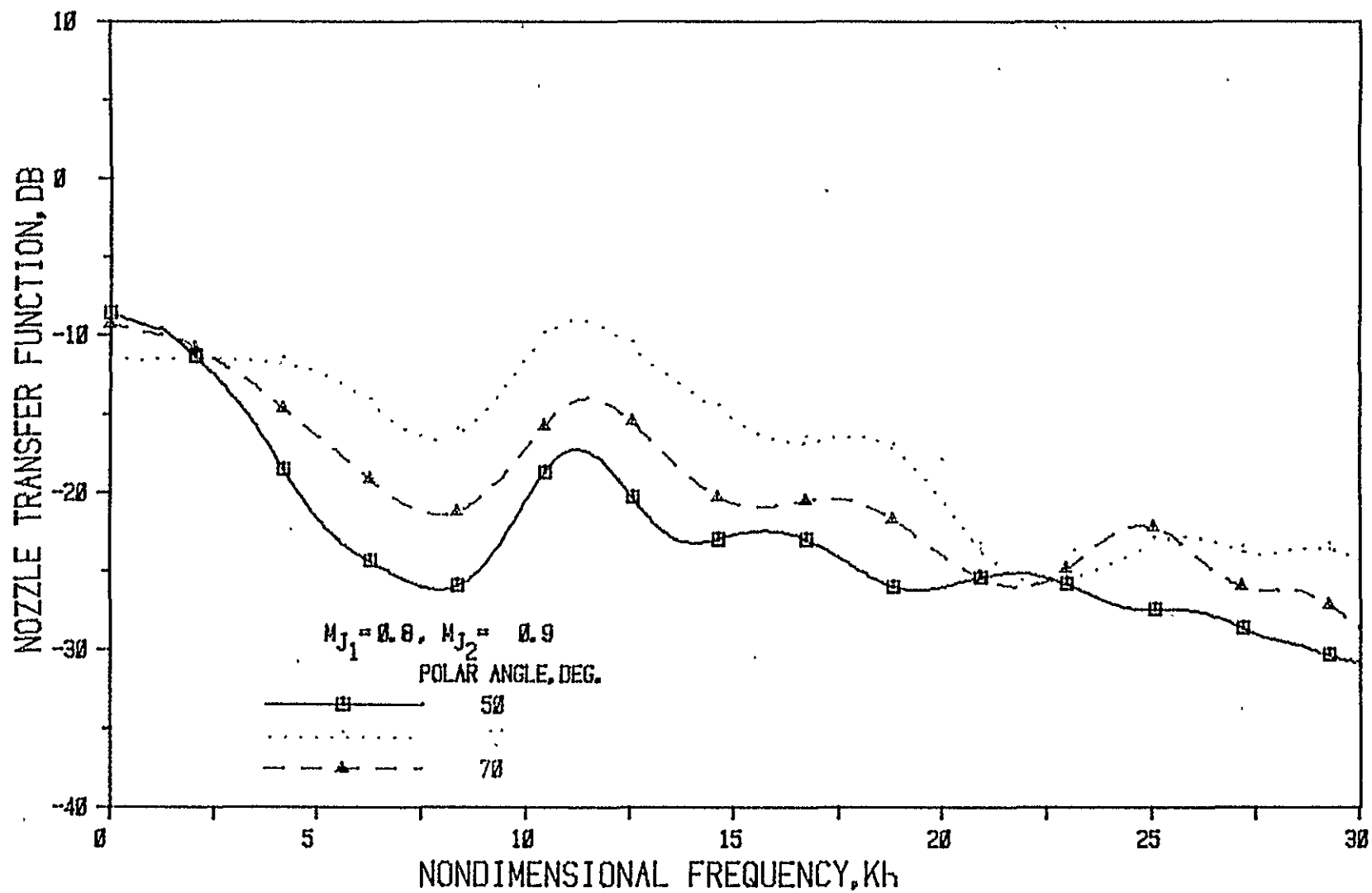


Figure 30(b) Nozzle N 3 ( $L/h = 5$ , Convergence Angle = 20 Deg.); Source At Fan

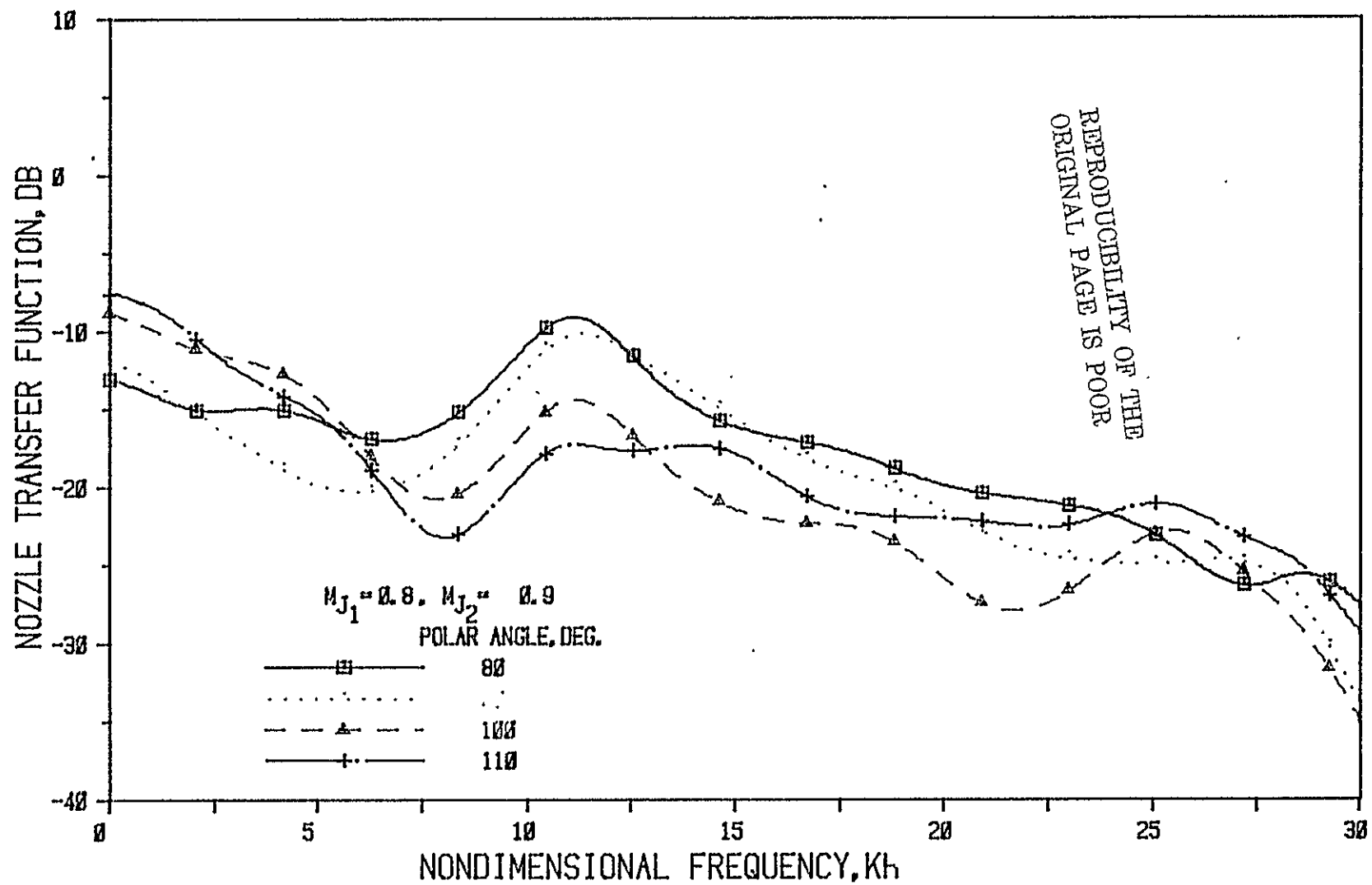


Figure 30(c) Nozzle N 3 ( $L/h = 5$ , Convergence Angle =  $20^\circ$ ); Source At Fan

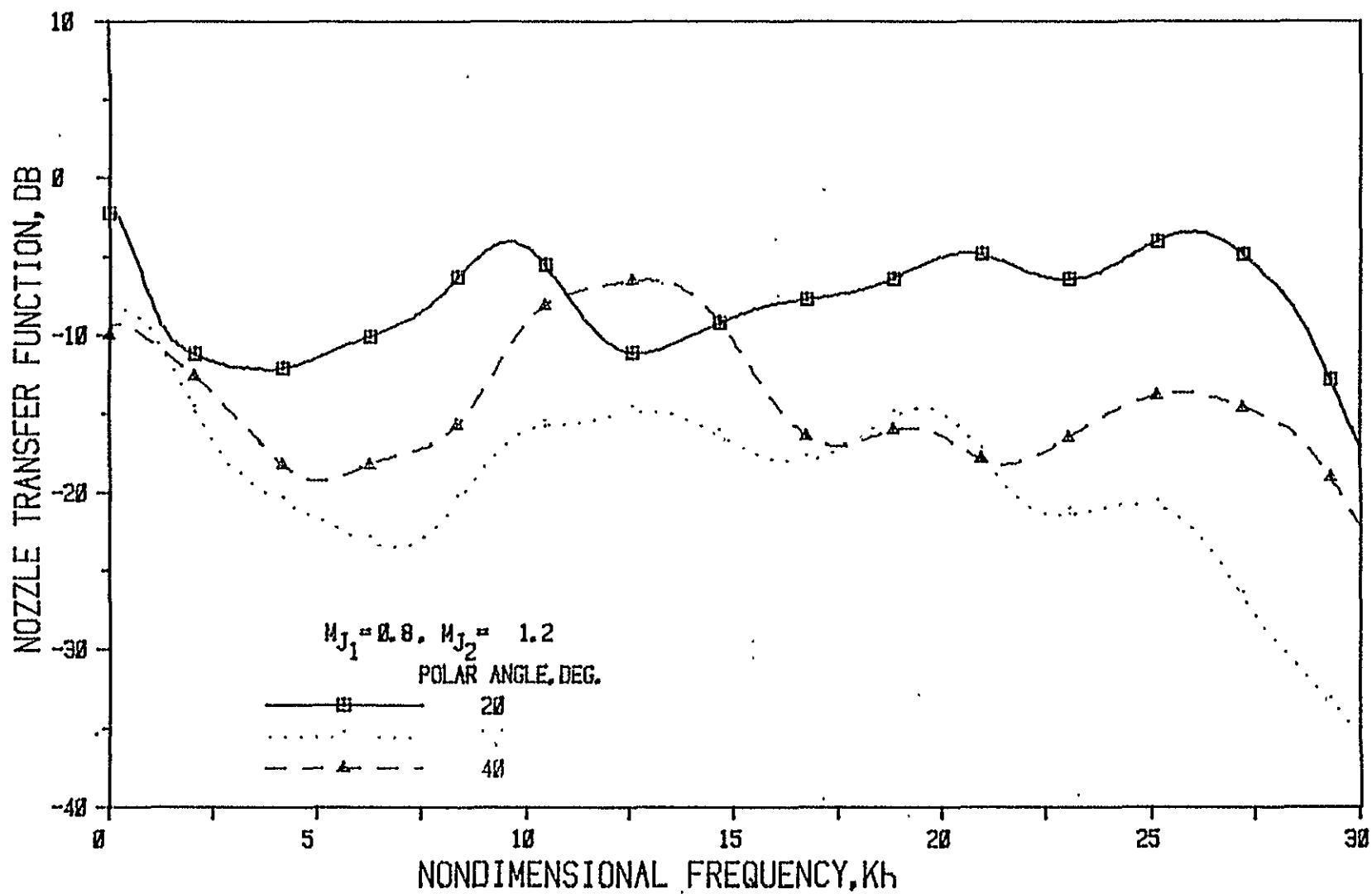


Figure 31(a) Nozzle N 3 (  $L/h = 5$ , Convergence Angle = 20 Deg.); Source At Fan

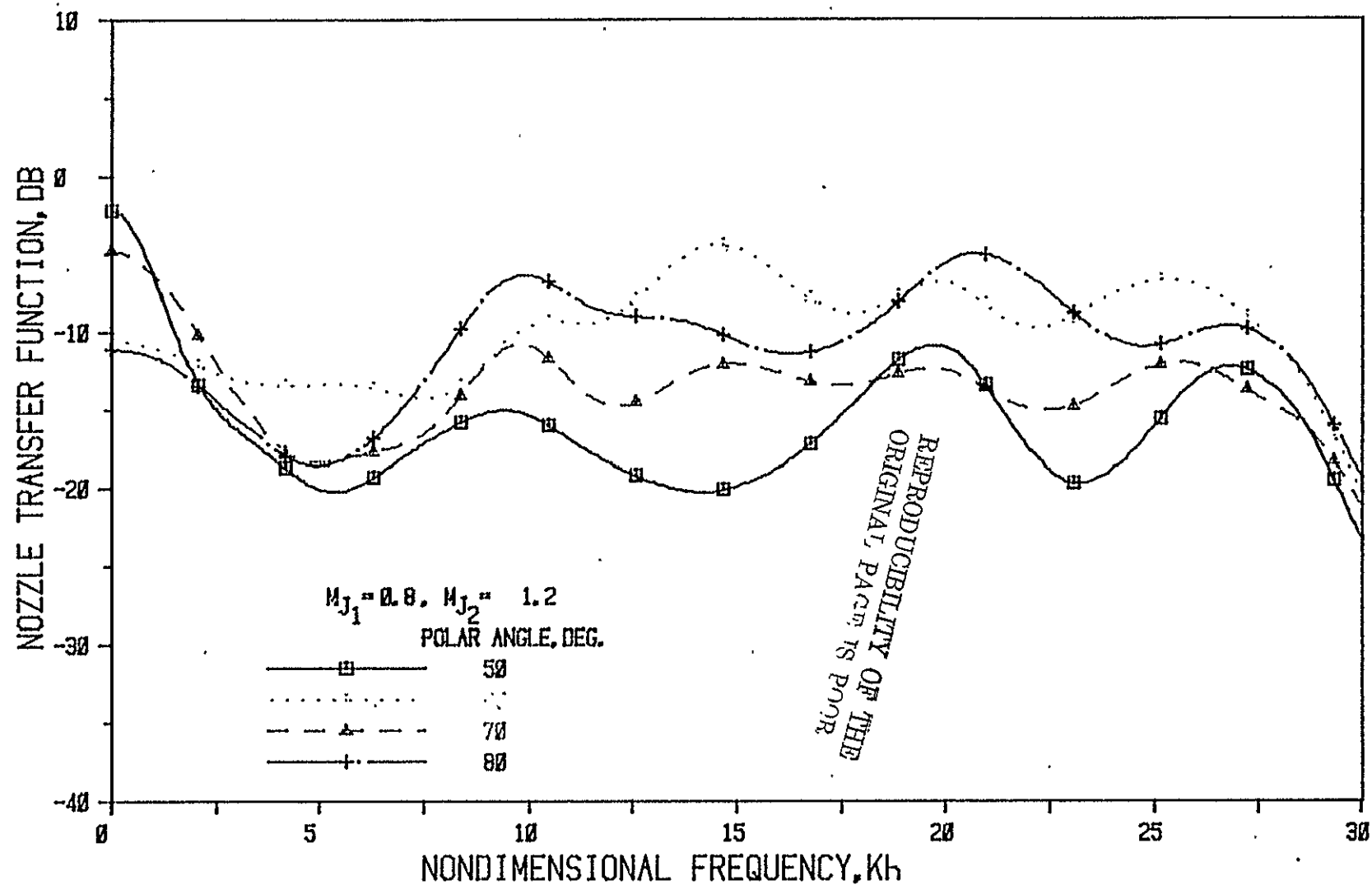


Figure 31(b) Nozzle N 3 (  $L/h = 5$ , Convergence Angle =  $20^\circ$  ); Source At Fan

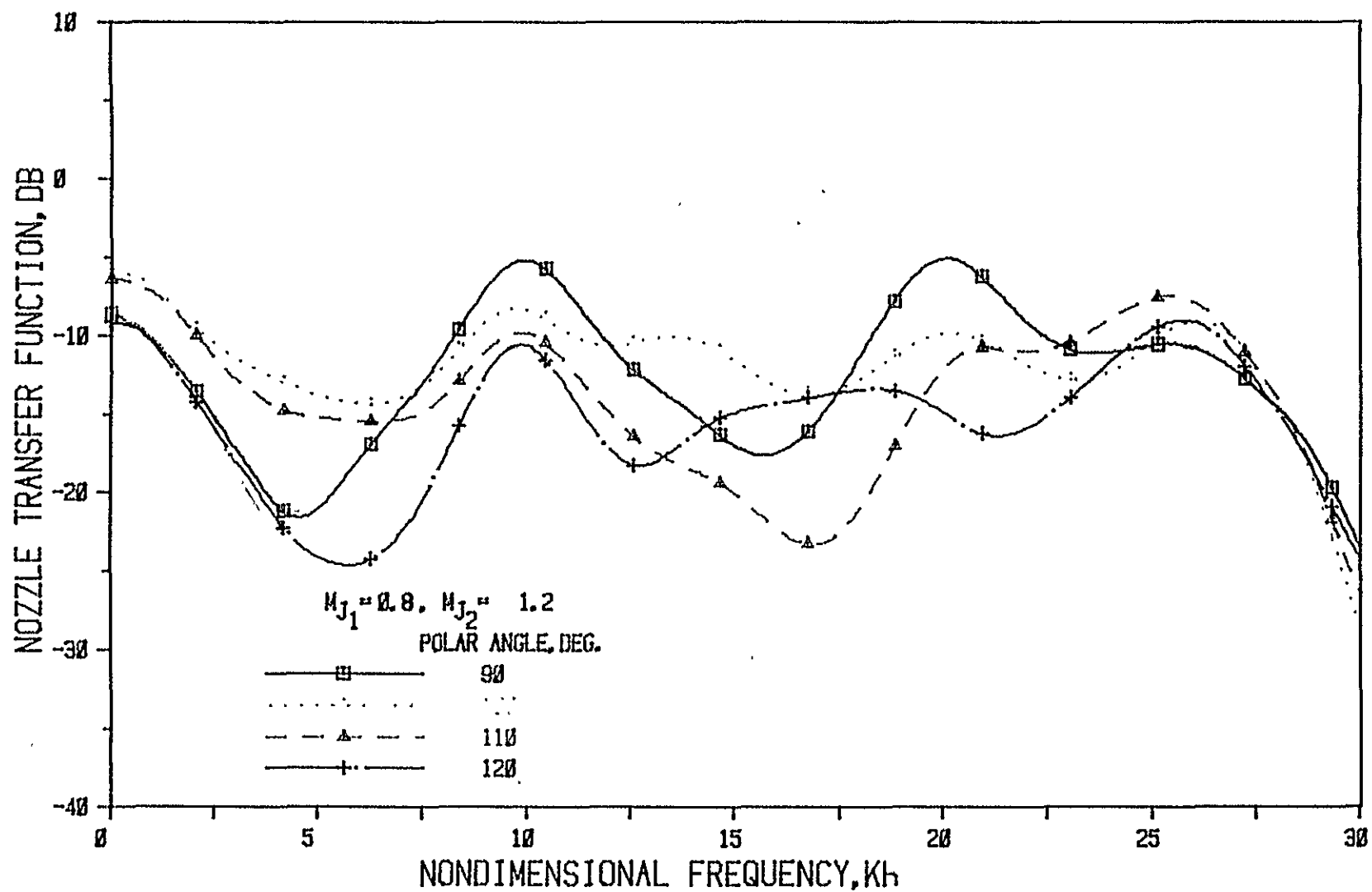


Figure 31(c) Nozzle N 3 ( $L/h = 5$ , Convergence Angle = 20 Deg.); Source At Fan

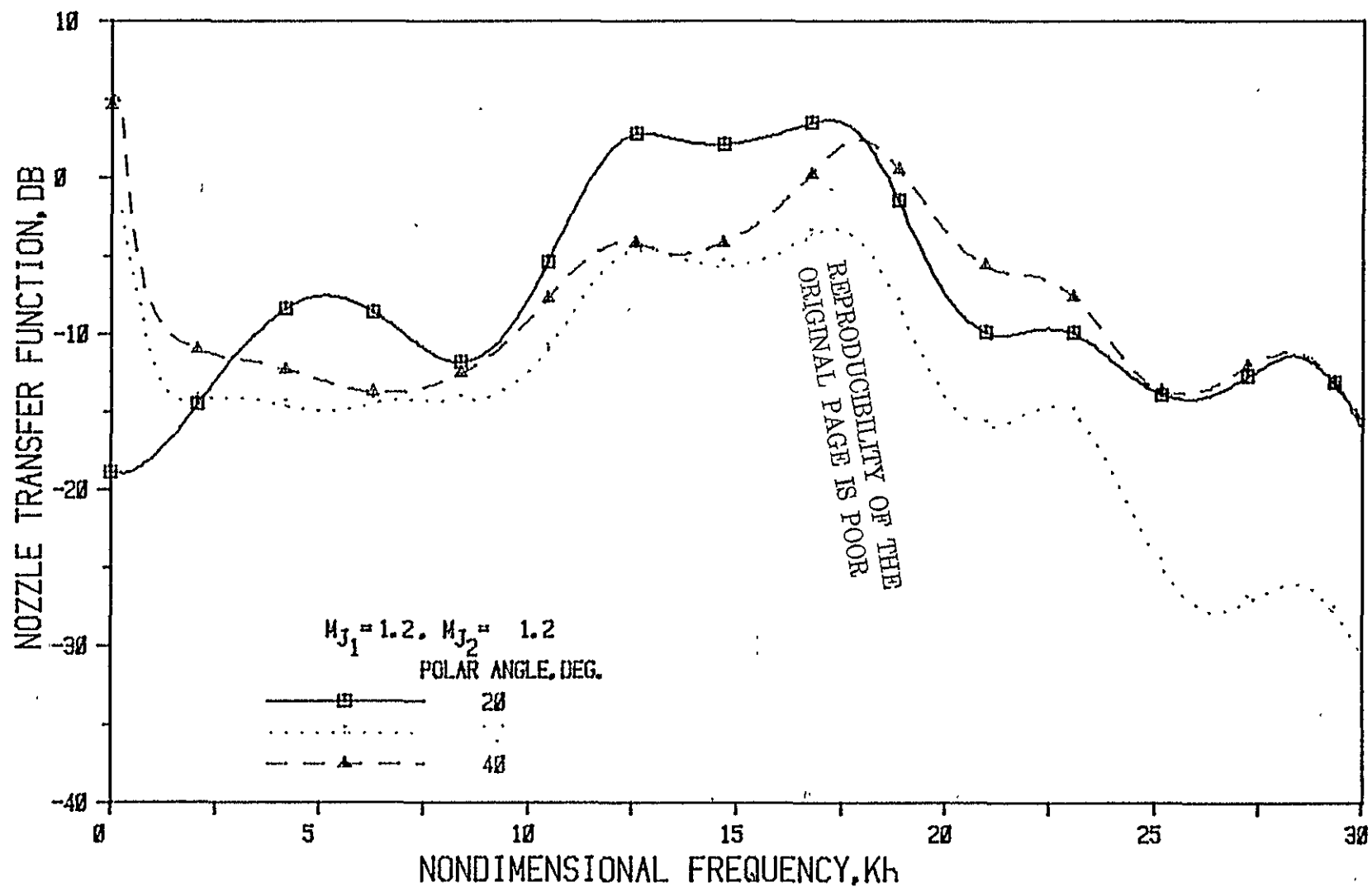


Figure 32(a) Nozzle N 3 (  $L/h = 5$ , Convergence Angle = 20 Deg.); Source At Fan

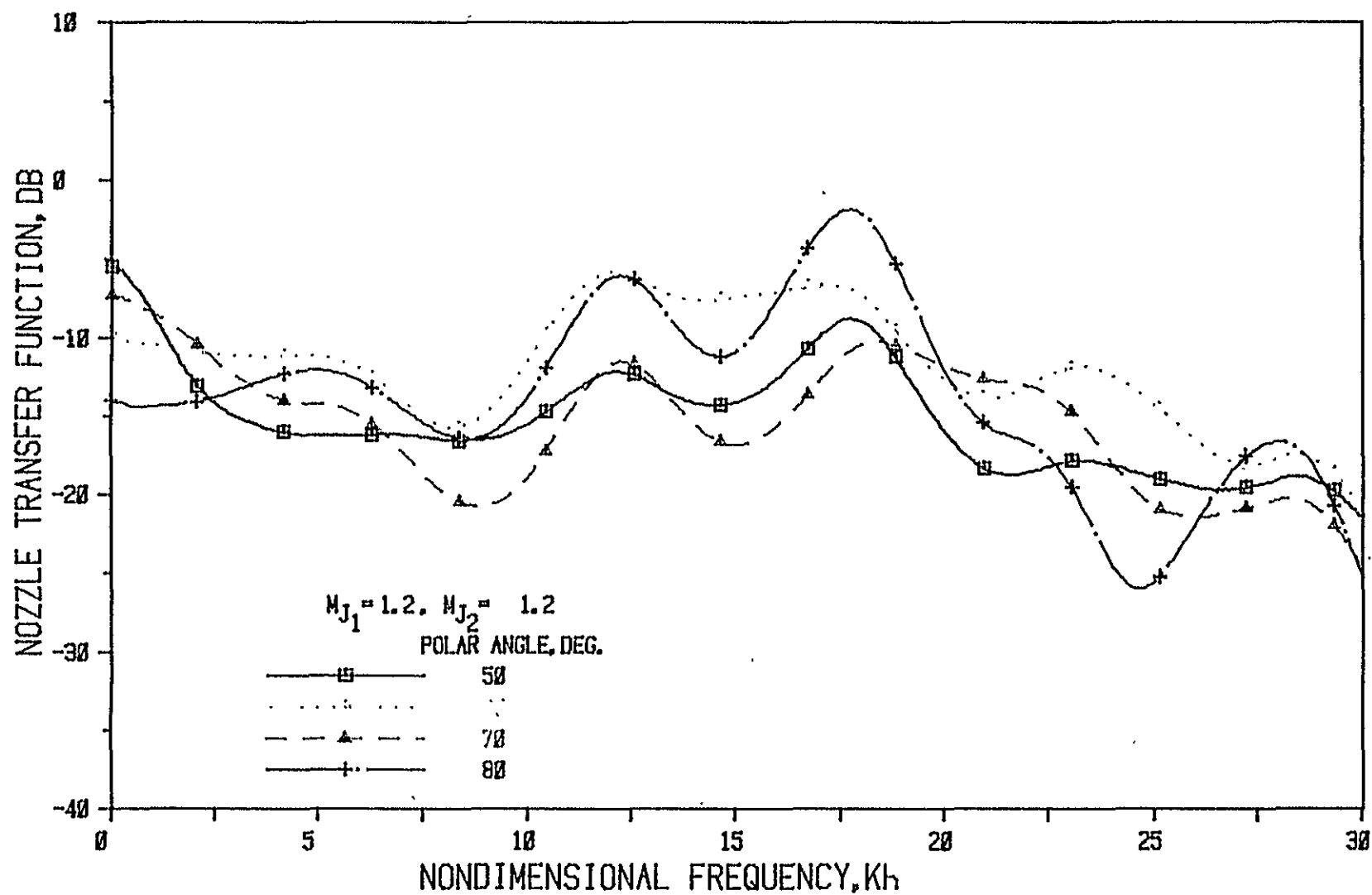


Figure 32(b) Nozzle N 3 (  $L/h = 5$ , Convergence Angle = 20 Deg.); Source At Fan

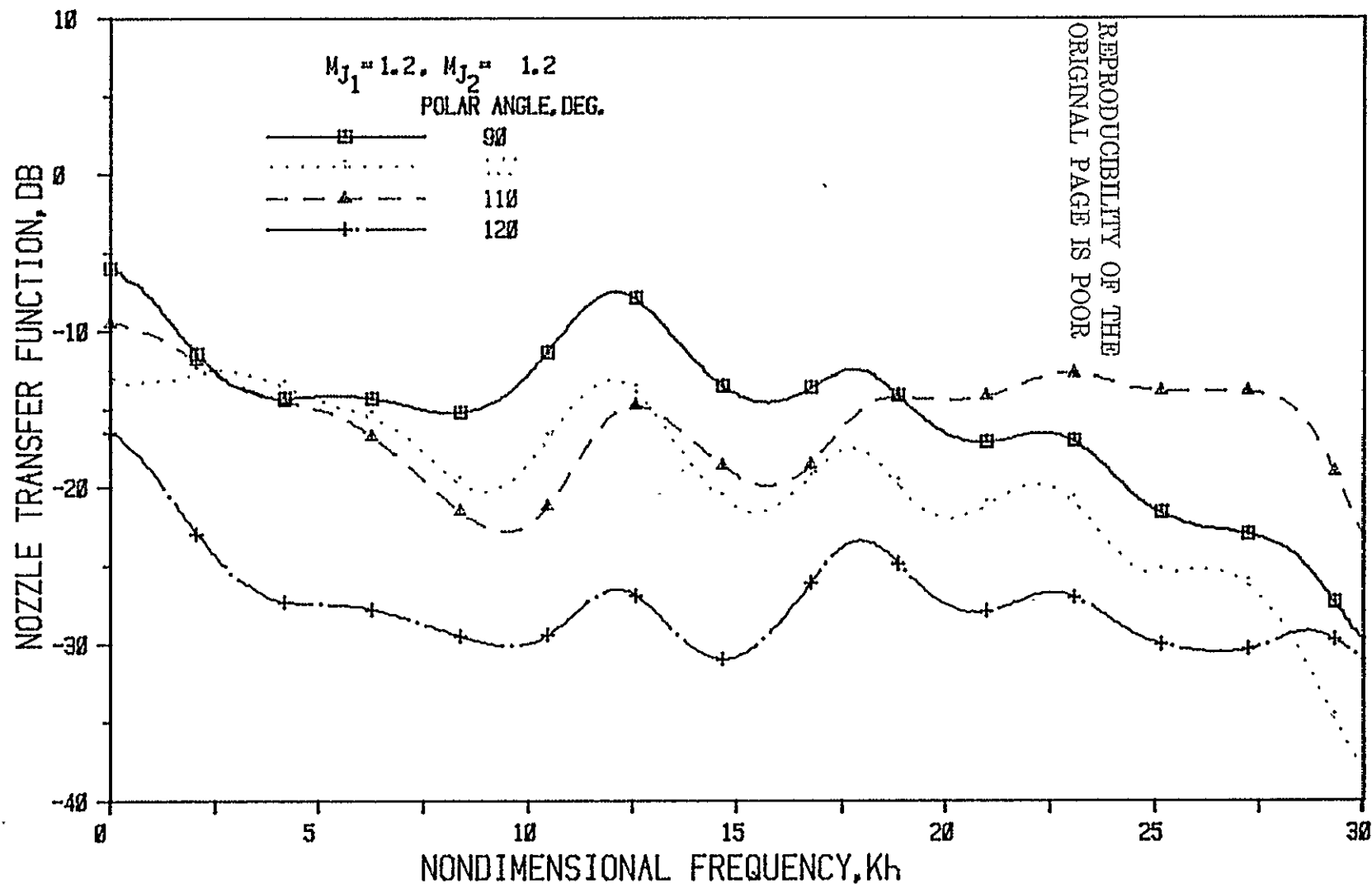


Figure 32(c) Nozzle N 3 (  $L/h = 5$ , Convergence Angle = 20 Deg.); Source At Fan



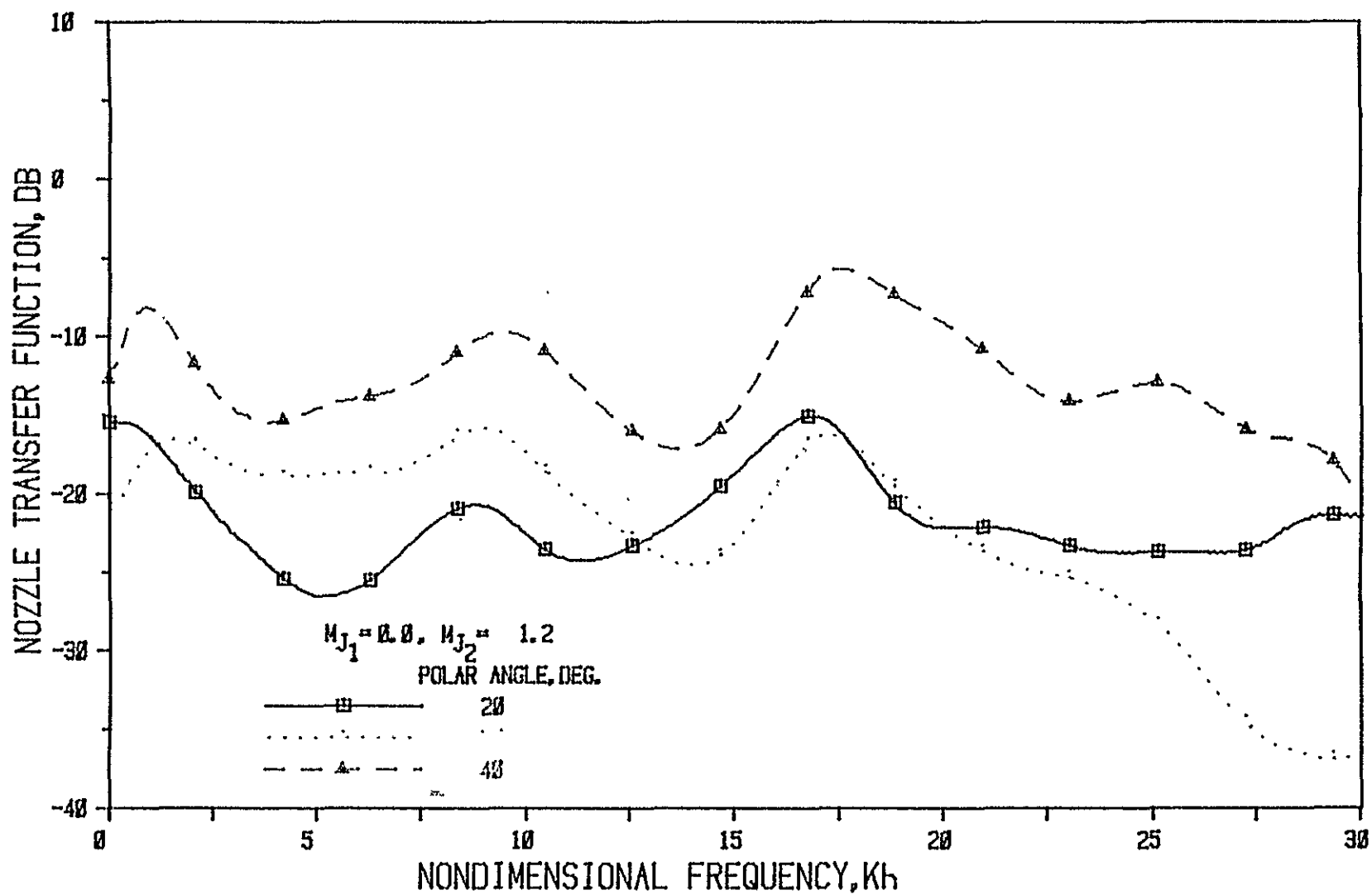


Figure 33(a) Nozzle N 3 ( $L/h = 5$ , Convergence Angle = 20 Deg.); Source At Fan

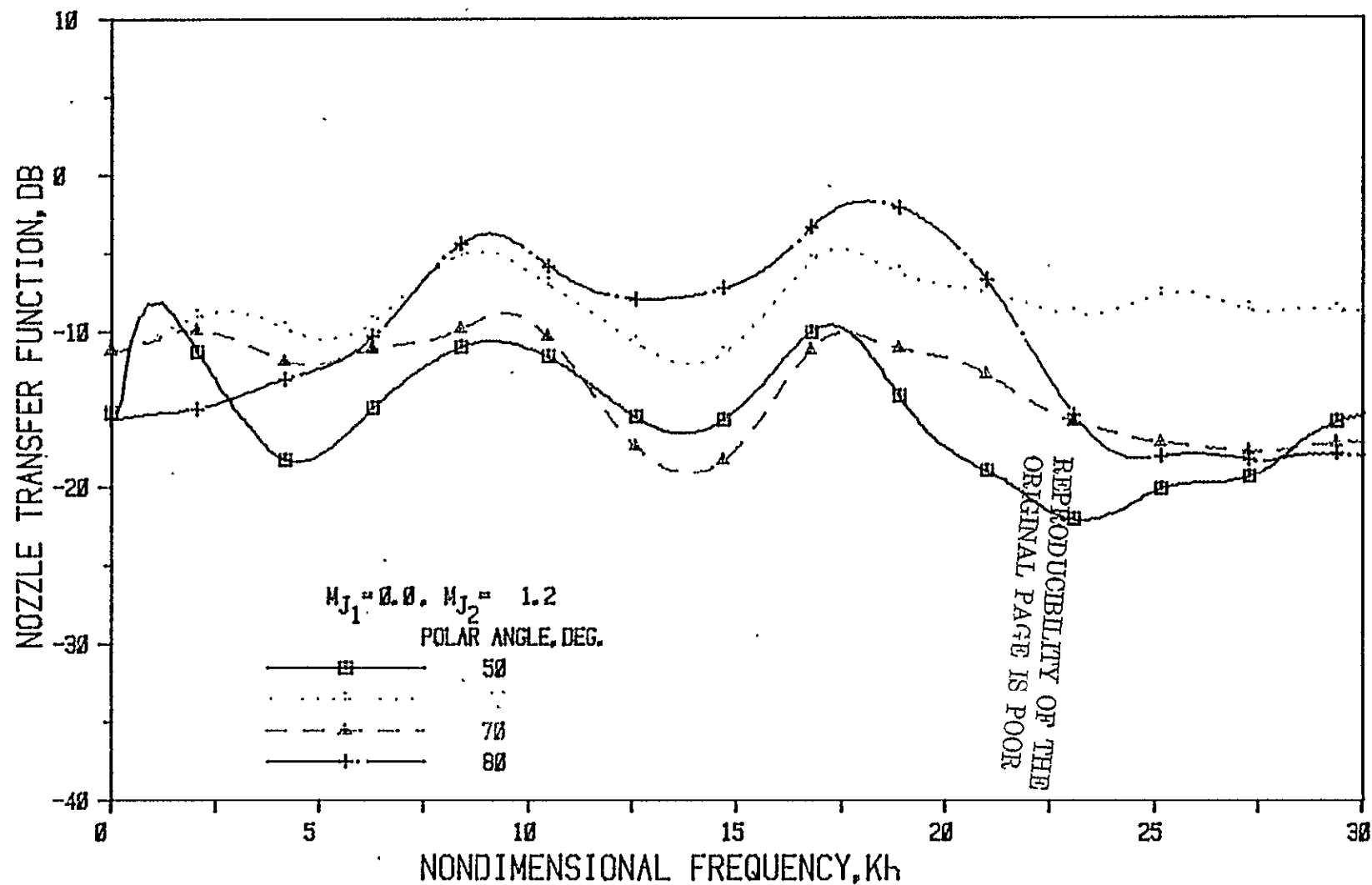


Figure 33(b) Nozzle N 3 (  $L/h = 5$ , Convergence Angle = 20 Deg.); Source At Fan

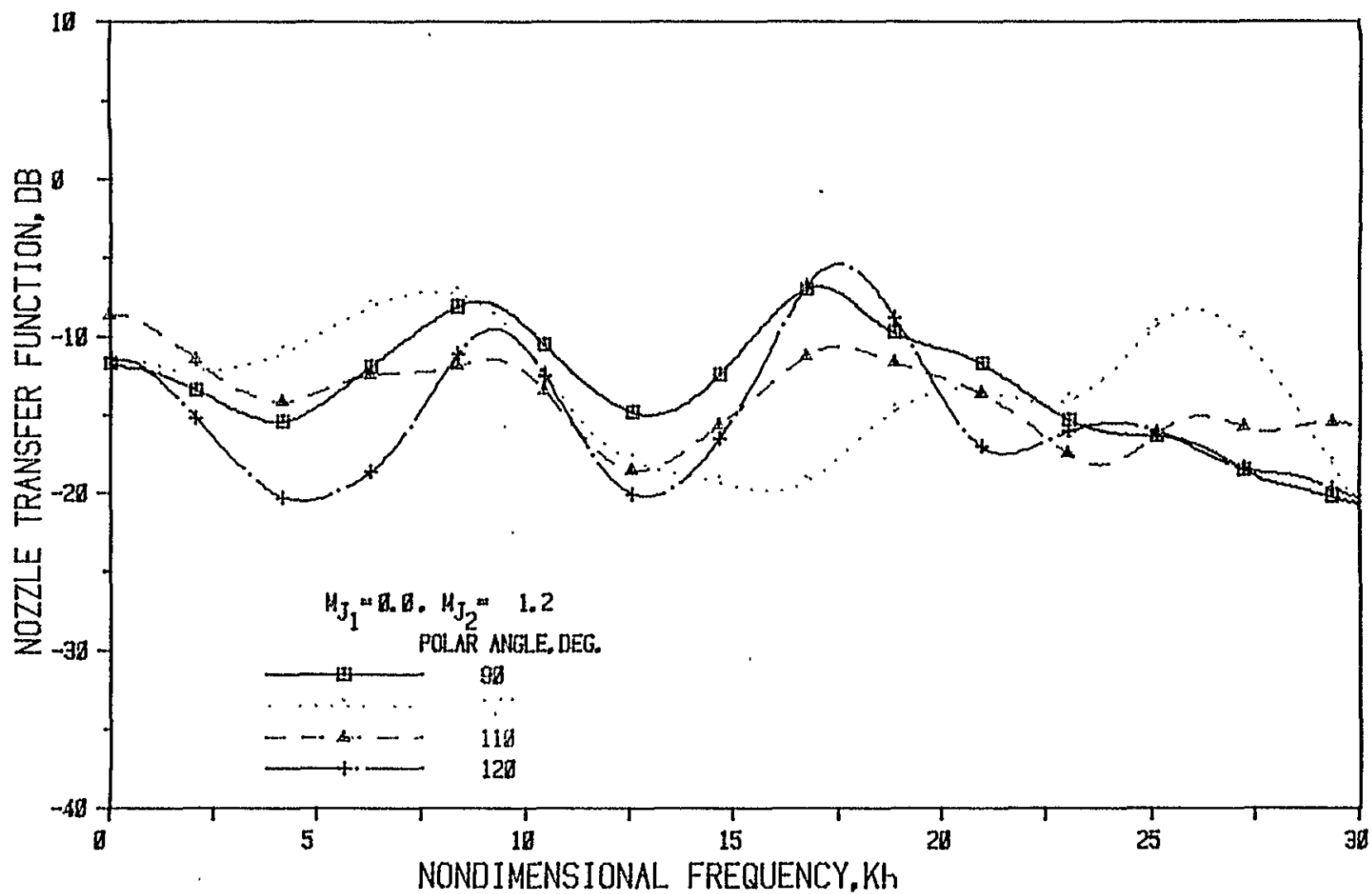


Figure 33(c) Nozzle N 3 ( $L/h = 5$ , Convergence Angle = 20 Deg.); Source At Fan

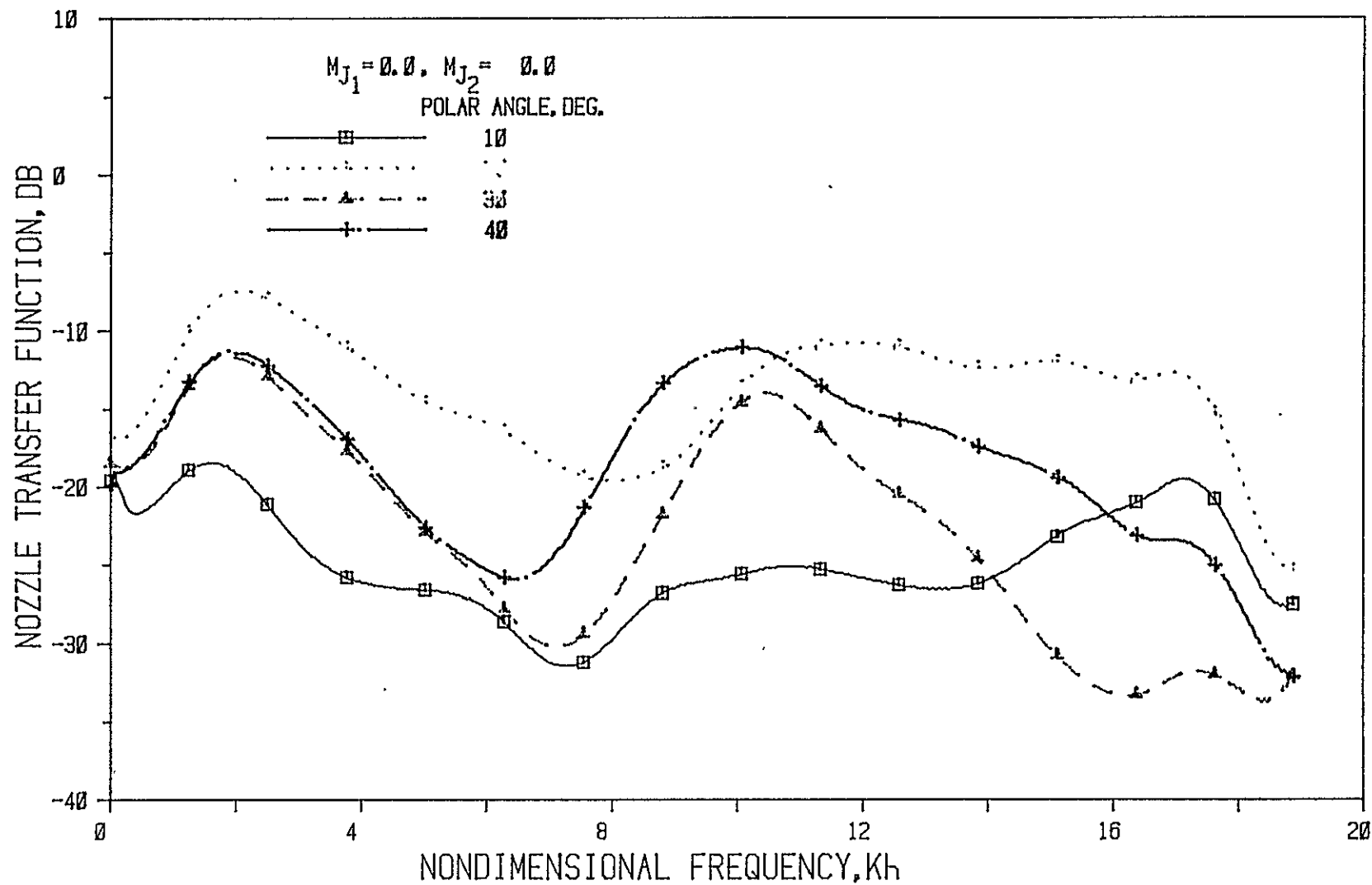


Figure 34(a) Nozzle N 4 ( $L/h = 1$ , Convergence Angle = 40 Deg.); Source At Fan

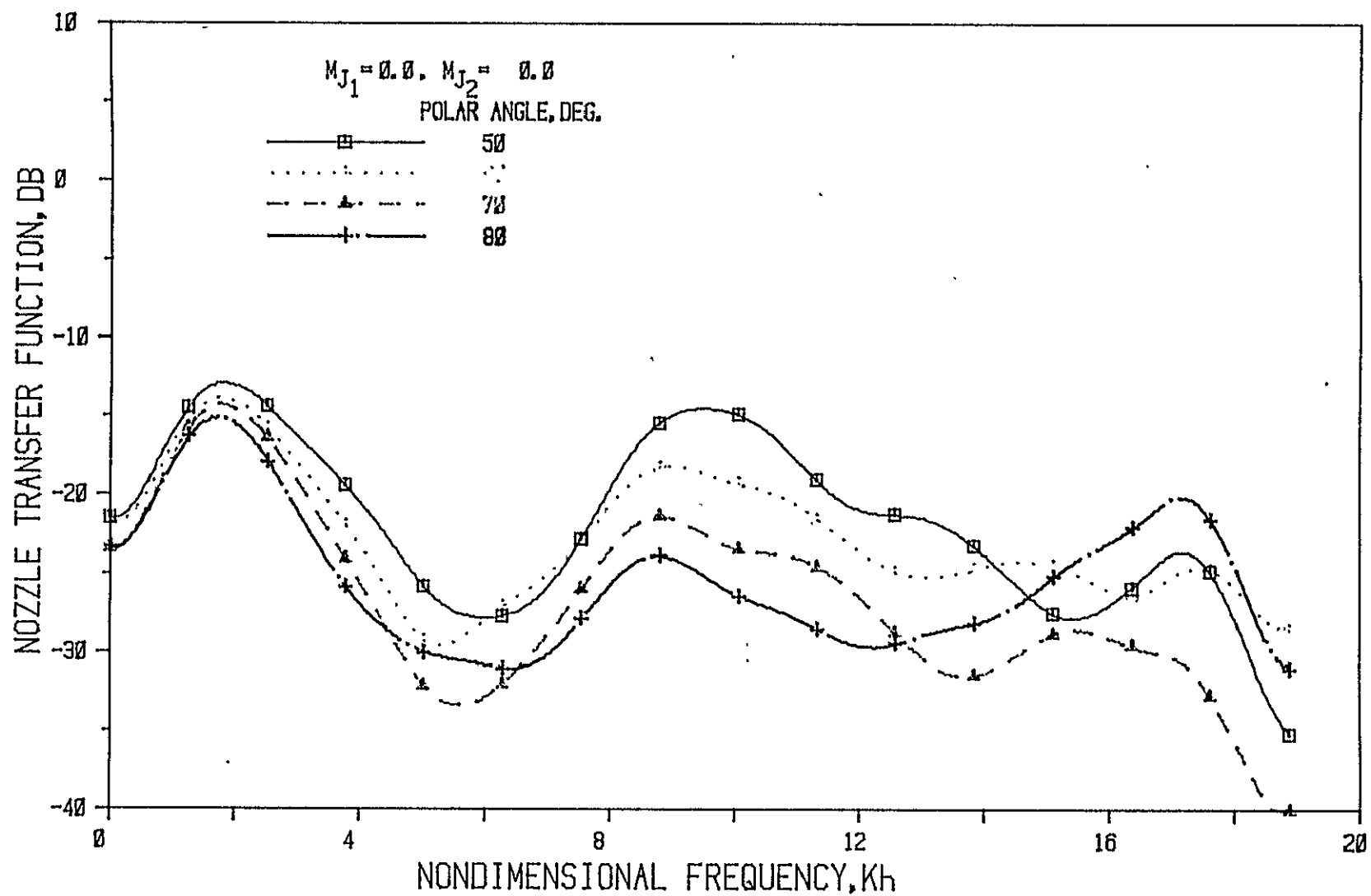


Figure 34(b) Nozzle N 4 ( $L/h = 1$ , Convergence Angle = 40 Deg.); Source At Fan

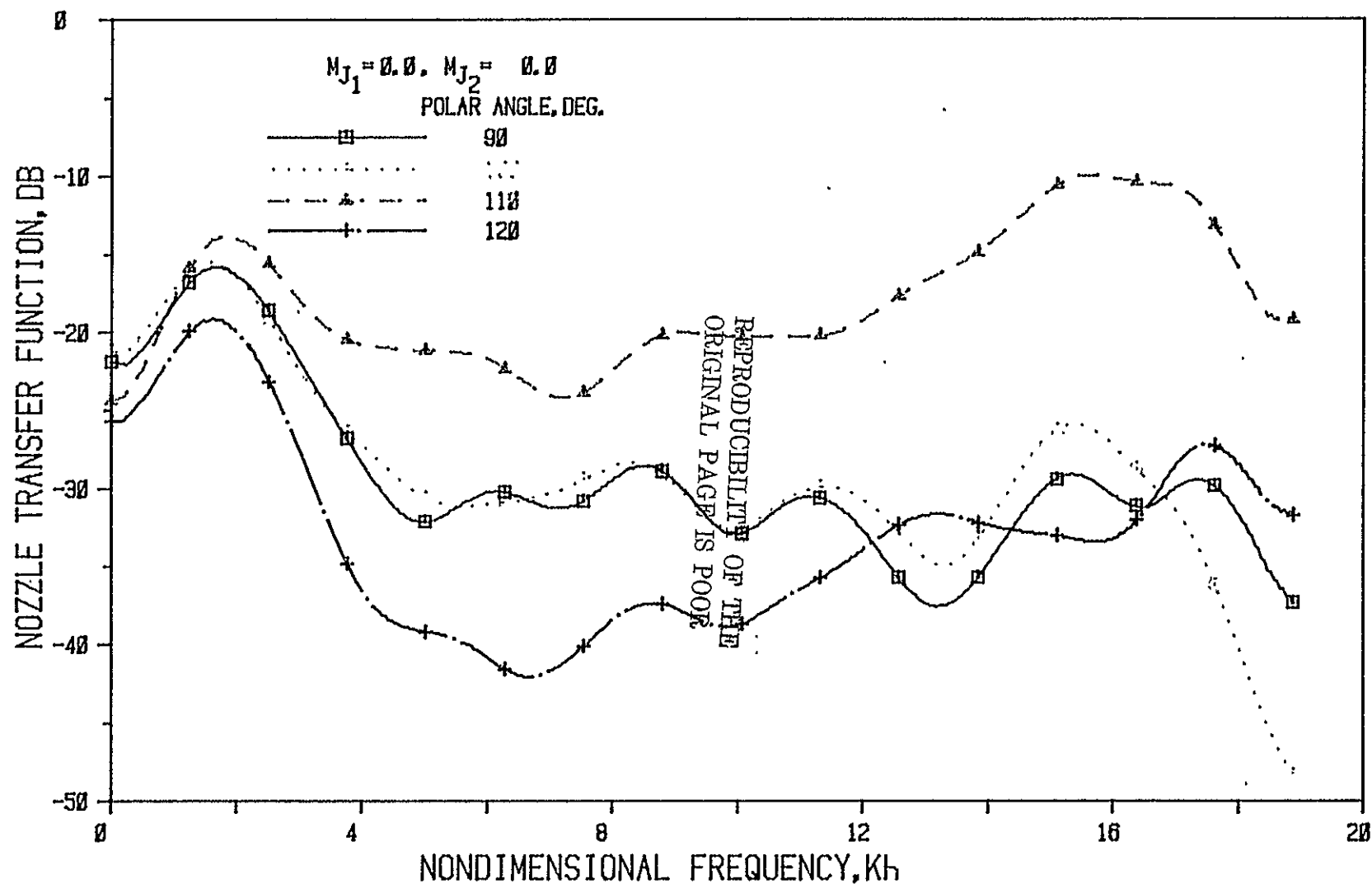


Figure 34(c) Nozzle N 4 (  $L/h = 1$ , Convergence Angle =  $40^\circ$  ); Source At Fan

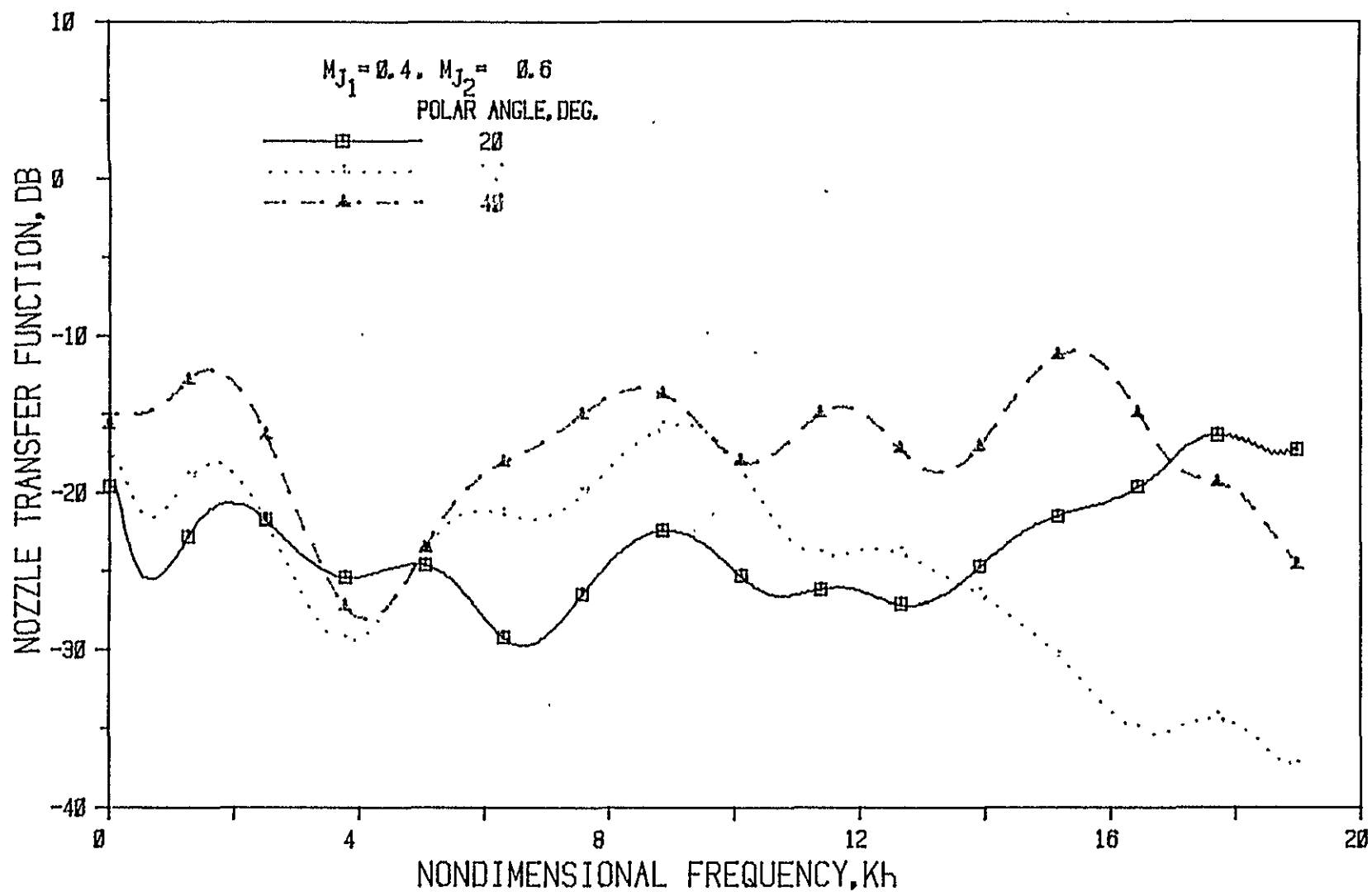


Figure 35(a) Nozzle N 4 ( $L/h = 1$ , Convergence Angle = 40 Deg.); Source At Fan

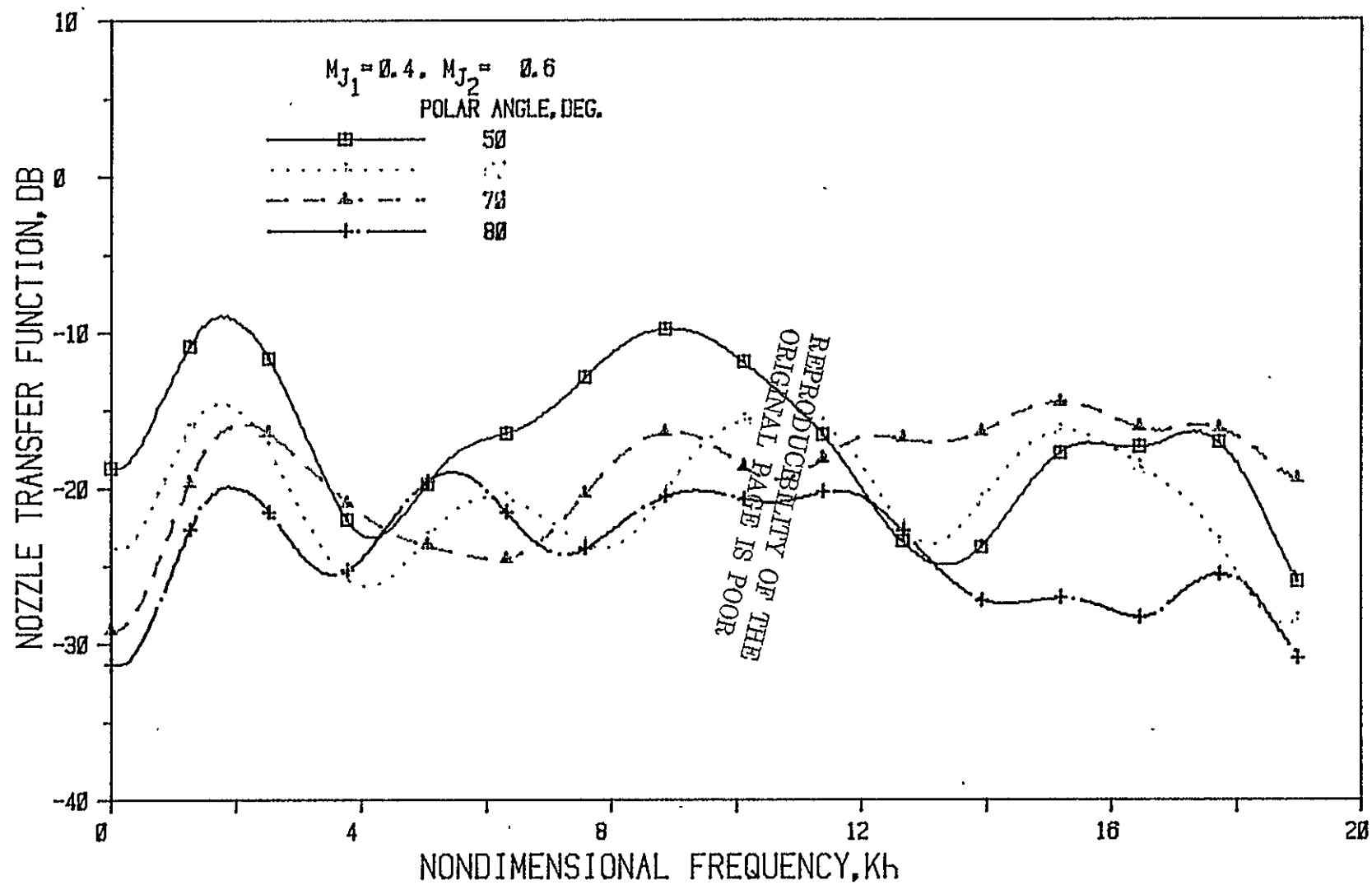


Figure 35(b) Nozzle N 4 ( $L/h = 1$ , Convergence Angle = 40 Deg.); Source At Fan



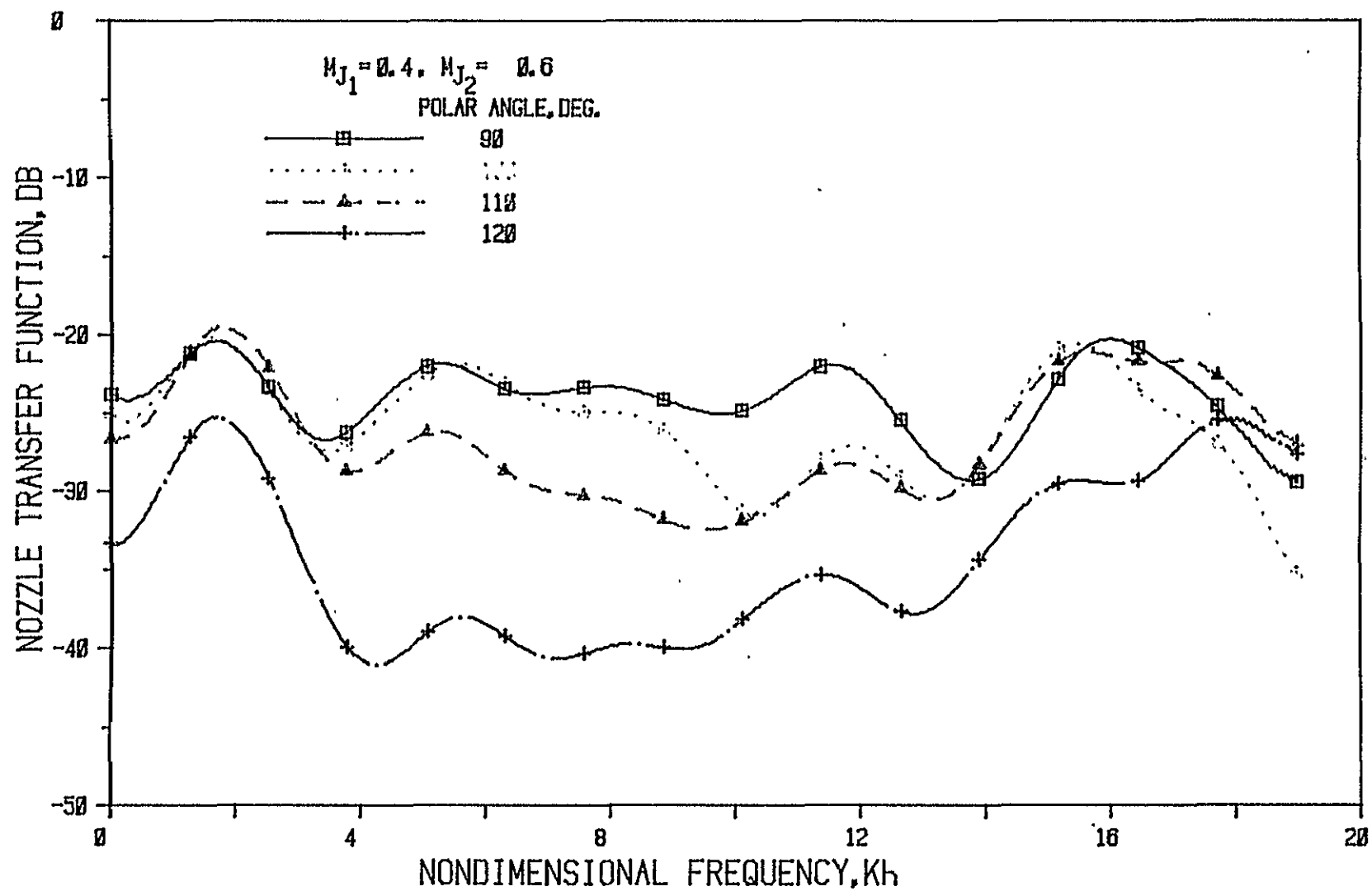


Figure 35(c) Nozzle N 4 ( $L/h = 1$ , Convergence Angle =  $40^\circ$ ); Source At Fan

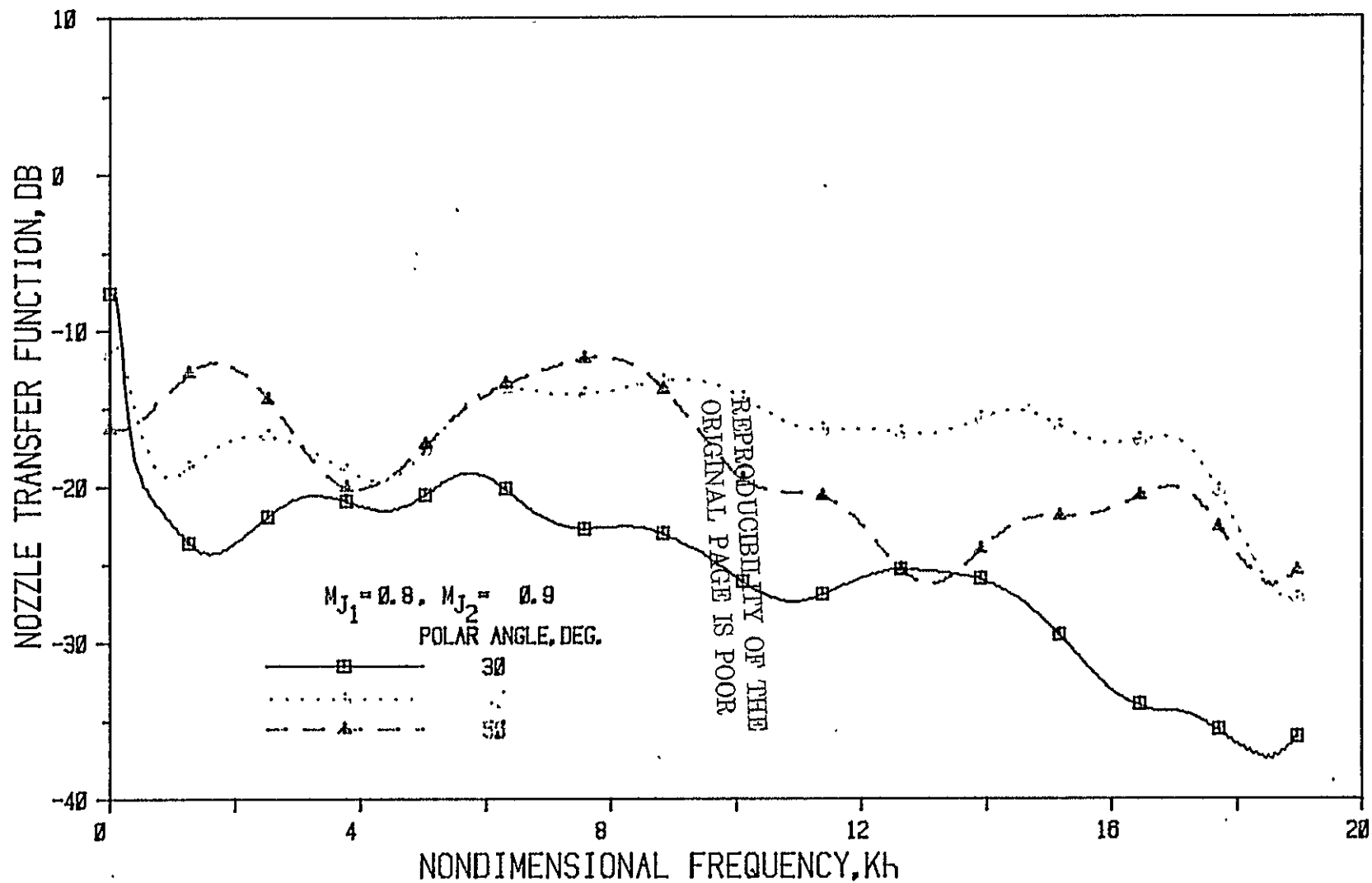


Figure 36(a) Nozzle N 4 (  $L/h = 1$ , Convergence Angle = 40 Deg.); Source At Fan

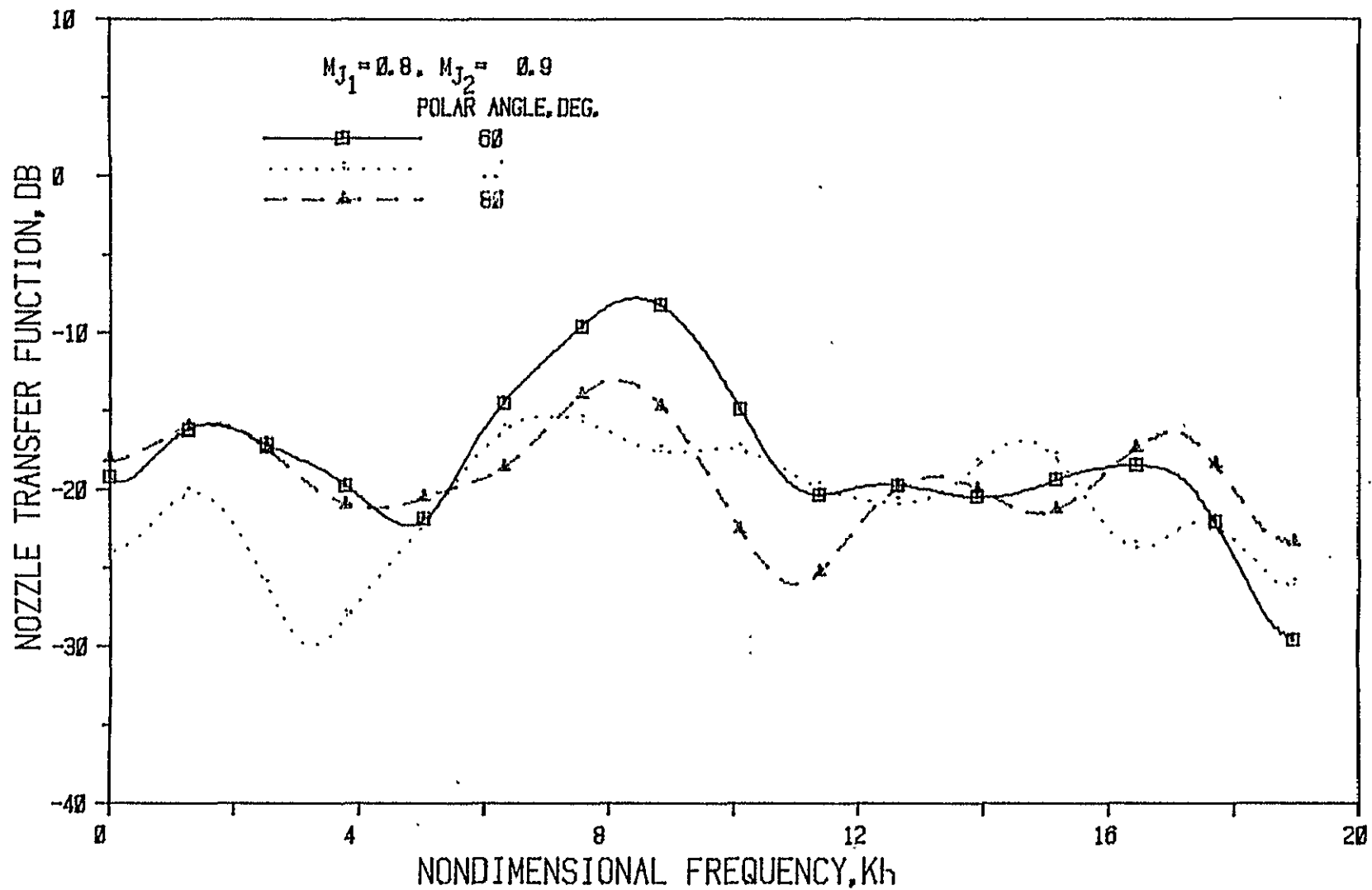


Figure 36(b) Nozzle N 4 ( $L/h = 1$ , Convergence Angle = 40 Deg.); Source At Fan

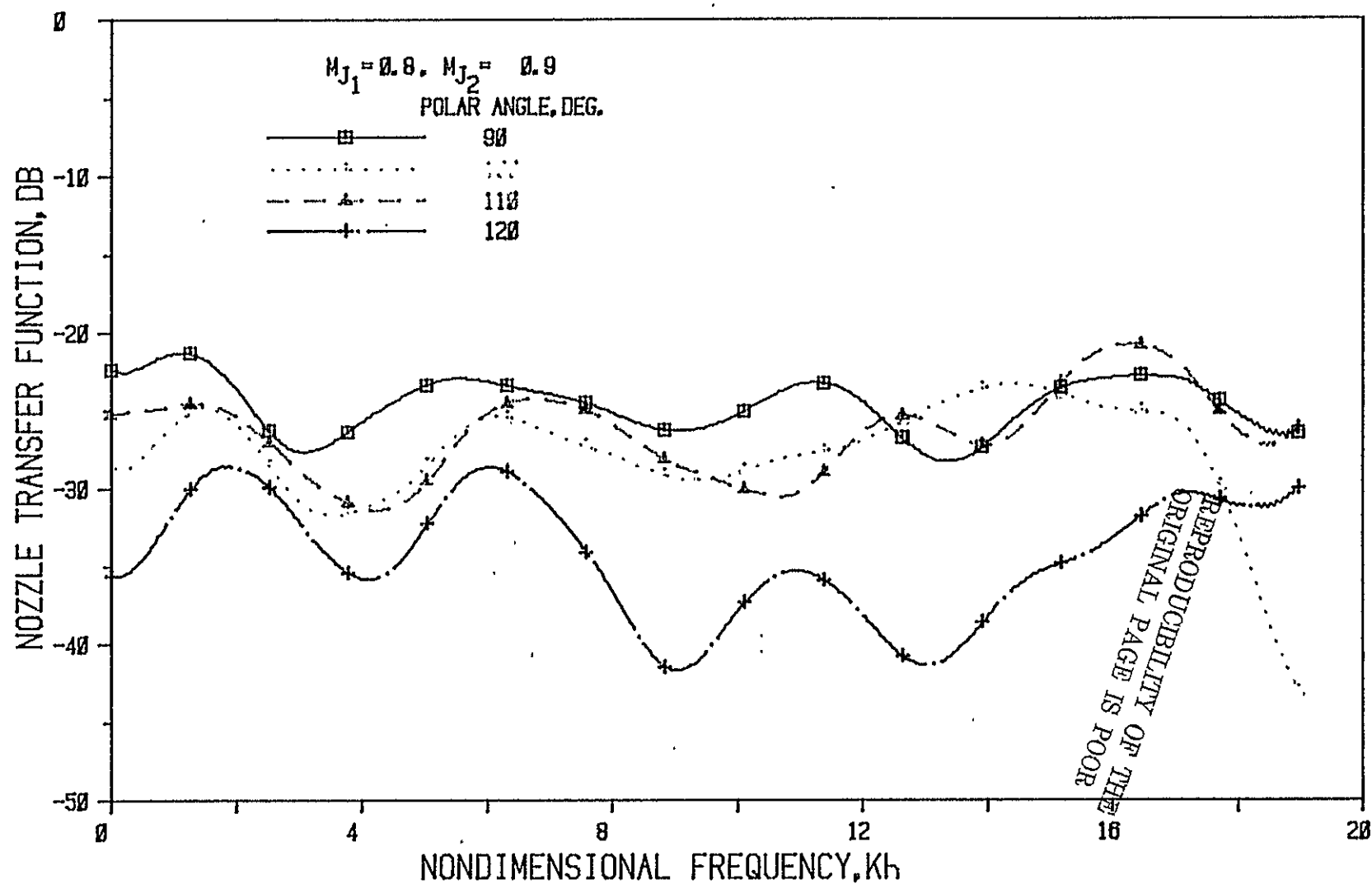


Figure 36(c) Nozzle N 4 (  $L/h = 1$ , Convergence Angle =  $40^\circ$  ); Source At Fan

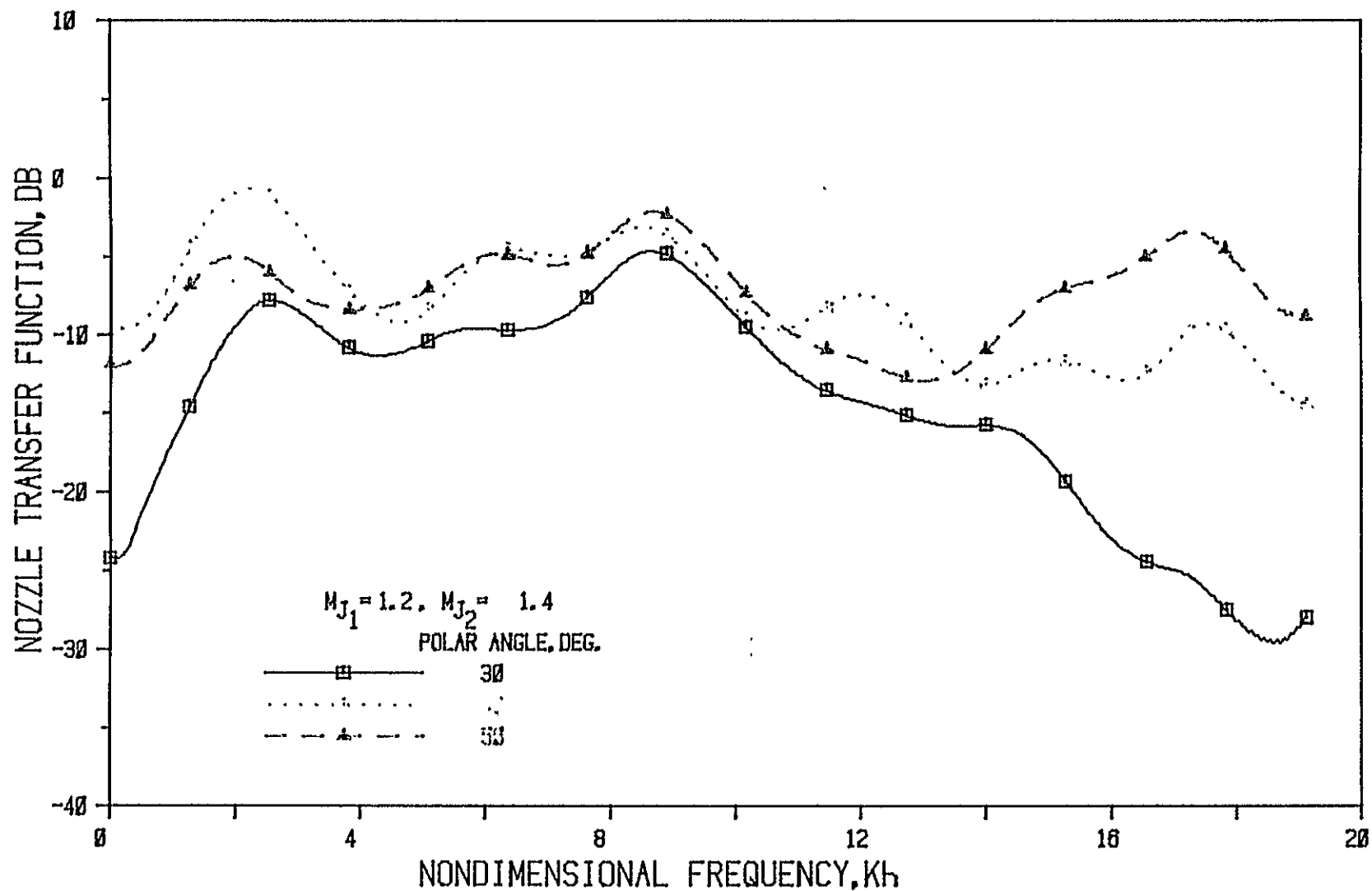


Figure 37(a) Nozzle N 4 ( $L/h = 1$ , Convergence Angle =  $40^\circ$ ); Source At Fan

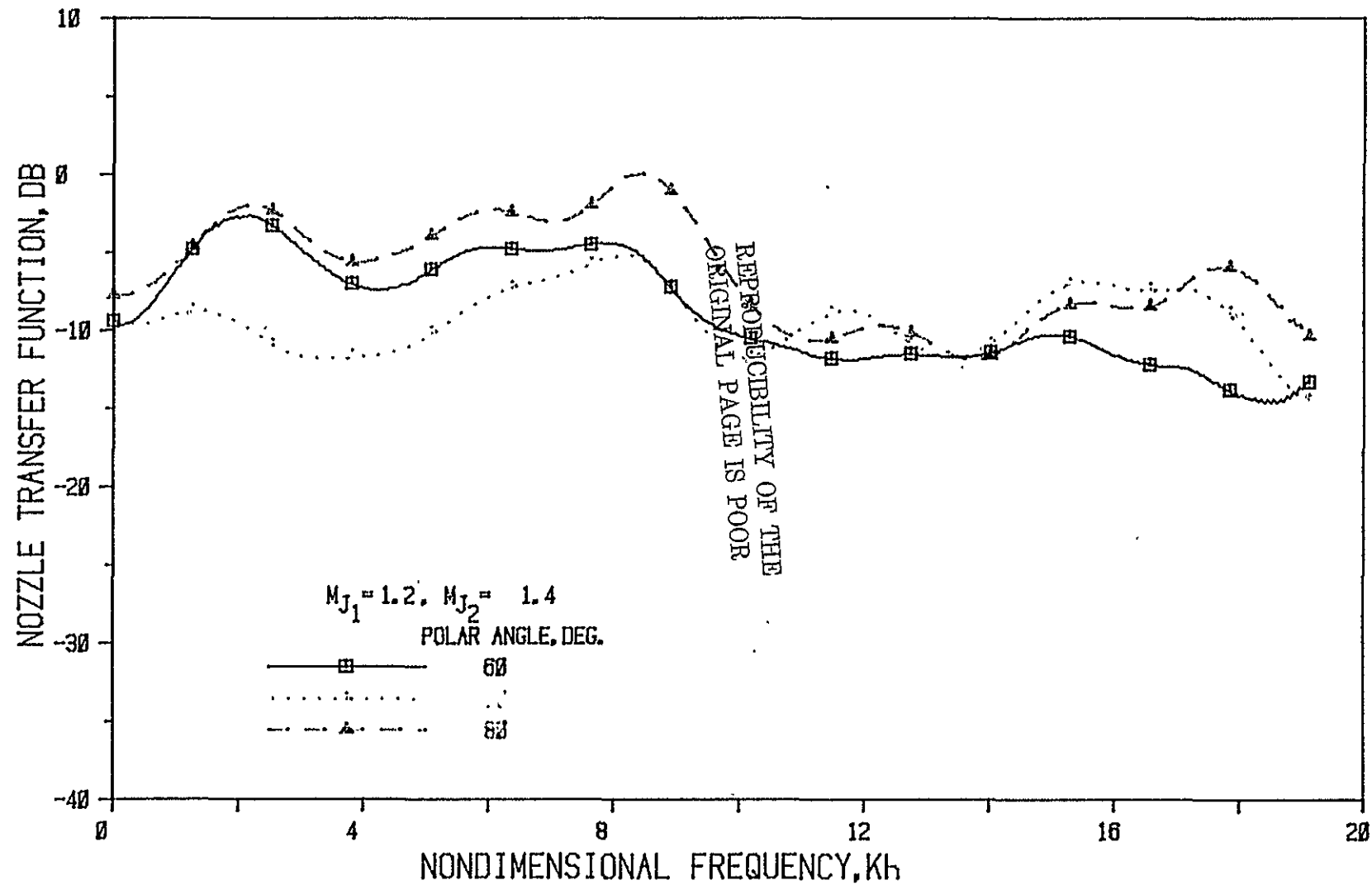


Figure 37(b) Nozzle N 4 (  $L/h = 1$ , Convergence Angle = 40 Deg.); Source At Fan

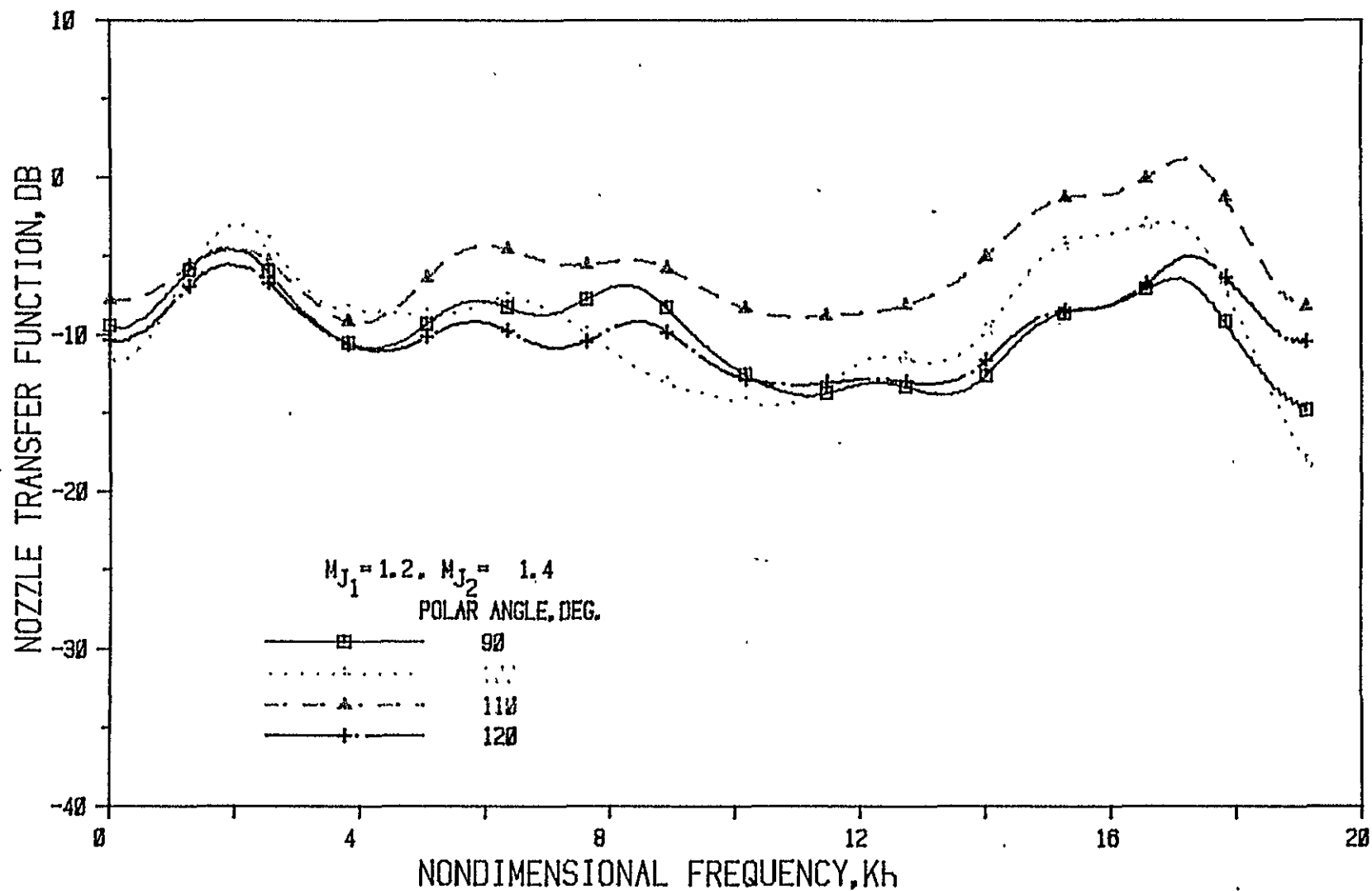


Figure 37(c) Nozzle N 4 ( $L/h = 1$ , Convergence Angle = 40 Deg.); Source At Fan

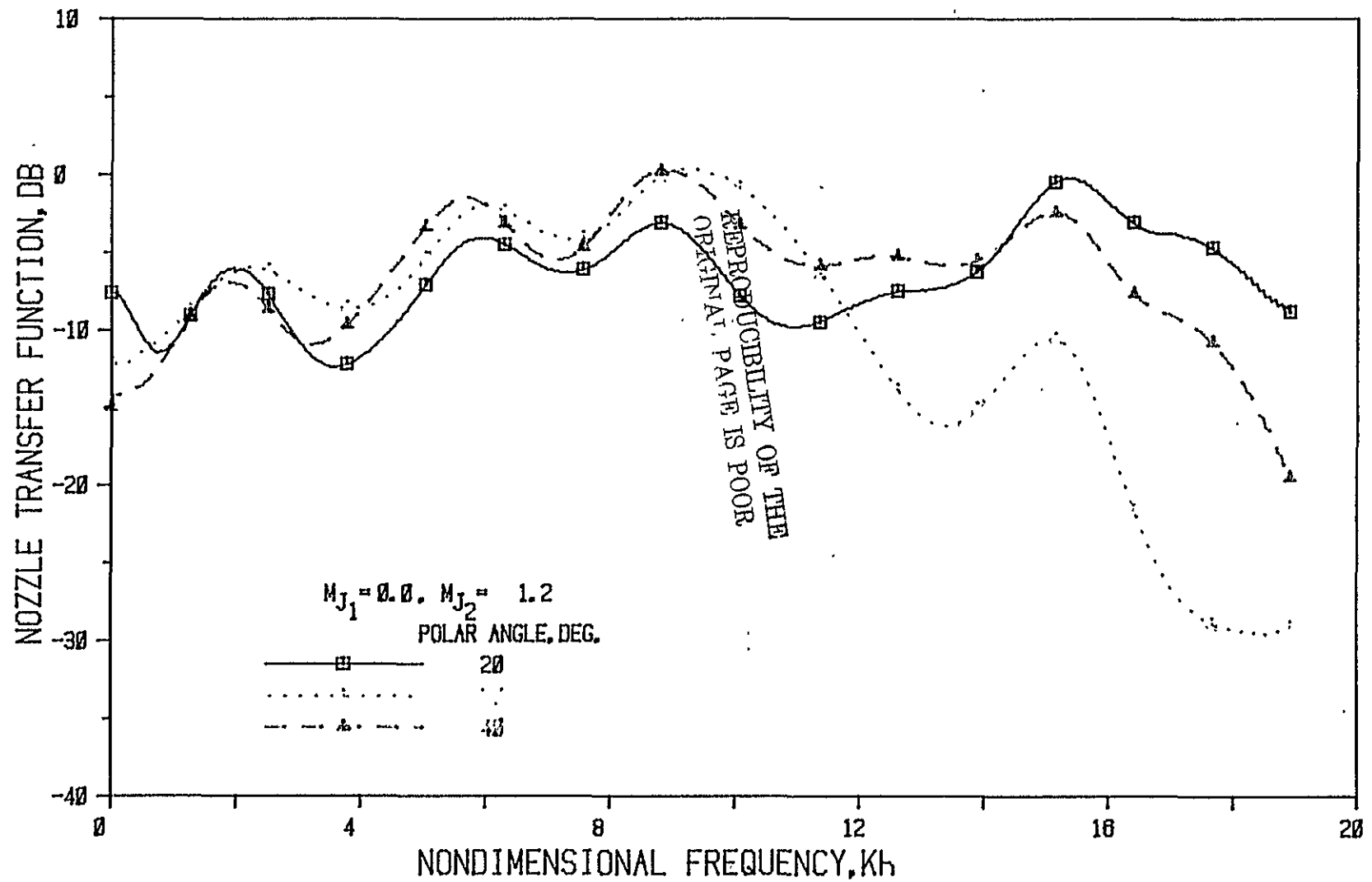


Figure 38(a) Nozzle N 4 (  $L/h = 1$ , Convergence Angle = 40 Deg.); Source At Fan



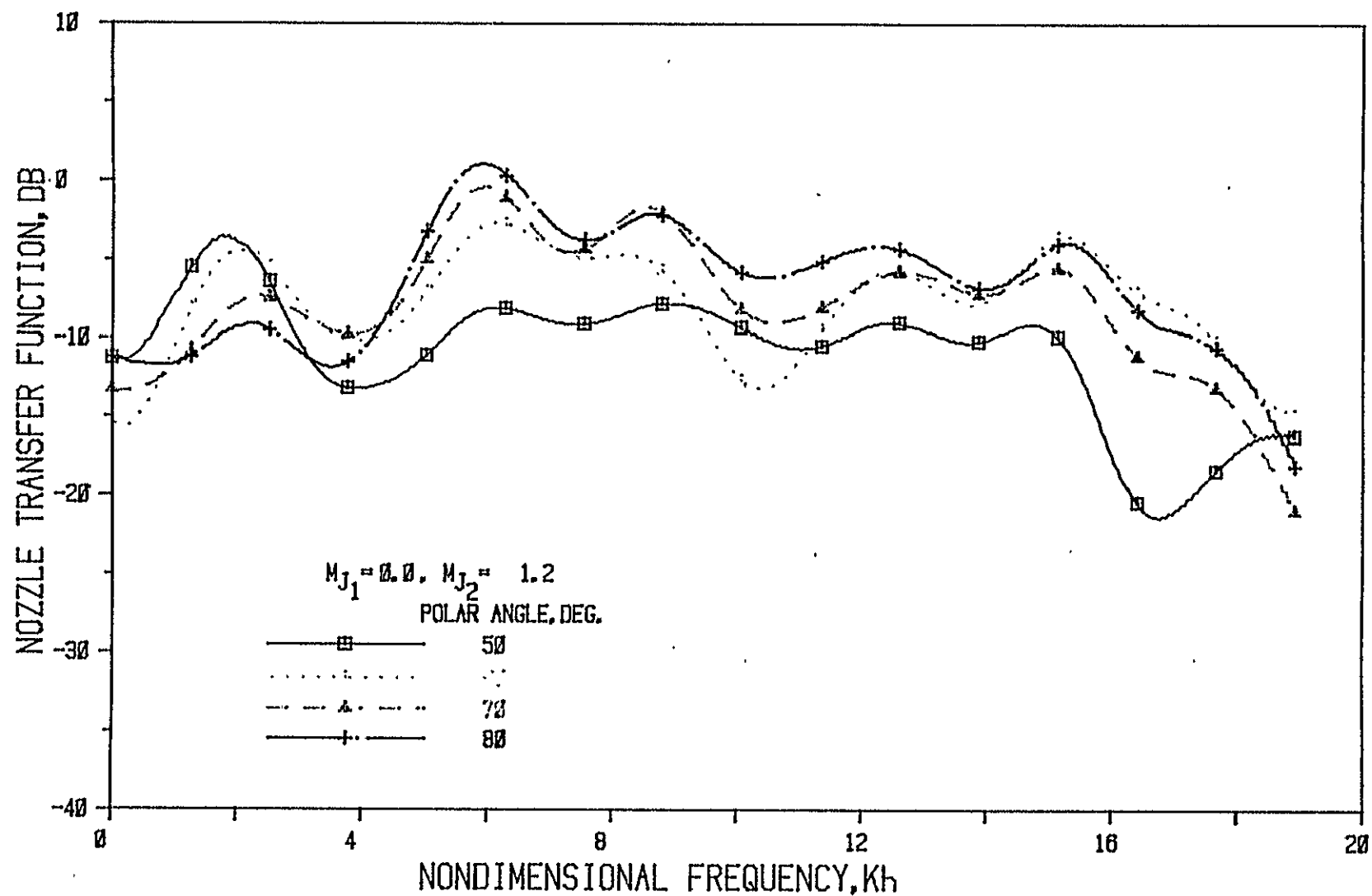


Figure 38(b) Nozzle N 4 ( $L/h = 1$ , Convergence Angle = 40 Deg.); Source At Fan

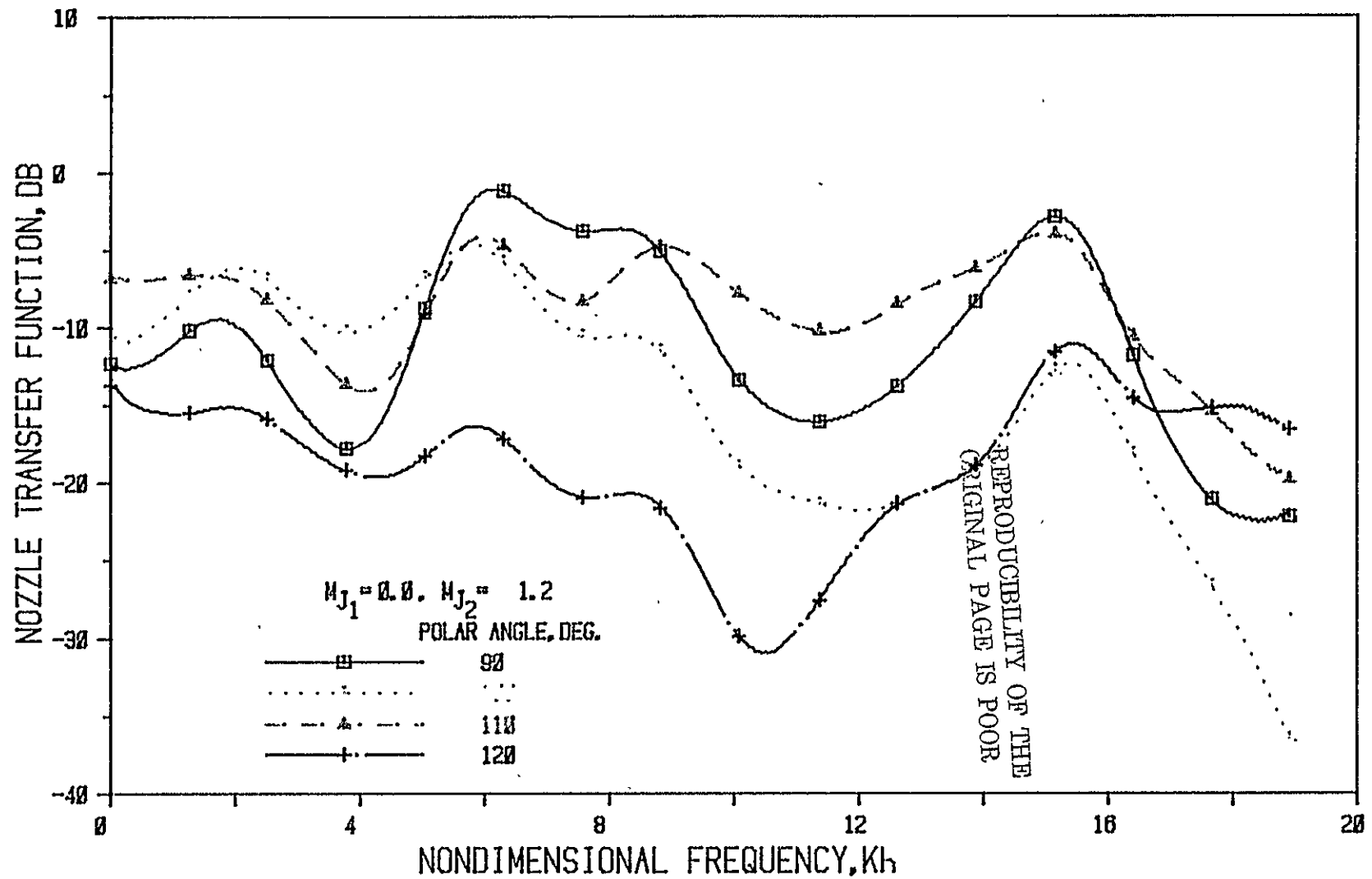


Figure 38(c) Nozzle N 4 ( $L/h = 1$ , Convergence Angle = 40 Deg.); Source At Fan

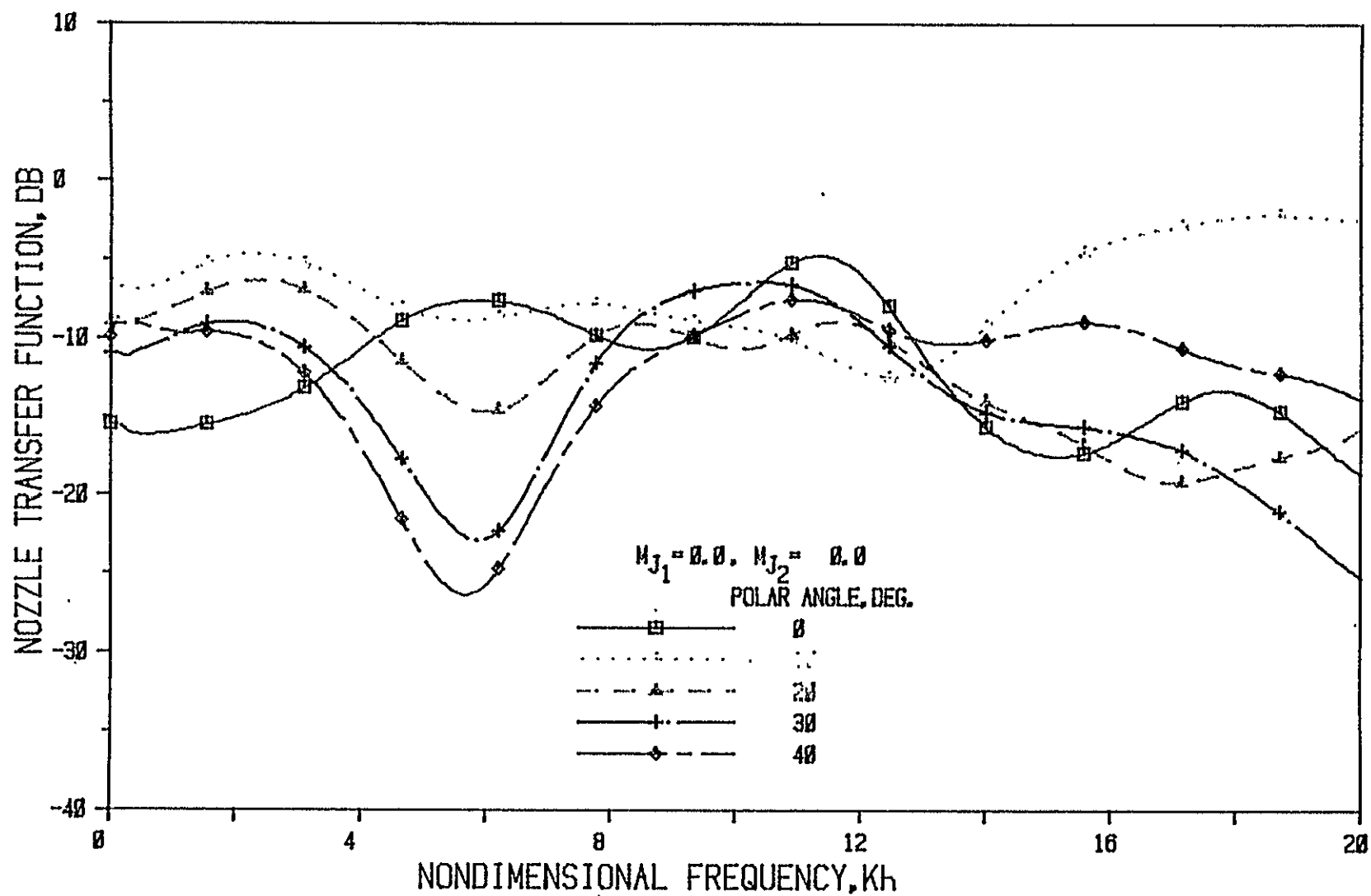


Figure 39(a) Nozzle N 5 ( $L/h = 3$ , Convergence Angle = 40 Deg.); Source At Fan

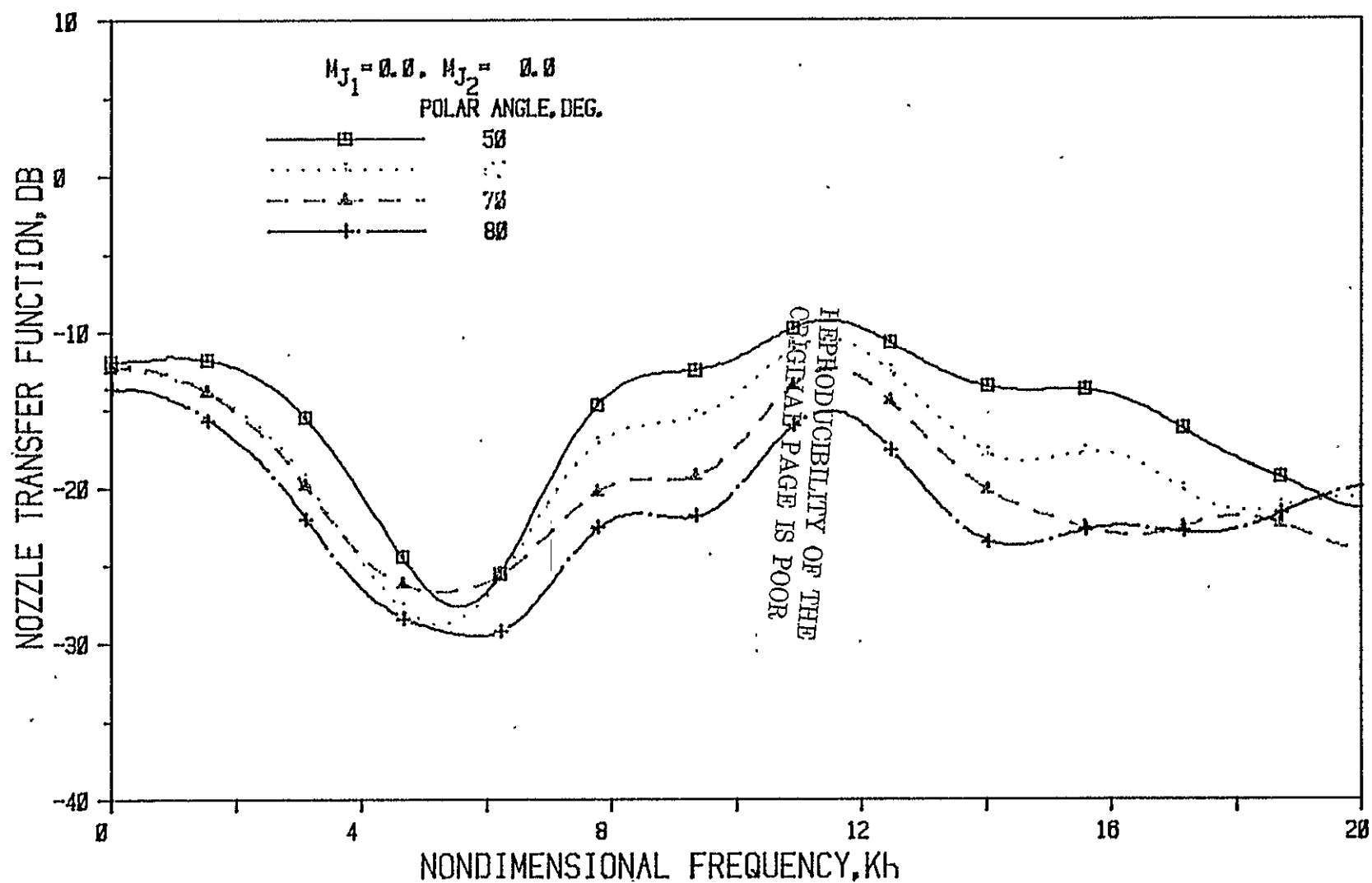


Figure 39(b) Nozzle N 5 ( $L/h = 3$ , Convergence Angle =  $40^\circ$ ); Source At Fan

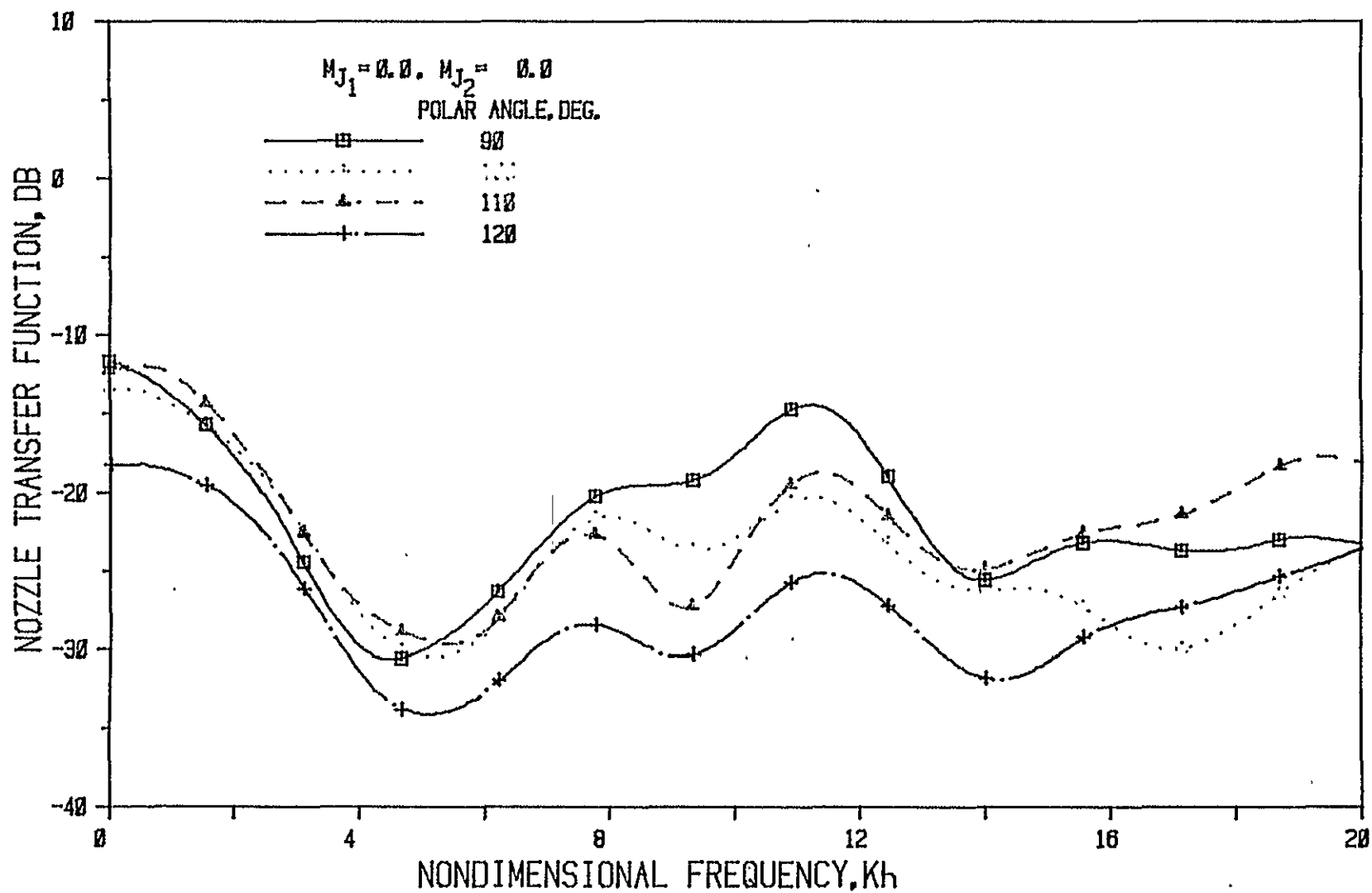


Figure 39(c) Nozzle N 5 ( $L/h = 3$ , Convergence Angle = 40 Deg.); Source At Fan

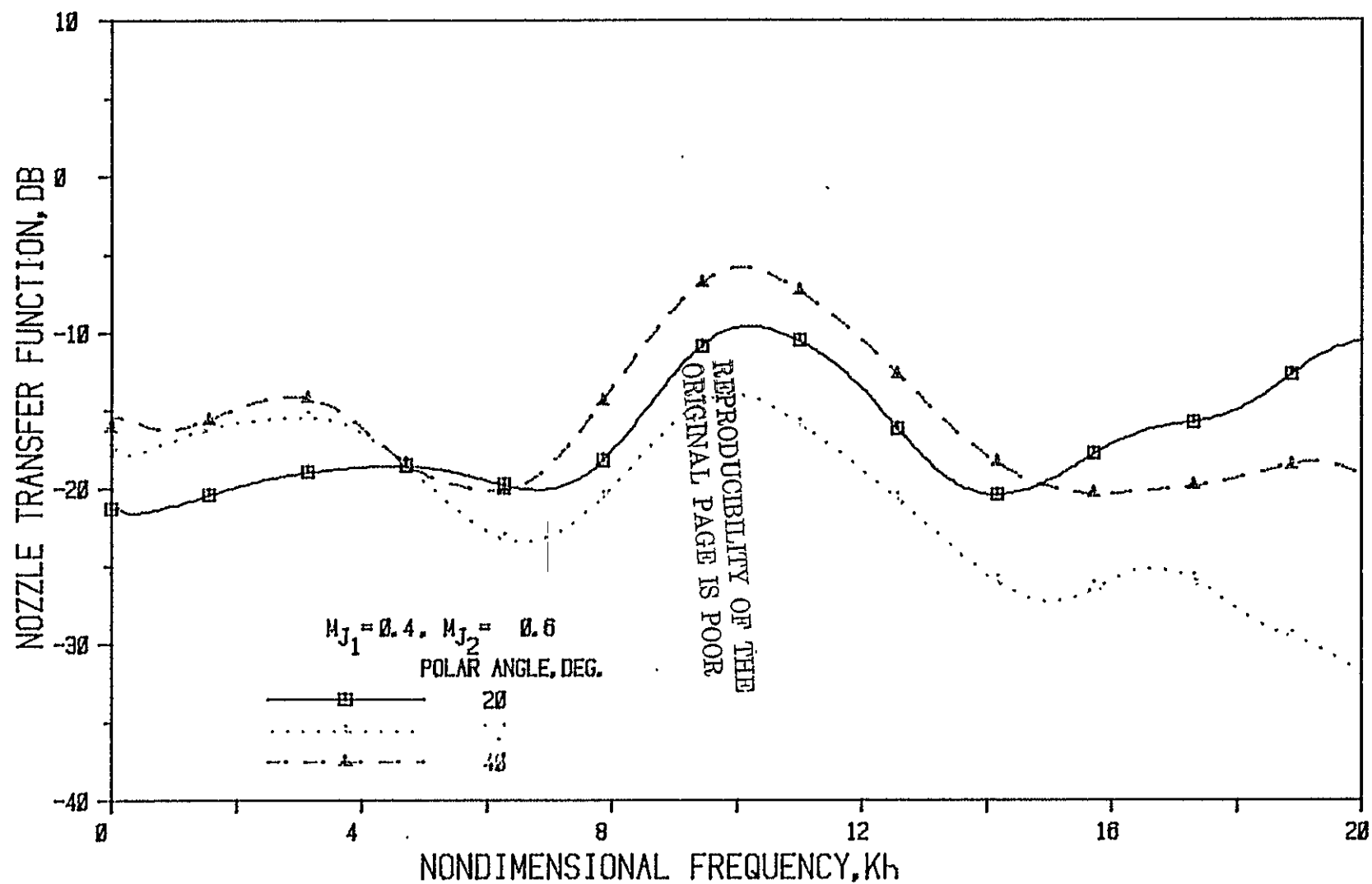


Figure 40(a) Nozzle N 5 ( $L/h = 3$ , Convergence Angle = 40 Deg.); Source At Fan

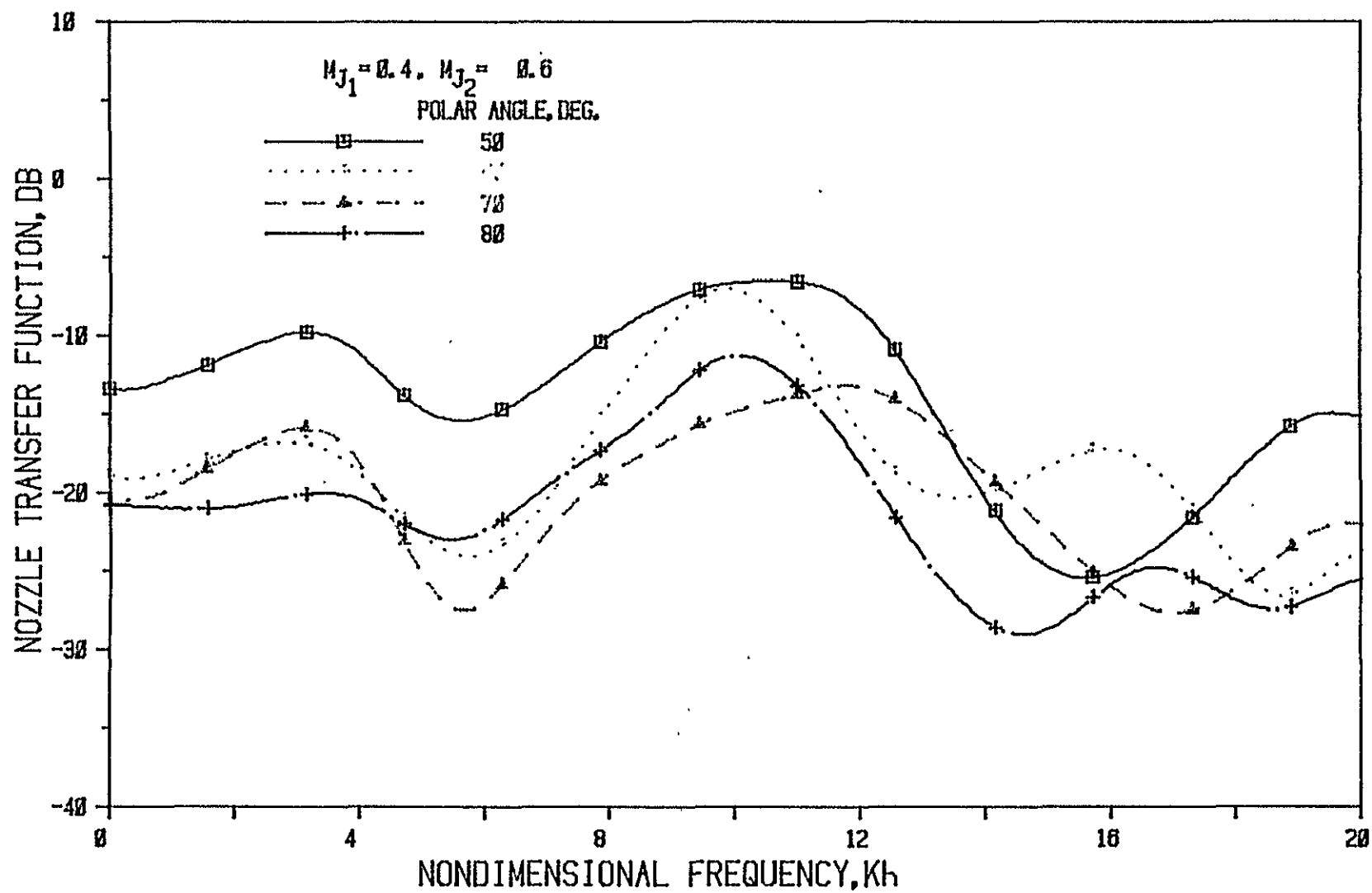


Figure 40(b) Nozzle N 5 ( $L/h = 3$ , Convergence Angle = 40 Deg.); Source At Fan

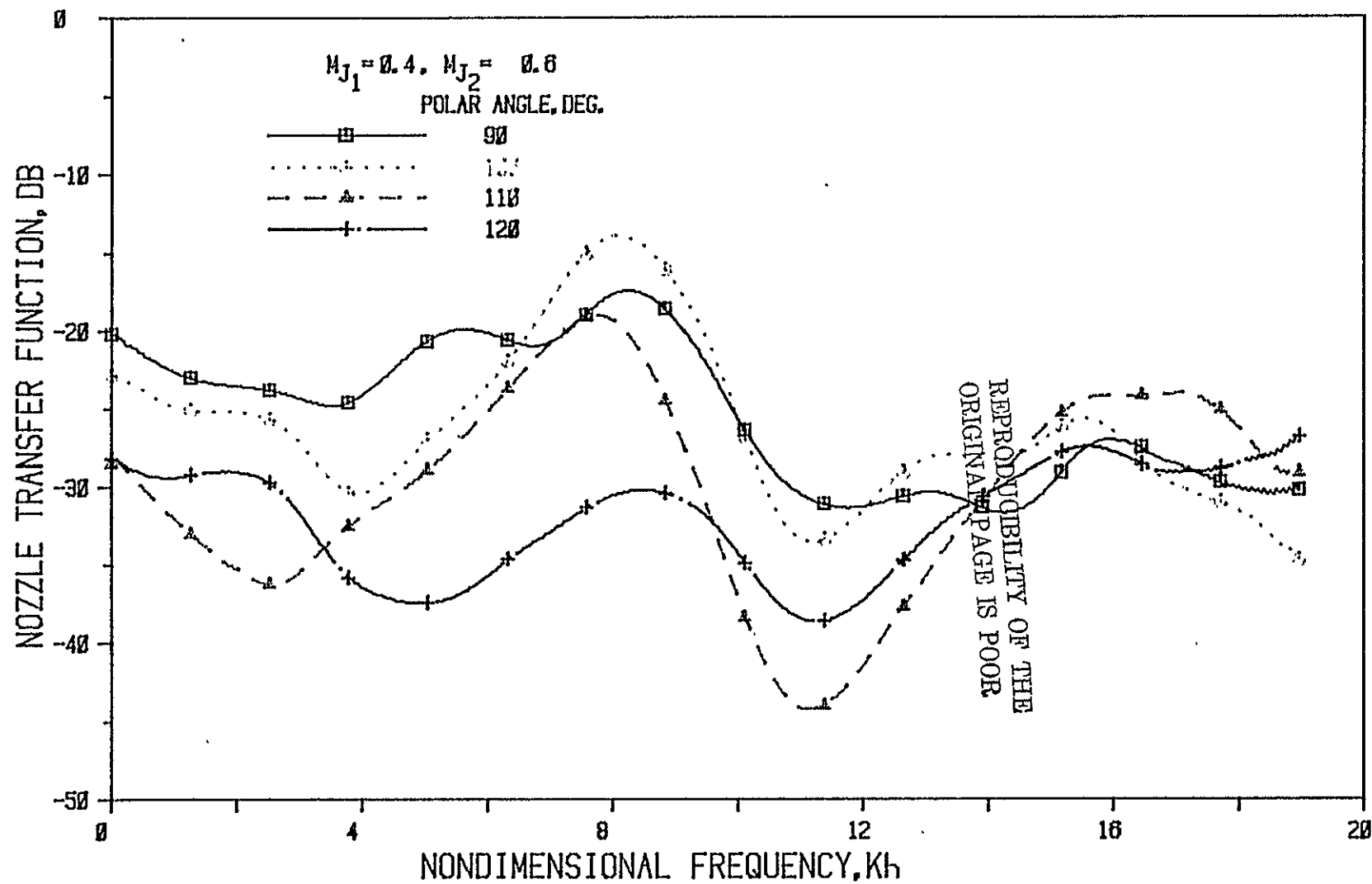


Figure 40(c) Nozzle N 4 (  $L/h = 1$ , Convergence Angle = 40 Deg.); Source At Fan



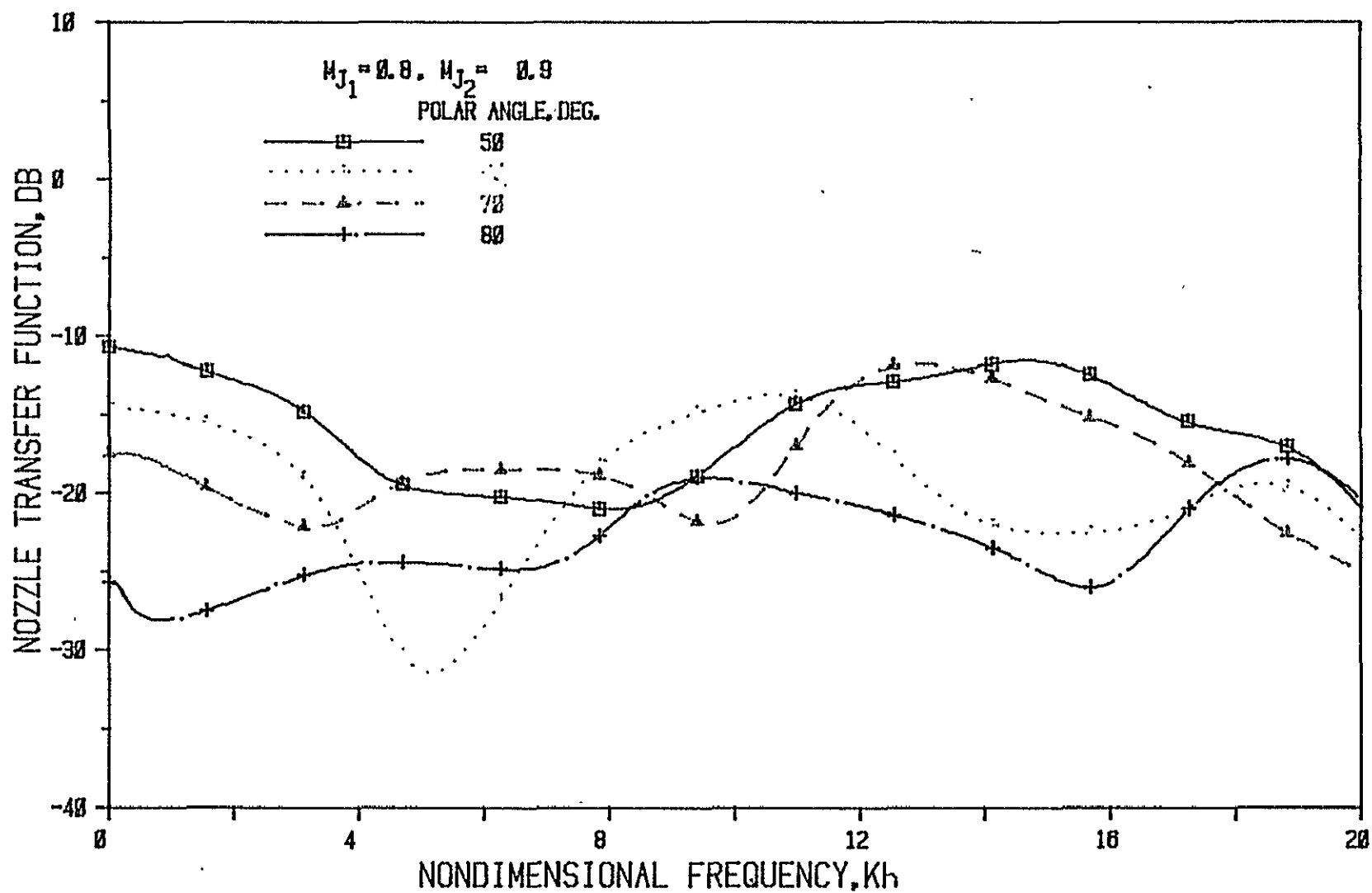


Figure 41(a) Nozzle N 5 ( $L/h = 3$ , Convergence Angle =  $40^\circ$ ); Source At Fan

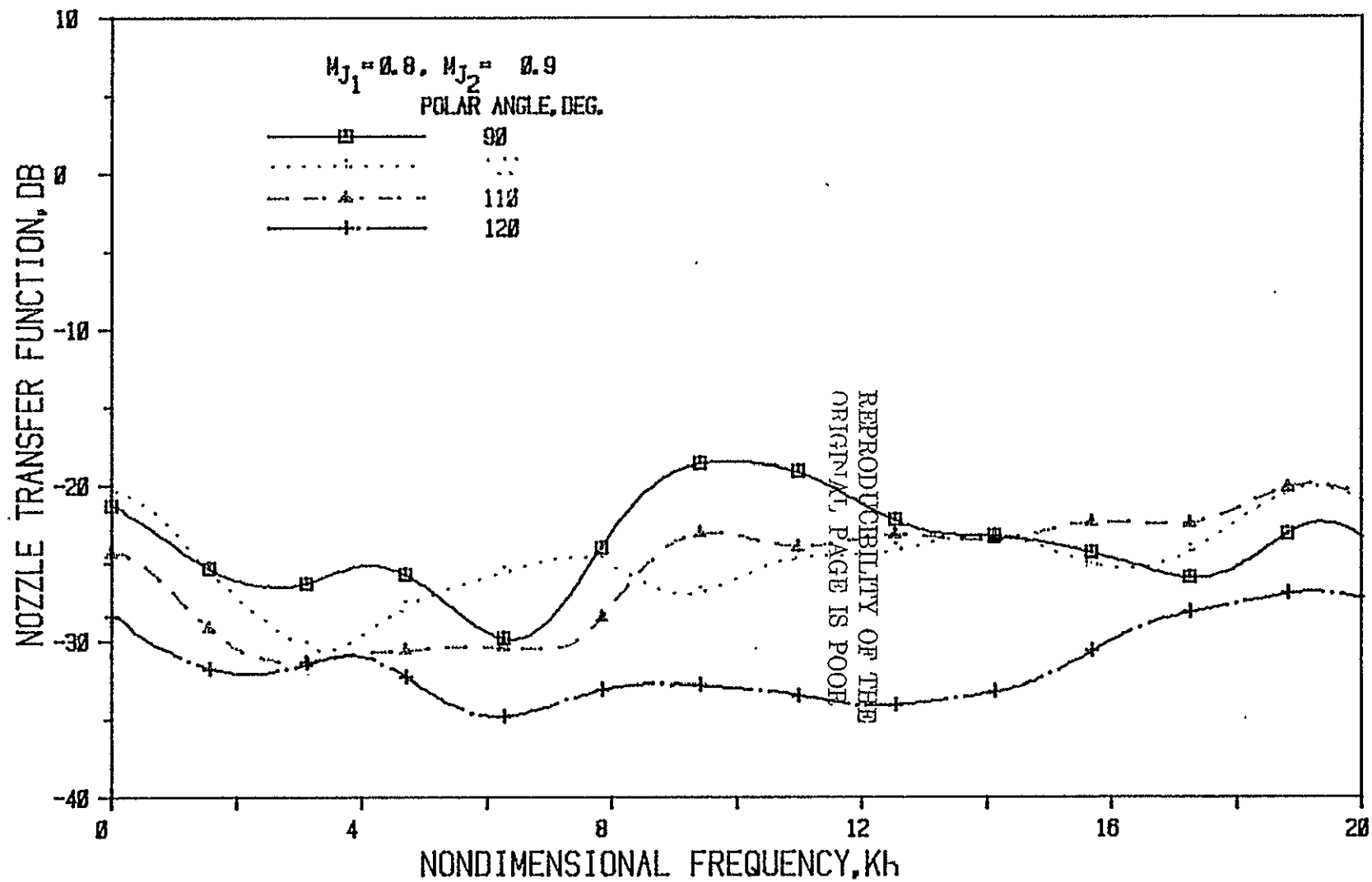


Figure 41(b) Nozzle N 5 ( $L/h = 3$ , Convergence Angle =  $40^\circ$ ); Source At Fan

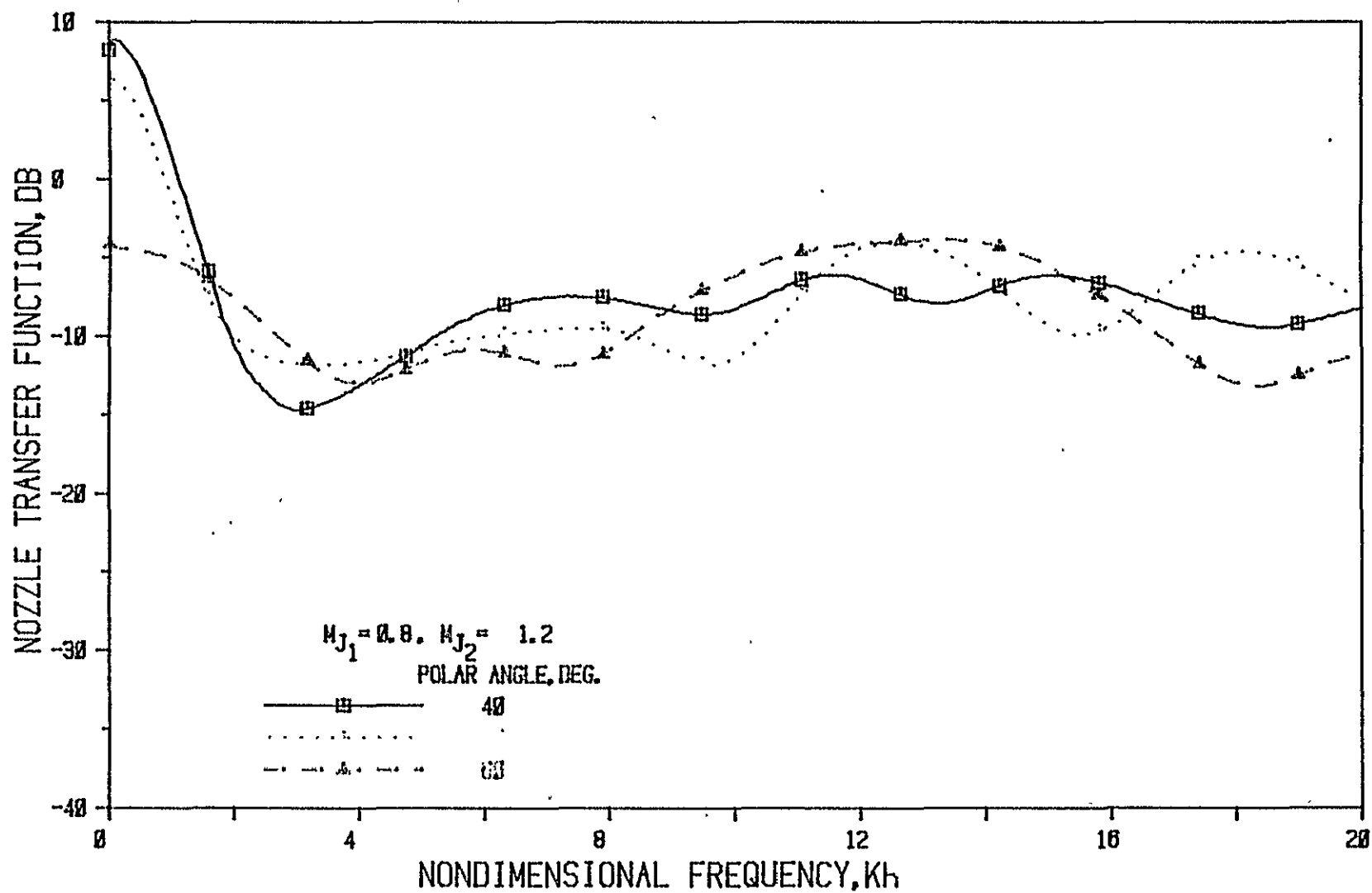


Figure 42(a) Nozzle N 5 ( $L/h = 3$ , Convergence Angle = 40 Deg.); Source At Fan

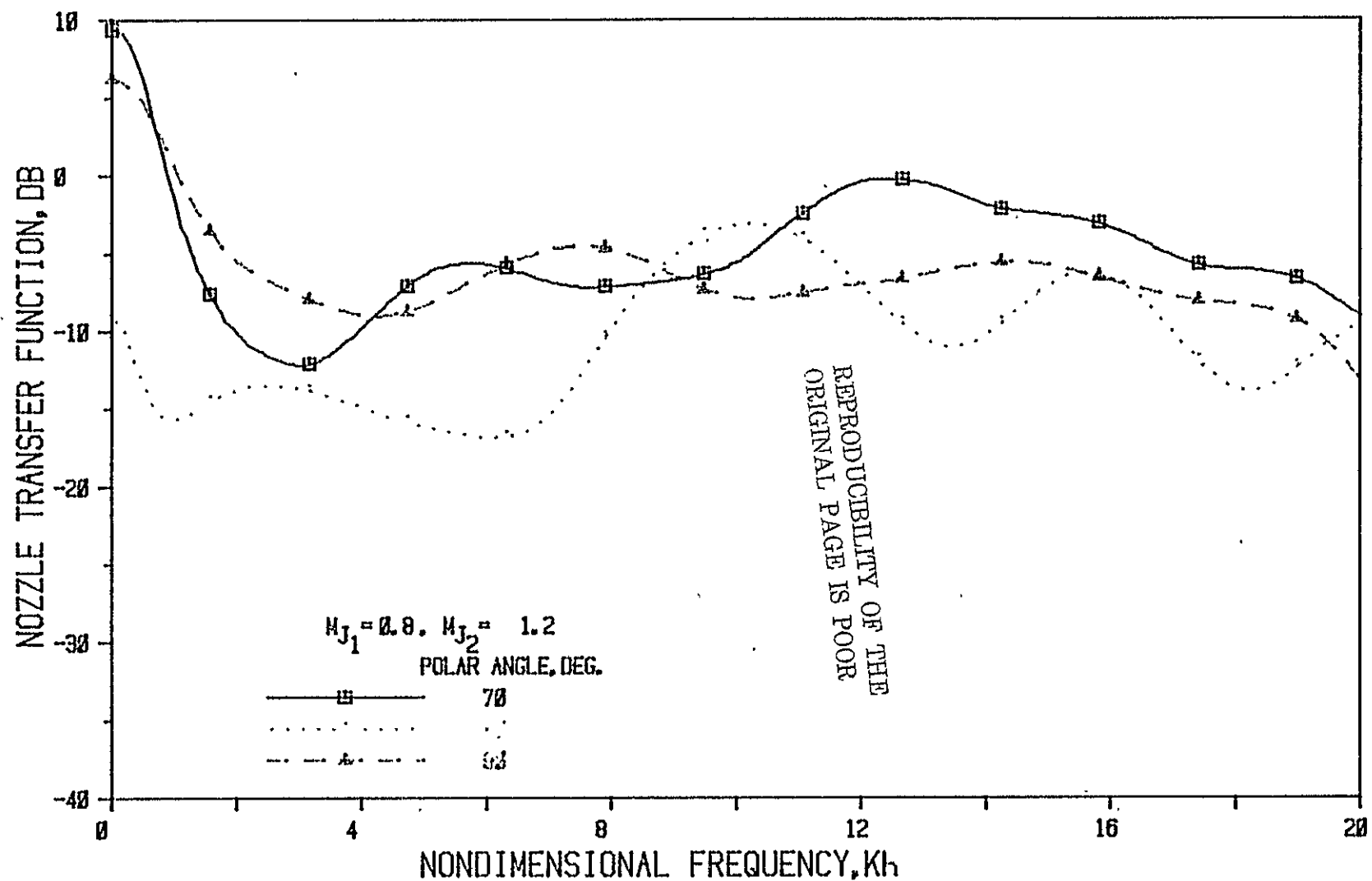


Figure 42(b) Nozzle N 5 (  $L/h = 3$ , Convergence Angle = 40 Deg.); Source At Fan

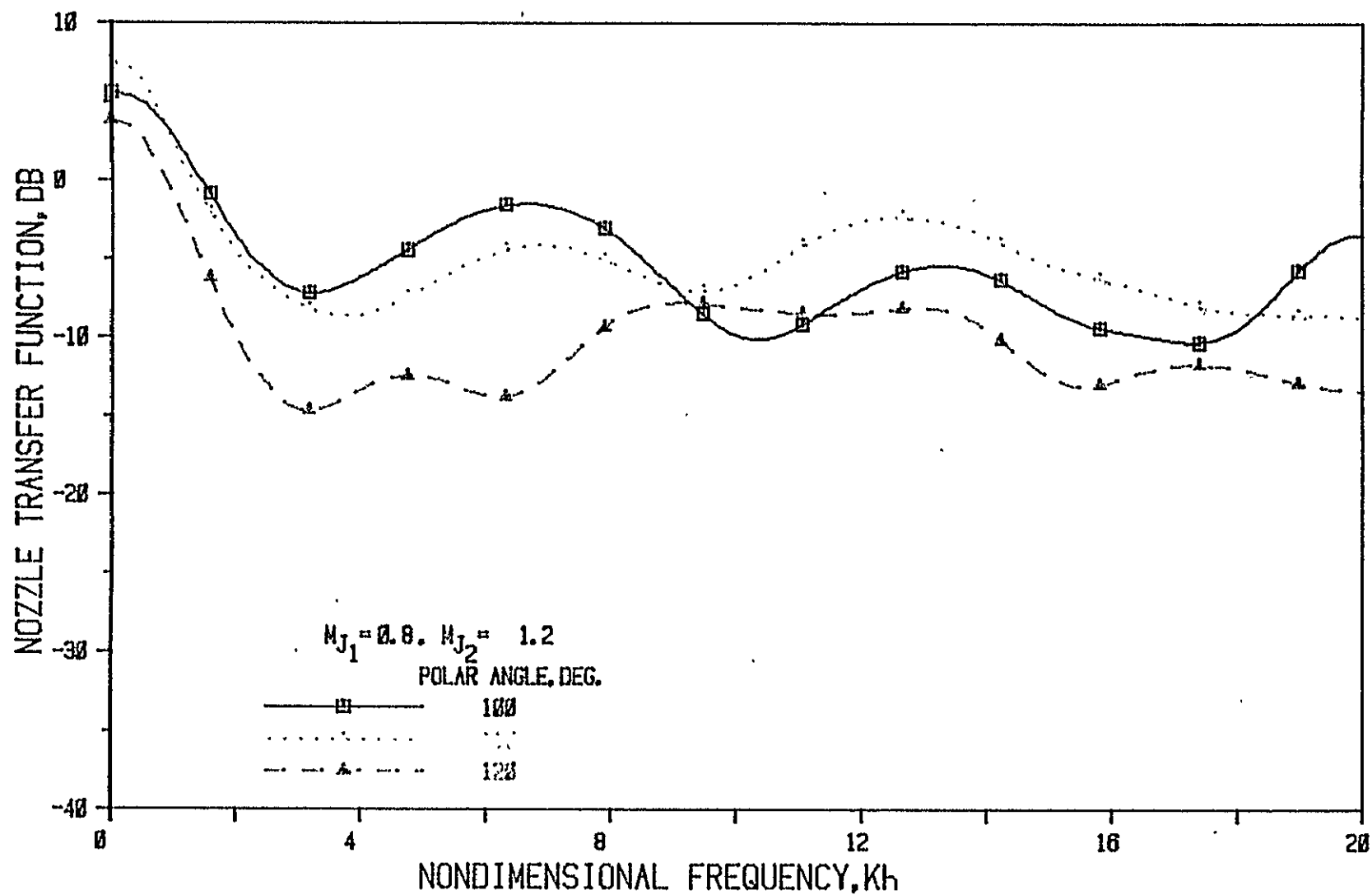


Figure 42(c) Nozzle N 5 ( $L/h = 3$ , Convergence Angle = 40 Deg.); Source At Fan

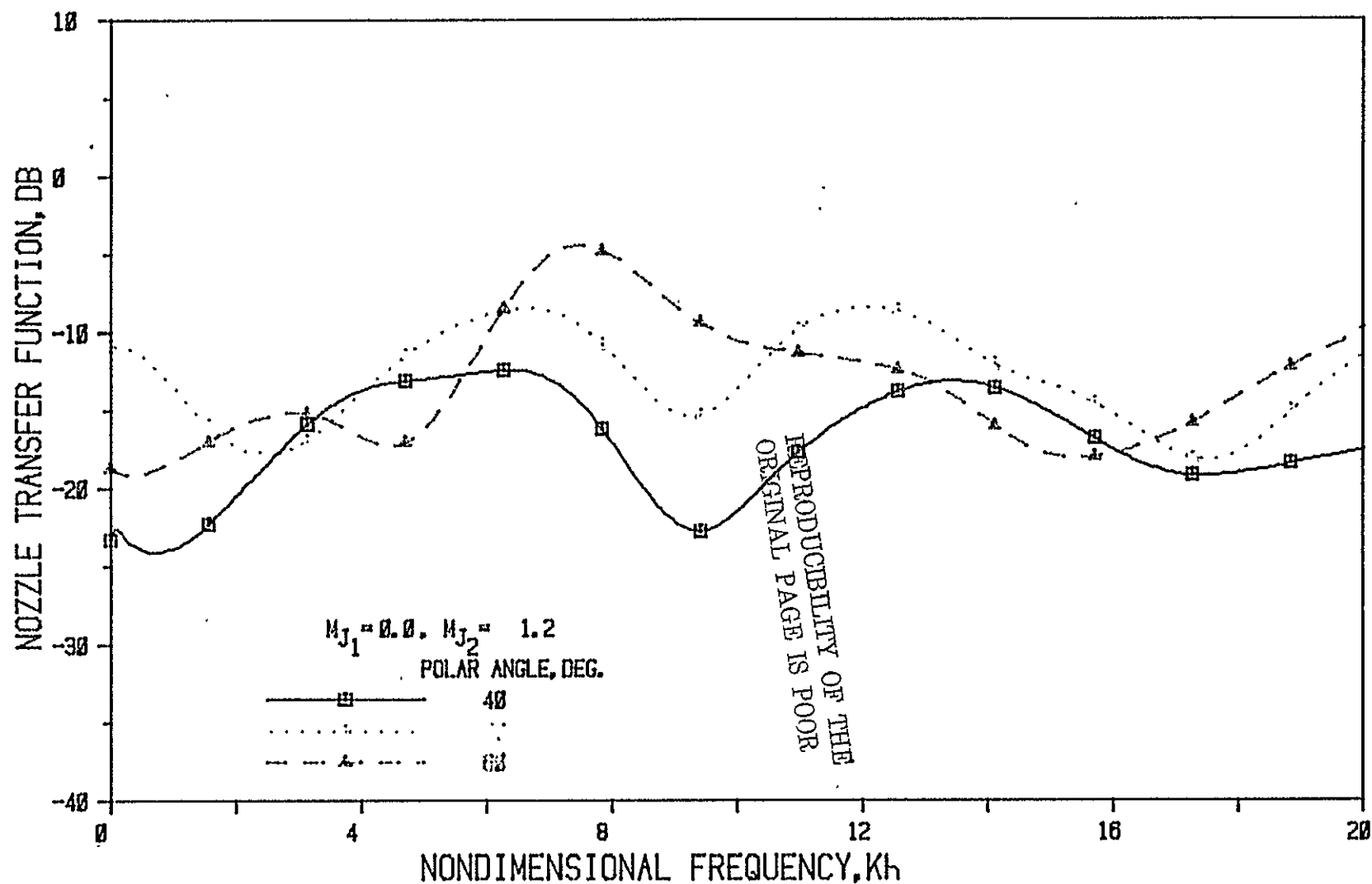


Figure 43(a) Nozzle N 5 ( $L/h = 3$ , Convergence Angle = 40 Deg.); Source At Fan

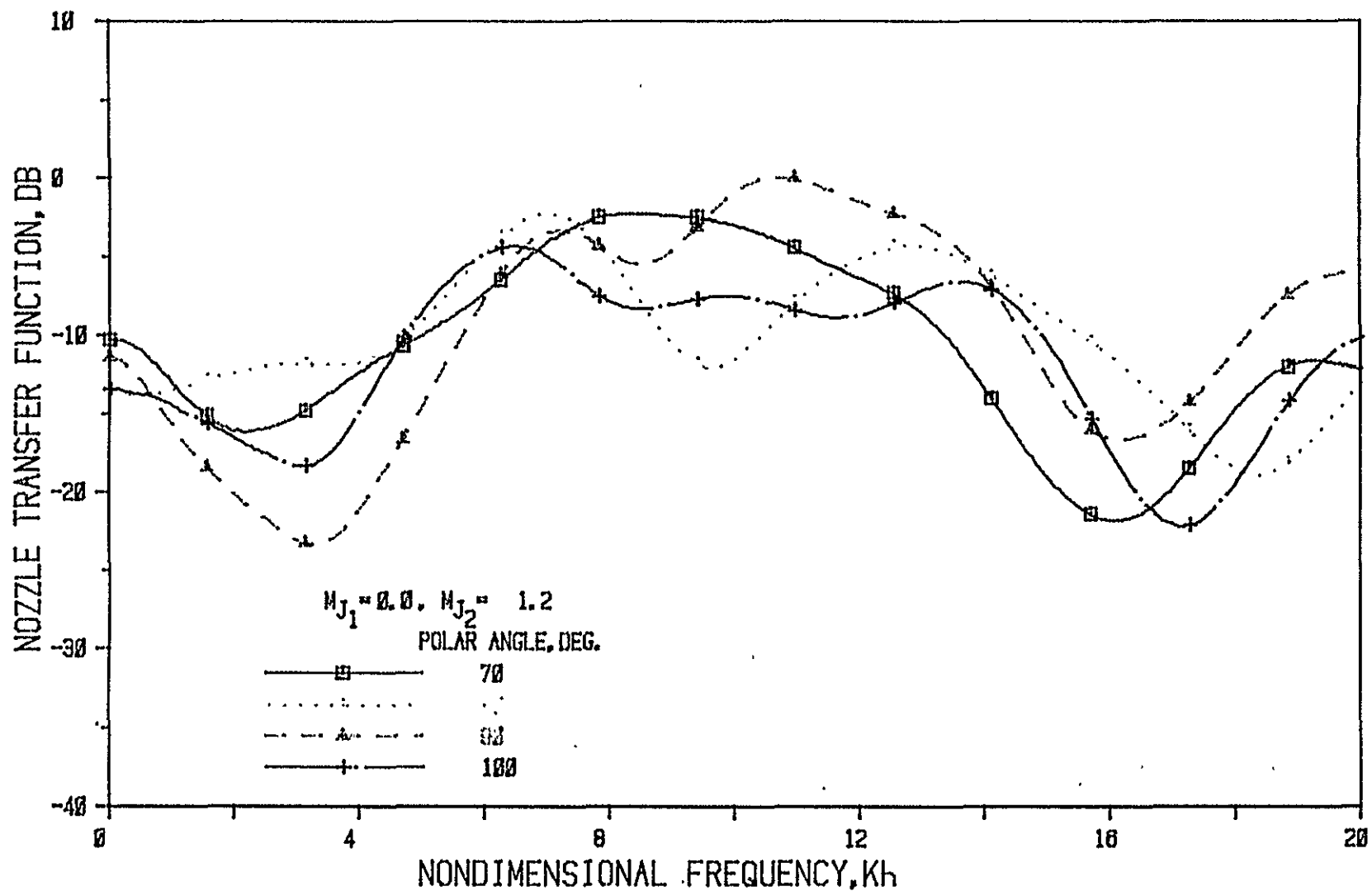


Figure 43(b) Nozzle N 5 ( $L/h = 3$ , Convergence Angle = 40 Deg.); Source At Fan

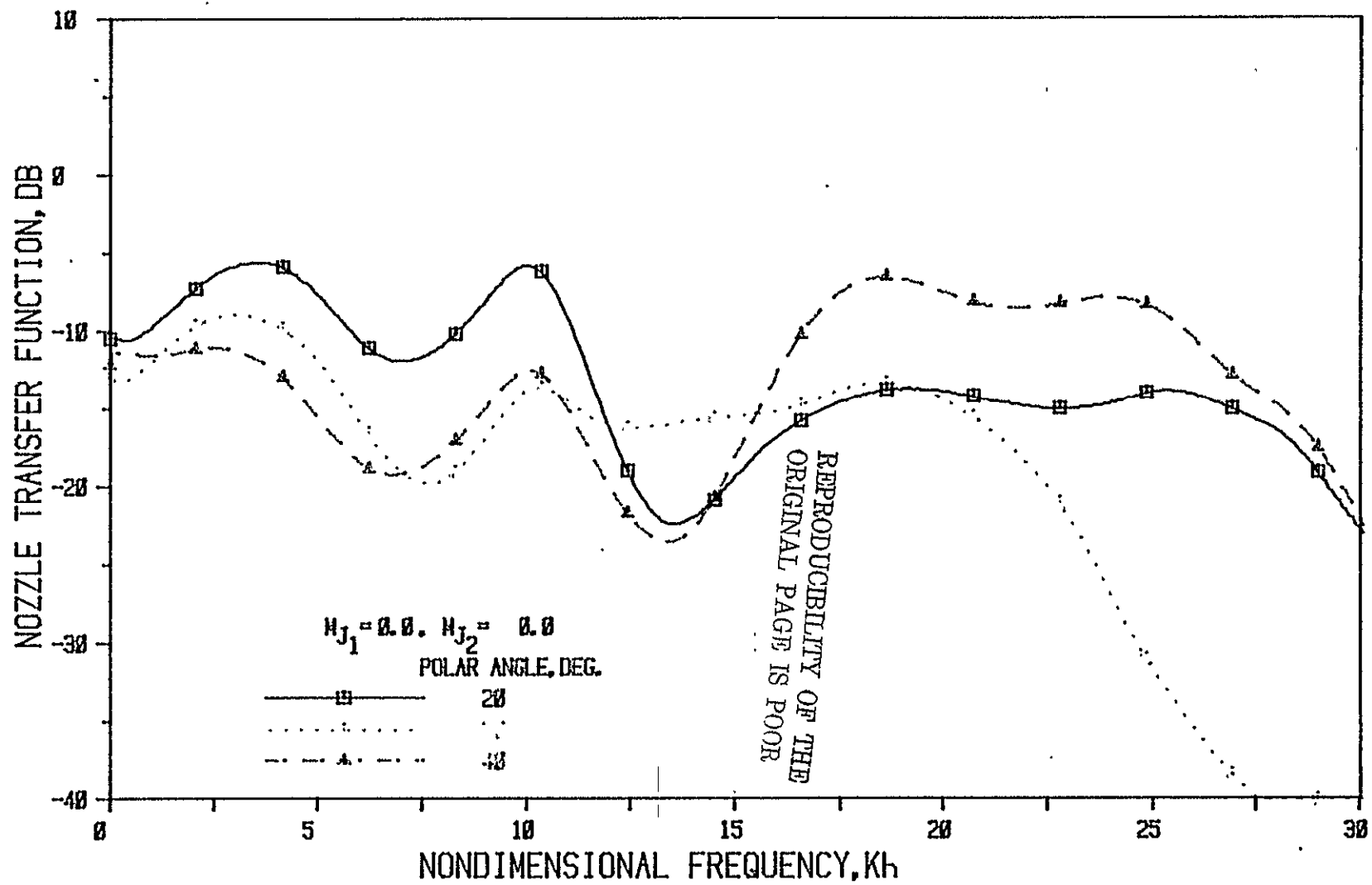


Figure 44(a) Nozzle N 6 ( $L/h = 5$ , Convergence Angle = 40 Deg.); Source At Fan



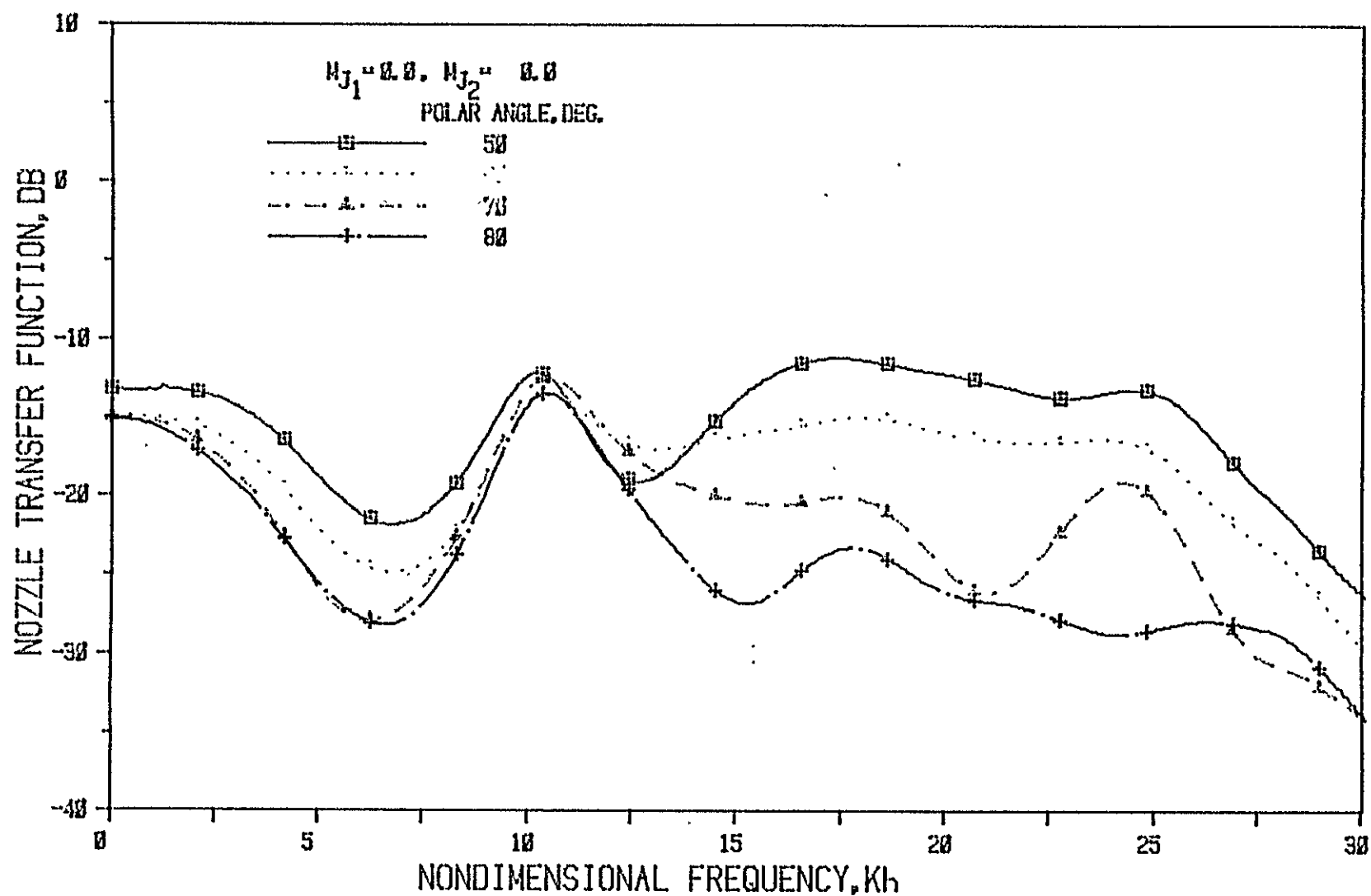


Figure 44(b) Nozzle N 6 ( $L/h = 5$ , Convergence Angle =  $40^\circ$ ); Source At Fan

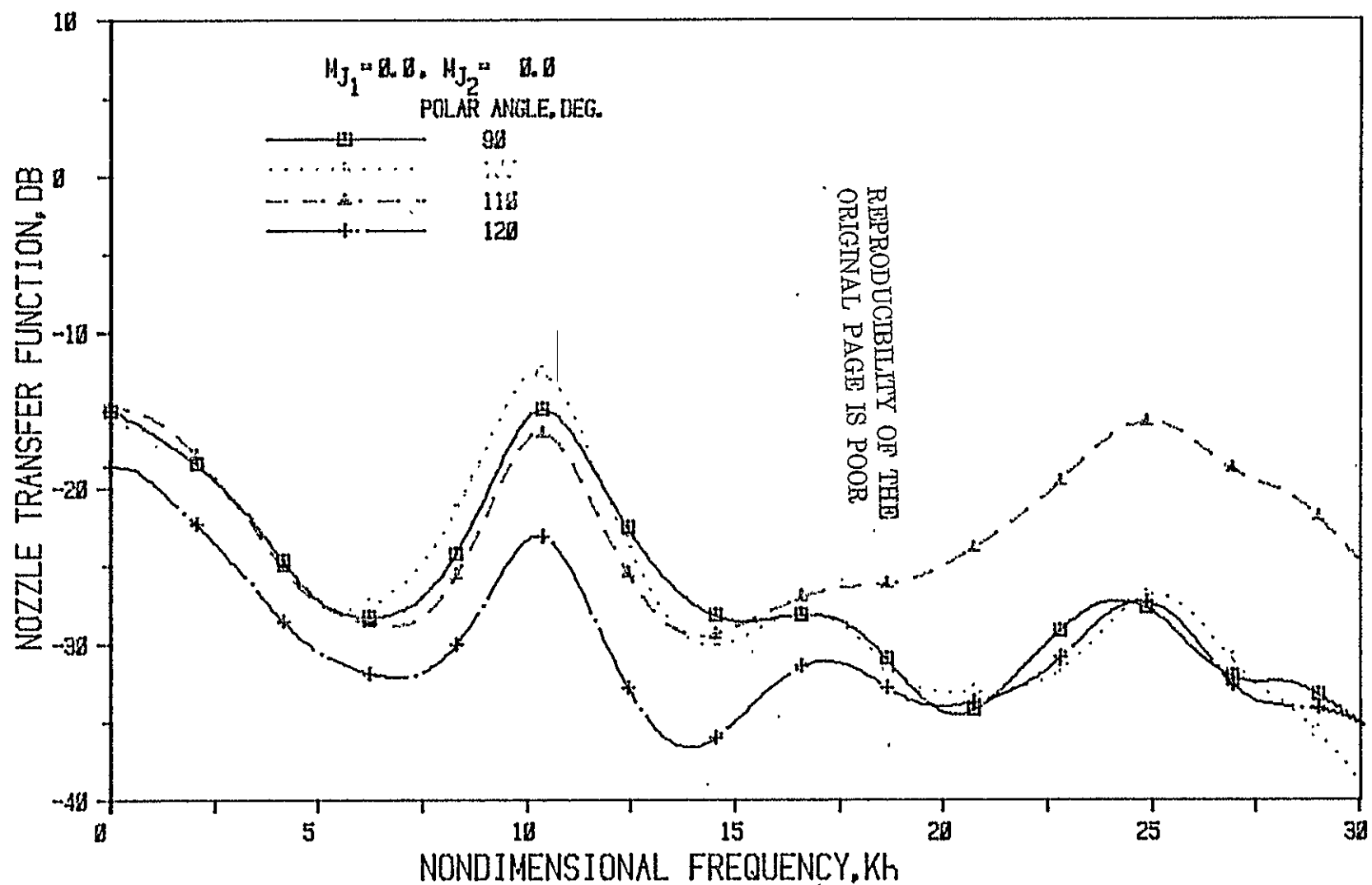


Figure 44(c) Nozzle N 6 ( $L/h = 5$ , Convergence Angle =  $40^\circ$ ); Source At Fan

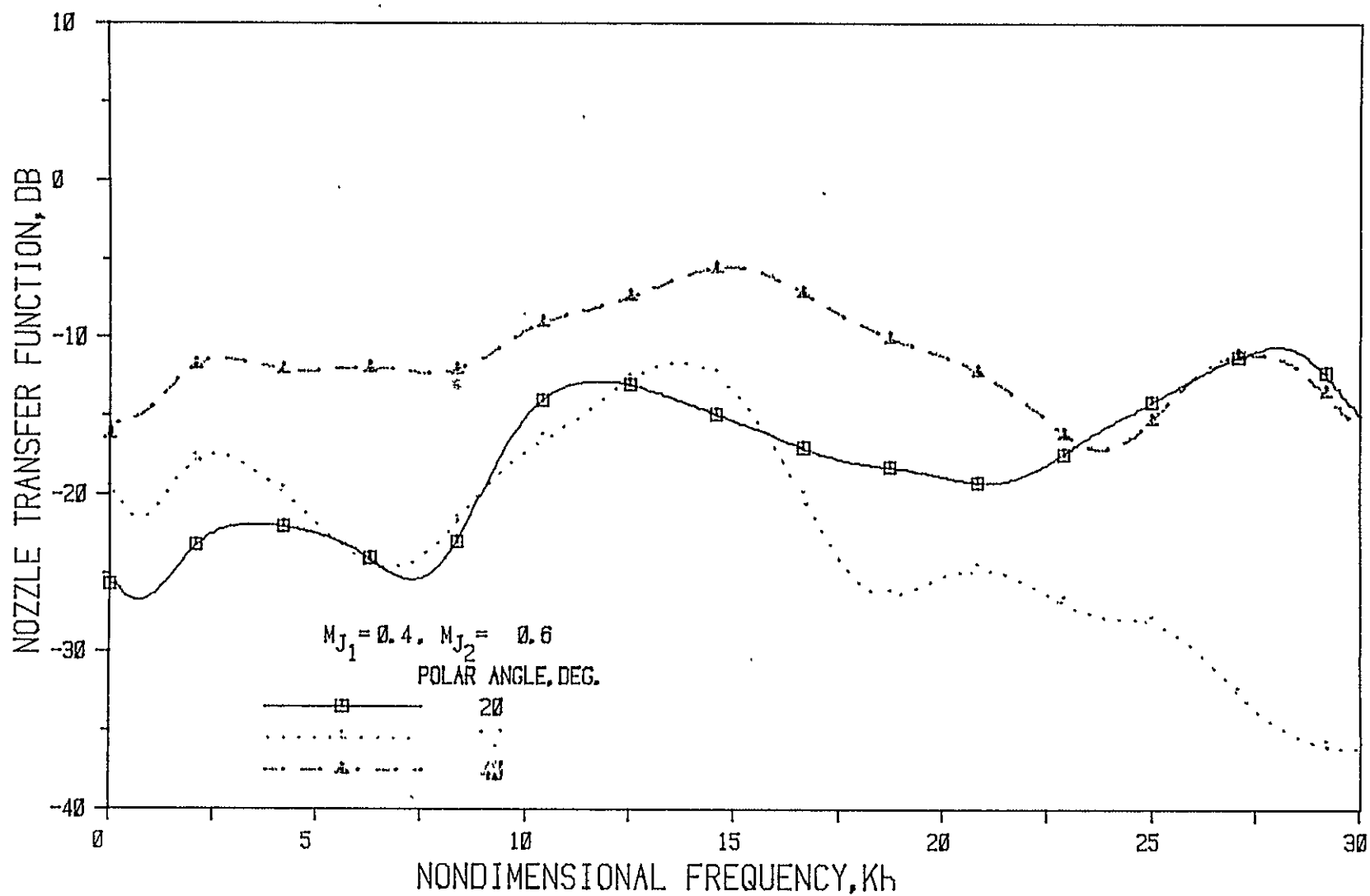


Figure 45(a) Nozzle N 6 ( $L/h = 5$ , Convergence Angle = 40 Deg.); Source At Fan

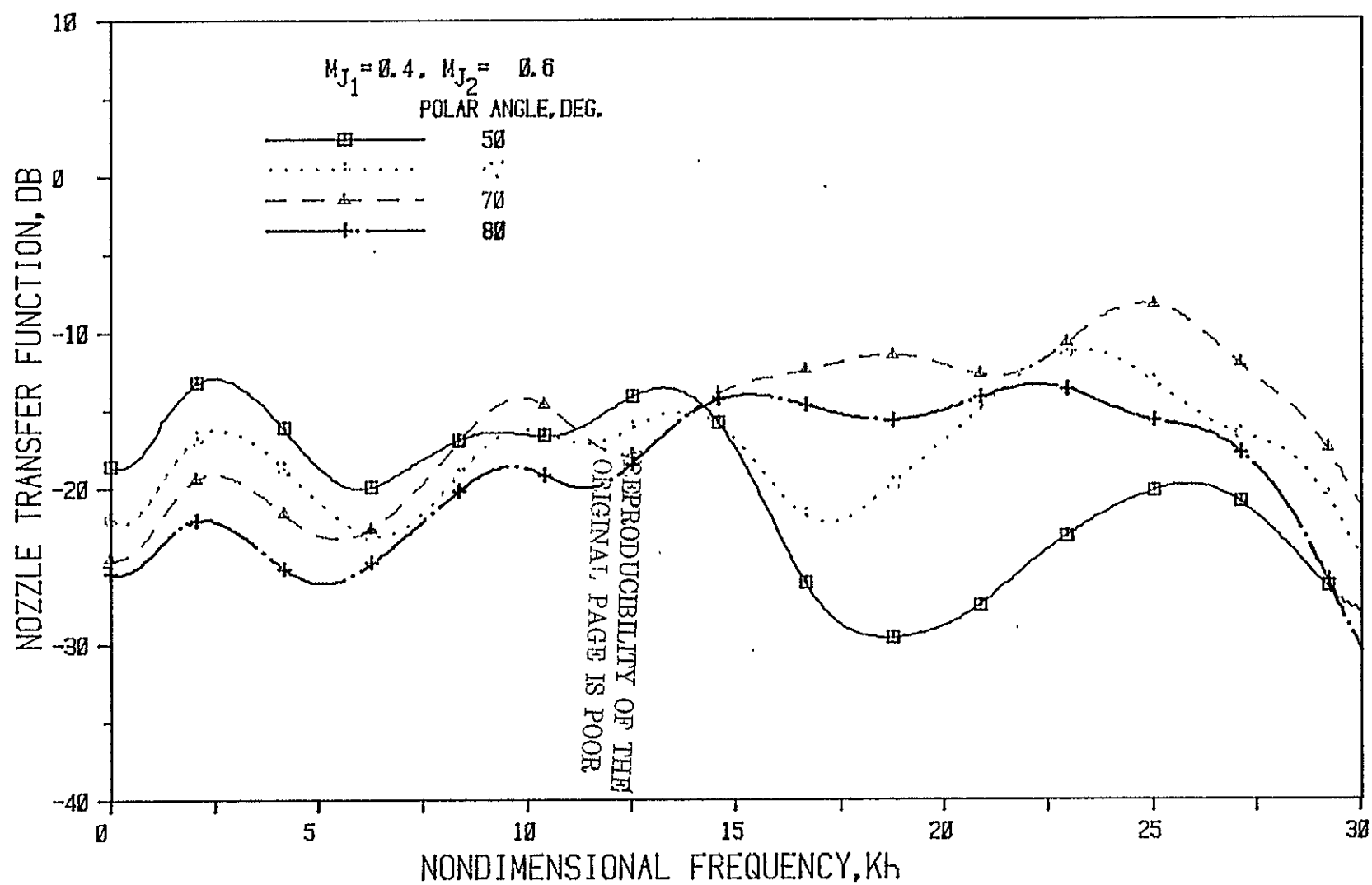


Figure 45(b) Nozzle N 6 ( $L/h = 5$ , Convergence Angle =  $40^\circ$ ); Source At Fan

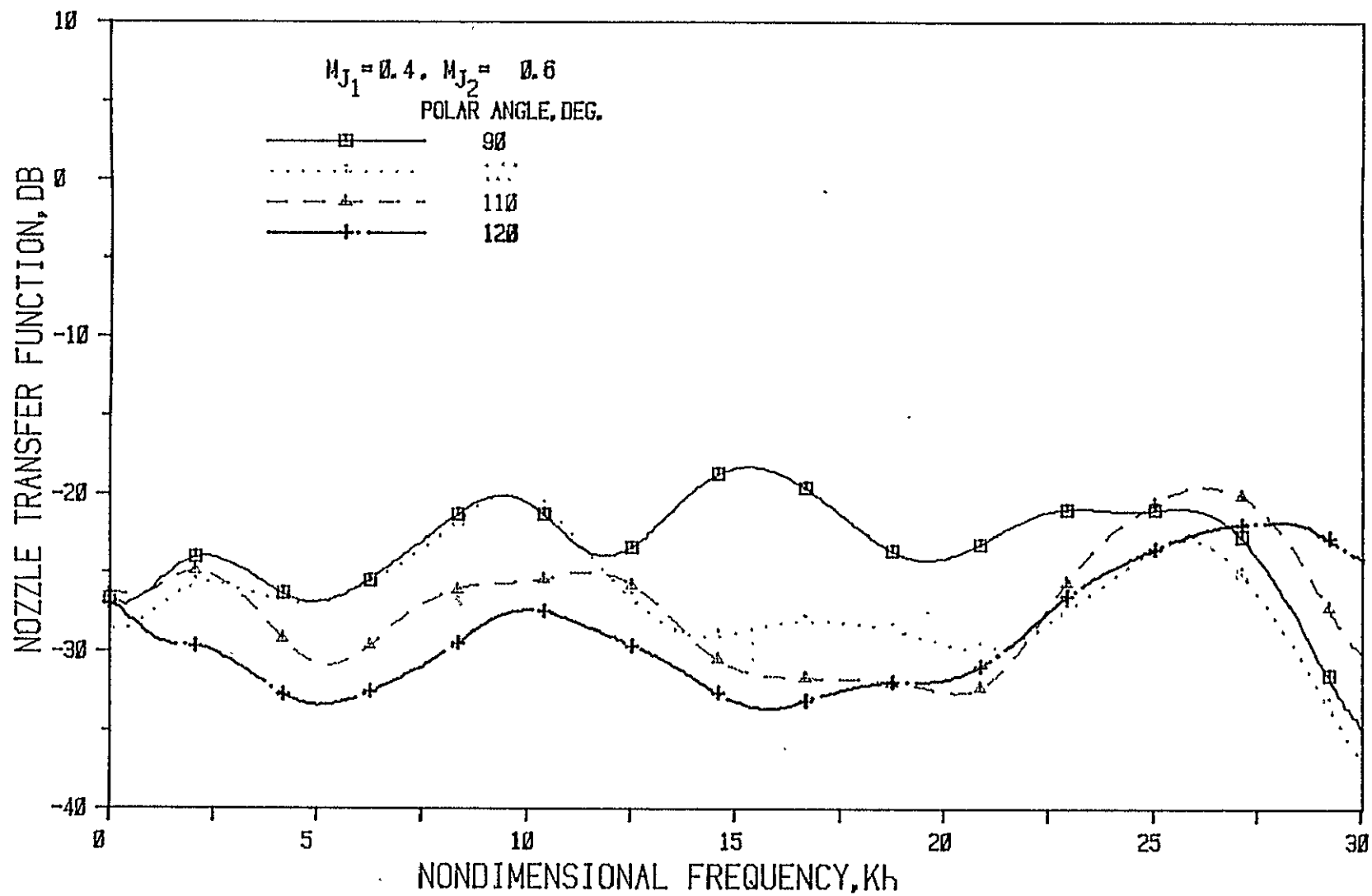


Figure 45(c) Nozzle N 6 ( $L/h = 5$ , Convergence Angle = 40 Deg.); Source At Fan

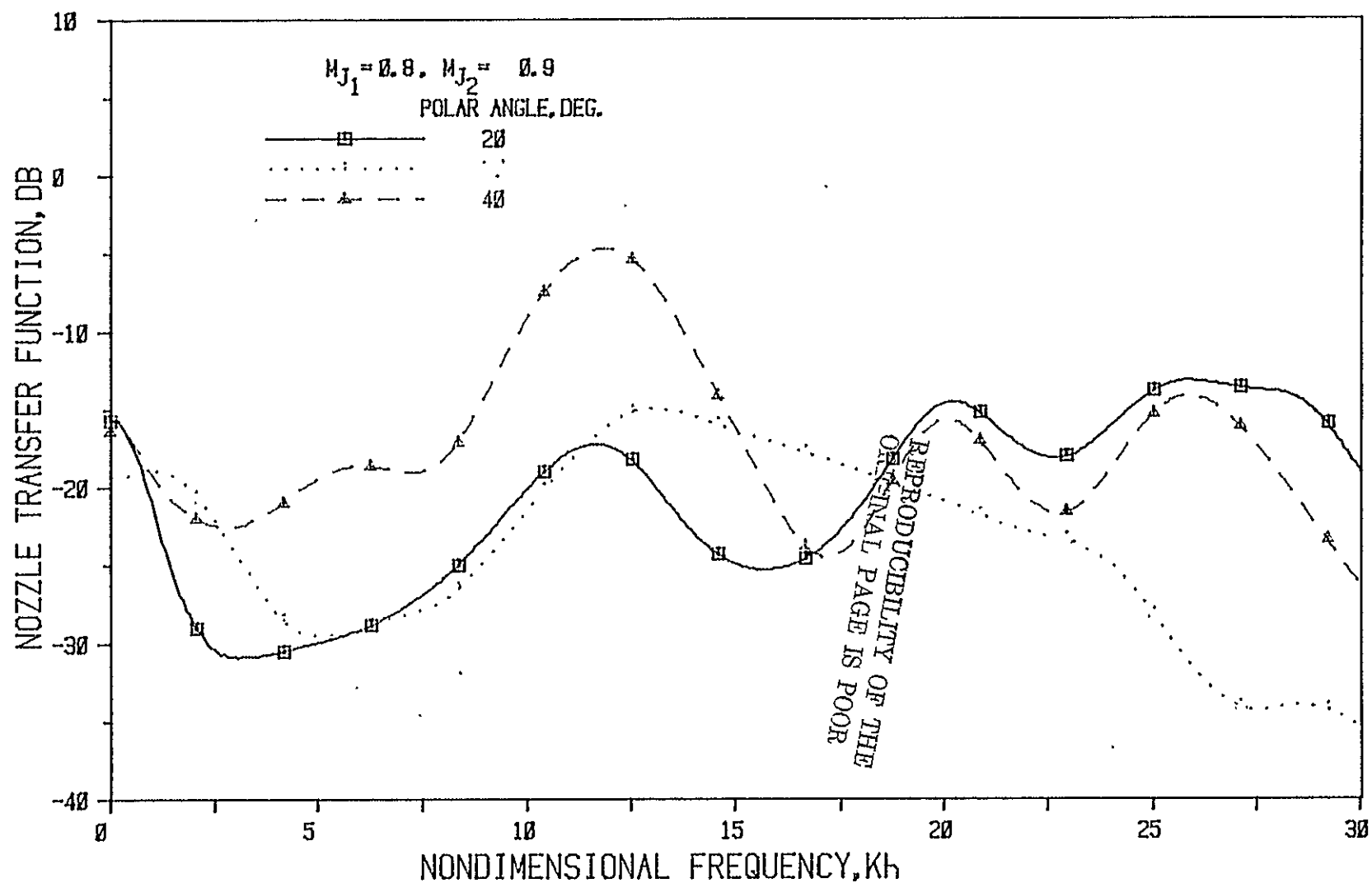


Figure 46(a) Nozzle N 6 (  $L/h = 5$ , Convergence Angle = 40 Deg.); Source At Fan

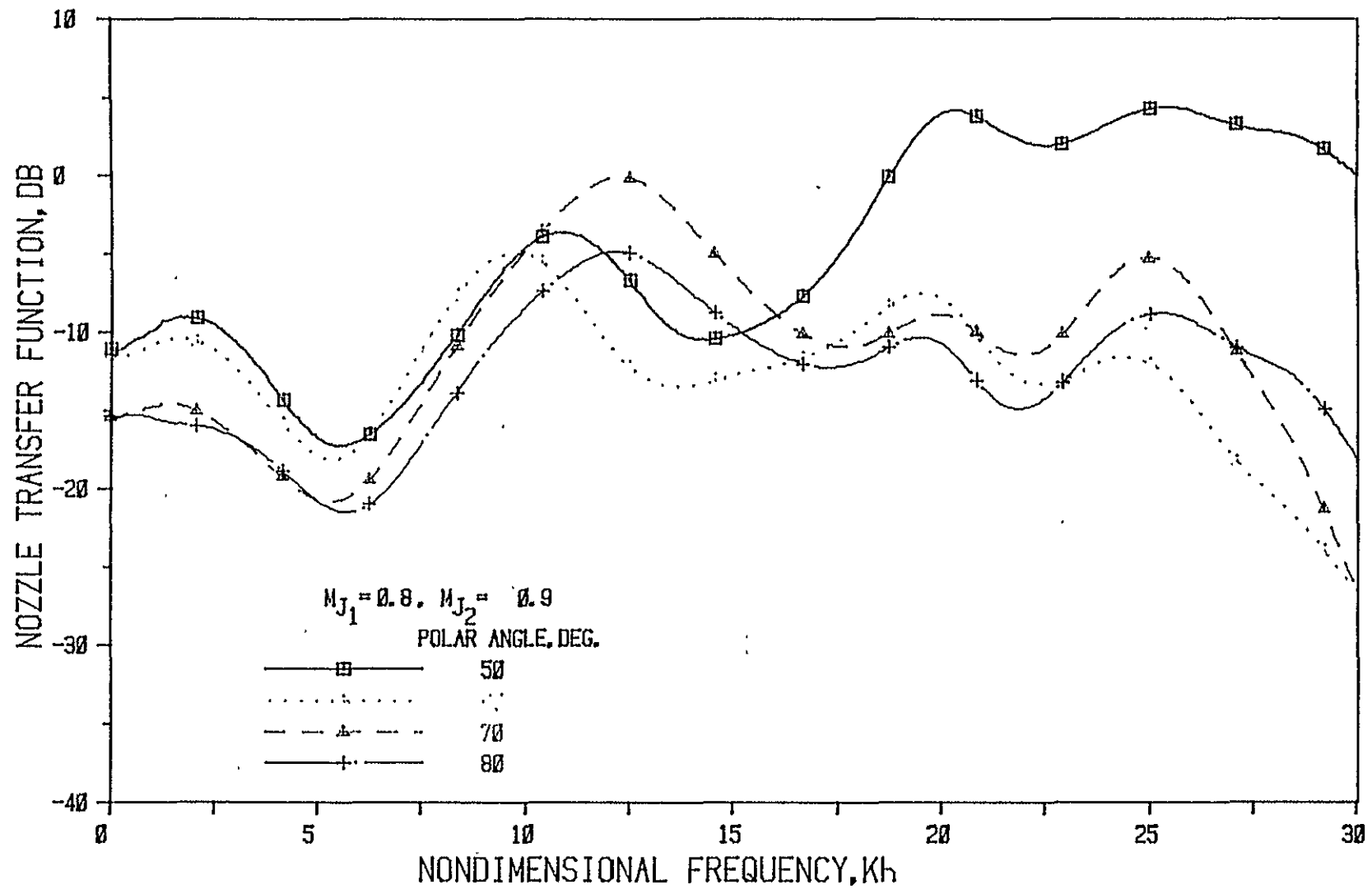


Figure 46(b) Nozzle N 6 ( $L/h = 5$ , Convergence Angle =  $40^\circ$ ); Source At Fan

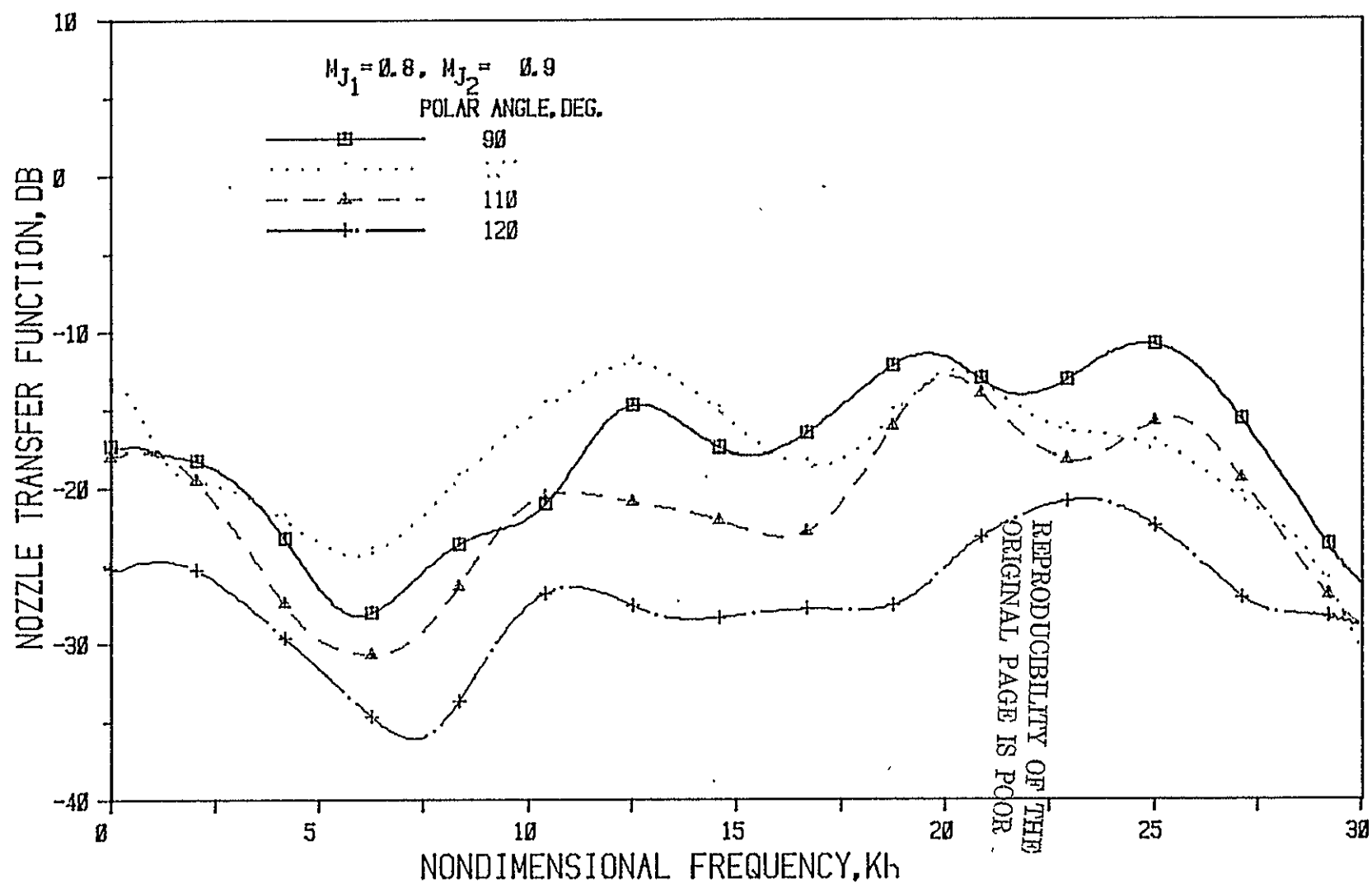


Figure 46(c) Nozzle N 6 (  $L/h = 5$ , Convergence Angle =  $40^\circ$  ); Source At Fan



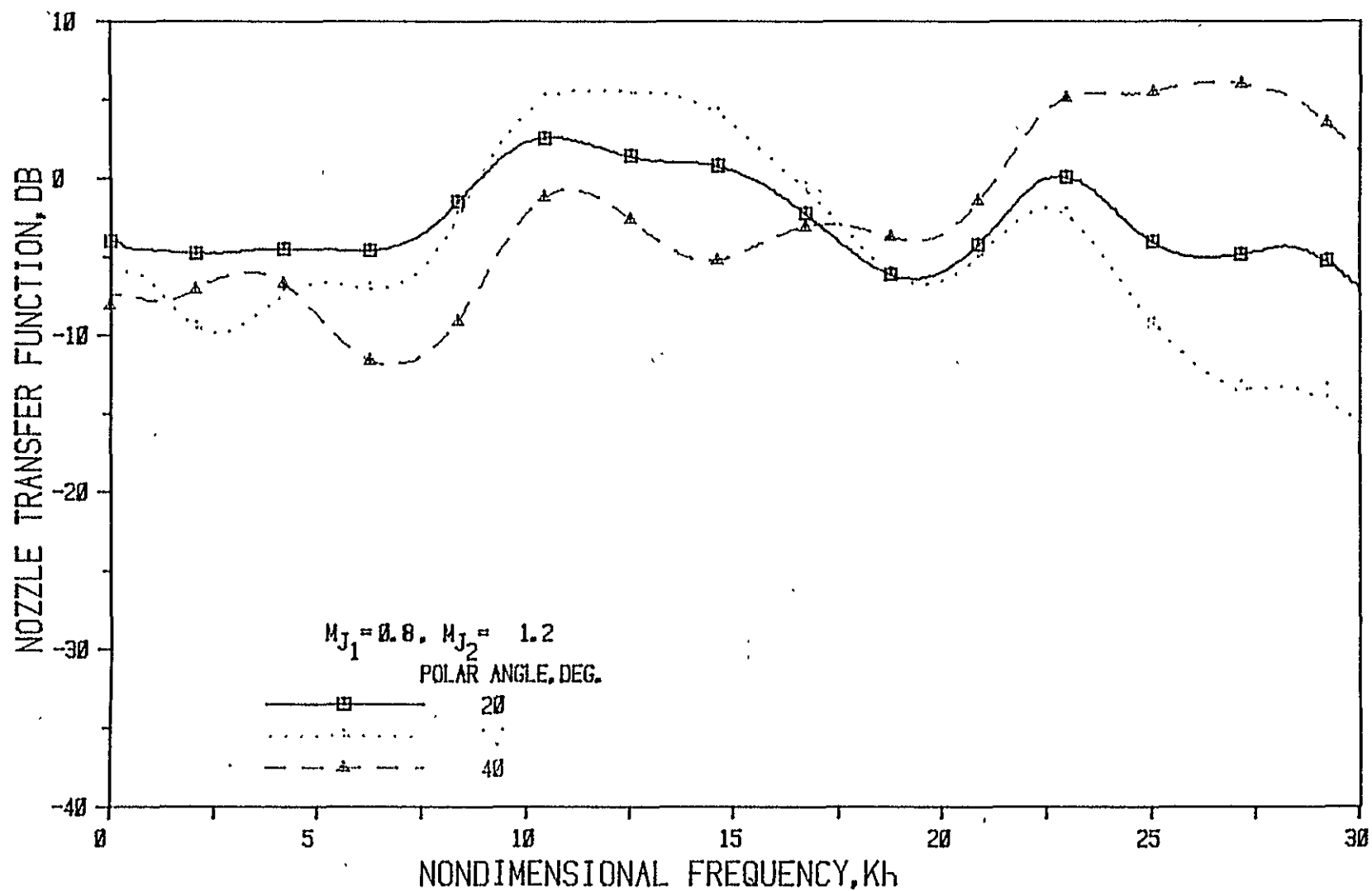


Figure 47(a) Nozzle N 6 (  $L/h = 5$ , Convergence Angle = 40 Deg.); Source At Fan

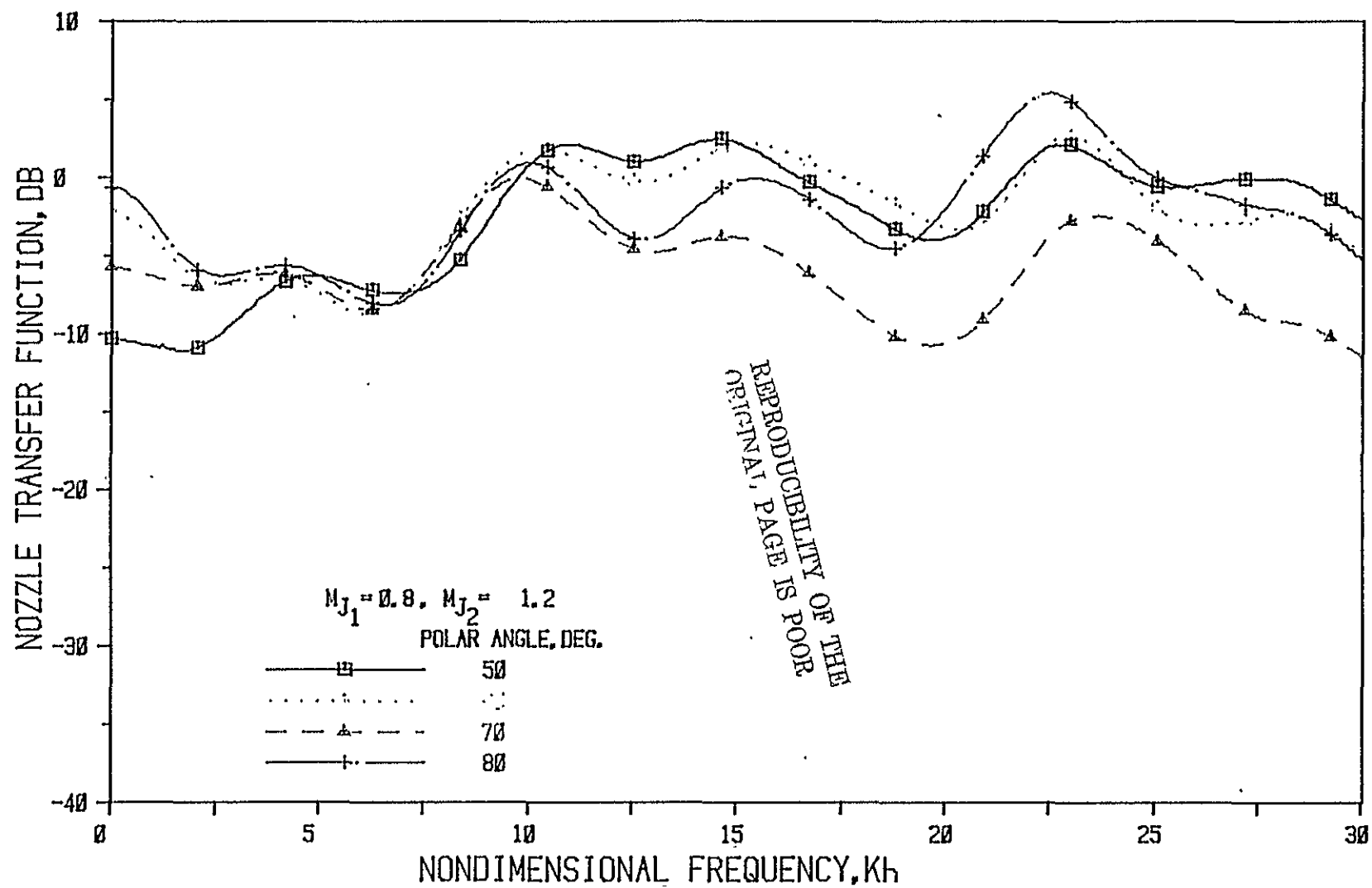


Figure 47(b) Nozzle N 6 ( $L/h = 5$ , Convergence Angle = 40 Deg.); Source At Fan

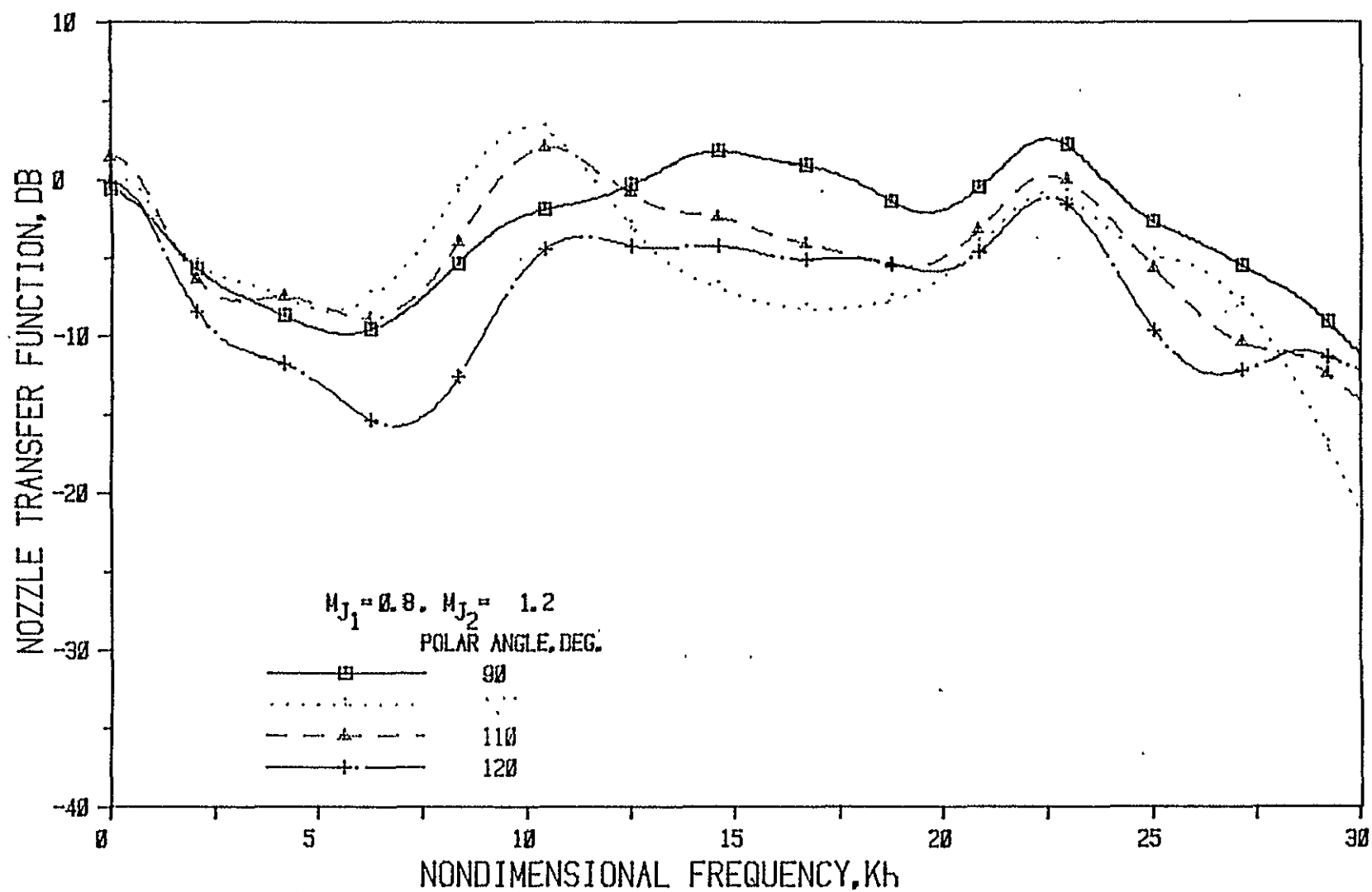


Figure 47(c) Nozzle N 6 ( $L/h = 5$ , Convergence Angle = 40 Deg.); Source At Fan

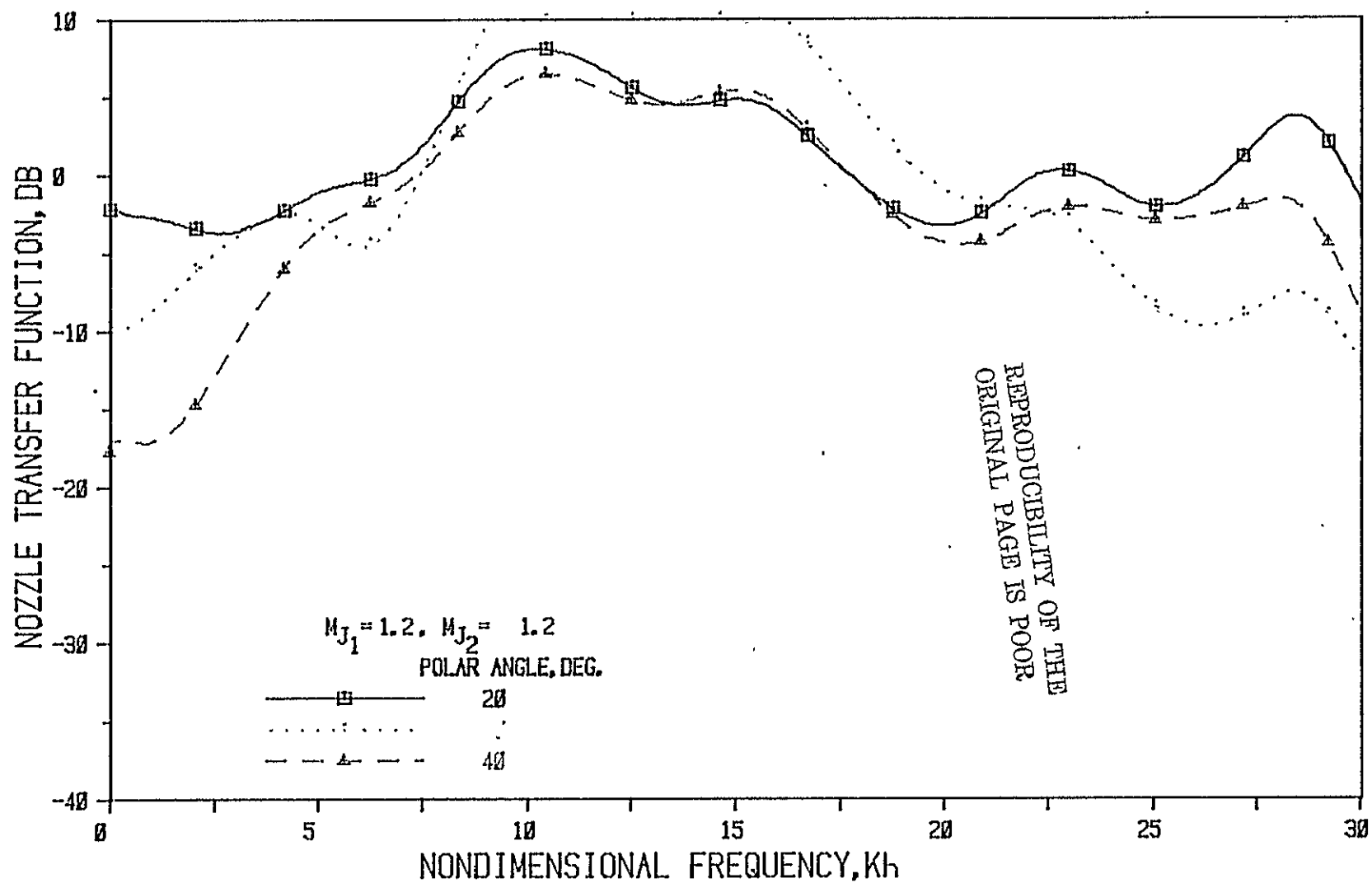


Figure 48(a) Nozzle N 6 (  $L/h = 5$ , Convergence Angle = 40 Deg.); Source At Fan

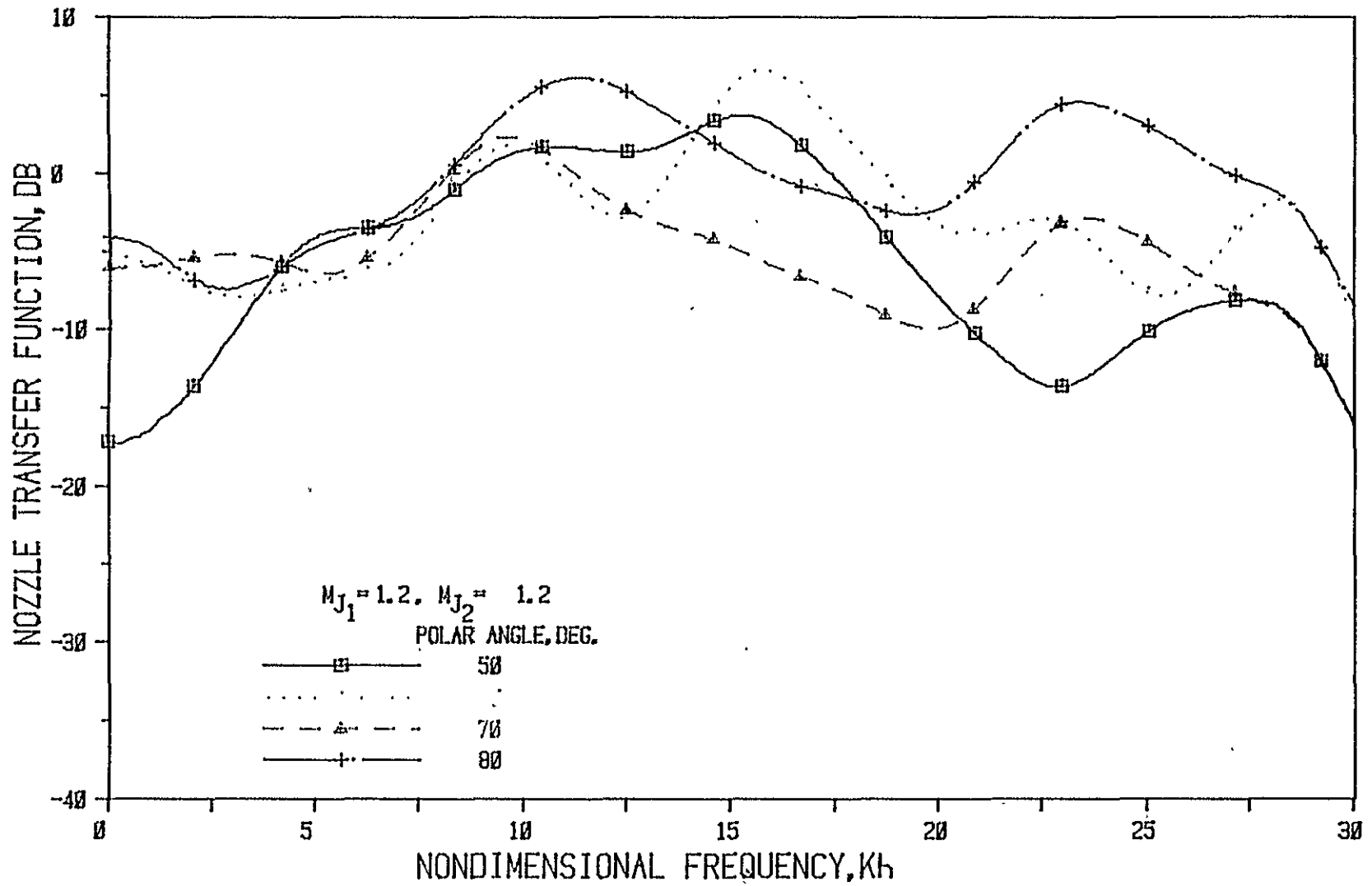


Figure 48(b) Nozzle N 6 ( $L/h = 5$ , Convergence Angle = 40 Deg.); Source At Fan

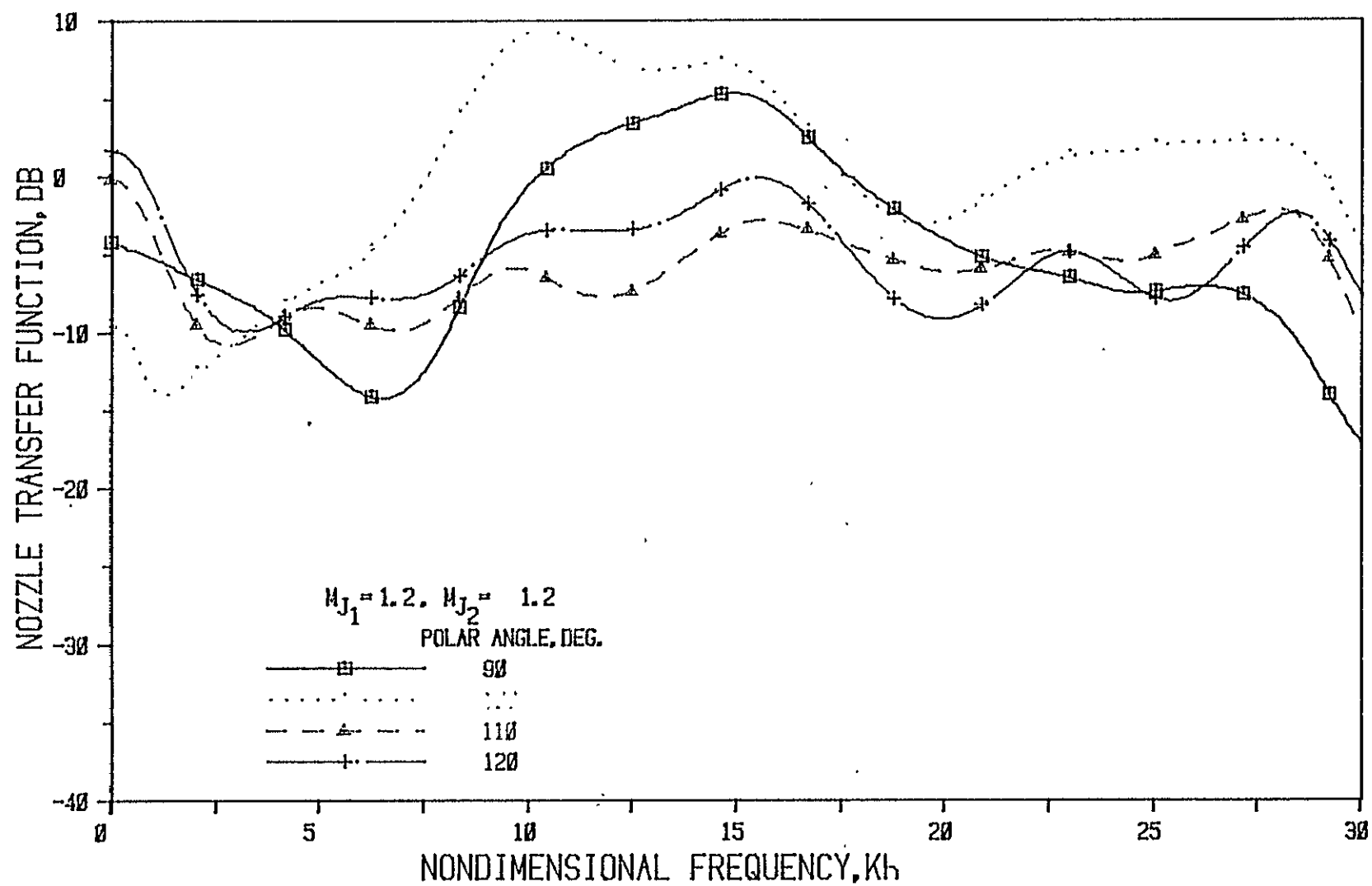


Figure 48(c) Nozzle N 6 ( $L/h = 5$ , Convergence Angle = 40 Deg.); Source At Fan

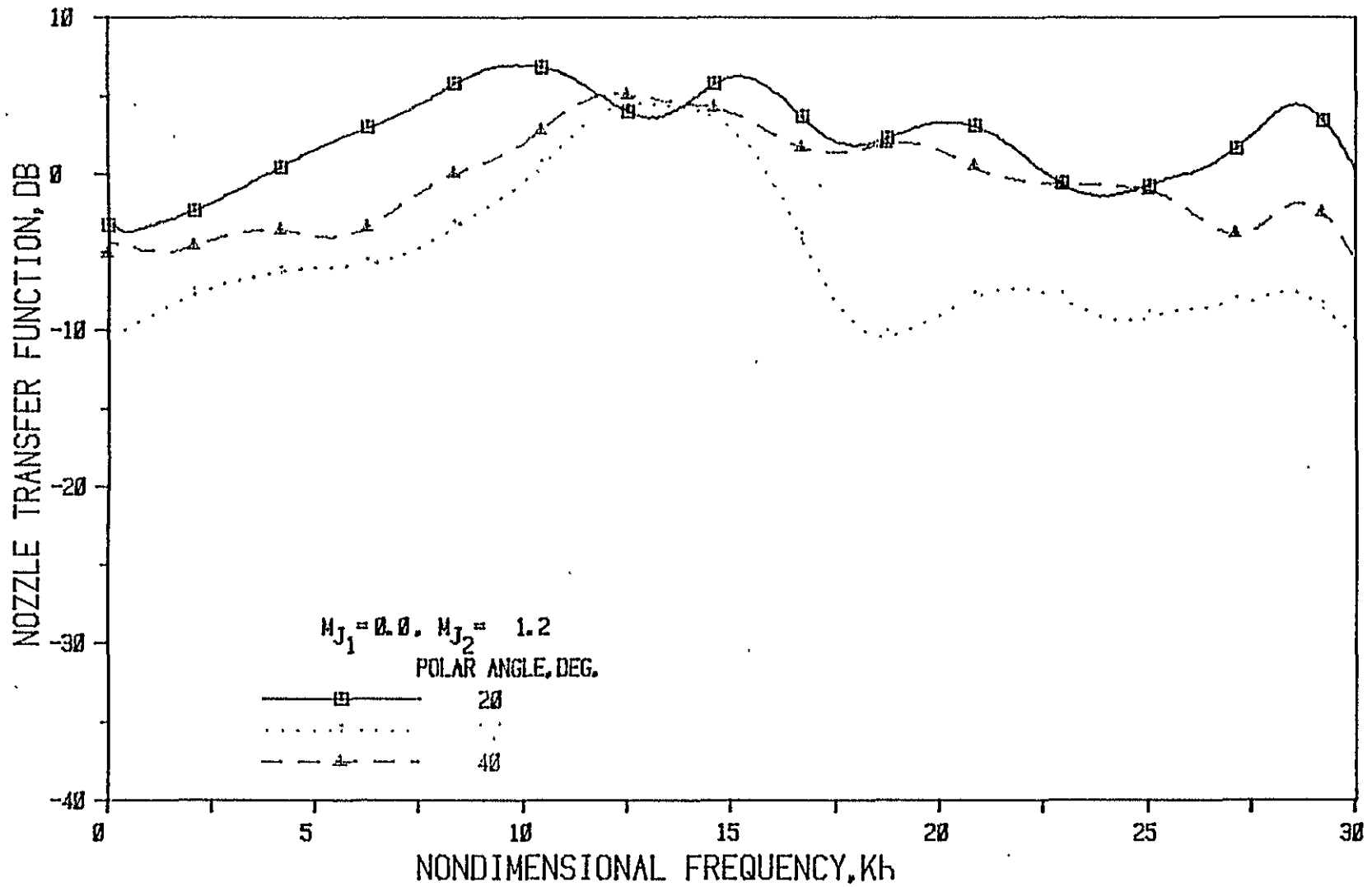


Figure 49(a) Nozzle N 6 ( $L/h = 5$ , Convergence Angle = 40 Deg.); Source At Fan

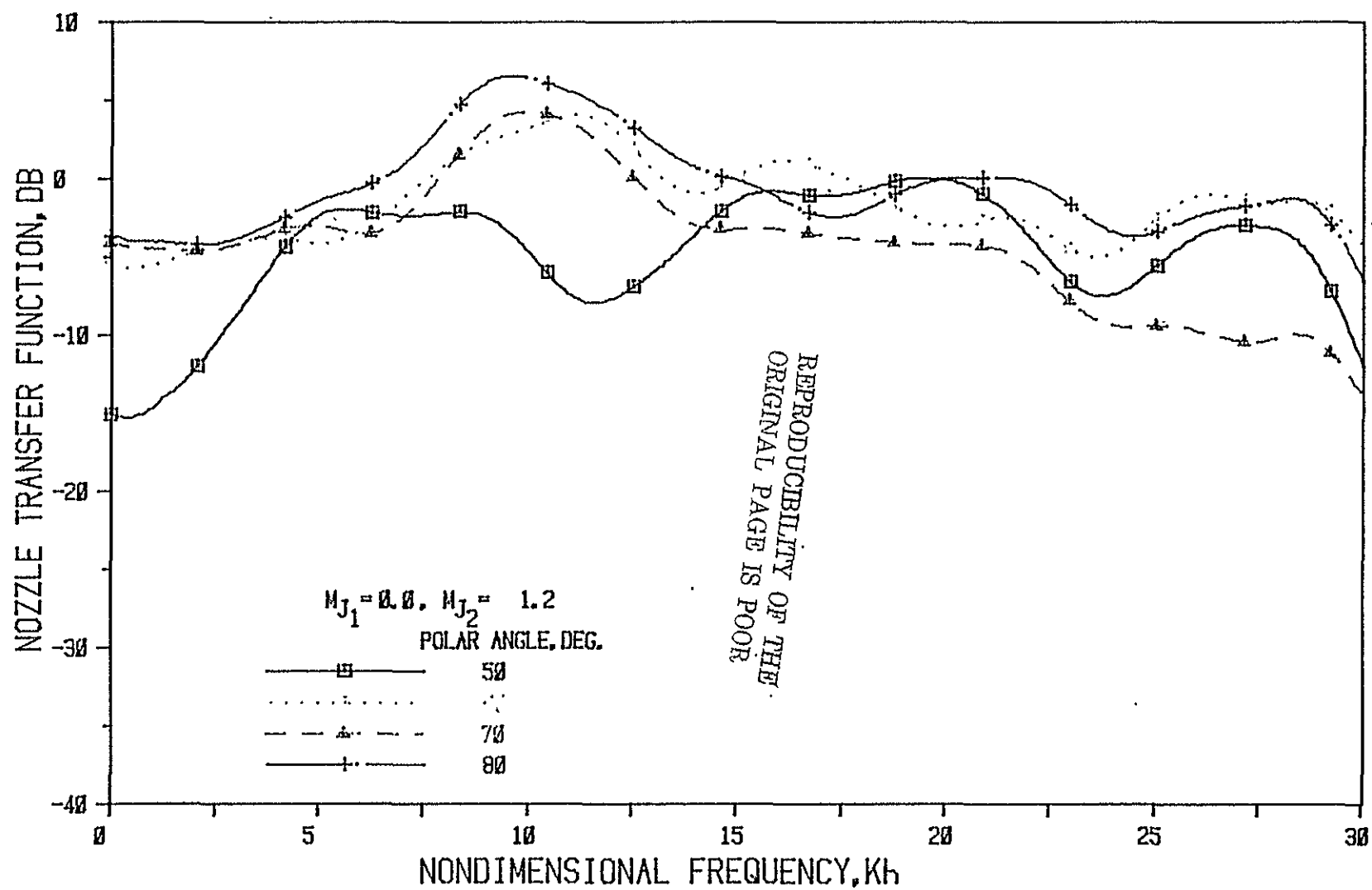


Figure 49(b) Nozzle N 6 ( $L/h = 5$ , Convergence Angle =  $40^\circ$ ); Source At Fan



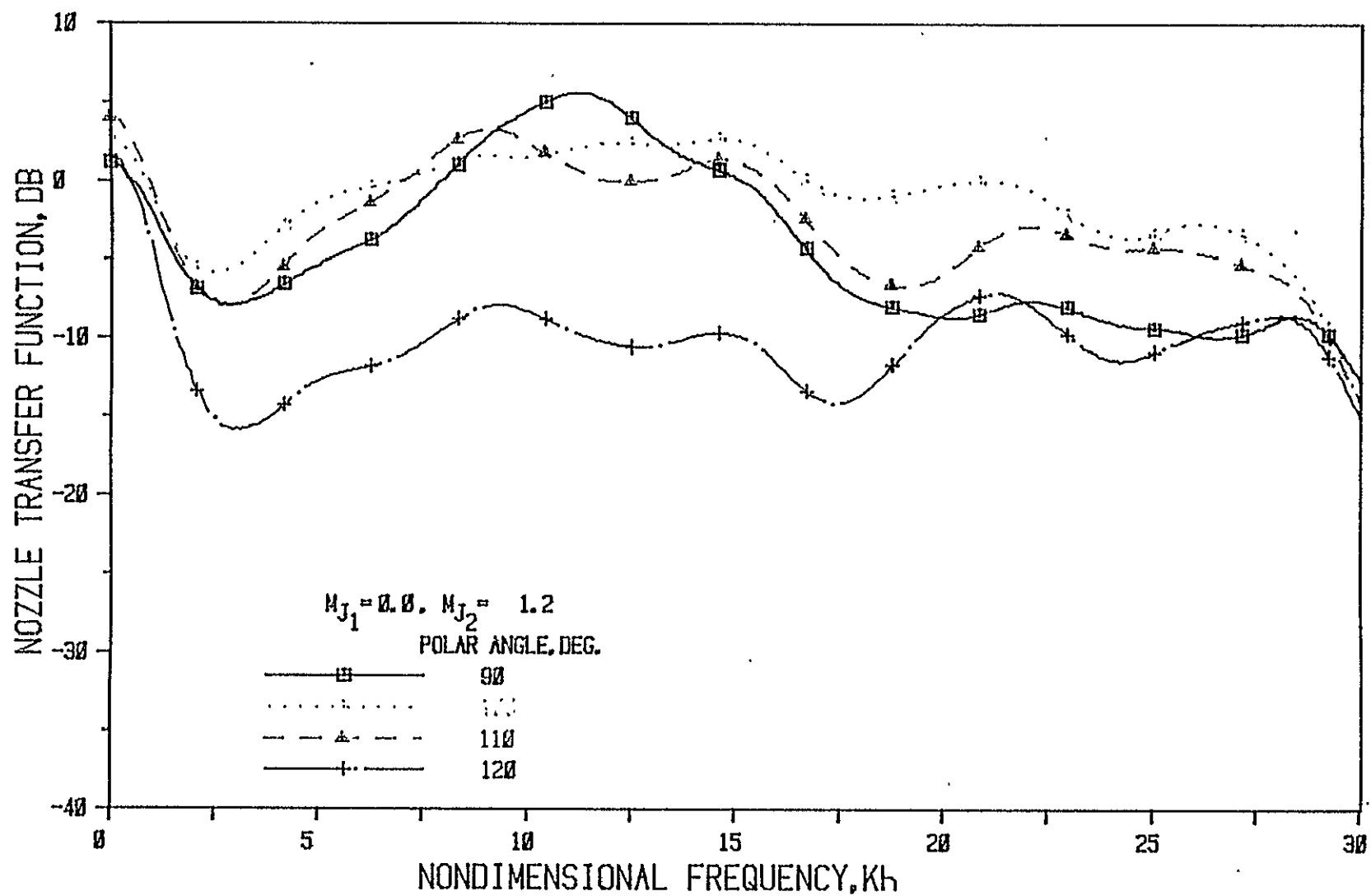


Figure 49(c) Nozzle N 6 ( $L/h = 5$ , Convergence Angle =  $40^\circ$ ); Source At Fan

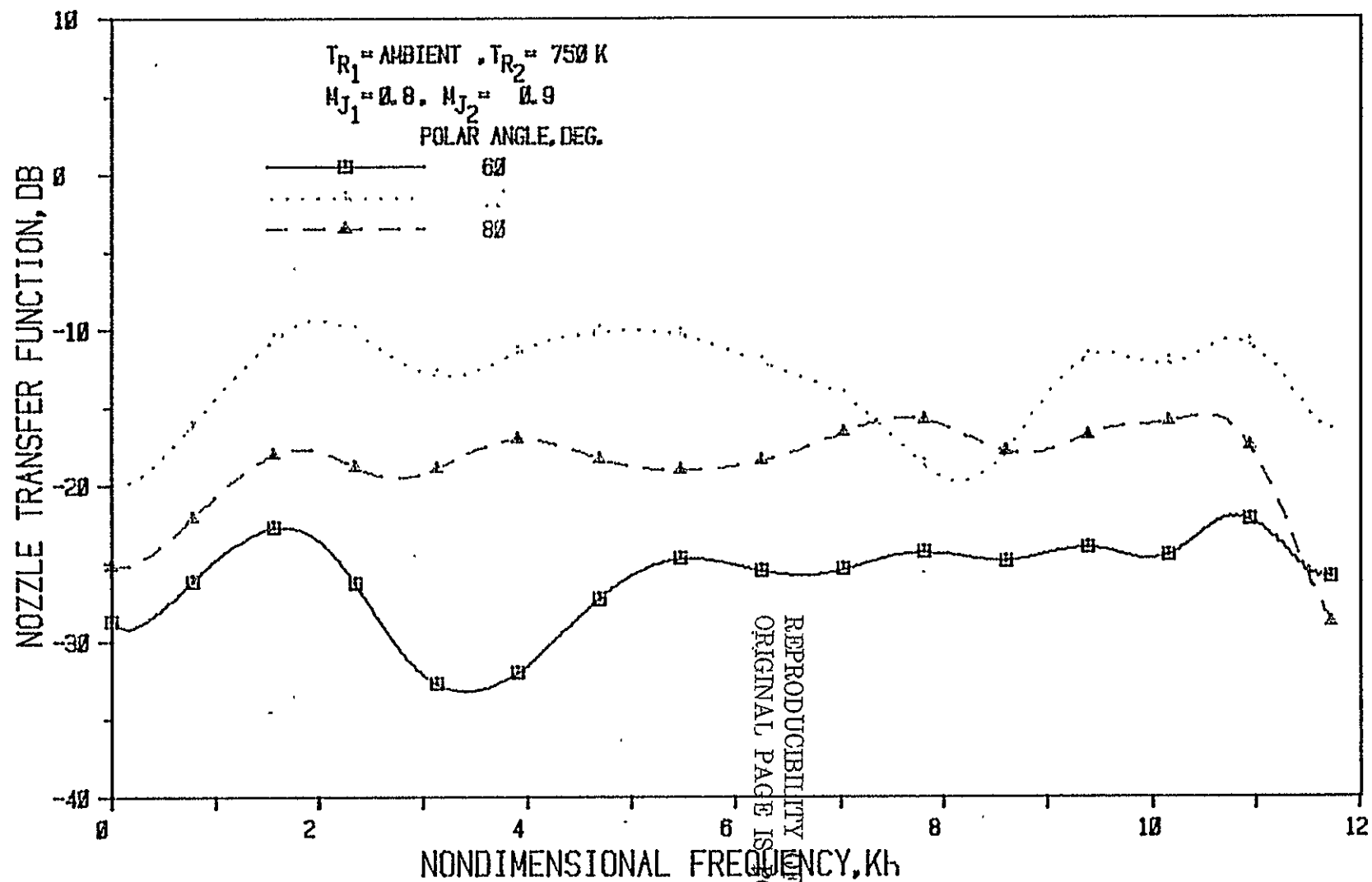


Figure 50(a) Nozzle N1 ( $L/h = 1$ , Convergence Angle = 20 Deg.); Source At Fan

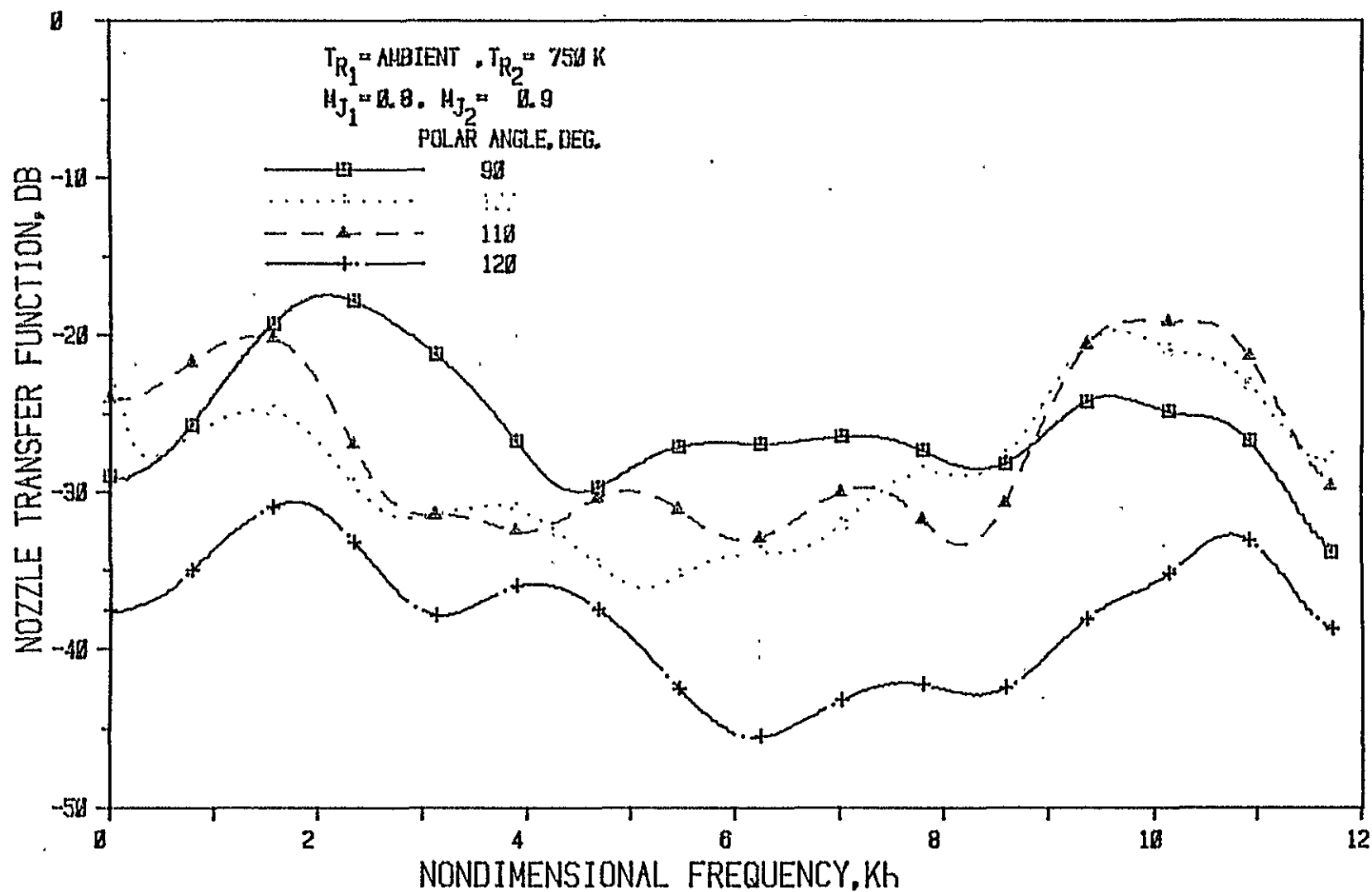


Figure 50(b) Nozzle N 1 (  $L/h = 1$  , Convergence Angle =  $20^\circ$  ); Source At Fan

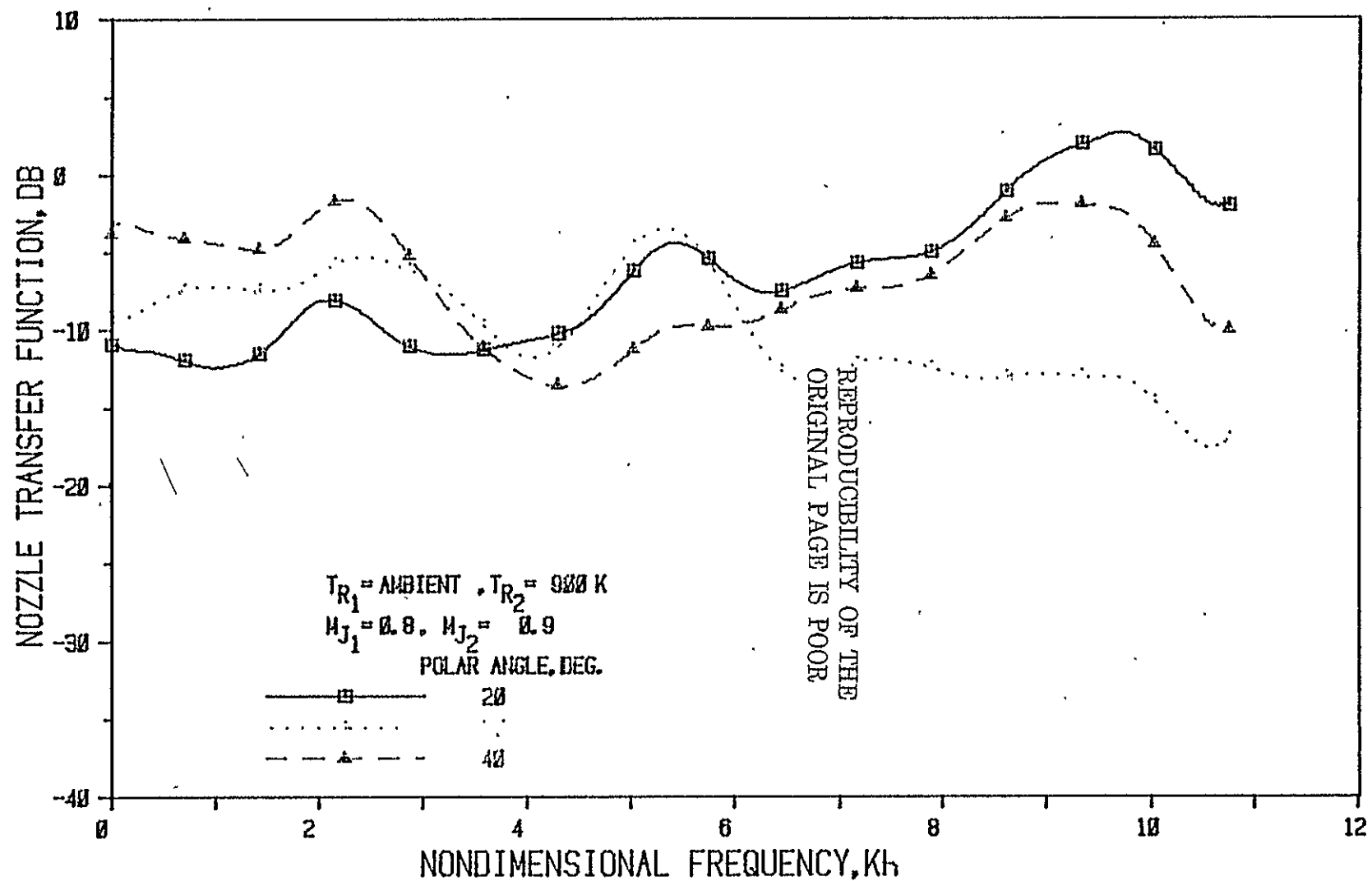


Figure 51(a) Nozzle N 1 (  $L/h = 1$ , Convergence Angle = 20 Deg.); Source At Fan

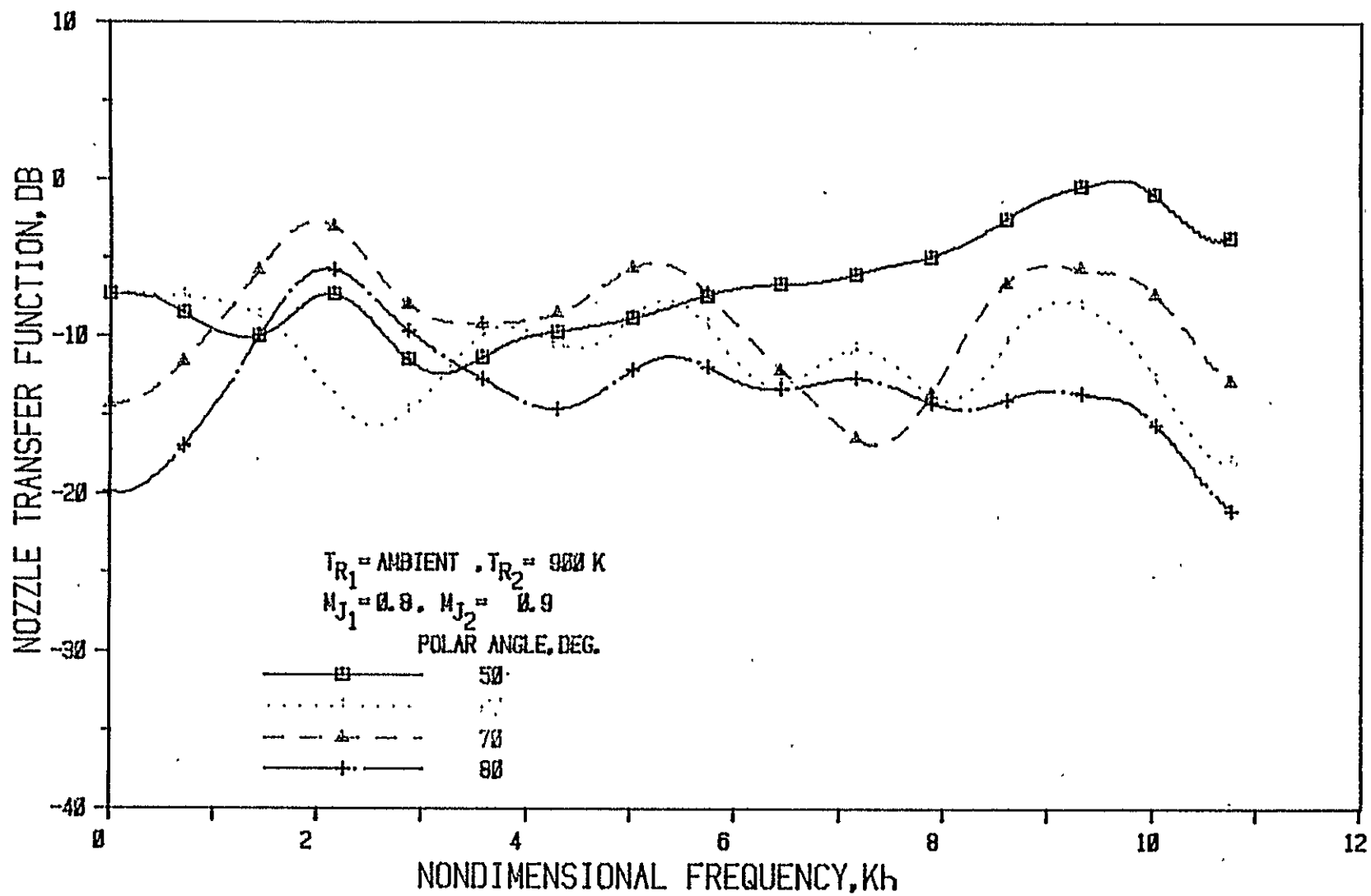


Figure 51(b) Nozzle N 1 (  $L/h = 1$  , Convergence Angle =  $20^\circ$  Deg. ); Source At Fan

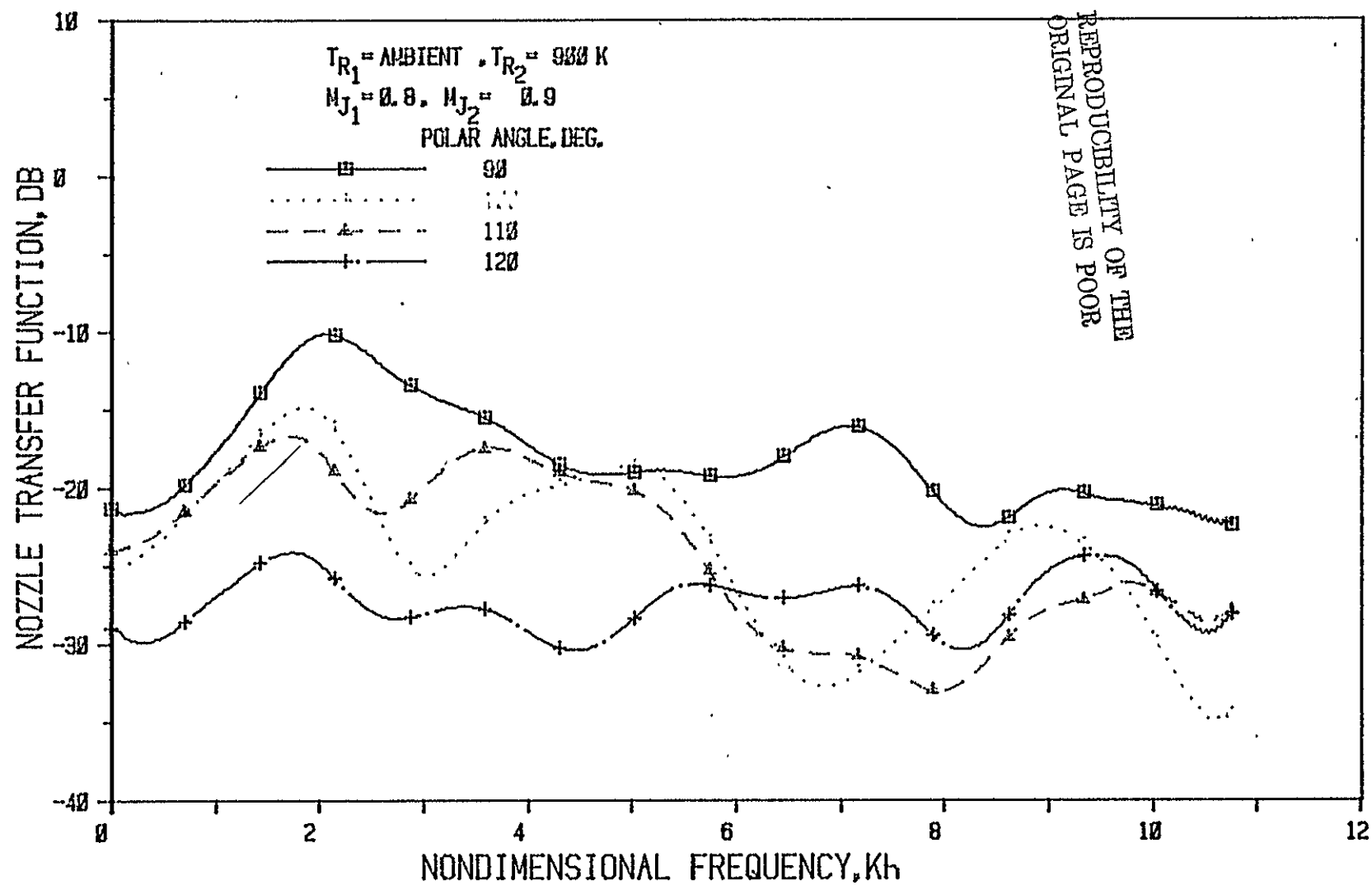


Figure 51(c) Nozzle N 1 (  $L/h = 1$ , Convergence Angle = 20 Deg.); Source At Fan

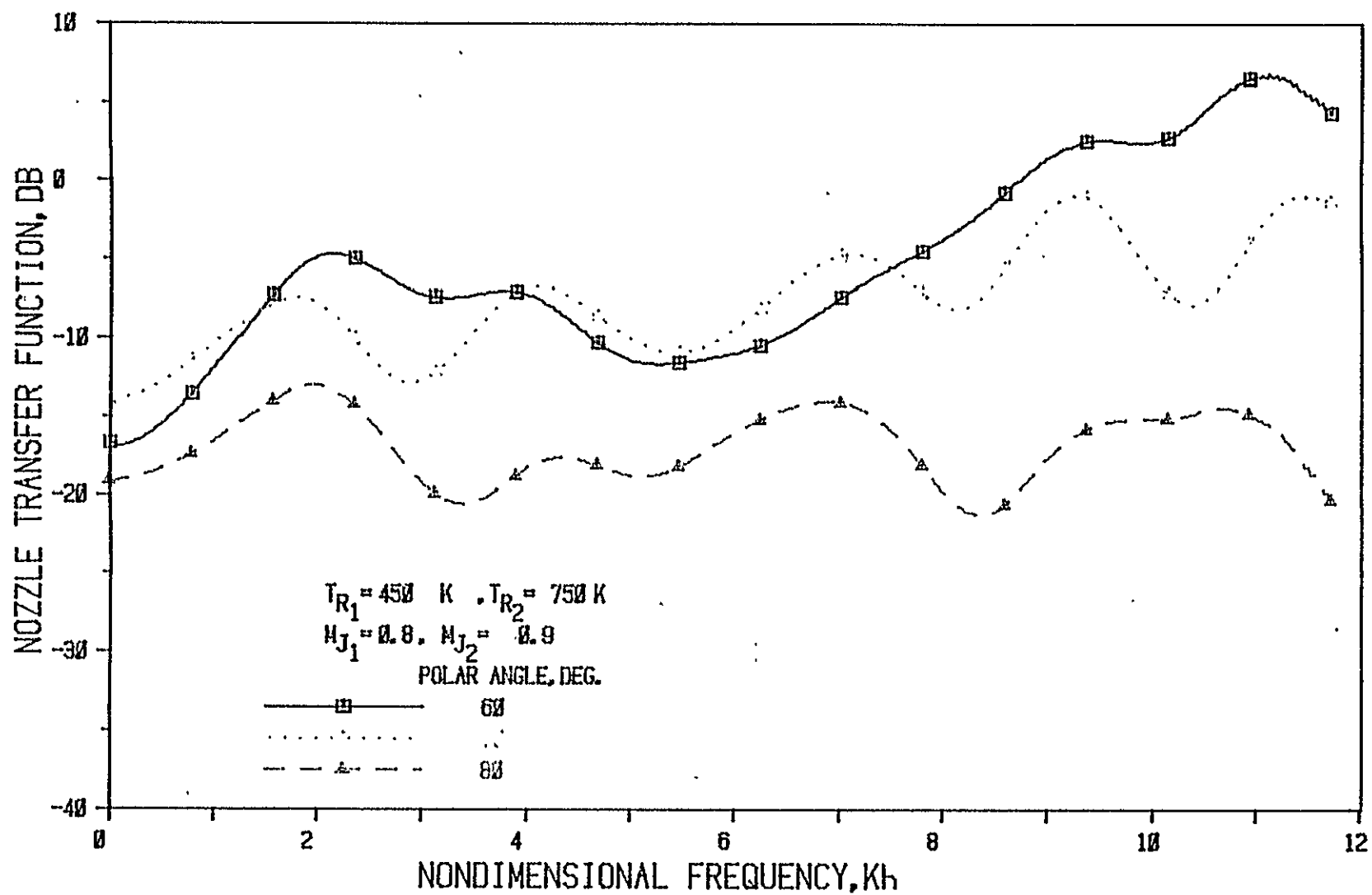


Figure 52(a) Nozzle N1 ( $L/h = 1$ , Convergence Angle =  $20^\circ$ ); Source At Fan

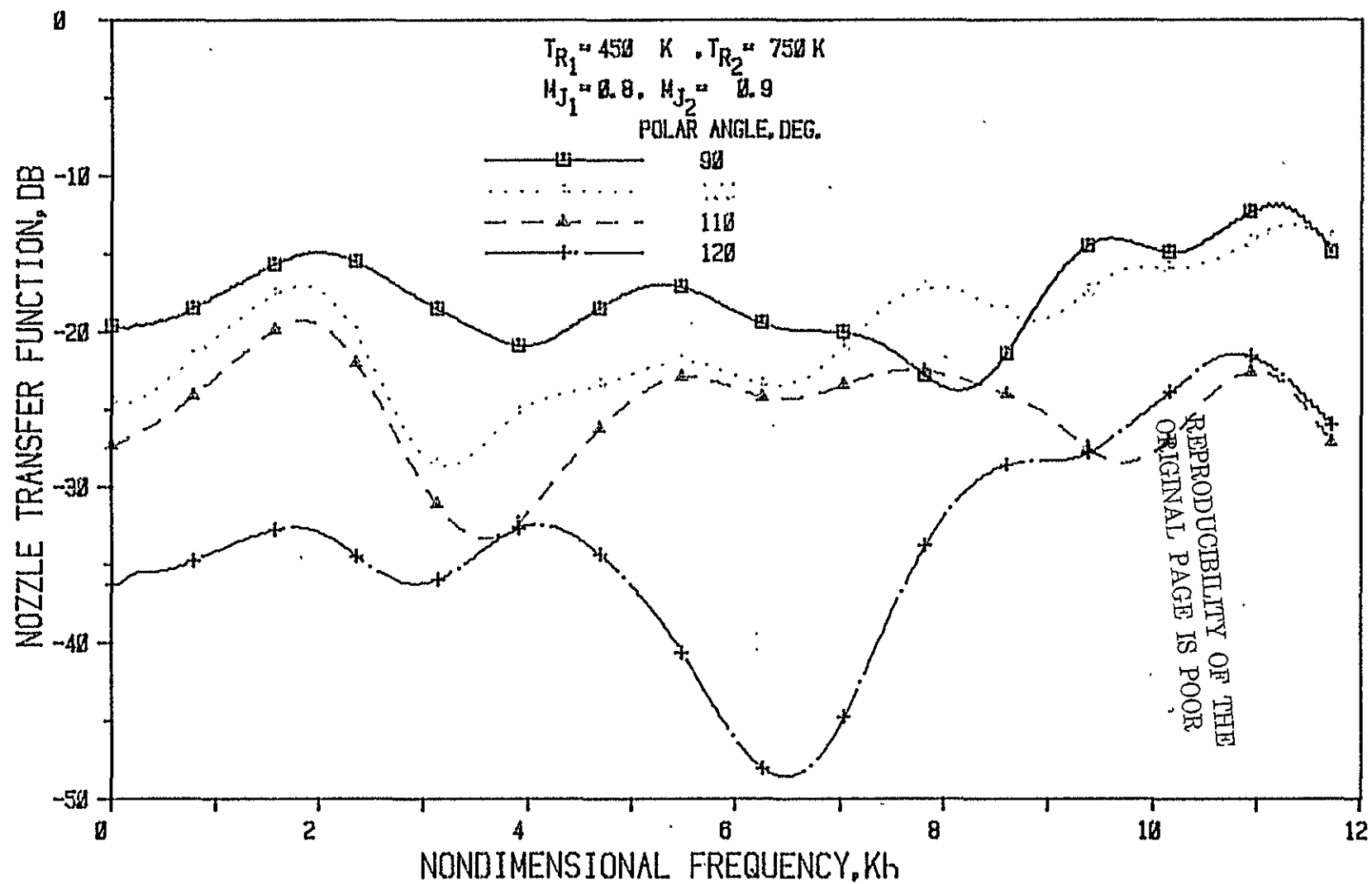


Figure 52(b) Nozzle N1 ( $L/h = 1$ , Convergence Angle =  $20^\circ$ ); Source At Fan



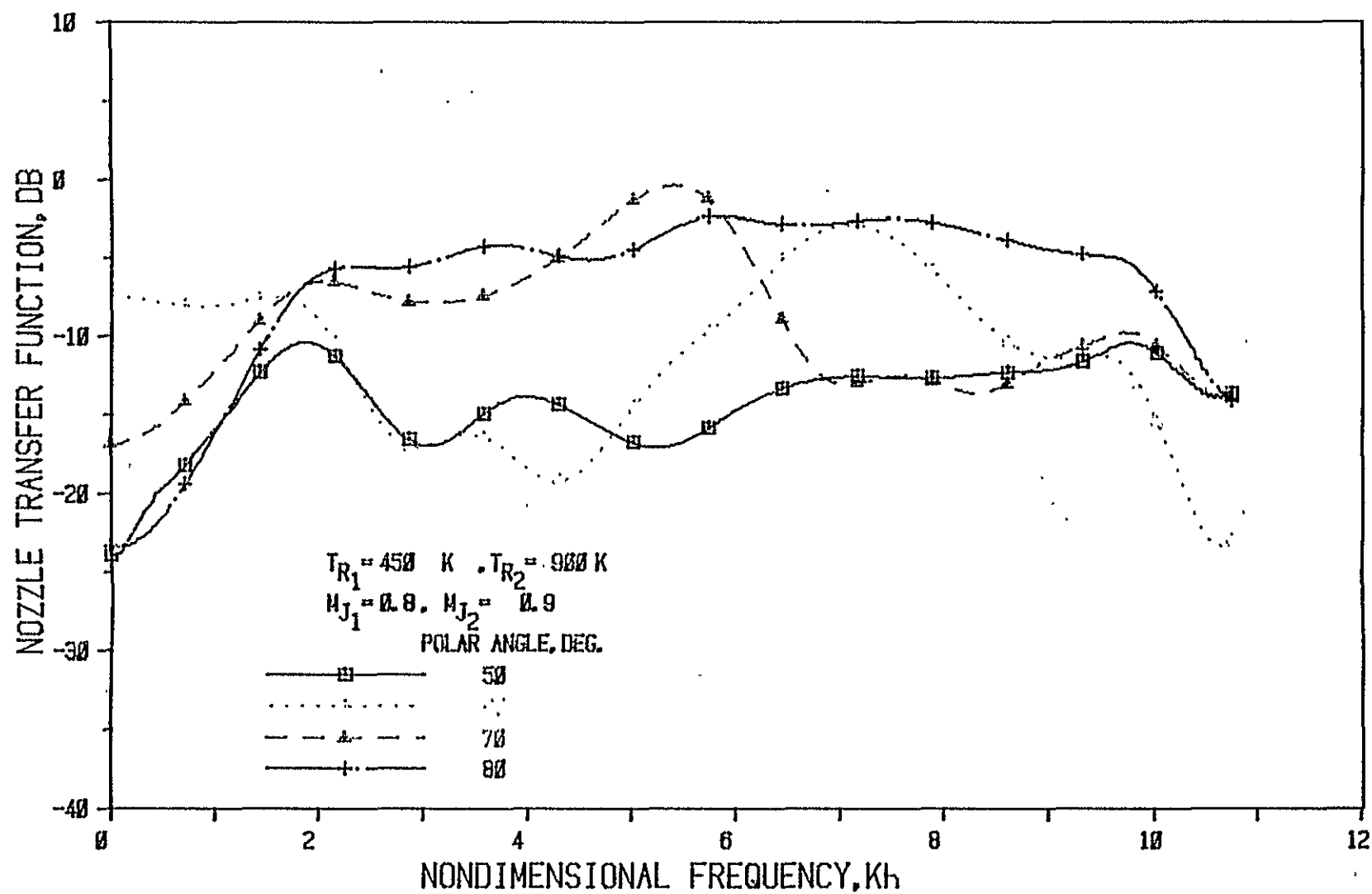


Figure 53(a) Nozzle N 1 (  $L/h = 1$  , Convergence Angle =  $20^\circ$  ); Source At Fan

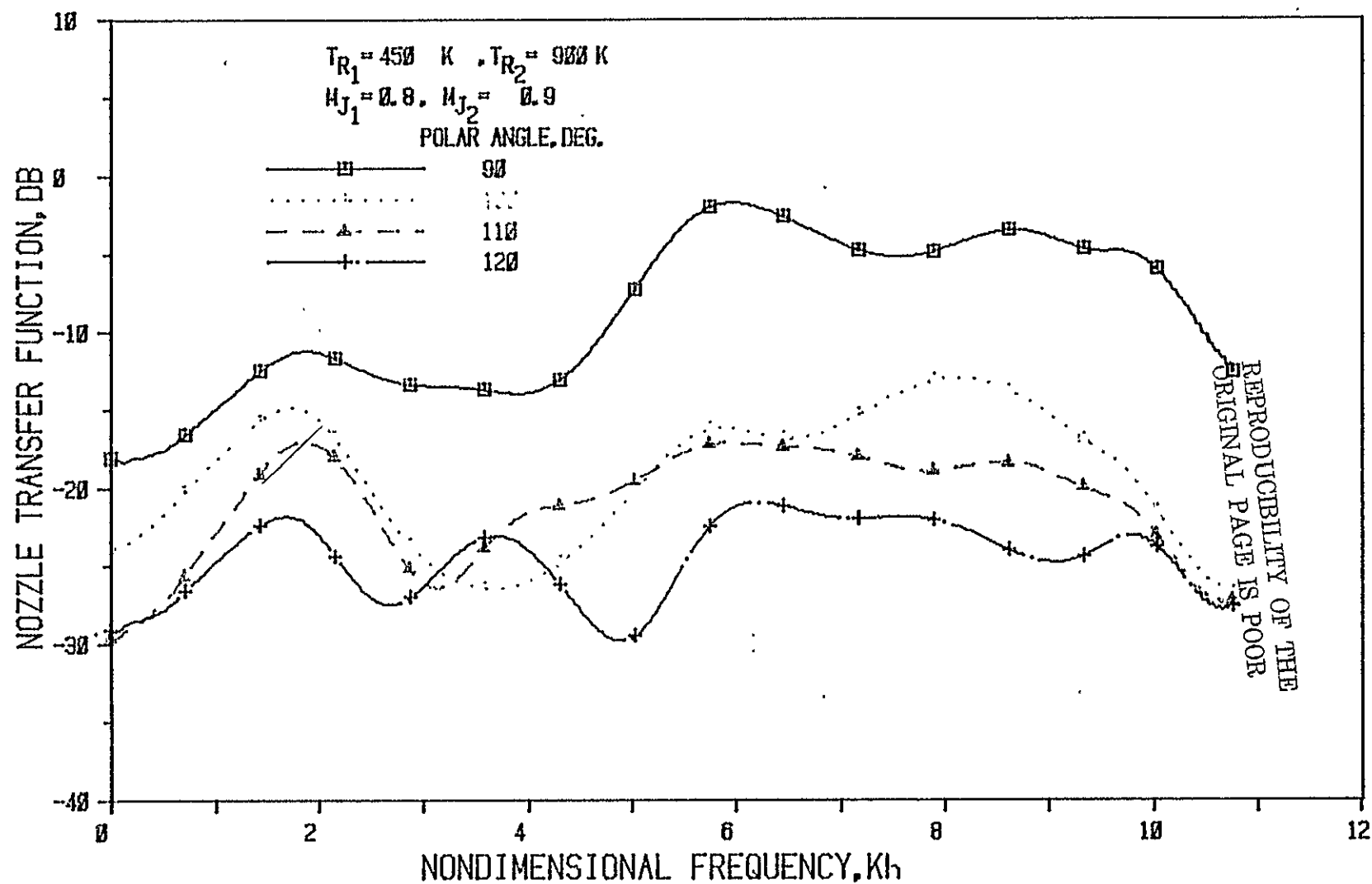


Figure 53(b) Nozzle N 1 (  $L/h = 1$  , Convergence Angle =  $20^\circ$  ); Source At Fan

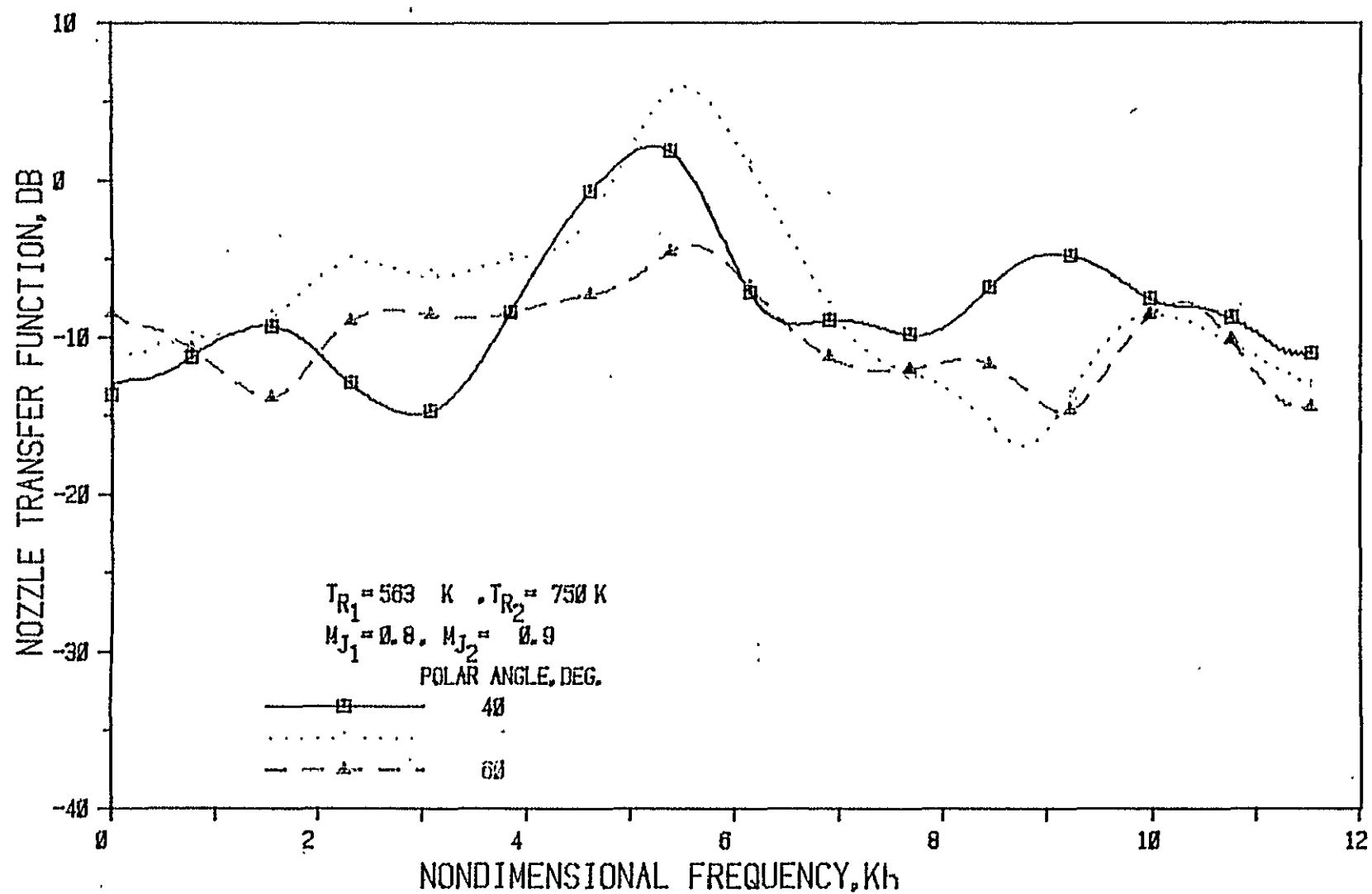


Figure 54(a) Nozzle N1 ( $L/h = 1$ , Convergence Angle = 20 Deg.); Source At Fan

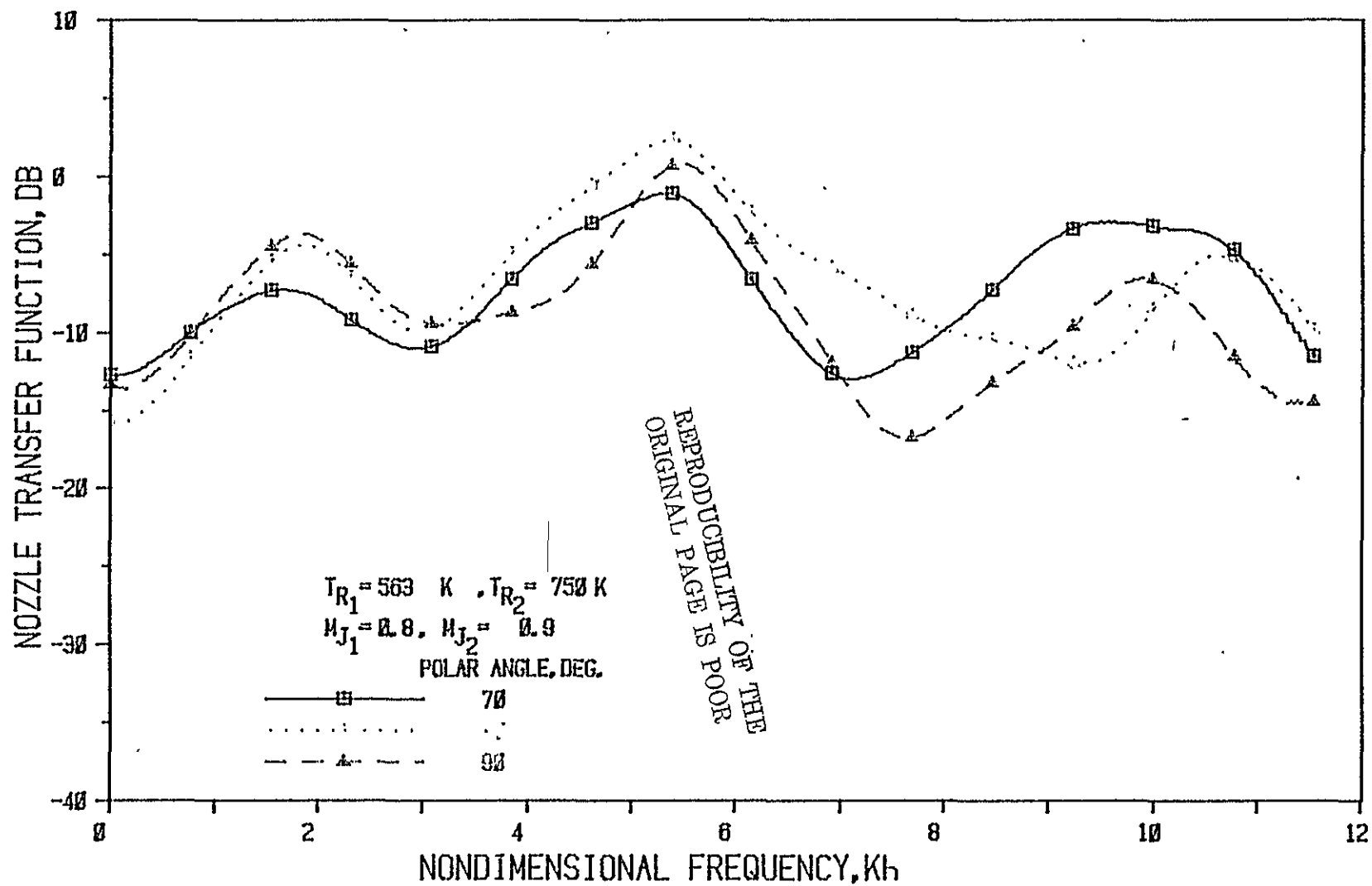


Figure 54(b) Nozzle N 1 (  $L/h = 1$ , Convergence Angle =  $20^\circ$  ); Source At Fan

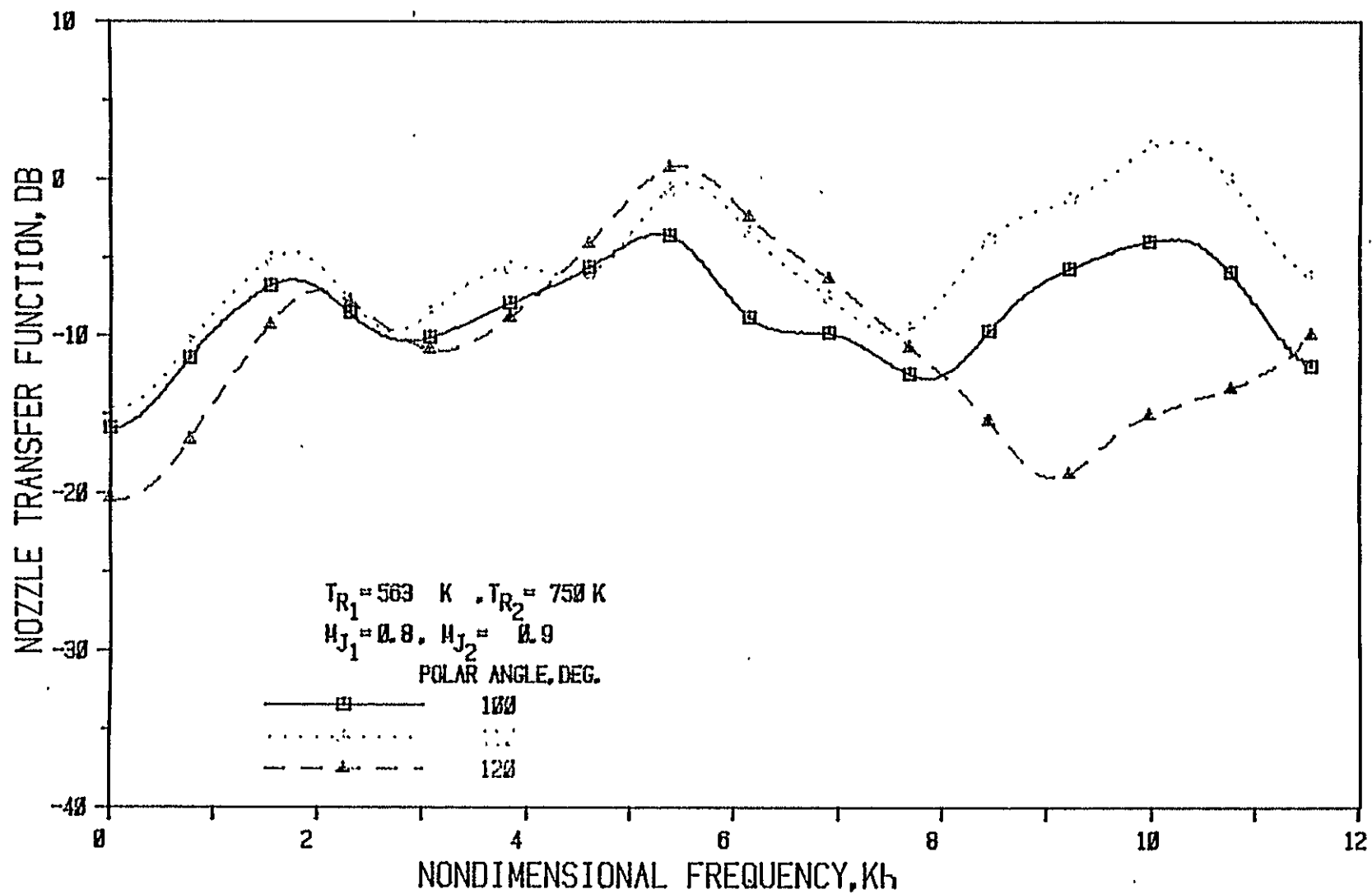


Figure 54(c) Nozzle N 1 (  $L/h = 1$  , Convergence Angle =  $20^\circ$  Deg. ); Source At Fan

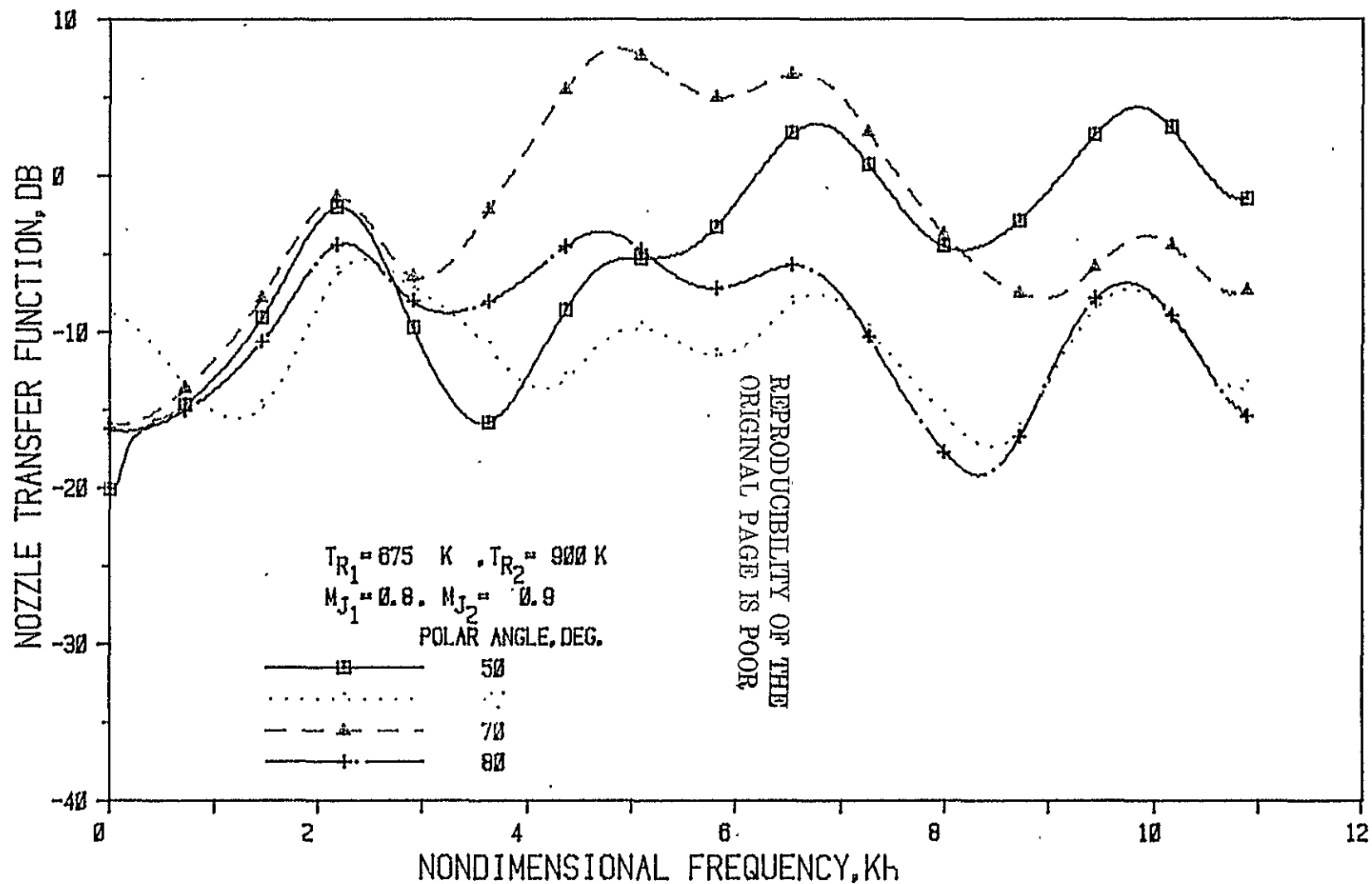


Figure 55(a) Nozzle N 1 (  $L/h = 1$  , Convergence Angle = 20 Deg. ) ; Source At Fan

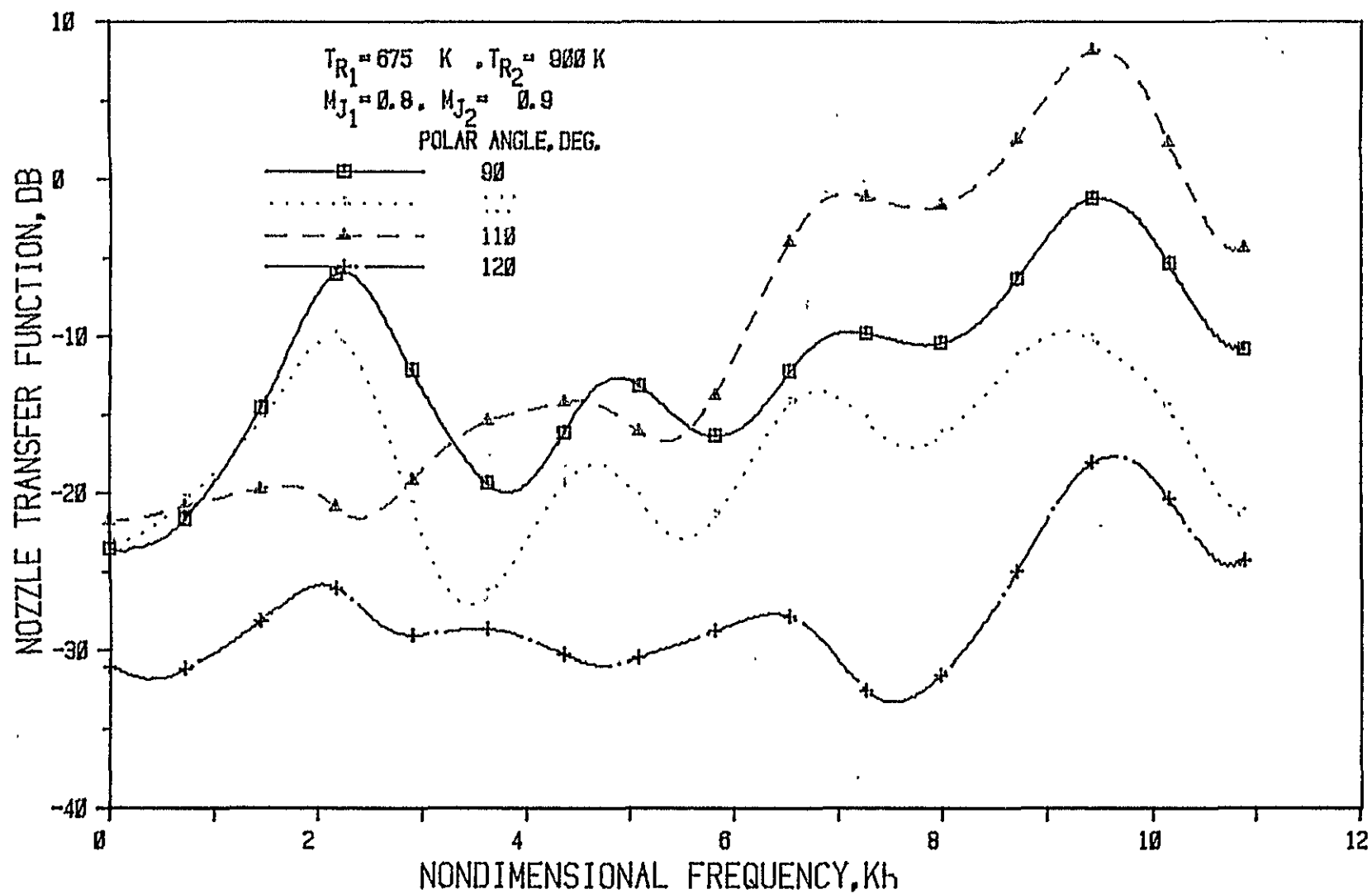


Figure 55(b) Nozzle N1 (  $L/h = 1$  , Convergence Angle =  $20^\circ$  ); Source At Fan

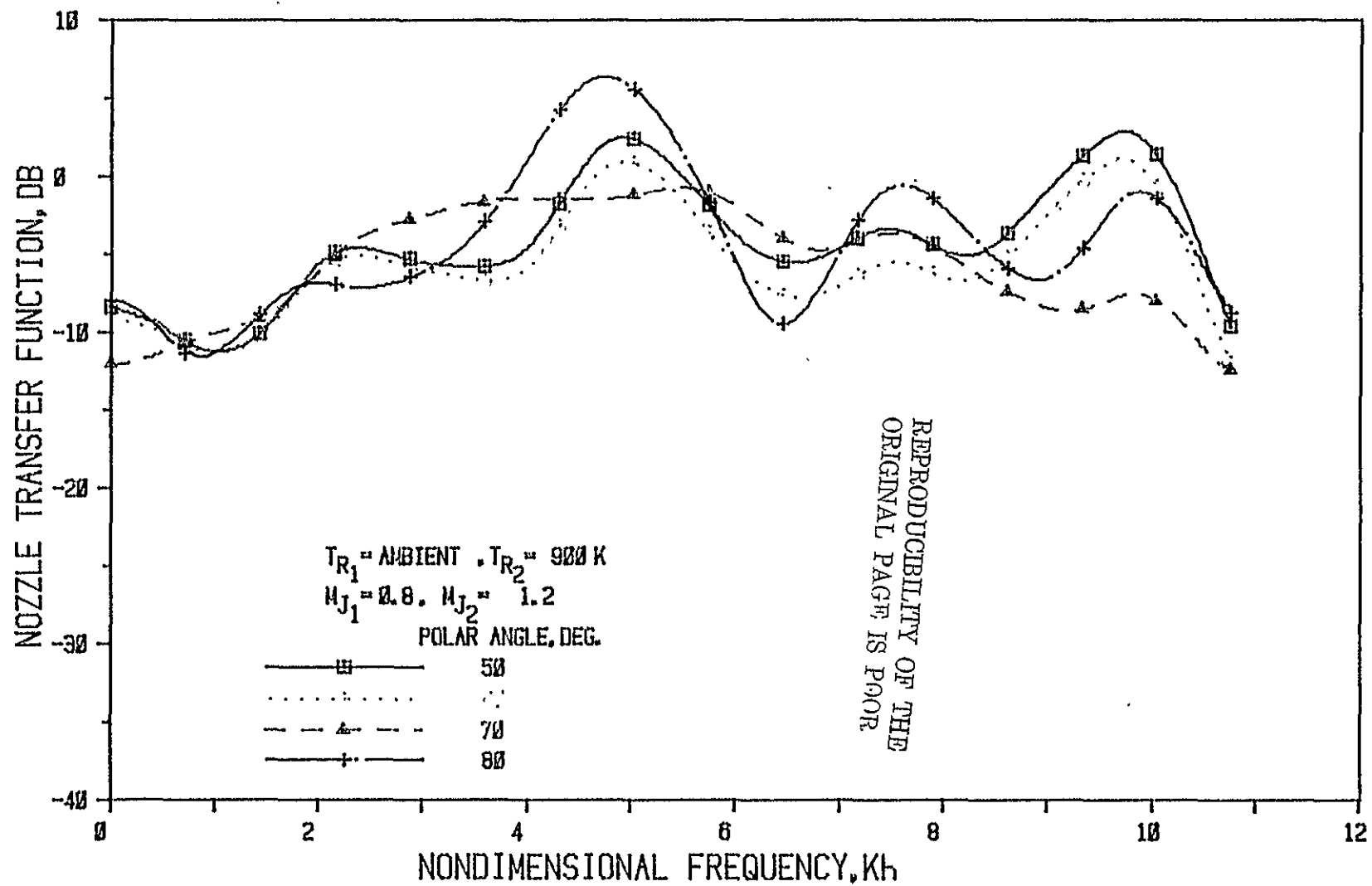


Figure 56(a) Nozzle N1 ( $L/h = 1$ , Convergence Angle = 20 Deg.); Source At Fan



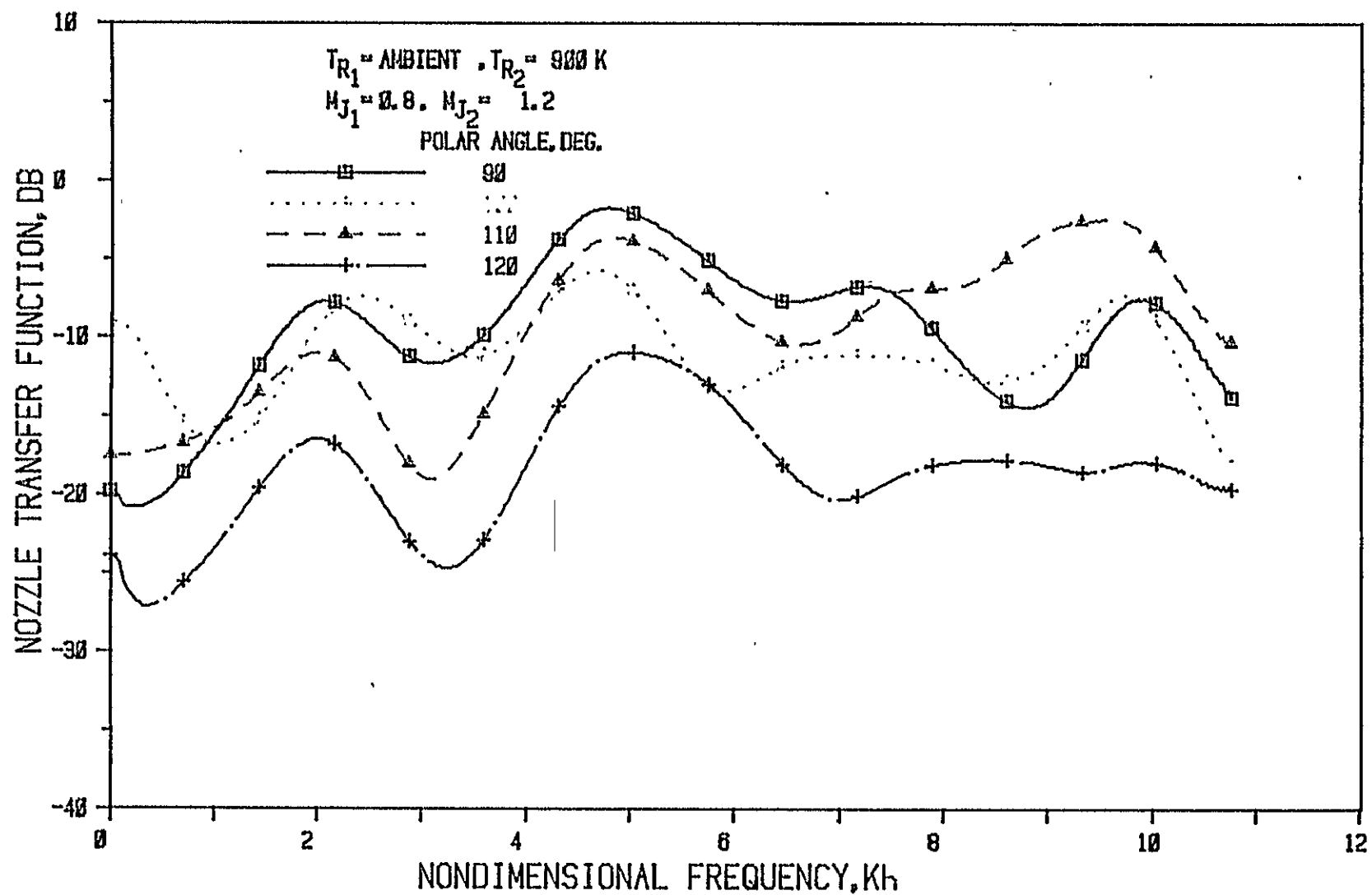


Figure 56(b) Nozzle N1 ( $L/h = 1$ , Convergence Angle = 20 Deg.); Source At Fan

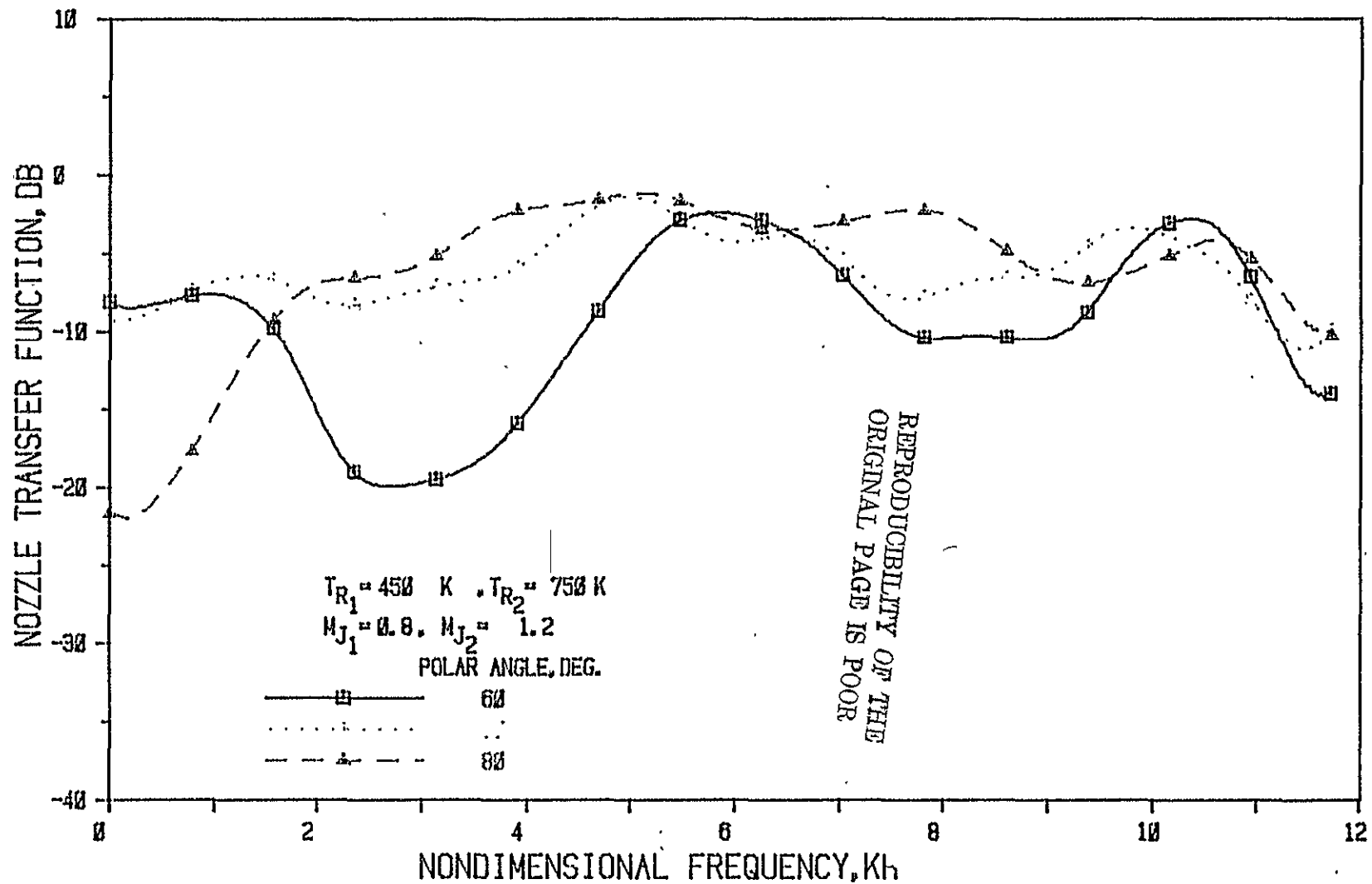


Figure 57 Nozzle N1 (  $L/h = 1$  , Convergence Angle = 20 Deg. ); Source At Fan

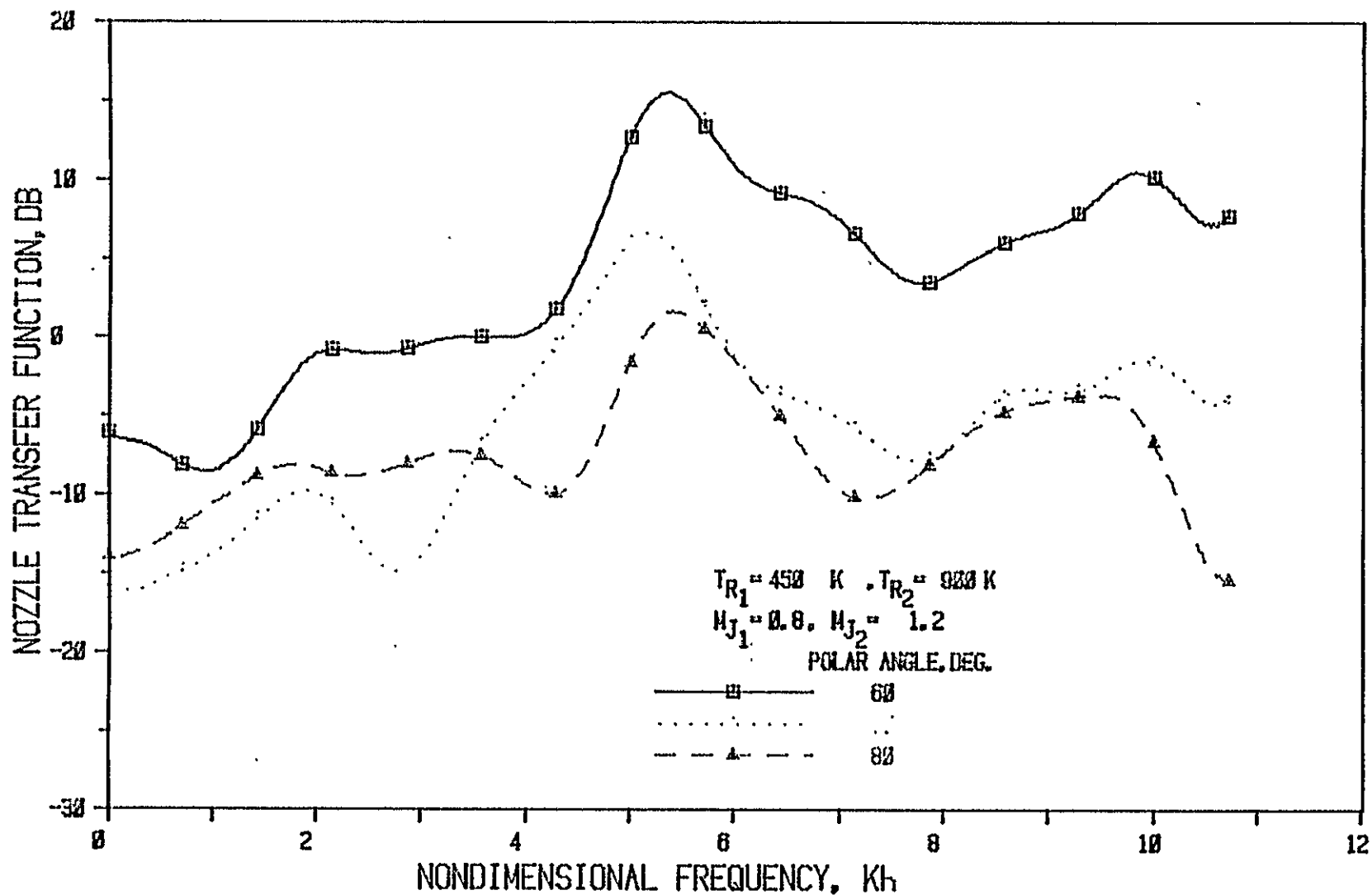


Figure 58(a) Nozzle N 1 ( $L/h = 1$  Convergence Angle =  $20^\circ$ ); Source At Fan

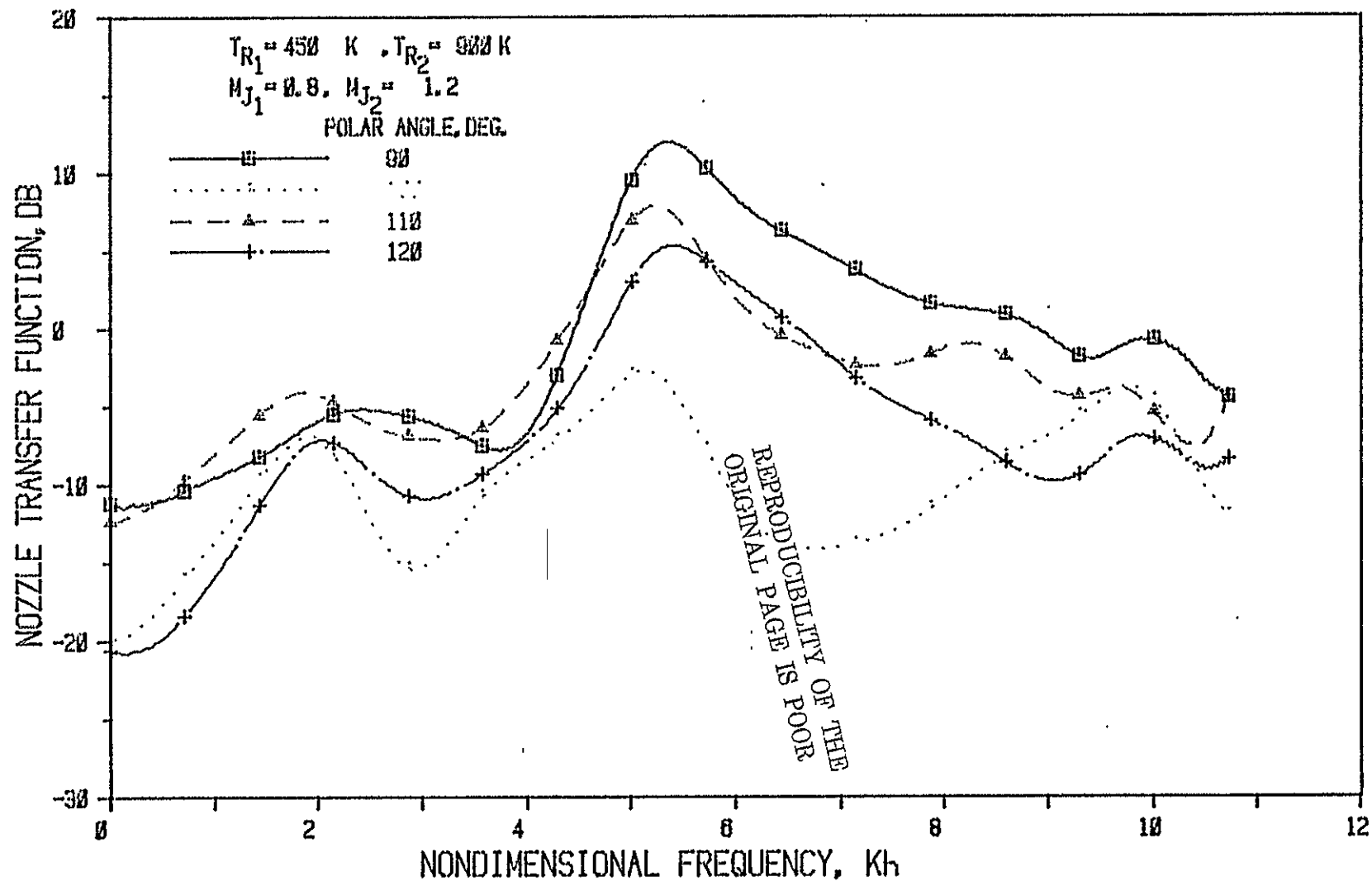


Figure 58(b) Nozzle N 1 ( $L/h = 1$  Convergence Angle =  $20^\circ$ ); Source At Fan

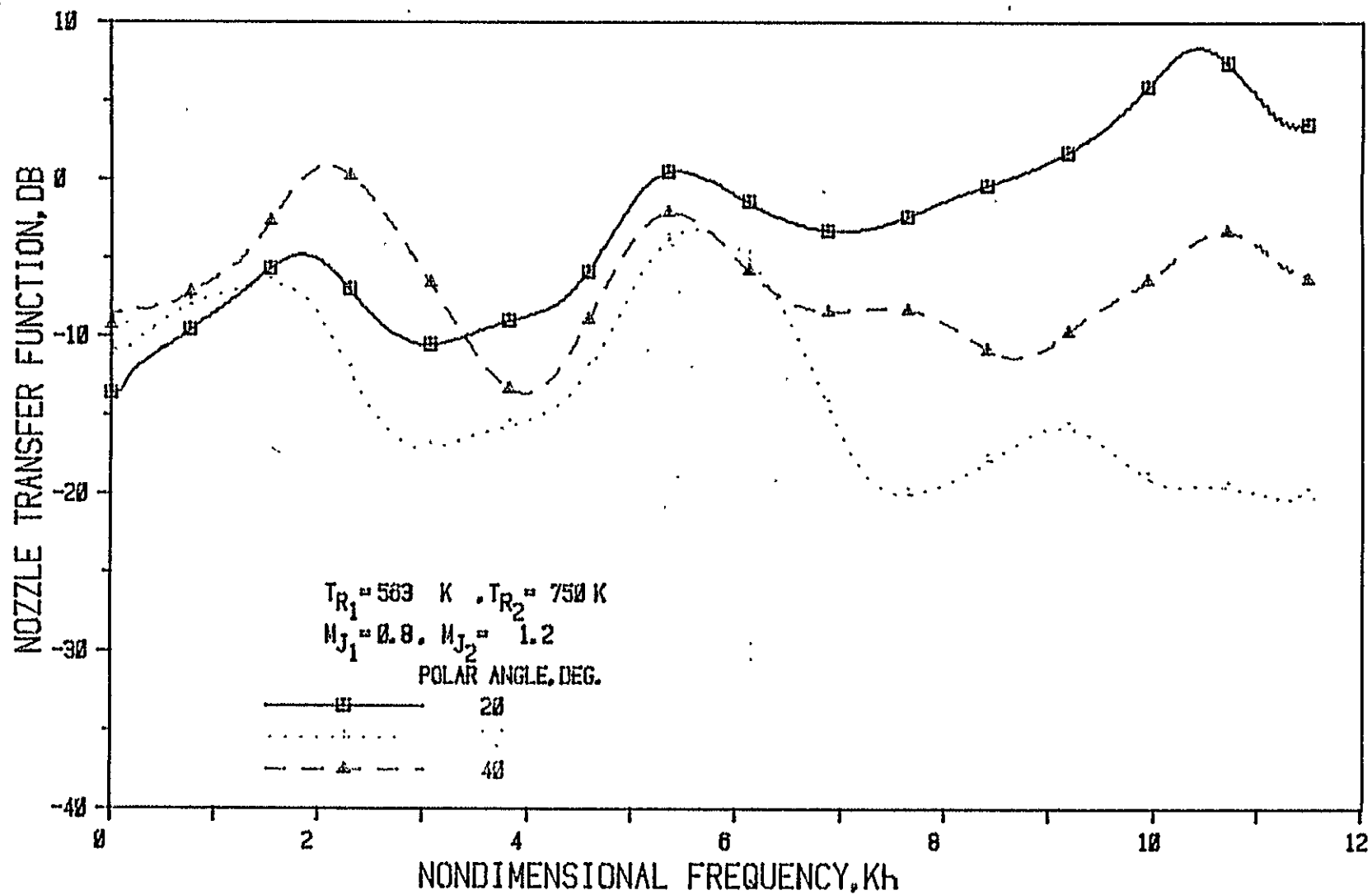


Figure 59(a) Nozzle N 1 (  $L/h = 1$  , Convergence Angle = 20 Deg. ); Source At Fan

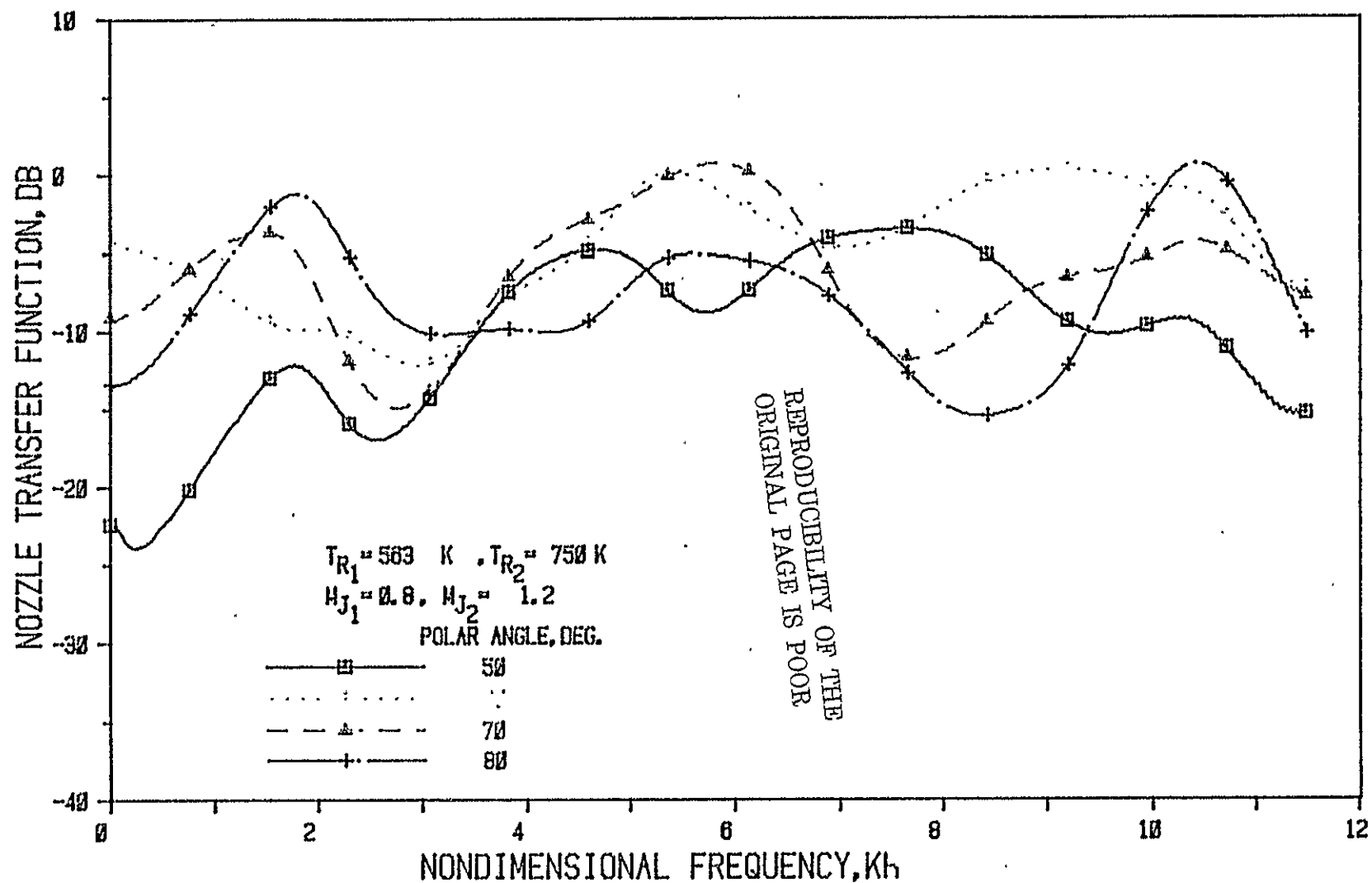


Figure 59(b) Nozzle N 1 (  $L/h = 1$  , Convergence Angle =  $20^\circ$  ); Source At Fan

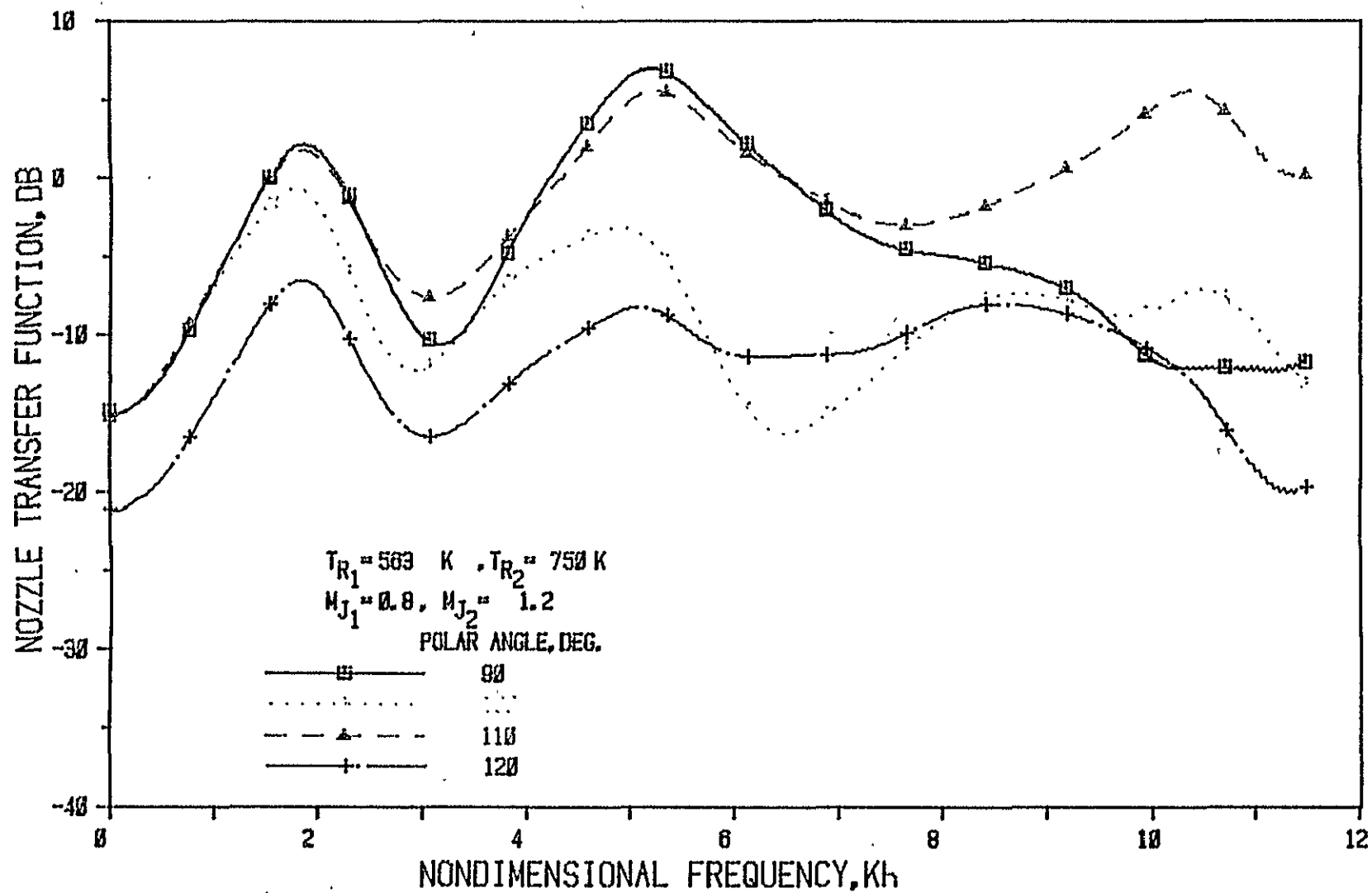


Figure 59(c) Nozzle N 1 ( $L/h = 1$ , Convergence Angle = 20 Deg.); Source At Fan

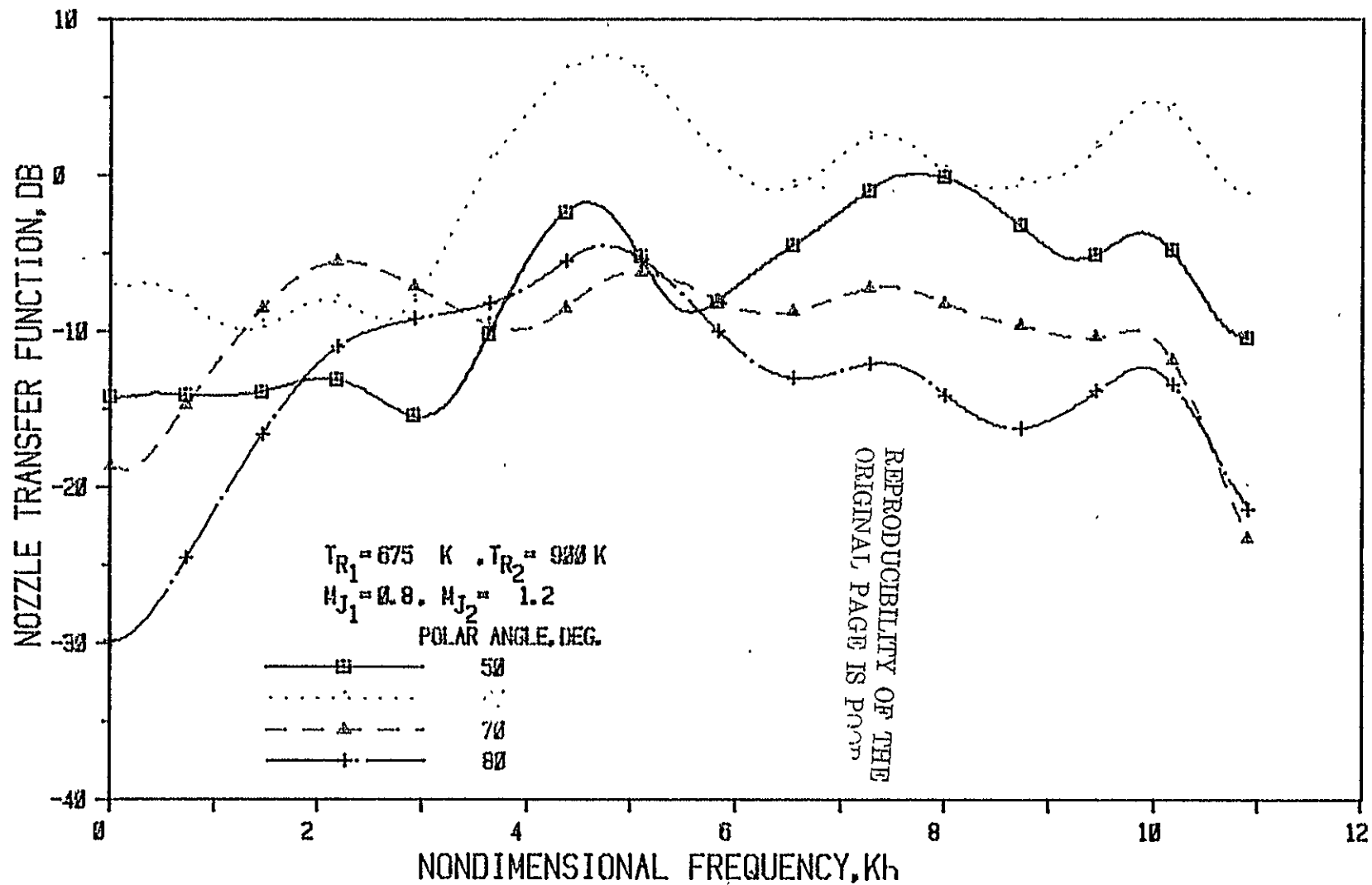


Figure 60(a) Nozzle N 1 (  $L/h = 1$ , Convergence Angle = 20 Deg.); Source At Fan



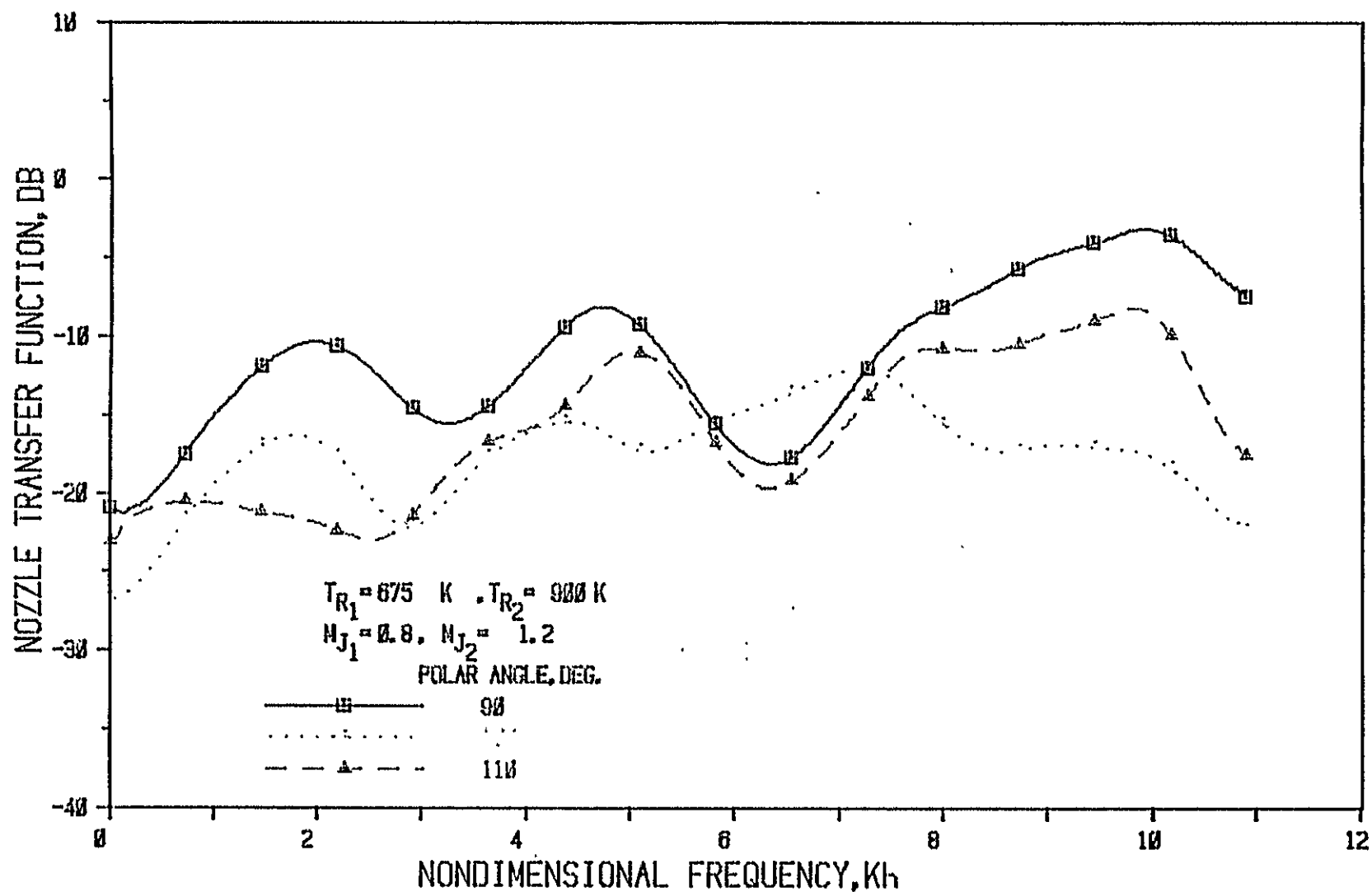


Figure 60(b) Nozzle N 1 ( $L/h = 1$ , Convergence Angle =  $20^\circ$  Deg.); Source At Fan

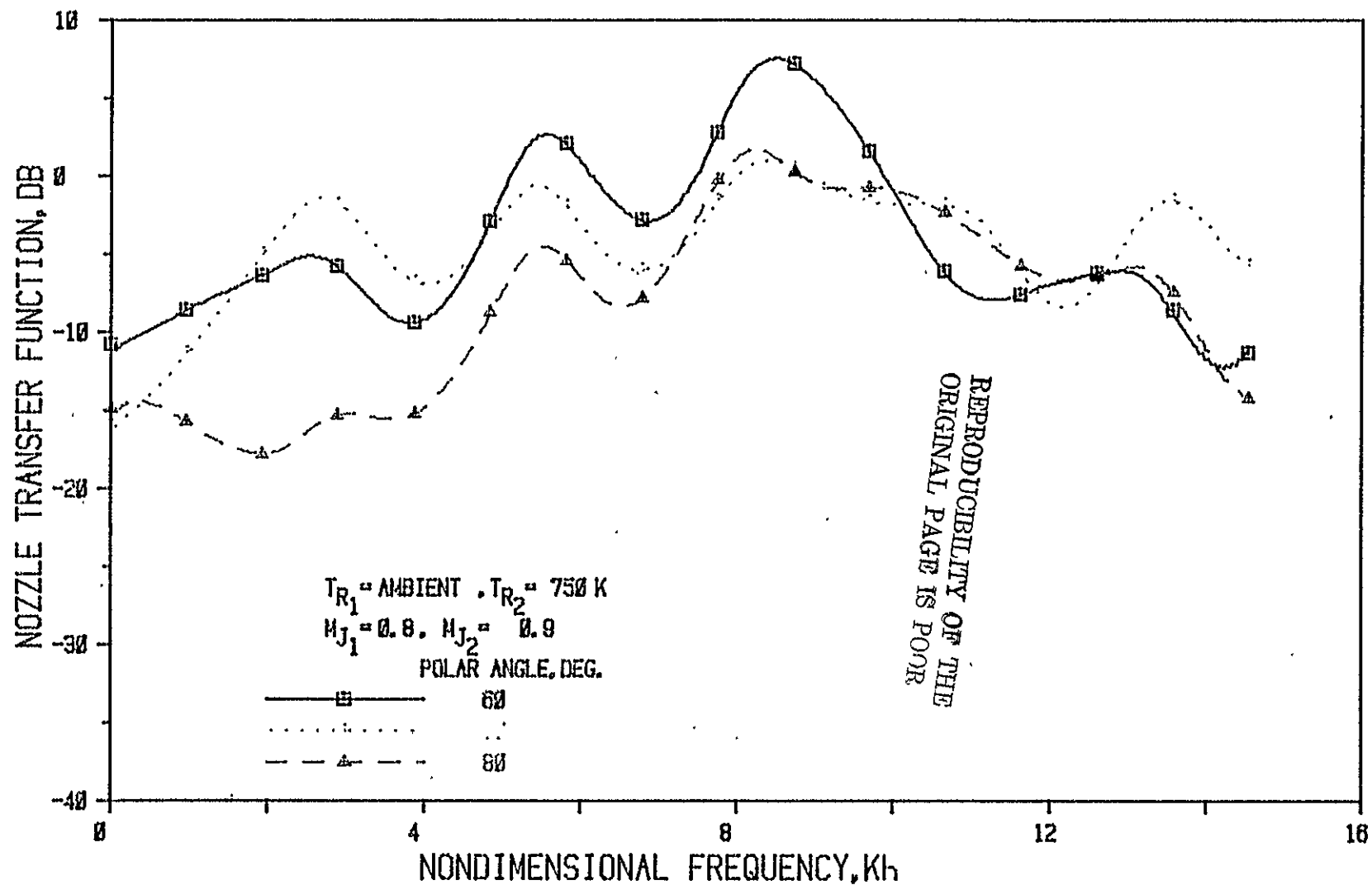


Figure 61(a) Nozzle N 2 (  $L/h = 3$  , Convergence Angle = 20 Deg. ); Source At Fan

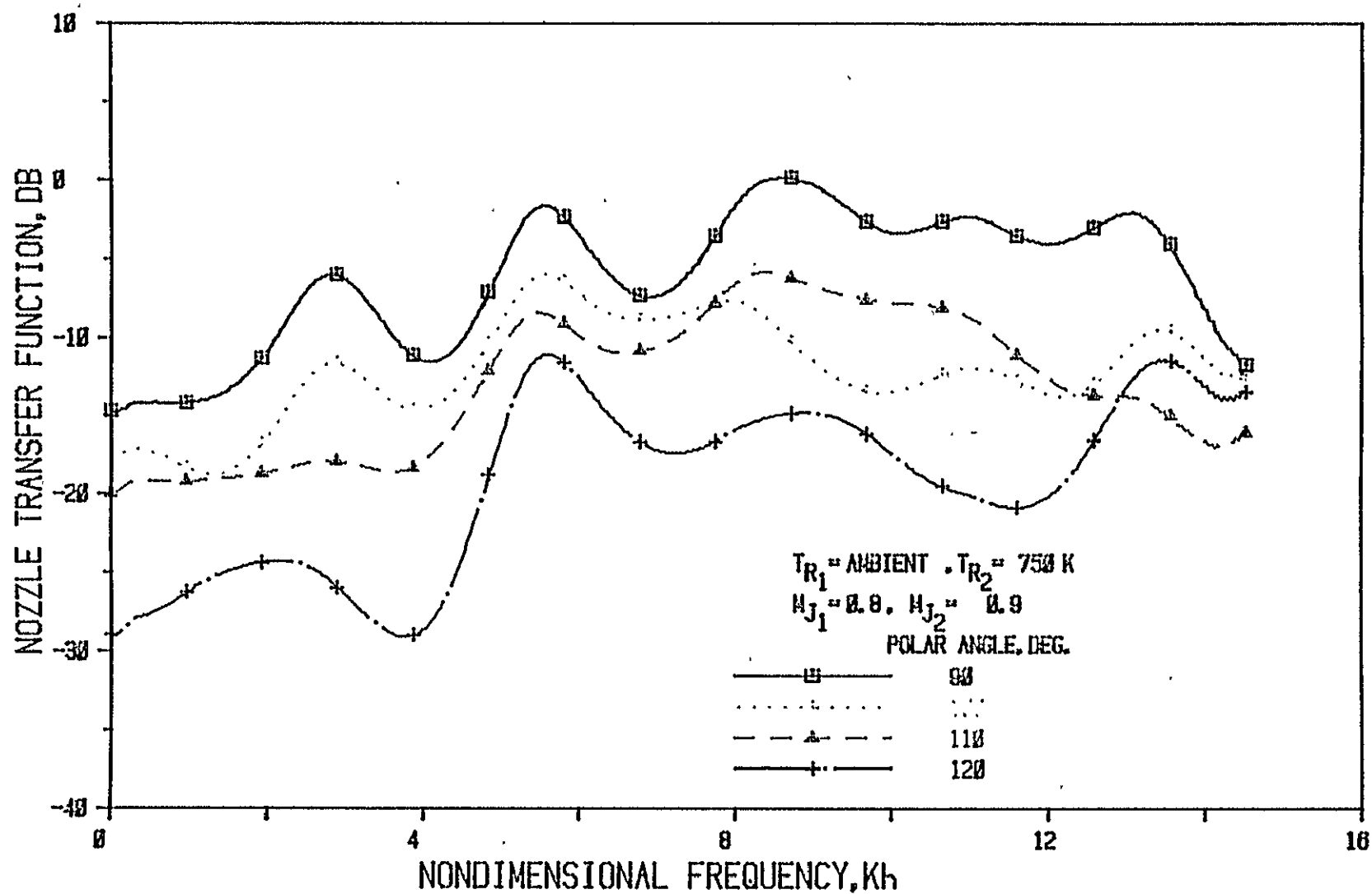


Figure 61(b) Nozzle N 2 (  $L/h = 3$ , Convergence Angle = 20 Deg.); Source At Fan

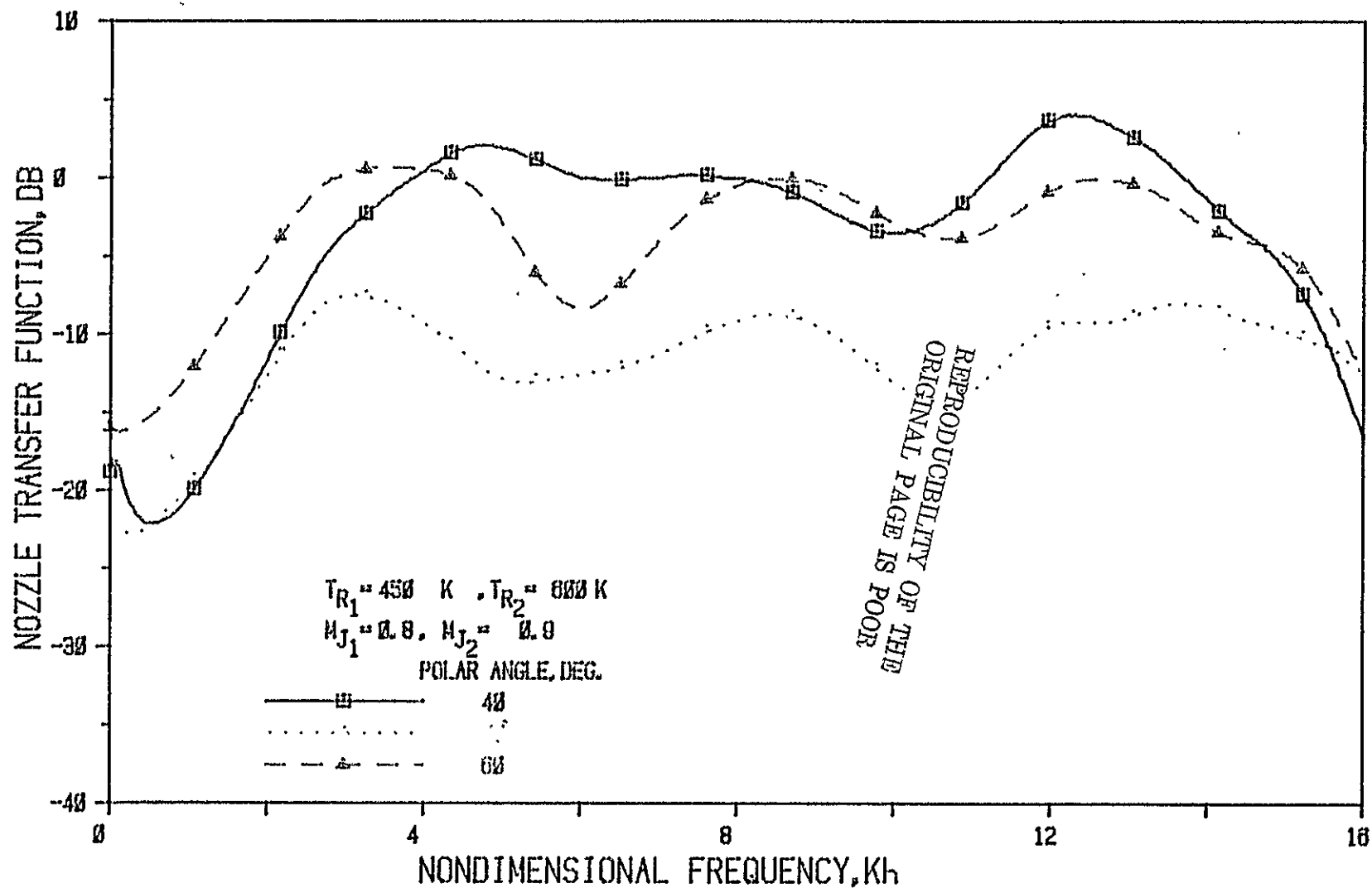


Figure 62(a) Nozzle N 2 (  $L/h = 3$ , Convergence Angle =  $20^\circ$  ); Source At Fan

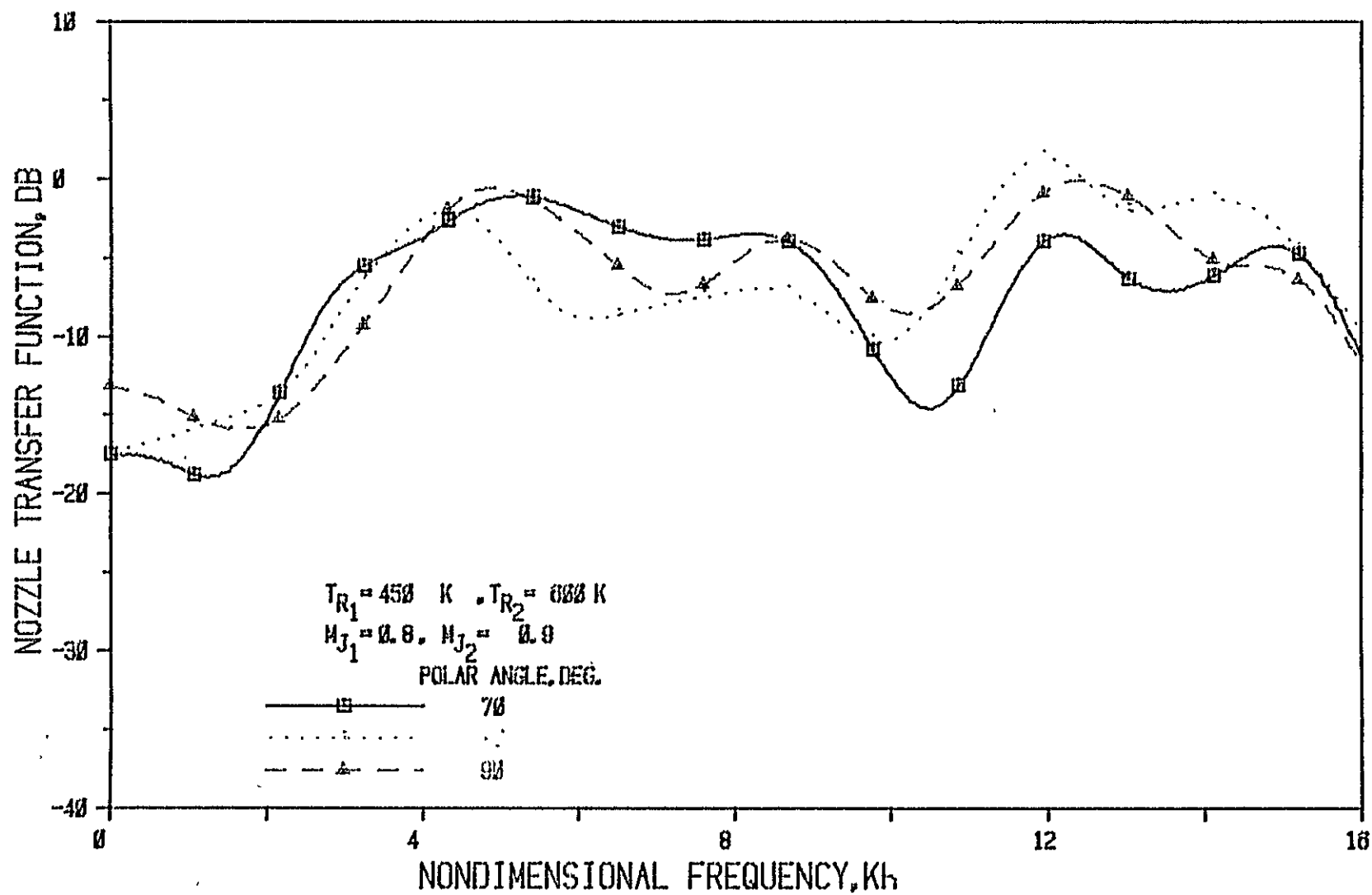


Figure 62(b) Nozzle N 2 ( $L/h = 3$ , Convergence Angle = 20 Deg.); Source At Fan

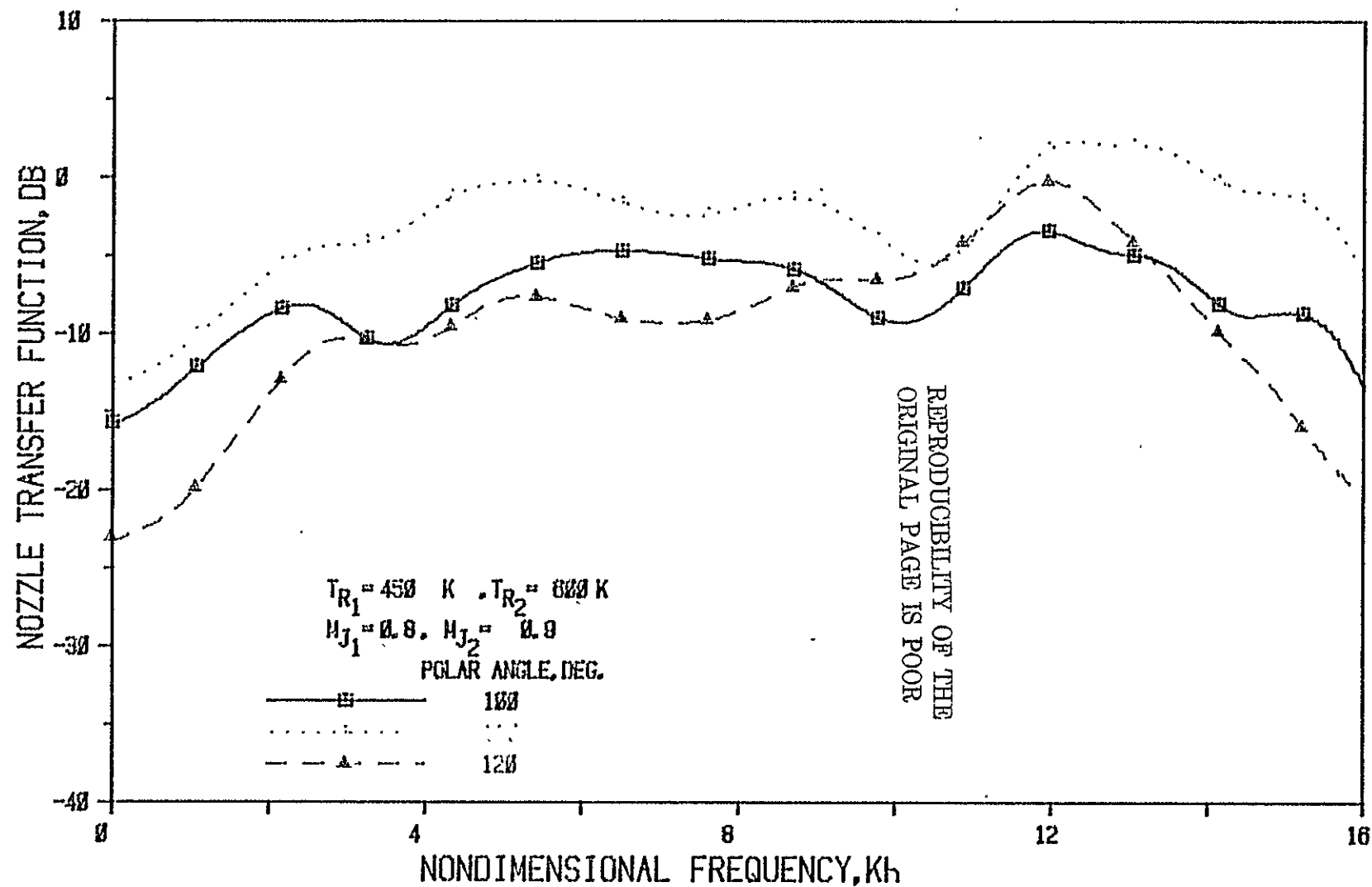


Figure 62(c) Nozzle N 2 (  $L/h = 3$  , Convergence Angle =  $20^\circ$  ); Source At Fan

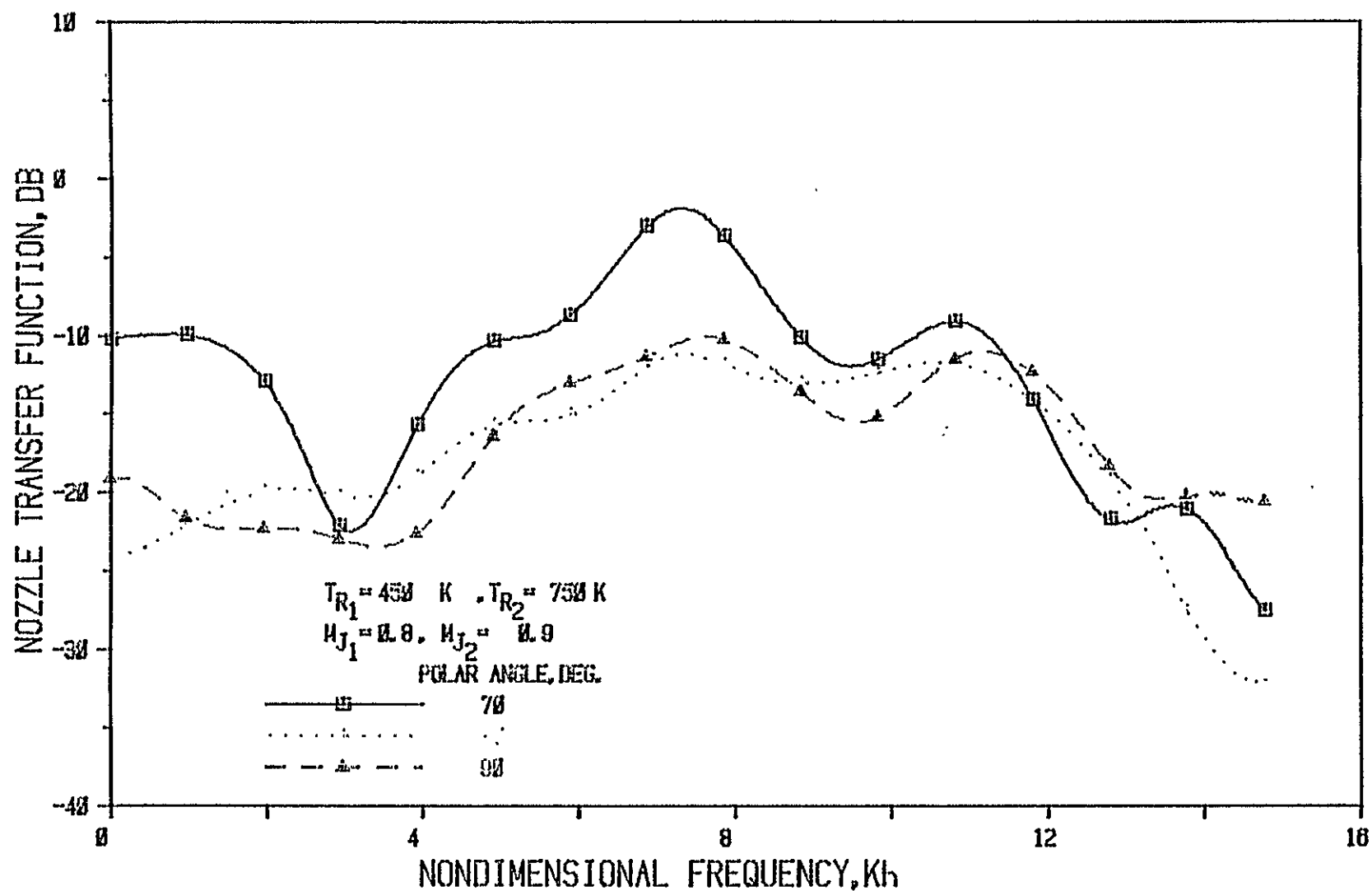


Figure 63(a) Nozzle N 2 (  $L/h = 3$  , Convergence Angle =  $20^\circ$  ) ; Source At Fan

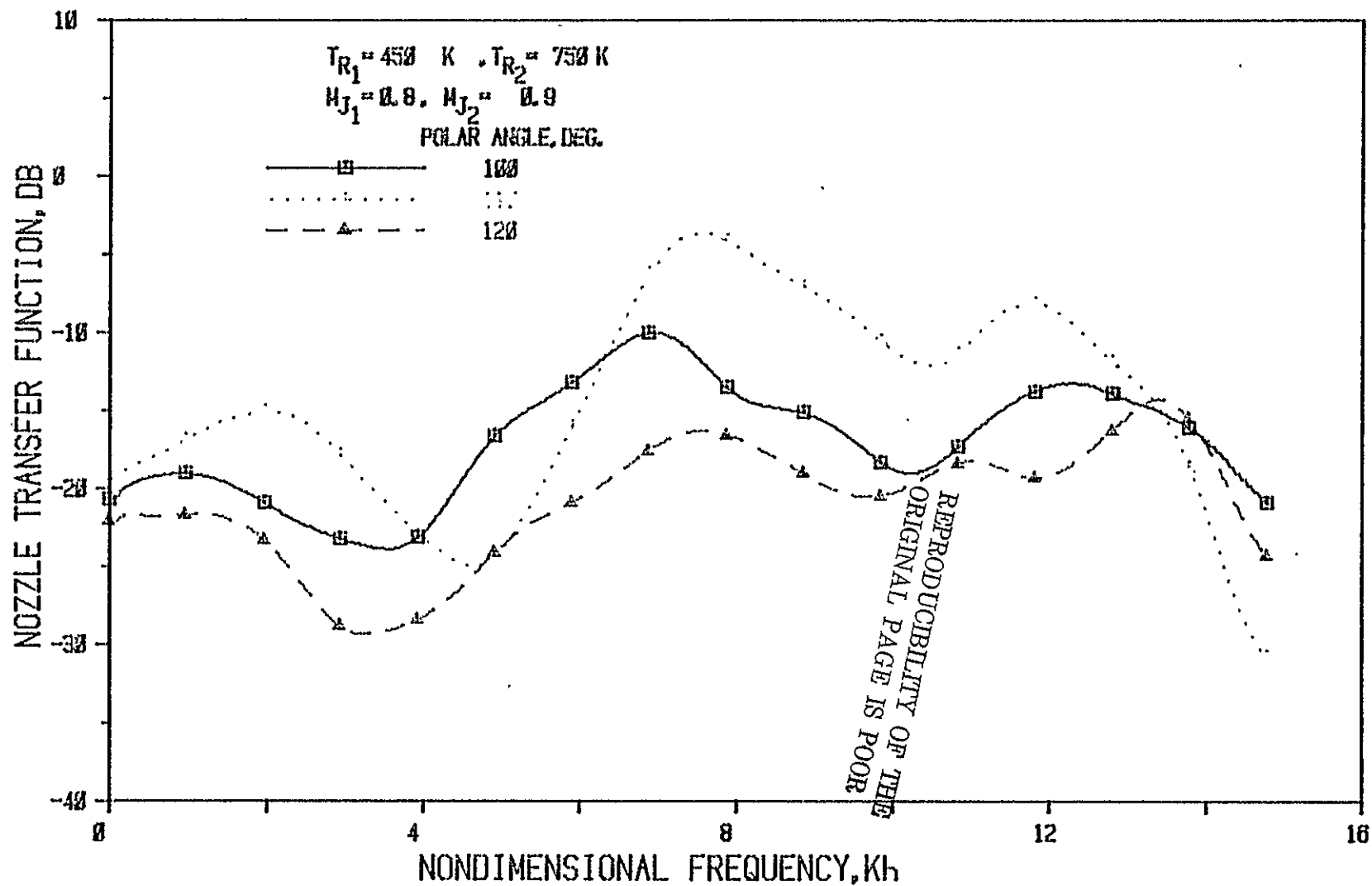


Figure 63(b) Nozzle N 2 (  $L/h = 3$  , Convergence Angle =  $20^\circ$  ); Source At Fan



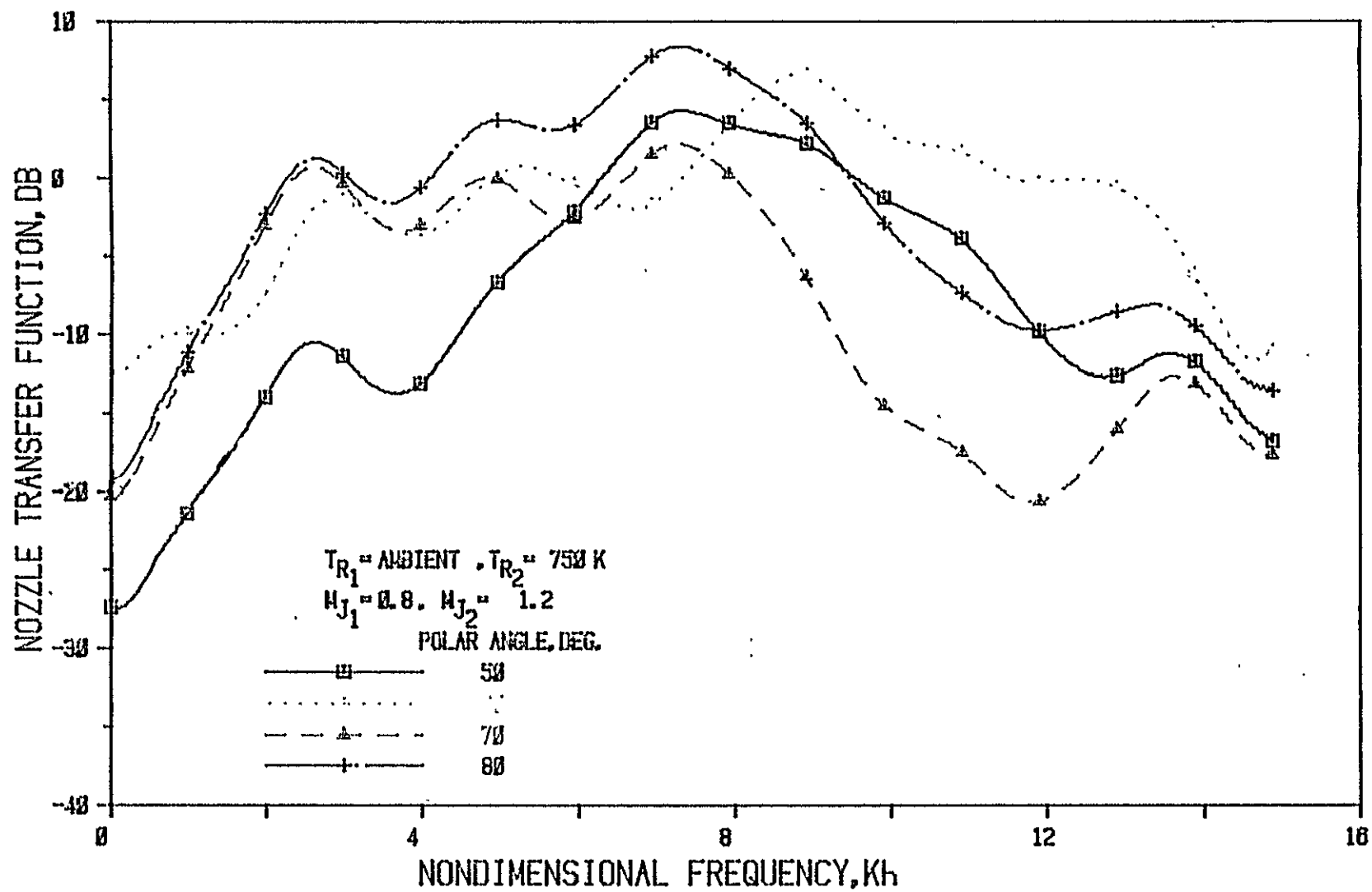


Figure 64(a) Nozzle N 2 (  $L/h = 3$  , Convergence Angle =  $20^\circ$  ); Source At Fan

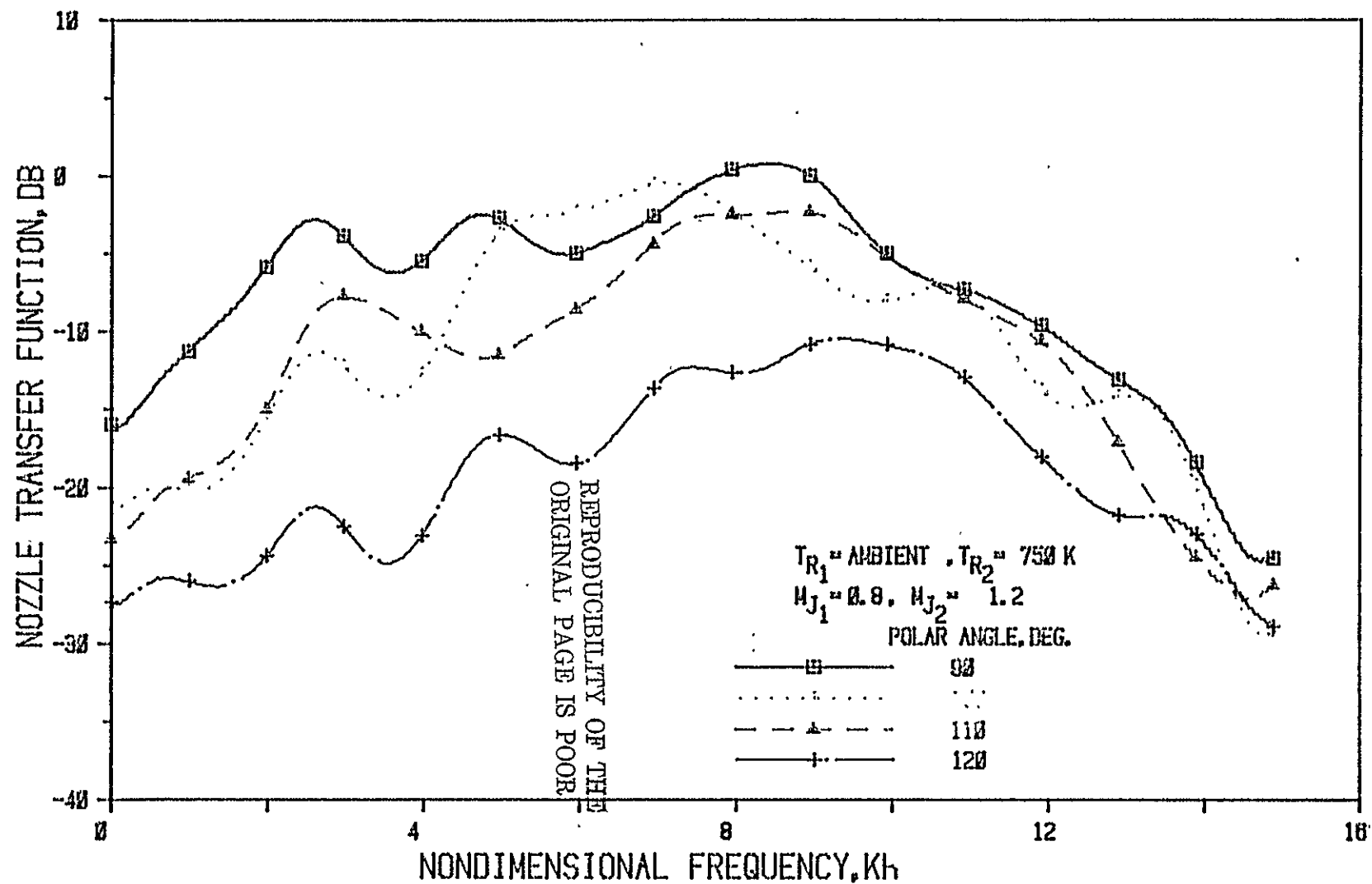


Figure 64(b) Nozzle N 2 (  $L/h = 3$ , Convergence Angle =  $20^\circ$  ); Source At Fan

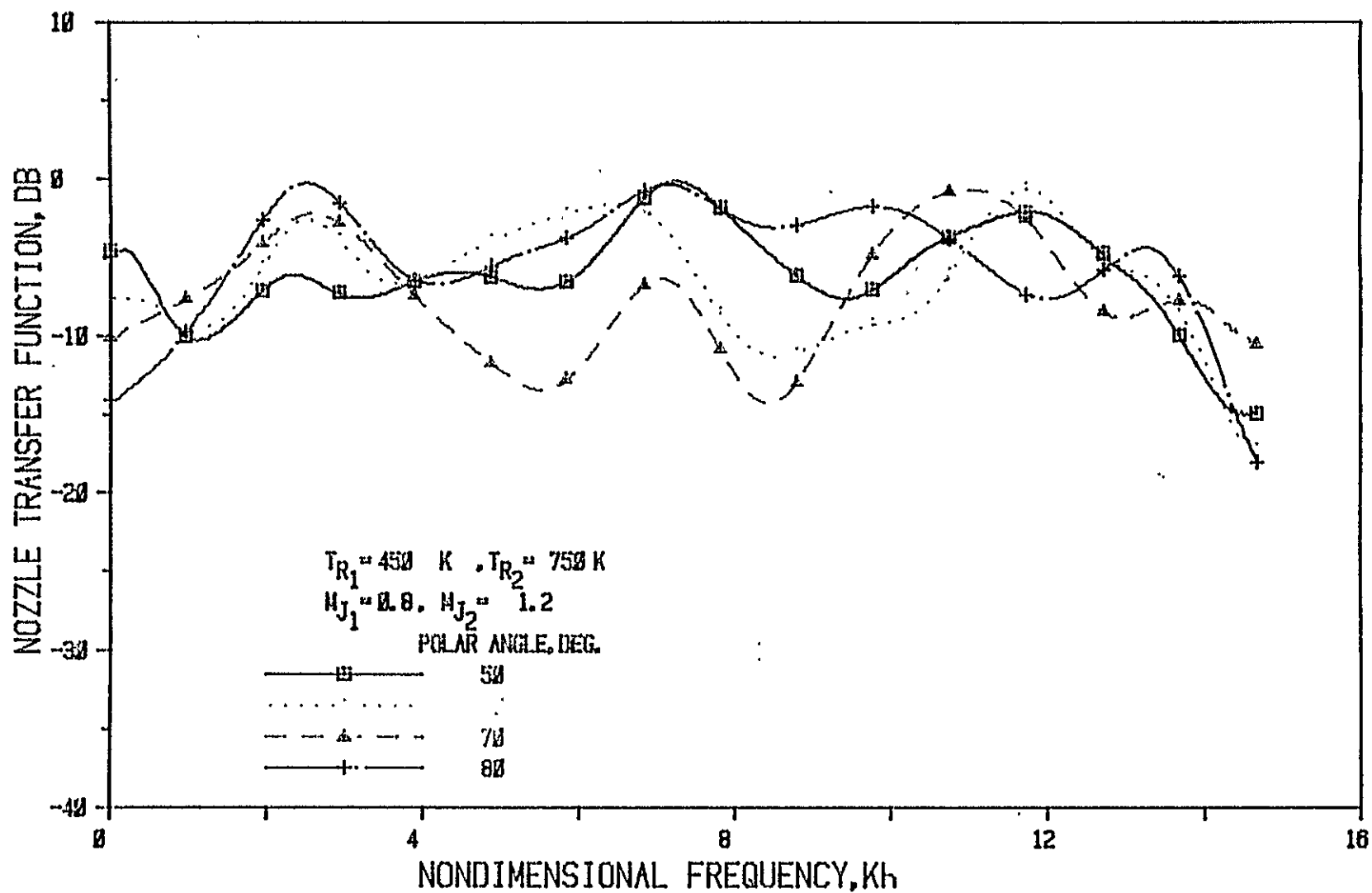


Figure 65(a) Nozzle N 2 ( $L/h = 3$ , Convergence Angle = 20 Deg.); Source At Fan

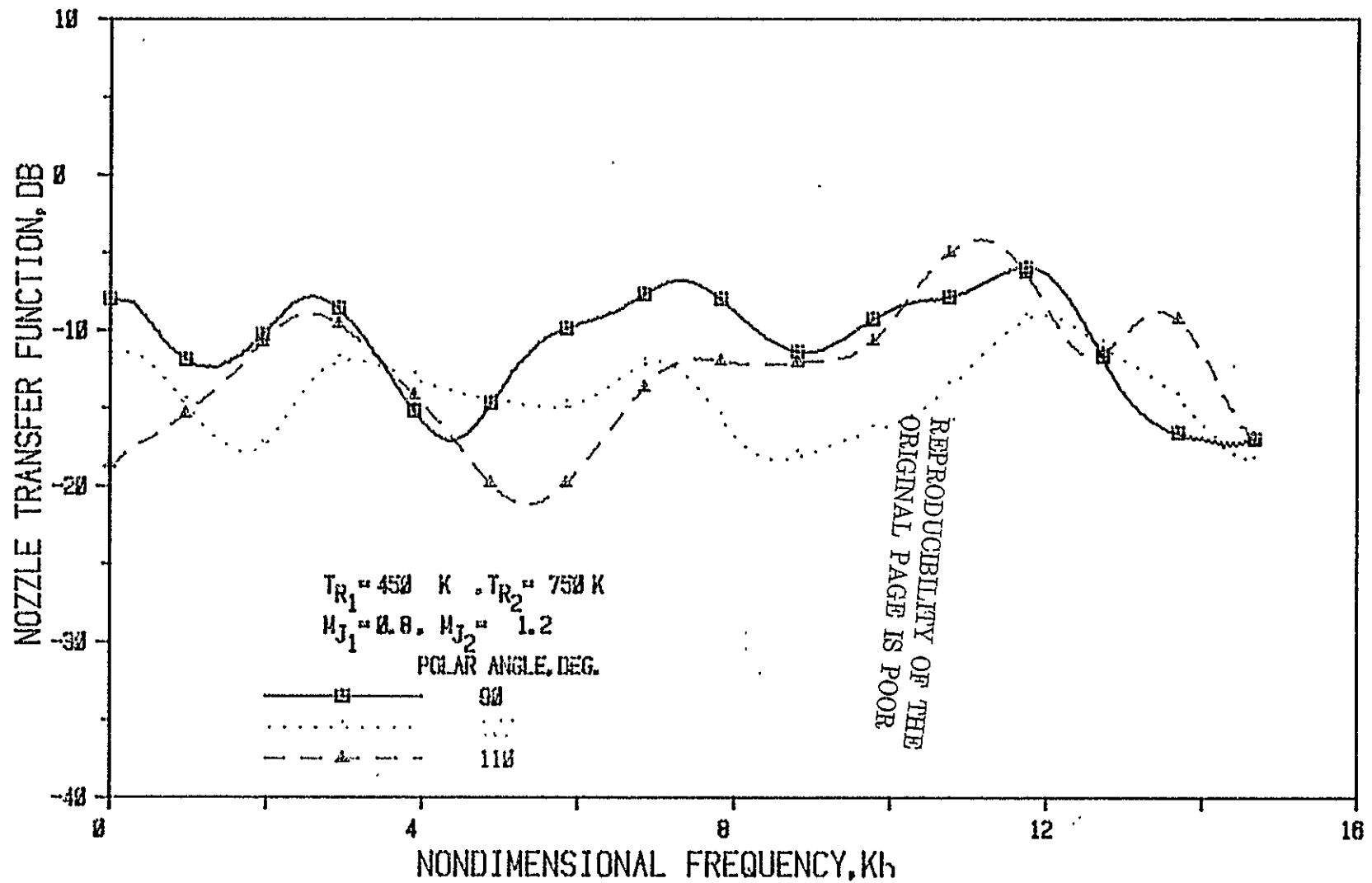


Figure 65(b) Nozzle N 2 (  $L/h = 3$  , Convergence Angle = 20 Deg. ); Source At Fan

## 6. LIST OF SYMBOLS

$A_D$	duct area
$C_D$	speed of sound in the duct
$C_O$	ambient speed of sound
$h$	annulus height
$K$	wave number
$L$	protrusion of primary nozzle exit beyond that of the secondary nozzle
$M_D$	Mach number in the duct
$M_{J_1}$	primary jet Mach number
$M_{J_2}$	secondary jet Mach number
$P_{amb}$	ambient pressure
$R$	primary nozzle radius
$T_{amb}$	ambient temperature
$T_{R_1}$	primary reservoir temperature
$T_{R_2}$	secondary reservoir temperature
$\alpha$	convergence angle of the secondary nozzle

## REFERENCES

1. Dean, P. D.; Salikuddin, M.; Ahuja, K. K.; Plumblee, H. E.; and Mungur, P.: Studies of the Acoustic Transmission Characteristics of Coaxial Nozzles with Inverted Velocity Profiles. NASA Contract NAS3-20797, NASA CR-(to be assigned).